

**Geobiological Coupling of Hydrothermal Vent Fluids with Endosymbiotic
Primary Producers of *Bathymodiolus* Mussels from
Hydrothermal Vents on the Mid-Atlantic Ridge**

Dissertation
zur Erlangung des Grades eines
Doktors der Naturwissenschaften
- Dr. rer. nat. -

dem Fachbereich Biologie/Chemie der
Universität Bremen
vorgelegt von

Frank Zielinski

Bremen
Juli 2008

Die Untersuchungen zur vorliegenden Doktorarbeit wurden am Max-Planck-Institut für Marine Mikrobiologie in Bremen durchgeführt.

1. Gutachter:

2. Gutachterin:

Weitere Prüfer:

Tag des Promotionskolloquiums:

"Mutual aid is met with even amidst the lowest animals, and we must be prepared to learn some day, from the students of microscopical pond-life, facts of unconscious mutual support, even from the life of micro-organisms. Of course, our knowledge of the life of the invertebrates, [...], is extremely limited; and yet, even as regards the lower animals, we may glean a few facts of well-ascertained cooperation. The numberless associations [...] are practically quite unexplored; but the very fact of their existence indicates that they must be composed on about the same principles [...]."

Petr Alekseevich Kropotkin, 1902

(*1842 †1921 - Geologist, Anarchist, Revolutionist)

Mutual Aid: A factor of evolution. 1902. London: William Heinemann, p. 13

SUMMARY	6
ZUSAMMENFASSUNG	7
I INTRODUCTION	9
1 The global system of oceanic spreading ridges	11
1.1 What are oceanic spreading ridges?	11
1.2 Types of oceanic spreading ridges	12
2 Hydrothermal circulation	13
2.1 The principle of hydrothermal circulation	15
2.2 Ultramafic-hosted settings	16
2.2.1 Serpentinization	16
2.2.2 Abiogenic methanogenesis	18
2.2.3 Lost City	19
2.3 Back-arc basin spreading centers and sediment-hosted settings	19
2.4 Global occurrence of hydrothermal vent fields	20
2.5 The basis for chemosynthesis at hydrothermal vents	21
3 Intermezzo: The 19th century roots of the symbiosis concept and its meaning in the 21st century	21
4 Deep-sea hydrothermal vents – chemosynthesis based ecosystems	23
4.1 Hydrothermal symbioses	26
4.1.1 Vent invertebrates with endosymbiotic bacteria	26
4.1.2 Vent invertebrates with episymbiotic bacteria	28
4.1.3 Vent protists with symbiotic bacteria	29
4.2 Non-vent marine chemosynthetic symbioses	29
4.2.1 Cold seeps	30
4.2.2 Whale falls and sunken wood	31
4.2.3 Marine sediments	32
4.3 Phylogeny of marine chemosynthetic symbionts	34
4.4 Energy sources, energy conservation, and carbon assimilation	34
4.4.1 Sulfur-oxidizing chemoautotrophs	35
4.4.2 Methane-oxidizing chemoheterotrophs	39
5 Deep-sea bathymodiolin mussels - chemosymbiotic bivalves	41
5.1.1 Phylogeny of chemosymbiotic bivalves	41
5.1.2 The genus <i>Bathymodiolus</i>	42
6 Thesis goal	45
II RESULTS AND DISCUSSION	46
1 Habitat characterization	46
1.1 Working question	46
1.2 Results of <i>in situ</i> microsensor measurements	47
1.3 <i>In situ</i> versus on board measurements	48
1.3.1 Sulfide as a paradigm for discrepancies between <i>in situ</i> and on board measurements	48
1.3.2 <i>In situ</i> techniques of sulfide detection	49

1.3.3	Summary	50
1.4	Gradients in hydrothermal diffuse flow	50
1.5	Outlook	52
2	Endosymbiont diversity	54
2.1	Assessment of endosymbiotic diversity	54
2.2	Chemoautotrophic and methanotrophic endosymbionts	54
2.3	“ <i>Candidatus</i> Endonucleobacter bathymodioli”	55
2.4	Conclusion	55
2.5	Outlook	57
2.5.1	Re-assessment of endosymbiotic diversity of <i>B. puteoserpentis</i>	57
2.5.2	Further research on “ <i>Ca. E. bathymodioli</i> ”	57
2.5.3	Further research on intranuclear bacteria in marine metazoa	60
3	Endosymbiont activity	62
3.1	Evaluation of endosymbiotic activity by physiological experiments	63
3.2	Results of H ₂ and H ₂ S consumption experiments	63
3.3	Effect of mussel transplantation on hydrogen consumption rates	64
3.4	Carbon assimilation in the presence of hydrogen or sulfide	66
3.5	Outlook / Experimental improvements	67
3.5.1	Consumption experiments	67
3.5.2	Carbon fixation experiments	71
3.5.3	Cultivation	72
4	General conclusions	73
III	REFERENCES	74
	ACKNOWLEDGEMENTS	83
IV	LIST OF PUBLICATIONS AND MANUSCRIPTS	84
1	Publications and manuscripts presented in this thesis	84
2	Contributions to other publications	85
3	Publications as a result of research cruises	85
	<i>IN SITU</i> MEASUREMENTS OF HYDROGEN SULFIDE, OXYGEN, AND TEMPERATURE IN DIFFUSE FLUIDS OF THE ULTRAMAFIC-HOSTED LOGATCHEV HYDROTHERMAL VENT FIELD (MID-ATLANTIC RIDGE): IMPLICATIONS FOR SYMBIONT-CONTAINING <i>BATHYMODIOLUS</i> MUSSELS	87
	WIDESPREAD OCCURRENCE OF AN INTRANUCLEAR BACTERIAL PARASITE IN VENT AND SEEP MUSSELS	107
	THE SULFUR-OXIDIZING ENDOSYMBIONT OF THE HYDROTHERMAL VENT MUSSEL <i>BATHYMODIOLUS PUTEOSERPENTIS</i> (BIVALVIA: MYTILIDAE) USES HYDROGEN AS AN ENERGY SOURCE	133
	CURRICULUM VITAE	158

Summary

This thesis was accomplished within the Priority Program SPP 1144 “From Mantle to Ocean” which investigates the energy-, material-, and life cycles at hydrothermal vents on the slow-spreading Mid-Atlantic Ridge. Two hydrothermal settings which differ prominently in their fluid composition are examined within the SPP: the ultramafic-hosted Logatchev vent field (14°45’N) and a cluster of basalt-hosted vent fields at 4°48’S. In contribution to the SPP the research group “Hydrothermal Symbioses” investigates the conversion of geochemical energy into biomass, particularly of hydrothermal vent mussels belonging to the genus *Bathymodiolus* through their chemoautotrophic and methanotrophic endosymbionts. To address this energy transfer the symbiosis research project focuses on the diversity, abundance, distribution, biomass, and activity of these endosymbiotic bacteria in regard to differing physico-chemical conditions. This PhD project aimed to (i) describe the physico-chemical conditions in Logatchev mussel habitats by means of *in situ* measurements, (ii) investigate the endosymbiotic diversity of *B. puteoserpentis* (Logatchev) using the 16S rRNA gene as a phylogenetic marker, and (iii) evaluate the activity of endosymbiotic bacteria as judged from H₂ and H₂S consumption and CO₂ assimilation in response to the two differing hydrothermal settings. (I) *In situ* measurements using microsensors revealed abundant H₂S and O₂ in diffuse fluids emanating from the mussel beds. Thus, Logatchev mussel habitats, previously suggested to be deficient in free sulfide, comply with the requirements of aerobic sulfur-oxidation. (II) Cloning and sequencing of the 16S rRNA gene revealed three phylotypes in *B. puteoserpentis*. Two were related to sulfur- and methane-oxidizing symbionts. The third phylotype was identified as an intranuclear bacterial parasite which was subsequently found to be widespread in hydrothermal vent and cold seep mussels of the genus *Bathymodiolus* and termed “*Candidatus* Endonucleobacter bathymodioli”. FISH and deconvolution microscopy revealed an unusual cell cycle, the first to be reported from an intranuclear parasite of metazoans. (III) Consumption of H₂ and H₂S along with CO₂ assimilation, indicative of energy conservation and thus actively metabolizing endosymbionts, implied that endosymbiotic chemoautotrophy may be sulfur-based at basalt-hosted vent settings but hydrogen-based at ultramafic-hosted vents. Indeed, the mussel population inhabiting the ultramafic-hosted Logatchev vent field may oxidize 270-670 liters of hydrogen per hour. Endosymbionts of *B. puteoserpentis* may therefore play an appreciable role as H₂-oxidizing primary producers and thus in converting H₂-derived geochemical energy into biomass. In fact, H₂ has not been shown previously to be utilized by symbionts of invertebrates from reducing environments.

Zusammenfassung

Die vorliegende Arbeit wurde im Rahmen des Schwerpunktprogramms SPP 1144 "Vom Mantel zum Ozean" angefertigt, das die Energie-, Stoff-, und Lebenszyklen an Hydrothermalquellen des langsam spreizenden Mittel-Atlantischen Rückens untersucht. Zwei sich vornehmlich in ihrer Fluidzusammensetzung unterscheidende Hydrothermalfelder werden im Rahmen des SPP untersucht: Logatchev bei 14°45'N, geologisch charakterisiert durch das Auftreten von ultramafischem Mantelgestein, und eine Ansammlung von Hydrothermalfeldern bei 4°48'S auf basaltischem Untergrund. Die Arbeitsgruppe "Hydrothermale Symbiosen" untersucht im Rahmen des SPP die Umwandlung geochemischer Energie in Biomasse, insbesondere von Muscheln der Gattung *Bathymodiolus* mittels ihrer chemoautotrophen und methanotrophen Endosymbionten. Dazu konzentriert sich das Symbioseprojekt auf die Diversität, Abundanz, Verteilung, Biomasse und Aktivität dieser endosymbiontischen Bakterien unter Berücksichtigung unterschiedlicher physikalisch-chemischer Bedingungen. Das Ziel der vorliegenden Doktorarbeit war es, (i) physikalisch-chemische Parameter in Muschelhabitaten des Logatchev Hydrothermalfeldes (LHF) mit Hilfe von *in situ* Messungen zu beschreiben, (ii) die endosymbiontische Diversität in *B. puteoserpentis* (Logatchev) mit Hilfe des 16S rRNA Gens als phylogenetischem Marker zu untersuchen und (iii) die Aktivität endosymbiontischer Bakterien auf der Basis des Verbrauches an H₂- und H₂S und der Assimilation von CO₂ zu evaluieren, und zwar in Abhängigkeit der geologisch unterschiedlichen hydrothermalen Standorte. (I) *In situ* Messungen mit Mikrosensoren offenbarten reichlich H₂S und O₂ in diffusen Fluiden über den Muschelansammlungen. Muschelhabitate des LHF erfüllen demnach die Voraussetzungen für die aerobe Oxidation reduzierter Schwefelverbindungen. Bisher wurde angenommen, dass diffuse Fluide des LHF nur unzureichend freie Sulfide enthalten würden. (II) Das Klonen und Sequenzieren der 16S rRNA Gene offenbarte drei Phylotypen in *B. puteoserpentis*. Zwei davon zeigten eine Verwandtschaft mit schwefel- und methanoxidierenden Endosymbionten. Der dritte Phylotyp konnte als bakterieller Zellkernparasit identifiziert werden und wurde als „*Candidatus* Endonucleobacter bathymodioli“ beschrieben. Nachfolgende Untersuchungen zeigten, dass dieser Phylotyp in Muscheln der Gattung *Bathymodiolus* weitverbreitet ist, sowohl an Hydrothermalquellen als auch an kalten Gasaustritten (cold seeps). Mit FISH und Dekonvolutionsmikroskopie konnte ein ungewöhnlicher Zellzyklus nachgezeichnet werden. Zellkernbakterien waren bisher so gut wie unbekannt in der Gruppe der Metazoa und ein Entwicklungszyklus ist zuvor nicht in vielzelligen Tieren beschrieben worden. (III) H₂- und H₂S-Verbrauch bei gleichzeitiger Assimilation von CO₂, ein Indikator für Energiekonservierung und folglich für aktiv Stoffwechsel-betreibende Endosymbionten, deuten darauf hin, dass endosymbiontische Chemoautotrophie an basaltischen Hydrothermalquellen auf reduzierten Schwefelverbindungen basiert während ultramafische Hydrothermalquellen eher H₂-verstoffwechselnde Endosymbionten unterstützen. Tatsächlich deuten H₂-Verbrauchsexperimente darauf hin, dass die LHF Muschelpopulation 270-670 Liter H₂ pro Stunde oxidiert. Die Endosymbionten von *B. puteoserpentis* spielen demnach eine beachtliche Rolle als H₂-oxidierende Primärproduzenten und folglich bei der Umwandlung von H₂-basierter geochemischer Energie in Biomasse. In dieser Arbeit wurde erstmals nachgewiesen, dass H₂ eine Energiequelle für Invertebratensymbionten in reduzierenden Habitaten darstellen kann.

I Introduction

The work presented in this thesis was accomplished within the Priority Program SPP 1144 (“From Mantle to Ocean”) funded by the German Research Foundation (Fig. 1). The multi-disciplinary program was launched in October 2003 and aims to investigate the energy-, material-, and life cycles at **HYDROTHERMAL VENTS** on the **SLOW-SPREADING MID-ATLANTIC RIDGE** (MAR). Two integrated study sites were chosen to address the energy and mass transfer from the mantle to the ocean: the **ULTRAMAFIC-HOSTED** Logatchev hydrothermal vent field at 14°45’N and the **BASALT-HOSTED** hydrothermally active area at 4°48’S (Fig. 2). As many as four hydrothermal vent fields have been discovered in this region as a result of this Priority Program: Red Lion, Comfortless Cove, Turtle Pits and Wideawake [1]. The occurrence of hydrothermal vents in two different geological settings, a characteristic thus far unique to the MAR provides a unique chance to study their relative contribution to the overall energy and mass transfer at a slow-spreading **MID-OCEAN RIDGE**.

In contribution to the Priority Program the research group “Hydrothermal Symbioses” in which this PhD was based investigates the transfer of geochemical energy to **HYDROTHERMAL VENT MUSSELS** via their bacterial **ENDOSYMBIONTS**. In the absence of light these symbionts synthesize organic carbon compounds *de novo* from dissolved CO₂ or CH₄ by means of **CHEMOSYNTHESIS** and thus form the basis of a hydrothermal food chain. The energy for carbon primary production comes from reduced chemical species and is provided with **HYDROTHERMAL FLUIDS**.

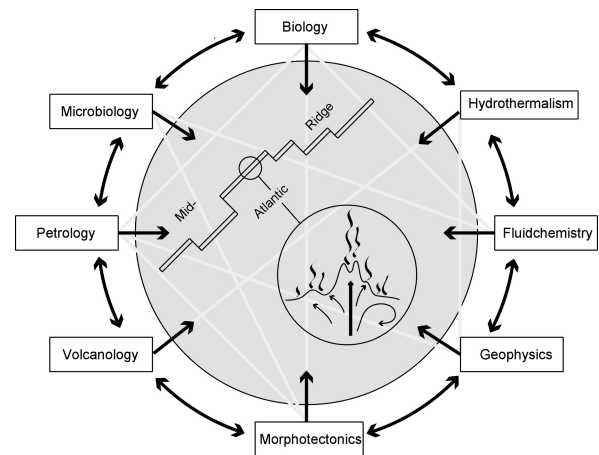


Fig. 1. Logo of the Priority Program SPP 1144. The manifold scientific disciplines involved in the program are shown.

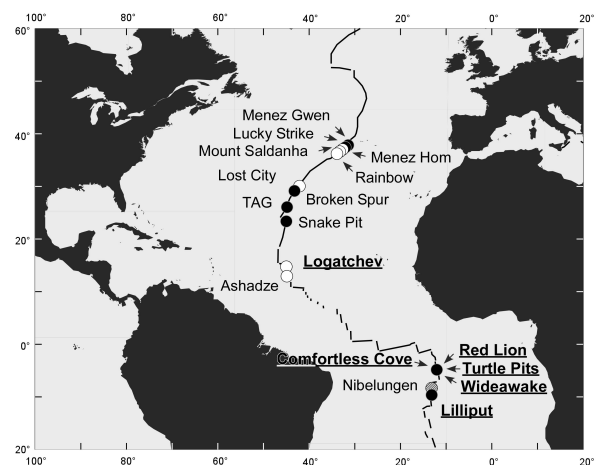


Fig. 2. Map showing currently known hydrothermal vent fields along the Mid-Atlantic Ridge. The study sites investigated during the Priority Program SPP 1144 are underlined. White and black circles denote ultramafic-hosted and basalt-hosted vent fields, respectively. Fluids of the Nibelungen field (grey circle) indicate an ultramafic-hosted setting, however, only basaltic rocks were recovered thus far [2].

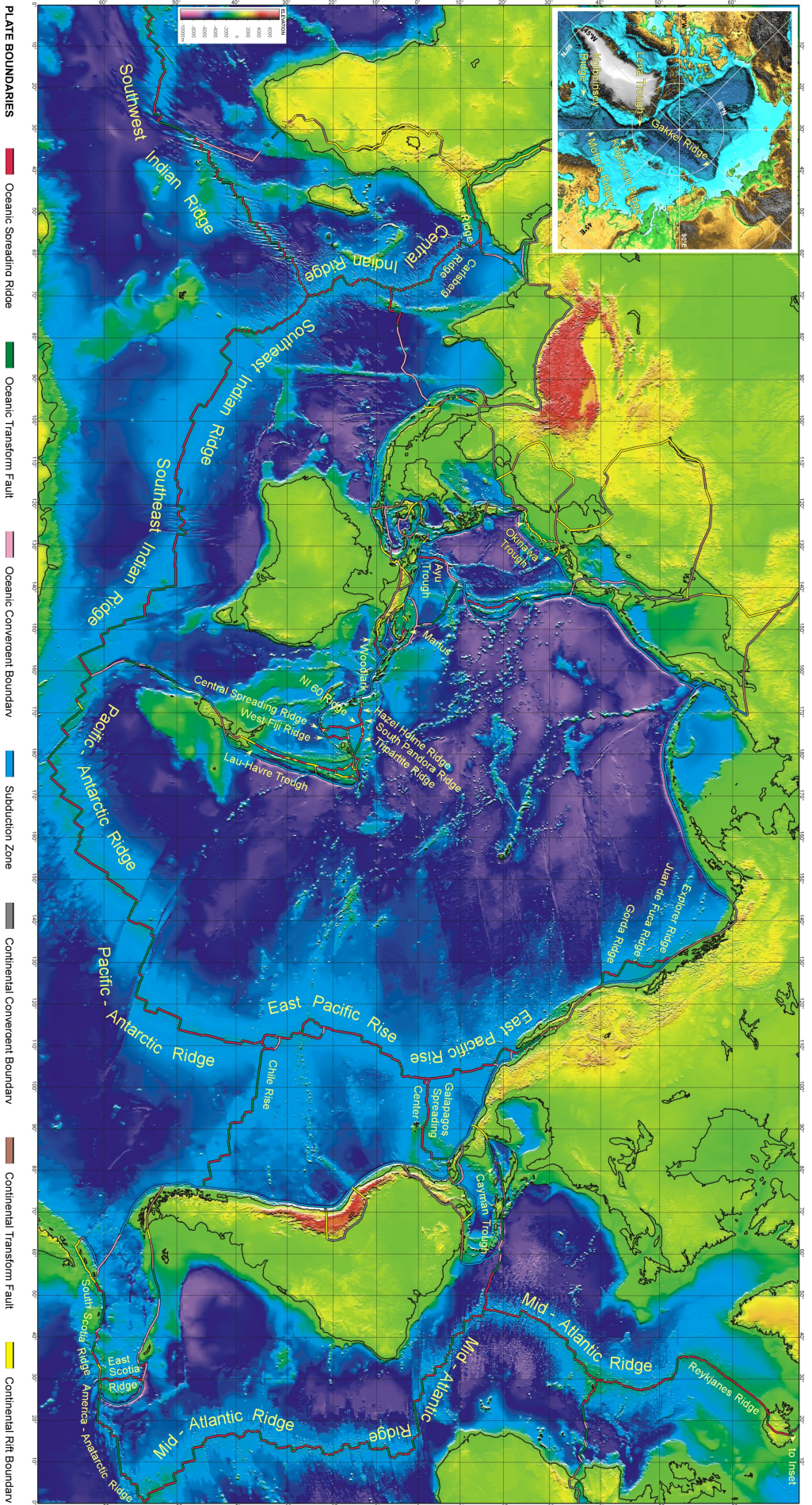


Fig. 3. Boundaries of Earth's tectonic plates. Oceanic spreading ridges are emphasized in red whereas oceanic transform faults are shown in green. Modified from [3]. Designation of oceanic spreading ridges after [3-8]. The huge Pacific plate borders to many small plates at its western extension. Several of these small plates are characterized by volcanic arcs, back-arc basins, and back-arc spreading ridges. Back-arc spreading ridges displayed in the figure are: Lau-Havre Trough (Kermadec plate hosting the Lau Back-Arc Basin), Hazel-Holme Ridge, South Pandora Ridge, Tripartite Ridge, NI 60 Ridge (New Hebrides and Balmorel Reef plates hosting the North-Fiji Back-Arc Basin), Manus - spreading ridges of the Manus plate (hosting the Manus Back-Arc Basin), Woodlark - spreading ridges of Woodlark plate (hosting the Woodlark Back-Arc Basin), Mariana Trough (Mariana Plate hosting the Mariana Back-Arc Basin), Okinawa Trough (Okinawa plate). *Inset:* Northern extension of the Mid-Atlantic Ridge showing the ultraslow-spreading ridges north of Iceland

Hydrothermal vent research is located at the interface of geology, chemistry, and biology. Vent ecosystems can not be understood in detail without basic knowledge in all of these fields and more detailed knowledge in, for example, plate tectonics, fluid chemistry, microbiology, and physiology. The following chapters aim to provide this background and the terms highlighted in bold will be explained and defined.

Chapter 1 gives an introduction to the global system of oceanic spreading ridges along which hydrothermal venting occurs throughout the oceans. Chapter 2 explains the principle of hydrothermal circulation and introduces the different geological settings in which hydrothermal convection cells occur. The emphasis will here be on ultramafic-hosted settings as much of the work presented in the 'Results and Discussion' section and the manuscripts is based on samples from the ultramafic-hosted Logatchev vent field. Chapter 2 will end with a short note on the life-supporting role of hydrothermal vents as a result of chemosynthesis before Chapter 3 will briefly deal with the symbiosis concept from a historic point of view. Chapter 4 will explain hydrothermal vent ecosystems and vent chemosynthetic symbioses in more detail but also make a detour to cognate communities of cold seeps, whale falls, sunken wood, and marine reducing sediments to present the bigger picture of the phylogeny and physiology of chemosynthetic symbionts. Chapter 5 introduces the chemosymbiotic bivalves in general and the deep-sea vent and seep mussels of the genus *Bathymodiolus* in particular since *B. puteoserpentis* and an undescribed *Bathymodiolus* species along with their endosymbionts are the main topics of this thesis. After introducing the goal of this PhD thesis in Chapter 6 the 'Results and Discussion' section will deal with the three major projects of this thesis: (i) *in situ* habitat characterization of *B. puteoserpentis*, (ii) bacterial diversity in *B. puteoserpentis*, and (iii) endosymbiont activity of *B. puteoserpentis* and *B. sp.* as judged from hydrogen and sulfide consumption and carbon assimilation in response to ultramafic- and basalt-hosted hydrothermal settings.

1 The global system of oceanic spreading ridges

1.1 What are oceanic spreading ridges?

Oceanic spreading ridges (OSR) are part of the boundaries that separate Earth's plates and are as such a result of plate tectonics themselves (Fig. 3) [3]. It is at OSR that plates are pulled apart by tectonic forces resulting in seafloor spreading and thus substantial continental drift over geological times [4]. OSR are hence also referred to as seafloor spreading centers. As magma ascends from Earth's interior (mantle) it partially melts and feeds volcanoes which eventually erupt to generate fresh oceanic crust [4,7,9]. While a small proportion of these

volcanic systems is found as spreading centers in back-arc basins close to subduction zones [10], the vast majority of all Earth's OSR forms a single, continuous, globe-encircling volcanic underwater mountain chain, known as the global mid-ocean ridge system, that typically lies at around 2000 to 5000 m depth [7]. This mountain range is divided into distinct actively spreading ridge segments bound by deep transform faults that offset the spreading axis resulting in a distinctive stepped appearance of the global mid-ocean ridge system (Fig. 3) [4]. Oceanic spreading ridges comprise ~67,000 km in length and account for almost nine-tenths of Earth's total area production (88%) while oceanic transform faults total 48,000 km contributing only negligibly to this production (1%). Together, they account for 44% of earth's plate boundaries [3].

1.2 Types of oceanic spreading ridges

According to their spreading rates, i.e. the speed at which two tectonic plates are pulled apart from each other, oceanic-spreading ridges can be classified into ultraslow- ($< 20 \text{ mm a}^{-1}$), slow- ($20\text{-}50 \text{ mm a}^{-1}$), intermediate- ($50\text{-}90 \text{ mm a}^{-1}$), fast- ($90\text{-}130 \text{ mm a}^{-1}$), and superfast- ($130\text{-}170 \text{ mm a}^{-1}$) spreading ridges (Table 1).

Table 1. Classification of mid-ocean ridges according to their spreading rates

Ridge category ^a	Spreading rate ^b	Example ^a
ultraslow-spreading	$< 20 \text{ mm a}^{-1}$	America-Antarctic Ridge, Gakkel Ridge, Knipovich Ridge, Lena Trough, Mohns Ridge, Southwest Indian Ridge
slow-spreading	$20\text{-}50 \text{ mm a}^{-1}$	Central Indian Ridge, Mid-Atlantic Ridge
intermediate-spreading	$50\text{-}90 \text{ mm a}^{-1}$	Galapagos Spreading Center, Gorda Ridge, East Pacific Rise (e.g. 21°N), Explorer Ridge, Juan de Fuca Ridge, Lau Basin Back-Arc Spreading Center, Southeast Indian Ridge
fast-spreading	$90\text{-}130 \text{ mm a}^{-1}$	East Pacific Rise (e.g. 8-13°N)
superfast spreading	$130\text{-}170 \text{ mm a}^{-1}$	East Pacific Rise (e.g. 27-32°S)

^a Ridge categories and examples compiled from various sources [4,5,7,11-13]; ^b Spreading rates from [7]

With the exception of ultraslow-spreading ridges all other mid-ocean ridges share certain characteristics. First, they have roughly the same crustal thickness (6-7 km), second, in plan view they have a characteristic stair-step geometry of volcanic rifts separated by perpendicular transform offsets (Fig. 3), and third, they generate a characteristic outcrop pattern of elongate, fault-bounded abyssal hills trending normal to the spreading direction [5]. Their differences lie primarily in their across-axis morphology (Fig. 4). Slow-spreading ridges have rugged rift mountains [5]. The paired flanks of the ridge axis are separated by a deep (typically 1-3 km) and wide (5-15 km) central rift valley. In contrast, intermediate-, fast-, and

superfast-spreading ridges have an only small axial rise (e.g. 100 m at 9°N on the East-Pacific Rise) with a very shallow (10-50 m) and narrow (50-1000 m) linear summit graben that is the locus for most volcanic and tectonic activity. Intermediate-, fast-, and superfast-spreading ridges tend to be dominated by volcanism, while the morphology of slow-spreading ridges is dominated more by tectonics [4,5,7,14].

Ultraslow-spreading ridges have only recently emerged as a unique, new class of mid-ocean ridges [5]. At ultraslow-spreading ridges the seismic crust is thinner (~1-4 km) than at other ridges. They uniquely possess amagmatic rifts that expose mantle rocks (peridotite) directly on the seafloor, with only scattered basalt and gabbro. Amagmatic segments can assume any orientation to the spreading direction sometimes forming oblique rifts and they can produce a unique “smooth” seafloor [5]. For example, the Gakkel ridge, the slowest-spreading ridge on earth, with spreading rates from 6-15 mm a⁻¹, has no transform offsets [9].

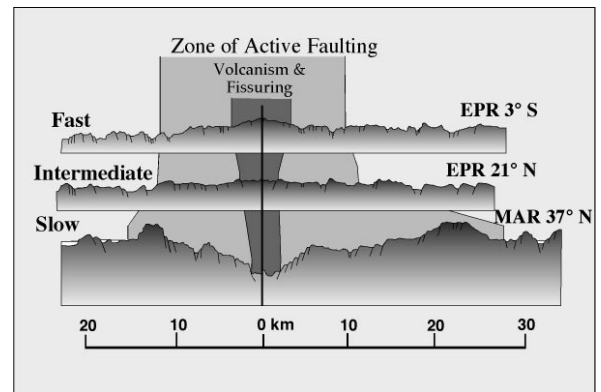


Fig. 4. Comparison of across-axis morphology of fast-, intermediate-, and slow-spreading mid-ocean ridges. From [14]. EPR – East Pacific Rise; MAR – Mid-Atlantic Ridge.

2 Hydrothermal circulation

Nearly 3.3 km² of oceanic crust are newly formed at mid-ocean ridges each year [15]. Along with the magma, heat is released from the Earth’s interior. While the majority of this heat loss occurs through conduction, approximately one-fifth of Earth’s total heat loss at mid-ocean ridges is effected by a convective process in which cold seawater percolates downward through fractured oceanic crust, is geothermally heated, and finally expelled back into the water column [12,15,16]. This process has been termed hydrothermal circulation.

It is a heat source such as a magma chamber underneath the volcanic mid-ocean ridge system that drives hydrothermal circulation. Other prerequisites are a permeable oceanic crust typically in the form of faulted and fissured igneous crust and seawater that saturates the crust [17]. During hydrothermal circulation seawater reacts with the host rock and is chemically modified. The composition of hot fluids that exit at vent fields thus reflects the composition of the rock, but also provides insights into rock structure, and the depth, size, and shape of the heat source [17]. The estimated yearly flux of hydrothermal fluids is of the order of 10¹⁴-10¹⁶ tons [16]. Thus, it has been estimated that the oceans circulate through hydrothermal systems

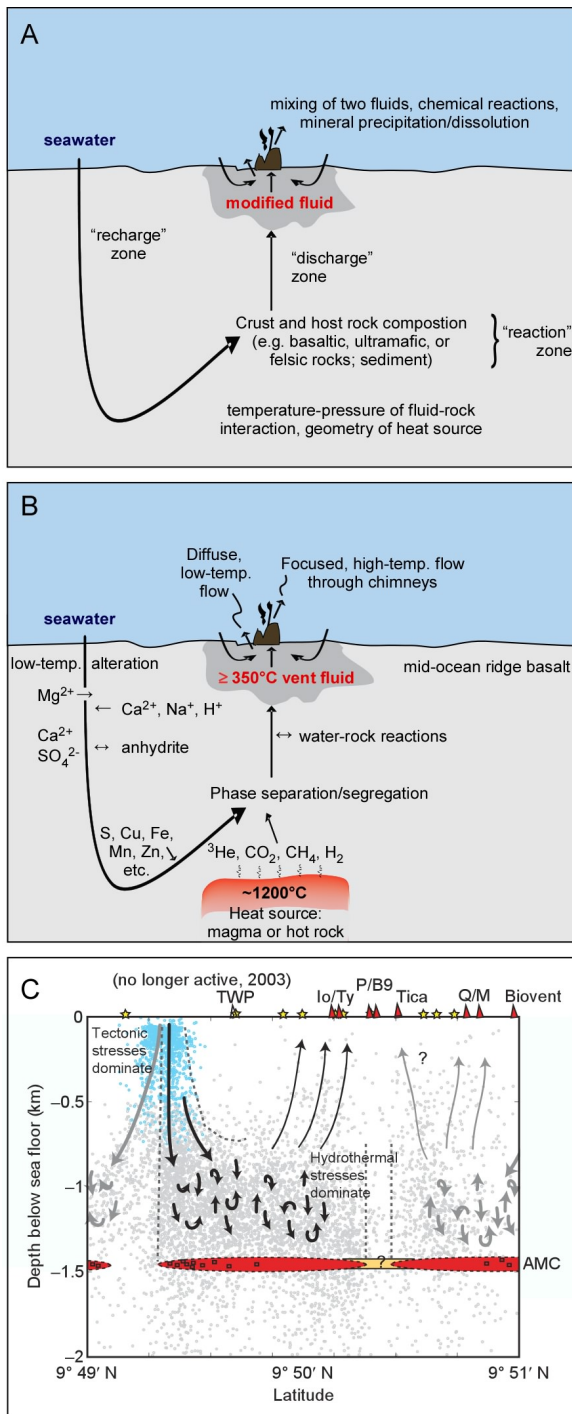


Fig. 5. Schematic drawing of a hydrothermal system. (A) Zones, components and processes involved in the generation of hydrothermal fluid. (B) Chemical evolution of the hydrothermal fluid during circulation through basaltic crust. From [17]. (C) Cartoon illustrating hydrothermal flow and the penetration depths of seawater at $9^\circ 50' \text{N}$ East Pacific Rise. Black arrows indicate a well-defined hydrothermal cell, while grey arrows denote inferred hydrothermal flow in adjacent cells. Light blue dots illustrate the area where tectonic stresses are likely to dominate, creating a zone of permeability. Light grey dots illustrate where hydrothermal stresses probably dominate. AMC – axial magma chamber. From [20].

on a timescale of 1 to 10 million years [18]. Recently, this number has been corrected to even shorter timescales by one order of magnitude to 1 to 10 thousand years [19].

Hydrothermal circulation has long been studied in basalt-hosted settings in which the host rock is exclusively or predominantly composed of mid-ocean ridge basalt. This was mainly a result of the fact that hydrothermal vent fields, initially discovered at the Galapagos Spreading Center and the East Pacific Rise are basalt-hosted. However, with further exploration of the global mid-ocean ridge system it became evident that hydrothermal circulation can occur in different settings in which the host rock is all but basaltic. For example, at ultra-slow spreading ridges mantle-derived ultramafic rocks (peridotite) dominate with only scattered basalt and gabbro [5], a situation that is also present at some portions of slow-spreading ridges [17,21]. At back-arc basin spreading centers the host rock composition can be felsic (comprising andesite, rhyolite, and dacite) instead of basaltic [10,17]. Finally, hydrothermal settings can also be sediment-hosted if they are associated with ridges in close vicinity to continental margins. Sediment-hosted vent fields are common at the Northeast Pacific Ridges (e.g. Juan de Fuca Ridge and Gorda Ridge) and at the Gulf of California section of the East Pacific Rise [17,22].

2.1 The principle of hydrothermal circulation

The principle of hydrothermal circulation has been elucidated using experimental and theoretical consideration but has primarily been developed for basalt-hosted hydrothermal settings [17]. Nevertheless, it is in general valid for all other hydrothermal settings as well, except for differences in the endmember fluid composition, i.e. the composition of the expelled fluid after hydrothermal circulation. Fig. 5 shows a schematic drawing of this principle. Table 2 summarizes the physico-chemical properties of endmember hydrothermal fluids venting from different settings.

According to the depth of the percolating seawater, the temperature within the crust, and chemical reactions between the seawater and the host rock, hydrothermal circulation can be subdivided into three distinct zones: a low-temperature “recharge” zone as part of the down-flowing limb, a high-temperature “reaction” zone, and a “discharge” zone as part of the up-flowing limb [17,19]. In the down-flowing limb and at temperatures up to about 40°C to 60°C, reactions between seawater and basalt result in alteration of basaltic minerals. As seawater penetrates deeper and is heated to temperatures above ~150°C, Mg²⁺ is removed from the fluid through precipitation with clays in exchange for Ca²⁺, Na⁺, and H⁺, the latter of which contributes to fluid acidification. Uptake of Ca²⁺ guarantees sufficient SO₄²⁻ precipitation (anhydrite: CaSO₄) as the SO₄²⁻ / Ca²⁺ ratio of seawater is ~3. A fraction of seawater sulfate is chemically reduced to sulfide. Other reactions include reaction of water with ferrous Fe-bearing minerals which results in reducing conditions. The sum of reactions occurring in the “recharge” zone results in a fluid that is slightly acidic, anoxic, alkali-rich, and Mg-poor relative to the surrounding seawater. At 425°C and ~400-500 bars this fluid then leaches S and metals (e.g. Cu, Fe, Mn, Zn) from the rock into solution in the deep “reaction” zone. If the fluid temperature and pressure exceed those of the boiling curve for seawater the fluid will separate into a low-salinity, vapor-rich phase and a brine phase (phase separation). During this partitioning, volatiles such as H₂S partition preferentially into the vapor-rich phase. A final process that can effect vent fluid compositions is the addition of magmatic volatiles to the circulating fluid, such as primordial helium (³He), CO₂, CH₄, and H₂. The evolved fluid in the “reaction” zone is very buoyant relative to cold seawater and thus rises at a rapid rate to the seafloor where it is expelled through polymetallic sulfide chimneys (“black smokers”) at temperatures that can exceed 400°C [17].

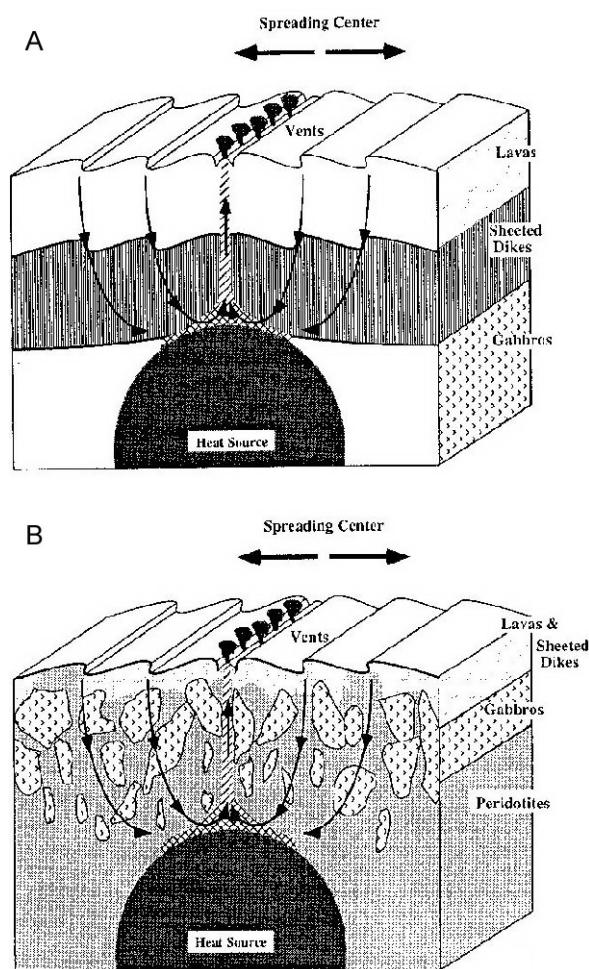


Fig. 6. Schematic model of the upper oceanic crust and hydrothermal circulation. (A) Crust entirely composed of basaltic rocks as is encountered at intermediate-, fast-, and superfast-spreading ridges. (B) Crust primarily composed of ultramafic rocks (peridotites) as is frequently encountered at slow-, and ultraslow-spreading ridges. From [23].

2.2 Ultramafic-hosted settings

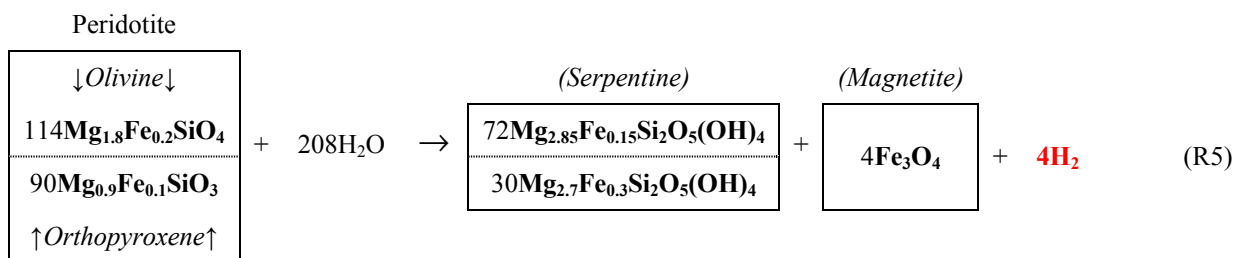
Ultramafic-hosted hydrothermal settings occur at slow- and ultraslow-spreading ridges as a result of tectonic processes [5,17]. In contrast to basalt-hosted settings where the upper oceanic crust is entirely composed of basaltic rocks, the upper crust in ultramafic-hosted settings is primarily composed of mantle-derived ultramafic rocks, i.e. peridotite (and serpentized peridotites), with basaltic lavas present as a thin veneer, and gabbros occasionally injected into the peridotites (Fig. 6) [5,23]. Thus, ultramafic-hosted hydrothermal systems differ in their fluid composition from basalt-hosted systems as a result of peridotite-seawater reactions [23]. The main difference is that hydrothermal fluids discharged from ultramafic-hosted vent fields contain large quantities of dissolved hydrogen and methane (Table 2) while these gases occur in only low amounts in fluids discharged from basaltic-hosted systems

[17,24-27]. The wealth of hydrogen in ultramafic-hosted hydrothermal systems results from a geochemical process known as serpentinization [23,24,26,28-31]. Methane is subsequently produced by abiogenic methanogenesis from CO_2 and hydrogen [26,32-35].

2.2.1 Serpentinization

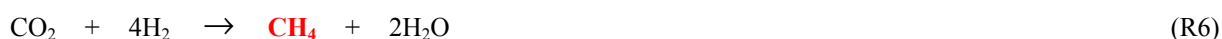
Serpentinization involves peridotite (an ultramafic mantle rock) which is mainly composed of the minerals olivine [$(\text{Mg,Fe})_2\text{SiO}_4$] and pyroxene [both orthopyroxene $(\text{Mg,Fe})\text{SiO}_3$ and clinopyroxene $\text{Ca}(\text{Mg,Fe})\text{Si}_2\text{O}_6$] [29]. In general, hydrolysis of olivine and pyroxene forms serpentine [$(\text{Mg,Fe})_3\text{Si}_2\text{O}_5(\text{OH})_4$], magnetite [Fe_3O_4] and hydrogen [26,28,29].

Depending on temperature and pressure Allen and Seyfried [28] proposed two sets of serpentinization reactions. In the first, at temperatures $> 350\text{-}400^\circ\text{C}$ and at 500 bar hydrogen



2.2.2 Abiogenic methanogenesis

Hydrogen released during serpentinization is subsequently consumed in a Fischer-Tropsch type (FTT) synthesis to abiogenically form methane (R6) [26,32,34]. Fischer-Tropsch synthesis is a well-known industrial process whereby CO_2 is converted to hydrocarbon gas by reaction with H_2 [26,32,34,35].



Magnetite formed during serpentinization likely plays a key role as a catalyst as it has been recognized as a potent catalyzing agent for producing CH_4 from CO_2 - H_2 gas mixtures [32]. Nevertheless, FTT methanogenesis following serpentinization proceeds only slowly and likely requires decades, thousands of years, and hundreds of thousands of years at 300°C , 200°C , and 100°C , respectively for full conversion of CO_2 to CH_4 [32]. The $\delta^{13}\text{C}$ values of methane from ultramafic-hosted hydrothermal vents, as well as the lack of a sediment source

Table 2. Range of endmember compositions of hydrothermal fluids venting from different settings

	Basalt	Ultramafic		Back-Arc	Sediment	Seawater
		High-temp.	Lost City			
T ($^\circ\text{C}$)	$\leq 407^*$	350-365	≤ 91	278-334	100-315	2
pH (at 25°C)	2.8-4.5	2.8-3.9	9-11	< 1 -5.0	5.1-5.9	8
H₂ mmol/kg	0.0005-38	13-19	< 1 -15	0.035-0.5	-	-
H₂S mmol/kg	0-19.5	1-2.5	< 0.064	1.3-13.1	1.10-5.98	-
CH₄ mmol/kg	0.007-2.58	0.13-3.5	1-2	0.005-.06	-	-
NH₃ mmol/kg	< 0.65	-	-	-	5.6-15.6	-
CO₂ mmol/kg	3.56-39.9	n.a.	b.d.	14.4-200	-	2.36
Fe $\mu\text{mol/kg}$	7-18700	2410-24000	-	13-2500	0-180	-
Na mmol/kg	10.6-983	438-553	479-485	210-590	315-560	464
Ca mmol/kg	4.02-109	28-67	< 30	6.5-89	160-257	10.2
K mmol/kg	1.17-58.7	20-24	-	10.5-79	13.5-49.2	10.1
Cl mmol/kg	30.5-1245	515-750	548	255-790	412-668	545
Mg mmol/kg	0	0	< 1	0	0	53
SO₄ mmol/kg	0	0-1.3	1-4	0	0	28

*thus far the highest temperature ever recorded from a hydrothermal vent [1]; n.a. – not analyzed, b.d. – below detection; Table from [17] based on [25,36-43] and extended for ultramafic-hosted high temperature fluids as analyzed by [24-26]

rich in organic matter suggest that the carbon source (CO₂) for the FTT synthesis is truly mantle-derived and not of thermogenic origin, i.e. by thermal decomposition of organic matter within sediments [34]. Besides methane, ethane and propane have been experimentally found after serpentinization of olivine at 300°C and 500 bars [32] and were subsequently confirmed in fluids venting from ultramafic-hosted settings [34]. Furthermore, straight chain saturated hydrocarbons with chain lengths between 16 and 29 carbon atoms have also been identified in fluids released from ultramafic-hosted vents [26,32]. Recent experiments indicated that chromite (a chromium-bearing component of pyroxene) could be the catalyst for the FTT synthesis of longer chain hydrocarbons [33].

2.2.3 *Lost City*

Lost City is a low-temperature vent field located off-axis on the slow-spreading Mid-Atlantic Ridge [36]. Consistent with its ultramafic-hosted setting, Lost City fluids are hydrogen- and methane rich but differ otherwise from fluids discharged from on-axis ultramafic-hosted vent fields. The main difference is the comparably low fluid temperature (28°-90°C) at a very high pH of 9-11 (Table 2). Upon mixing with seawater the alkaline fluids precipitate carbonate and hydroxide minerals thus, forming chimneys composed of calcite [CaCO₃], aragonite [CaCO₃], and brucite [Mg(OH)₂], while silica is found only in traces and sulfide minerals are completely absent [14,36,37,44]. It has been proposed that generation of Lost City fluids does not require heat from magma or cooling of recently solidified rock but instead is a result of exothermic serpentinization reactions. In fact, the isotopic composition of Lost City fluids is consistent with serpentinization reactions at 110°-150°C [38]. However, serpentinization is likely not a significant source of heat and it is more likely that the Lost City system is driven by deep penetration of fluids and access to heat from hot rock or magma [31].

2.3 Back-arc basin spreading centers and sediment-hosted settings

Compared to fluids discharged from basalt-hosted vents, fluids expelled from vent fields hosted in a felsic (andesite) setting (back-arc basin spreading centers) show elevated trace metals (e.g. Zn, Pb, As) and can be very acidic (pH < 1). The low pH may reflect an input of magmatic volatiles (e.g. SO₂) [17]. Fluids from sediment-hosted vent fields show a wide range in composition but are similar in exhibiting a higher pH (5-6 at 25°C), lower maximum temperatures, and lower metal contents than fluids from unsedimented settings [17] (Table 2).

2.4 Global occurrence of hydrothermal vent fields

Hydrothermal venting is known to discharge along mid-ocean ridges in every ocean and at all spreading rates [11]. To date, approximately 280 sites have been described (including back-arc spreading centers) and ~1000 are predicted to exist [11]. Roughly 145 sites have been confirmed by visual observation, while another 130 are inferred solely from water-column observations. Confirmed vent sites range from enormous sulfide constructs hosting multiple high-temperature chimneys to isolated patches of low-temperature diffuse-flow [11]. The term “site” used here is meant as a cluster of single vents (up to ~10 m) as -defined by Tarasov *et al.* [46]. For deep-sea vents Tarasov *et al.* suggested the following nomenclature:

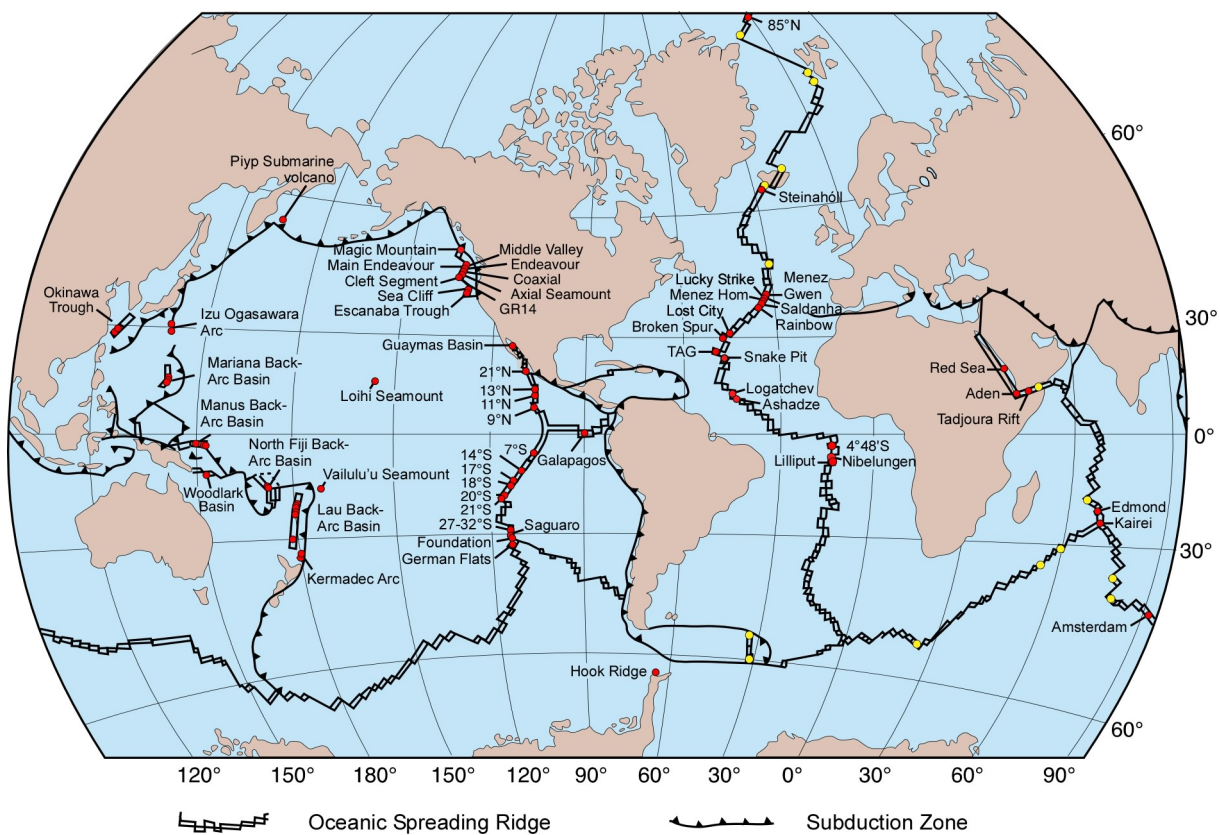


Fig. 7. Currently known deep-sea hydrothermal vent fields along oceanic spreading ridges. Red dots indicate visually confirmed fields while yellow dots denote inferred sites of venting from water-column anomalies. Shallow water vent fields (< 200 m water depth) are not included. A vent field on the ultraslow-spreading Gakkel Ridge (85°N, 85°E) was only recently discovered (<http://www.divediscover.who.edu>). In addition 4 vent sites were recently found in the Indian Ocean, 3 at the ultraslow-spreading Southwest Indian Ridge and one at the Central Indian Ridge (<http://www.interridge.org/node/230>). The coordinates have, however, not yet been released [45]. The 4°48'S area on the Mid-Atlantic Ridge comprises the vent fields: Red Lion, Comfortless Cove, Turtle Pits, and Wideawake. Vent fields at back-arc basins in the West Pacific are (from north to south): **Izu Ogasawara Arc**: Myojin Knoll, Sumisu Caldera, Suiyo Seamount, Kaikata Seamount, Nikko Seamount; **Okinawa Trough**: Hatoma Knoll, Minami-Ensei Knoll, North Iheya Knoll, Iheya Ridge, Izena Cauldron; **Mariana Back-Arc Basin**: Kagusa 2 seamount, North West Eifuku Seamount, Daikoku Seamount, Mariana Trough, Anemone Heaven, Snails Pit, East Diamante Seamount, North West Rota Seamount, Alice Spring Field; **Manus Back-Arc Basin**: Edison Seamount, Vienna Woods, Desmos Cauldron, Pacmanus Complex; **North Fiji Back-Arc Basin**: White Lady, Mussel Valley; **Lau Back-Arc Basin**: Kilo Moana, Tow Cam, ABE, Tu'i Malila, Vai Lili, Hine Hina; **Woodlark Basin**: Maccauley Caldera; **Kermadec Arc**: Brothers Seamount, Rumble III seamount, Rumble V seamount, Calypso Vents. Figure modified from [17]. Vent fields compiled from [1,2,6,46,47].

“vent”, i.e. a single active structure/opening; “site”, i.e. a cluster of single vents (up to ~10 m in diameter); “field”, i.e. a cluster of sites (up to several hundred m in diameter); “group of fields”, i.e. a cluster of fields (within ~1 km in diameter) [46]. Fig. 7 shows a compilation of currently known vent fields along oceanic spreading ridges.

2.5 The basis for chemosynthesis at hydrothermal vents

While approximately half of all hydrothermal fluids are currently believed to be discharged from the seafloor as high-temperature focused flow through chimneys, about an equal amount mixes with cold seawater and is emitted from the seabed as low-temperature diffuse-flow, typically at temperatures that are measured in tens of degrees Celsius [7]. These diffuse fluids have precipitated their mineral load but, importantly, still contain high concentrations of dissolved methane, reduced sulfur compounds, and - as for ultramafic-hosted settings - hydrogen. It is mainly these chemicals that provide the necessary energy for free-living prokaryotes and symbiotic bacteria at hydrothermal vents [48-51].

3 Intermezzo: The 19th century roots of the symbiosis concept and its meaning in the 21st century

Most (if not all eukaryotes) live in close association with bacteria (and other microbes) that either inhabit certain tissues of their hosts, or live externally on their hosts in a close physiological relationship. These associations have been categorized in a variety of ways that indicate whether a particular association is beneficial (mutualistic), harmful (parasitic) or without any effect (commensal) to one or more of the organisms involved and are referred to as mutualism, parasitism, and commensalism, respectively [52]. To comprehensively describe all these forms of close associations between different organisms the concept of symbiosis was put forward in the late sixties of 19th century [53]. Throughout the modern symbiosis literature the German biologist Anton de Bary (1831-1888) is usually acknowledged as the one who coined the term ‘symbiosis’, however, this view is somewhat too simplistic and neglects equally important contributions of other contemporaneous scientists.

The concept of symbiosis has deep historical roots in the late 19th century and is intimately linked with the finding that lichens – traditionally considered a distinct class of plants – are in fact an association of fungi and algae [53]. The dual nature of lichens was independently discovered in the late 1860ies by the Swiss botanist Simon Schwendener (1829-1919) and Anton de Bary. However, it was Schwendener who in 1867 first reported on his findings [54-56]. Within the next decade it became evident that a term describing this dual relationship was needed as it could not be described as parasitism. Schwendener himself

viewed lichens in terms of ‘slavery’ by a fungal master over captured algae, others referred to lichens as a ‘consortium’ or even as a ‘communistic arrangement’ [57]. Therefore, in 1877, the German botanist Albert Bernhard Frank (1839-1900) (who later coined the term “mycorrhiza” to describe the association between fungi and root plants) wrote: “We must bring all the cases where two different species live on or in one another under a comprehensive concept which does not consider the role which the two individuals play but is based on the mere coexistence and for which the term *Symbiotism* [Symbiotismus] is to be recommended” [58]. Perhaps unaware of Frank’s publication, de Bary introduced the term ‘Symbiosis’ [Symbiose] only shortly after in an address entitled “The phenomena of symbiosis” delivered at a general meeting of the Association of German Naturalists and Physicians at Cassel in 1878. In his lecture which provided the essence for his subsequently published book de Bary stated: “Parasitism, mutualism, lichenism etc. are each special cases of that one general association for which the term *symbiosis* is proposed as the collective name.” Symbiosis is the phenomenon in which ” differently named organisms live together” [59,60]. Clearly, both Frank and de Bary basically describe the same concept, and the terms they proposed, *Symbiotism* and *Symbiosis*, are semantically identical. Both their definitions specify a close physical (and/or metabolic) association between differently named organisms (usually different species) and do not include a judgement as to whether the two symbionts benefit or harm each other. Thus, Frank and de Bary should equally be acknowledged for their contributions to the symbiosis concept while it was both Schwendener and de Bary who first described non-parasitic associations.

Even though Frank and de Bary specified symbiosis as a neutral term and although de Bary explicitly included parasitism in his general definition the semantic meaning of symbiosis changed towards a mutually benefiting association in the early 20th century [52,61]. Today, symbiosis has two different meanings: Frank and de Bary’s classical one and a “modern” one restricted to the phenomenon of mutualism. Thus, in the 21st century there is still no clear and universally agreed definition of symbiosis [62]. However, as the mechanisms leading to the establishment of mutually benefiting or parasitic associations are often similar on the molecular level [63] and as formerly parasitic associations may evolve into beneficial relationships it makes little sense to assign symbiosis strictly to mutually benefiting associations. Instead mutualism, parasitism, and commensalism should be regarded as different phenomena of symbiosis as was originally suggested by Frank and de Bary. However, old habits are likely to die hard.

4 Deep-sea hydrothermal vents – chemosynthesis based ecosystems

Unlike all other major ecosystems on Earth, which are driven by photosynthesis, hydrothermal vent ecosystems are based on chemosynthesis. In *sensu stricto* chemosynthesis refers to the capability of bacteria and archaea to use the energy of inorganic reduced chemical compounds to synthesize biomass from CO₂. These organisms are referred to as chemo-litho-autotrophs or short chemoautotrophs. In *sensu lato* chemosynthesis also includes those microbes that use organic methane as an energy and carbon source to build up biomass [48,64,65]. These organisms are referred to as methanotrophs and belong to the large group of chemo-organo-heterotrophs. However, unlike methanotrophs all other chemo-organo-heterotrophs are not considered chemosynthetic. Nevertheless, the discovery that C₂-C₄ hydrocarbons, i.e. ethane, propane, and butane, are abiogenically produced at ultramafic-hosted hydrothermal vents [34] should expand the concept of chemosynthesis to include those chemo-organo-heterotrophs that use abiogenically produced hydrocarbons as an energy and carbon source. Even though based on chemosynthesis hydrothermal vent ecosystems are not independent of photosynthesis (as is often wrongly argued). Many chemosynthetic prokaryotes, most protists, and all metazoans found at vents are obligate aerobes, i.e. they use and depend on oxygen for respiration. Clearly, the wealth of dissolved oxygen in the deep-sea is ultimately derived from photosynthesis in the oceans euphotic zones and from photosynthesis on land.

Although some vent animals rely on free-living chemosynthetic prokaryotes as their primary source of carbon, vent invertebrates that dominate the biomass of the communities have gone a step further and rely on symbiotic chemosynthetic bacteria. Both partners are inferred to benefit nutritionally from these symbioses. The host facilitates excess to the substrates that are necessary for chemosynthetic metabolism (e.g. reduced sulfur compounds, methane, oxygen, CO₂). In exchange, the bacterial symbionts fix carbon that supports the growth and maintenance of host biomass [64,65]. Primary production by chemosynthetic bacterial symbionts contributes considerably to the biogeochemical cycling of carbon and substrates at hydrothermal vents [64]. Thus, chemosynthetic symbionts are part of the manifold interactions between the lithosphere and biosphere at seafloor spreading centers.

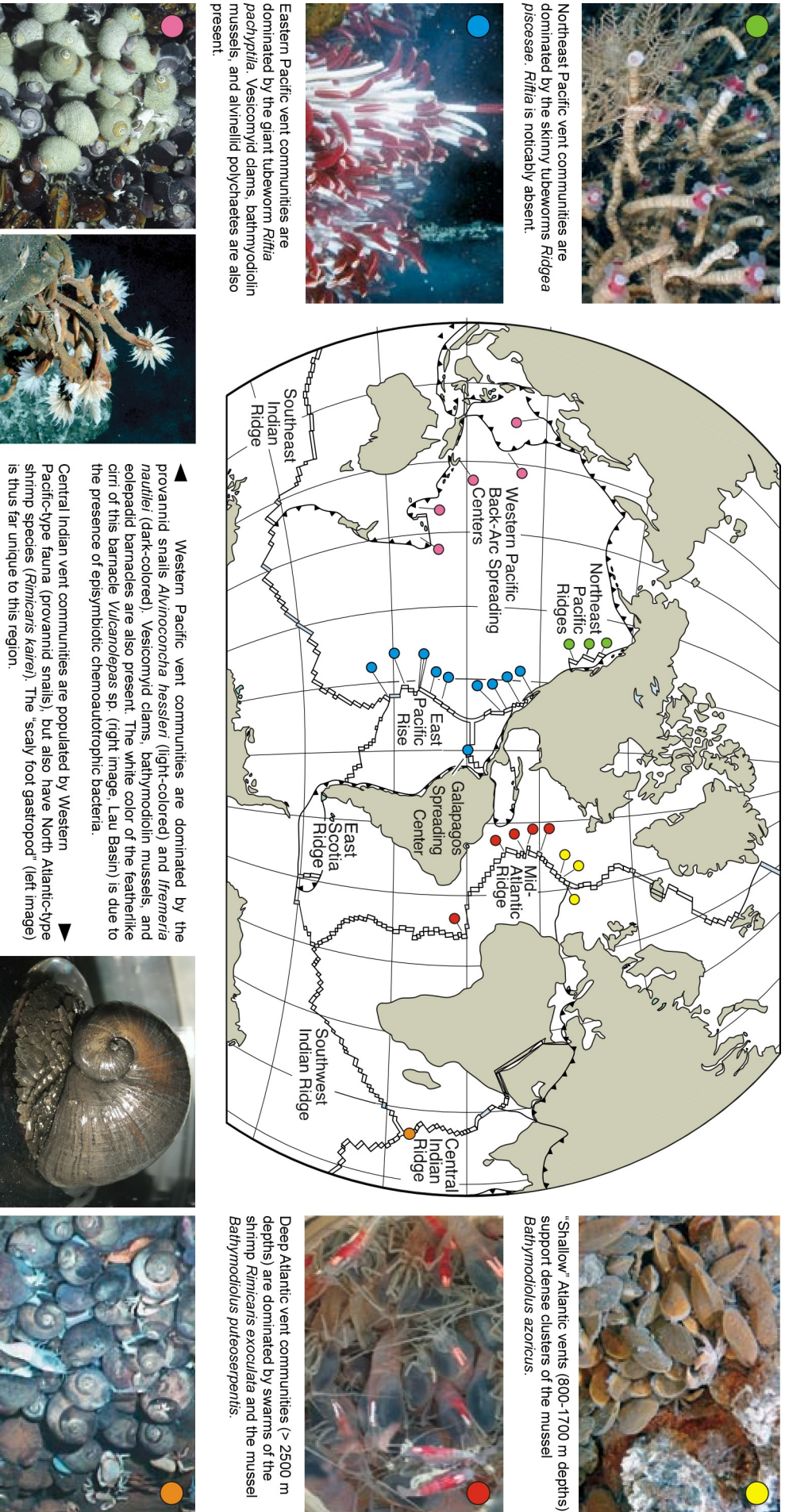


Fig. 8. Biogeography of hydrothermal vent invertebrates hosting chemosynthetic symbiotic bacteria. To date, there are six distinct biogeographic regions as indicated by colored circles. Green - Northeast Pacific Ridges; Blue - East Pacific Rise; Pink - Western Pacific back-arc spreading ridges; yellow - Mid-Atlantic Ridge near the Azores; red - deep (> 2500 m) Mid-Atlantic Ridge; orange - Indian Ocean Ridges. Figure modified from [66] based on figures and images provided in [7,49,67].

Table 3. Invertebrate and protist taxa hosting chemosynthetic bacterial symbionts

Phylum	Common name	Symbiont location			Habitat	type
		Tissue	Cell			
“PROTISTA”						
Excavata						
Euglenozoa	euglenid	cell surface	epi		cs	c
Chromalveolata						
Alveolata: Ciliophora	ciliate	cytoplasm cell surface	endo epi	intra	hv sw,rs	c
METAZOA						
Porifera						
Demospongiae: Cladorhizidae	sponge	skeletal matrix	endo	extra	hv,cs	m
Nemata						
Desmodorida: Desmodoridae: Stilbonematinae	nematode	cuticle	epi		rs	
Monhysterida: Siphonolaimidae	nematode	gut lumen	endo	extra	rs	c
Mollusca						
Bivalvia: Protobranchia: Solemyidae	clam	gills	endo	intra	hv,cs,wf,rs	c
Bivalvia: Heterodonta: Lucinidae	clam	gills	endo	intra	hv,vs,wf,rs	c
Bivalvia: Heterodonta: Thyasiridae	clam	gills	endo	intra	hv,vs,wf,rs	c
Bivalvia: Heterodonta: Vesicomidae	clam	gills	endo	intra	hv,cs,wf	c
Bivalvia: Pteriomorpha: Mytilidae	mussel	gills	endo	intra	hv,cs,wf,sw	c/m
Gastropoda: Provannidae	snail	gills	endo	intra	hv	c
Gastropoda: Peltospiridae	snail	esophagus operculum	endo epi	intra extra	hv	
Gastropoda: Lepetodrilidae	limpet	gills	epi		hv	c
Annelida						
Polychaeta: Alvinellidae	worm	dorsal surface	epi		hv	c
Polychaeta: Siboglinidae	tubeworm	trophosome	endo	intra	hv,cs,wf,rs	c
Oligochaeta: Tubificidae	oligochaete	subcuticular	endo	extra	rs	c
Arthropoda						
Crustacea: Alvinocaridae	shrimp	exoskeleton	epi		hv	c

Abbreviations: c, chemoautotroph; m, methanotroph; cs, cold seep; hv, hydrothermal vent; rs, reducing sediment; sw, sunken wood; wf, whale fall. Table based on information provided in [64,65,68-74].

The ubiquity of chemosynthetic symbioses at hydrothermal vents was soon recognized. Subsequently, chemosynthetic symbioses were intentionally searched for and found in other habitats similar to hydrothermal vents that were characterized by reducing conditions. Coastal, intertidal, and subtidal reducing sediments were the first non-vent habitats to be investigated [65]. The discovery of cold seeps in 1984 – seven years after hydrothermal vents were discovered – revealed faunal communities very similar to vent communities [4,69,70]. Whale carcasses found on the seafloor in 1989 also uncovered abundant fauna relying on chemosynthetic bacterial symbionts and thus further expanded the spectrum of chemosynthesis-based marine habitats [71]. More recently, sunken wood such as shipwrecks and trees discharged into the coastal ocean by rivers and mudslides, as well as debris from marsh and mangrove plants or kelp falls have been recognized to support chemosynthetic faunal communities [75-77]. All these environments are characterized by elevated methane

and / or hydrogen sulfide concentrations and share similar fauna hosting chemosynthetic symbionts. To date chemosynthetic bacteria are known to associate with invertebrates from five metazoan phyla, i.e. sponges, nematodes, mollusks, annelids, and arthropods. [65]. Besides, protists have also been reported to host chemosynthetic bacteria; however, these associations remain clearly understudied. Table 3 lists invertebrate and protist taxa known to host chemosynthetic bacteria.

Invertebrate hosts harbor their bacterial partners either intracellularly or extracellularly as endosymbionts or externally as episymbionts. Whereas intracellular endosymbiotic bacteria are housed within cytoplasmic vacuoles of specialized cells referred to as “bacteriocytes”, episymbiotic bacteria are typically attached to the surfaces of their hosts [64,65]. Dual or multiple physiologically diverse endosymbionts can occur in some invertebrate hosts and both endo- and episymbionts can be associated with one and the same host.

4.1 Hydrothermal symbioses

Within 30 years of hydrothermal vent research more than 500 mainly metazoan species have been described from deep-sea hydrothermal vents around the world. By December 2006, the species list held 551 species belonging to twelve major metazoan phyla [68]. And new vent species are still being described at a rate of nearly two per month [49]. 83% of hydrothermal vent species and 45% of vent genera are endemic to hydrothermal vents. These values far exceed those found anywhere else in the marine environment [78]. Among described vent animals chemosynthetic bacteria are known to be associated with invertebrates from four metazoan phyla, i.e. sponges, mollusks, annelids, and arthropods (Table 4). Fig. 8 gives a biogeographic perspective on predominate hydrothermal vent invertebrates hosting chemosynthetic symbiotic bacteria.

4.1.1 Vent invertebrates with endosymbiotic bacteria

The star among hydrothermal vent symbioses and the most and best studied symbiont-bearing vent invertebrate is clearly the giant tubeworm *Riftia pachyptila* (Annelida: “Polychaeta”: Siboglinidae) (Fig. 8). *R. pachyptila* and all other siboglinid tubeworms described to date (Table 4) lack a mouth and a digestive system and depend completely on their endosymbiotic sulfur-oxidizing chemoautotrophic bacteria. The symbionts reside within a lobular and highly vascularized organ (the trophosome) that spans the interior of the animal’s body and functions specifically to house the bacteria. The host absorbs hydrogen sulfide, oxygen, and CO₂ through its well-irrigated plume and transports these substrates via its vascular system. For H₂S and O₂ transport the tubeworms have evolved special

hemoglobins that bind hydrogen sulfide and oxygen reversibly with high affinity at independent sites on the protein. This mechanism allows them to transport high concentrations of sulfide through their bodies without experiencing its toxic effects [7,49,64,65].

Among vent bivalves (Mollusca: Bivalvia) endosymbiotic bacteria have been found in clams of the genera *Calyptogena* (Vesicomidae), *Thyasira* (Thyasiridae), and *Acharax* (Solemyidae), and in mussels of the genera *Bathymodiolus* and *Gigantidas* (both Mytilidae)

Table 4. Hydrothermal vent invertebrates known to be associated with symbiotic bacteria

Higher ranking taxa		symbiosis	Geographic distribution*	Publications ^a					
Subordinate taxon	Genus			Title search			Topic search		
				1 ^b	2 ^c	Tot	1 ^b	2 ^c	Tot
<i>Porifera: Demospongiae</i>									
Cladorhizidae	<i>Cladorhiza</i>	epi	EP, MA,cs	1	0	1	5	1	6
<i>Annelida: "Polychaeta"</i>									
Siboglinidae	<i>Riftia</i>	endo	EP	59	71	130	240	229	469
	<i>Lamellibrachia</i>	endo	NP,WP,cs,sw	14	1	15	59	40	99
	<i>Ridgeia</i>	endo	NP,EP	18	1	19	39	24	63
	<i>Tevnia</i>	endo	EP	1	1	2	26	8	34
	<i>Oasisia</i>	endo	EP	1	0	1	10	2	12
	<i>Arcovestia</i>	endo	WP	1	0	1	4	1	5
	<i>Alaysia</i>	endo	WP	1	0	1	2	1	3
	<i>Siphonobrachia</i>	endo	WP	1	0	1	1	2	3
Alvinellidae	<i>Alvinella</i>	epi	EP	43	1	44	163	32	195
	<i>Paralvinella</i>	epi	EP,NP,WP	18	0	18	79	8	87
<i>Mollusca: Bivalvia</i>									
Vesicomidae	<i>Calyptogena</i>	endo	EP,NP,WP,cs,wf	64	5	69	175	111	286
Mytilidae	<i>Bathymodiolus</i>	endo	CI,EP,MA,PA,WP,cs	76	13	89	168	104	272
Thyasiridae	<i>Thyasira</i> ^d	endo	MA,cs	12	5	17	61	34	95
Solemyidae	<i>Acharax</i>	endo	WP,cs	4	0	4	13	5	18
Mytilidae	<i>Gigantidas</i>	endo	WP	0	0	0	2	0	2
Lucinidae	<i>Bathyaustriella</i> ^c	endo	WPR	1	0	1	1	0	1
<i>Mollusca: Gastropoda</i>									
Lepetodrilidae	<i>Lepetodrilus</i>	epi	EP,MA,NP,WP	7	0	7	39	7	46
Provannidae	<i>Ifremeria</i>	endo	WP	1	4	5	4	8	12
	<i>Alvinoconcha</i>	endo	CI,WP	0	0	0	1	1	2
Peltospiridae	scaly gastropod	endo, epi	CI	1	0	1	1	0	1
<i>Arthropoda: Crustacea</i>									
Alvinocarididae	<i>Rimicaris</i>	epi	CI,MA	25	0	25	99	23	122
Eolepadidae	<i>Vulcanolepas</i>	epi	WP	0	0	0	2	0	2

* If a genus occurs also at non-vent reducing environments, these environments are listed without their geographic location. ^a Publications as of January 2008 using ISI Web of Knowledge (v.4.0, Thomson Scientific). Numbers refer to the number of publication entries in the ISI databases. ^b search with genus only excluding words containing *symb**, ^c search with genus including words containing *symb**, ^d according to [79] and C. Borowski (MPI for Marine Microbiology, Bremen – personal communication). ^e symbionts have not yet been reported but are likely obligate within the Lucinidae [80]. Model representatives of vent invertebrate fauna are in bold. Abbreviations: CI, Central Indian Ridge; EP, East Pacific Rise; MA, Mid-Atlantic Ridge; NP, Northeast Pacific Ridges; PA, Pacific-Antarctic Ridge; WP, Western Pacific Ridges, cs, cold seeps; sw, sunken wood; wf, whale-falls. Table based on information provided in [64,65,68-71].

[64,65,79,81,82]. In all of these bivalves endosymbiotic bacteria reside within bacteriocytes in the gill epithelium. Whereas the endosymbionts of *Thyasira*, *Acharax*, and *Gigantidas* are not well characterized, *Calyptogena* and *Bathymodiolus* symbioses have received considerable scientific interest. Nevertheless, these symbioses remain understudied in comparison to the *Riftia* symbiosis (Table 4).

In hydrothermal systems of the Western Pacific back-arc spreading ridges two large endosymbiont containing snails, *Alviniconcha hessleri* and *Ifremeria nautilei* (Mollusca: Gastropoda: Provannidae), dominate the ecosystem (Fig. 8). Like the endosymbiont-containing vent bivalves they harbor sulfur-oxidizing chemoautotrophs in their gills [4,10]. With four phylogenetically distinct symbionts, *I. nautilei* hosts the most diverse endobacterial population known to date from a hydrothermal vent invertebrate (N. Dubilier, MPI for Marine Microbiology – personal communication).

Unlike all other endosymbiont containing vent mollusks which house their symbionts within their gills, the “scaly foot gastropod” (Mollusca: Gastropoda: Peltospiroidae) which has to date only been found on the Central Indian Ridge (Fig. 8) harbors sulfur-oxidizing bacteria within cells of its enormously enlarged esophageal gland. Another morphological adaptation makes this snail unique among vent invertebrates. Its operculum is modified into several hundred aligned scales composed of dense layers of iron sulfides and covered with filamentous episymbiotic bacteria. It has been hypothesized that the iron sulfide plates, whose purpose is unknown, are in fact mineralized by the snail’s episymbionts. [7,64].

Associations between limpets belonging to the family Lepetodrilidae (Mollusca: Gastropoda) and bacteria seem to be an intermediate between epi- and endosymbioses. In *Lepetodrilus fucensis* bacteria are partially embedded in the gill epidermis and may be endocytosed or fed on by the host [65].

4.1.2 Vent invertebrates with episymbiotic bacteria

In contrast to siboglinid polychaetes, polychaetes of the family Alvinellidae (Annelidae: “Polychaeta”) have a fully functional digestive tract and may not depend on endosymbionts. Yet, they host a diverse episymbiotic community on their dorsal surfaces including large filamentous bacteria visible to the naked eye. Both trophic and sulfide-detoxifying roles have been suggested for these bacteria [4]. However, as hydrogen sulfide does essentially not occur as dissolved sulfide in alvinellid habitats but rather as non-toxic soluble iron sulfide clusters [83] there is no need for episymbiotic sulfide detoxification. Alvinellid polychaetes live inside organic tubes in close proximity to active chimneys and high-temperature fluids [7]. They

tolerate permanent body temperatures between 50 and 55°C as has been demonstrated for *Paralvinella sulfincola*, a close relative of the well-studied Pompeii worm *Alvinella pompejana*. These are the highest body temperatures ever demonstrated for a marine metazoan [49]. For a short period they may survive even higher temperatures. For example, *A. pompejana* was observed curling around a high-temperature probe for a few minutes while the probe simultaneously recorded 105°C [84]. Adaptations to this high-temperature habitat depleted in oxygen include well developed gills with short diffusion distances between the external seawater and the blood, and hemoglobins with extremely high oxygen affinity [4].

Episymbiotic bacteria are also associated with shrimp belonging to the family Alvinocarididae (Arthropoda: Crustacea: Decapoda) and barnacles of the family Eolepadidae (Arthropoda: Crustacea: Cirripedia). For example, the alvinocarid shrimp *Rimicaris exoculata* which lives in dense swarms on chimney walls along the Mid-Atlantic Ridge hosts episymbiotic bacteria on its external carapace, mouthparts, and the inner surfaces of its enlarged gill chamber [4,7,74]. These bacteria are morphologically and phylogenetically similar to the filamentous bacteria associated with *A. pompejana* [4,64,65,74]. Adult shrimp derive most of their carbon and nitrogen from their episymbionts [4]. A particular feature of vent shrimp is their photoreceptors. The “eyes” of *R. exoculata* are considered to have evolved into a broad ocular plate that forms part of the shrimp’s dorsal surface. The plate’s novel photoreceptors apparently do not form a distinct image. Instead, they are highly sensitive to dim light, perhaps an adaptation for detecting radiation from orifices of hot black smokers and for allowing the shrimp to orient along the chimney walls [4,7].

A recent addition of invertebrates hosting episymbiotic bacteria are carnivorous *Cladorhiza* sponges (Demospongiae: Poecilosclerida: Cladorhizidae) which are known to host methanotrophic bacteria but had not formerly been recognized to occur at hydrothermal vents [85-87].

4.1.3 Vent protists with symbiotic bacteria

In contrast to the many vent invertebrate symbioses recognized to date only one vent protozoan-bacteria symbiosis has been reported thus far. The ciliate *Fulliculinopsis* sp. (Chromalveolata: Alveolata: Ciliophora) harbors bacteria in its cytoplasm. However, the chemolithoautotrophic nature of these endosymbionts remains to be confirmed [88].

4.2 Non-vent marine chemosynthetic symbioses

Cold seeps, whale falls, sunken wood, and reducing sediments are similar to hydrothermal vent habitats in that they can release methane and hydrogen sulfide into their

environment. Thus, invertebrate-bacteria associations similar to those found at vents also occur in these habitats. Non-vent habitats have extended the list of marine chemosynthetic symbioses to include the metazoan phyla Nemata (= Nematoda) and Echinodermata (Table 3). Among the phyla known from hydrothermal vents, non-vent reducing environments far expand the bivalve families Solemyidae, Thyasiridae, Lucinidae, Vesicomidae, and Mytilidae. Annelid hosts include additional siboglinid tubeworms and also comprise the gutless oligochaetes (Annelida: Clitellata).

4.2.1 Cold seeps

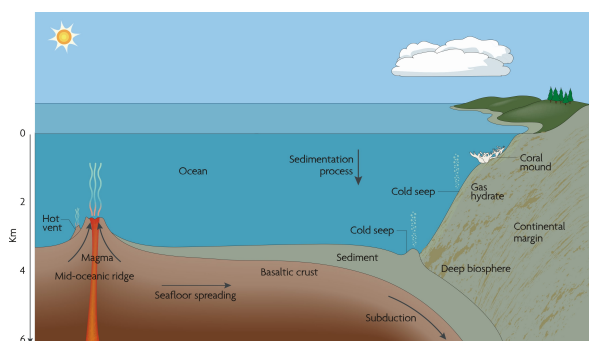


Fig. 9. Geological setting of cold seeps at an active margin. This cartoon shows a vertical section through oceanic and continental crust (from a mid-ocean ridge to plate subduction at a continental margin). Sinking particles form thick sediment piles on the ageing crust and on the margins. From [48].

Like hydrothermal vents, cold seeps are a result of plate tectonics. However, unlike hydrothermal vents which occur at mid-ocean and back-arc spreading ridges, i.e. where oceanic crust is formed, cold seeps are found at the opposite end of oceanic crust where it meets continental crust, i.e. at continental margins (Fig. 9). Due to the extended age of ocean seafloor at its outer edges, oceanic crust has accumulated a heavy layer of sediment here, usually several

kilometers thick. When this deposited sediment becomes compressed at continental margins as a result of subduction (active margin, Fig. 3) or because oceanic crust is forced toward the heavier continental crust at passive margins, subsurface pore fluids and gases are expelled, forming gas-hydrate deposits, gas chimneys, mud volcanoes, and diverse seep systems including hypersaline (brine) seeps, hydrocarbon seeps, oil and asphalt seeps, asphalt volcanoes, carbon dioxide seeps, and pockmarks [4,22,48,69,70]. Seep fluids are usually rich in methane and hydrogen sulfide which provide the energy for the chemosynthesis-based symbioses. However, unlike in vent ecosystems where these chemicals are of abiogenic (thermogenic) origin, they often are of biogenic (non-thermogenic) origin at cold seeps as a result of archaeal methanogenesis and bacterial sulfate reduction. However, abiogenic (thermogenic) methane can occur at seeps when buried organic matter is exposed to high temperature and pressure over time, for example at subduction zones, [64].

At the end of the millennium, 211 species were known from cold seeps of which one-third (61) belonging to 20 genera hosted symbiotic bacteria [69,70]. Of these only five species

belonging to three genera occurred both at hydrothermal vents and cold seeps: the siboglinid tubeworm *Lamellibrachia barhami*, the vesicomyid clam *Calyptogena pacifica*, and three species of bathymodiolin mussels (*B. adulooides*, *B. japonicus*, and *B. platifrons*). At the genus level, the solemyid clam *Acharax* was also shared between cold seeps and hydrothermal vents (13 symbiont-hosting genera were known back then from vents). Noticeably, clams are much more diverse at cold seeps and the tubeworms comprise different genera at vents and seeps (except for *L. barhami*). Thus, there is a great endemism at the species level at both seeps and vents but less endemism at the genus level [69,70]. This endemism among symbiont-bearing species is consistent with the fact that 83% of all species found at vents are endemic to vents. Only 6% of vent species are shared with cold seeps and another 11% are also recorded from non-vent/non-seep environments [78]. The similarities between the two habitats become more obvious at the family level with representatives belonging to the siboglinid tubeworms, solemyid, lucinid, thyasirid, and vesicomyid clams, as well as bathymodiolin mussels, and cladorhizid sponges (Table 4).

An interesting contribution of cold seeps to marine chemosynthetic symbioses are methanotrophic endosymbionts in the siboglinid tubeworm *Siboglinum poseidoni* (Annelida: “Polychaeta”) [89]. To date, all other known siboglinid tubeworms harbor exclusively chemoautotrophic endosymbionts. Among protists, a euglenid (Excavata: Euglenozoa) with episymbiotic sulfur-oxidizing chemoautotrophic bacteria is known from a seep site [90].

4.2.2 *Whale falls and sunken wood*

Baleen whales (Mammalia: Cetacea) attain body weights of 30-160 tons. The world population size of the 9 largest whale species has been estimated to comprise 1.4 million animals of which ~0.05% die each year [71]. This makes a total of ~70,000 whale carcasses that sink each year to the ocean floor. A sunken whale carcass provides a massive food fall to the normally organic-poor deep-sea floor. For example, the organic carbon input from a 40-t whale carcass to the underlying sediment is equivalent to that typically sinking from the euphotic zone to the abyssal sea in ~2000 years [71]. After removal of whale soft tissue by scavengers,

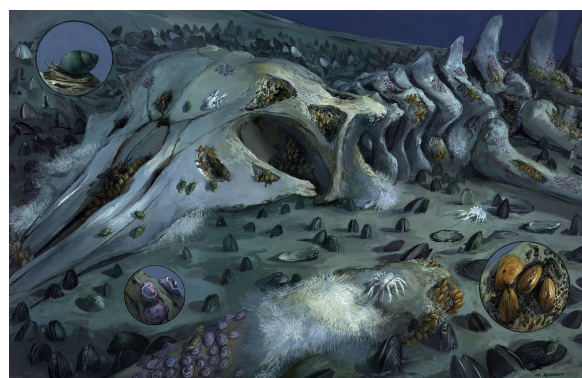


Fig. 10. Whale carcass habitat in its sulphophilic stage. Note the abundant bivalves half buried into the sediment as is typical for vesicomyid clams. Picture kindly provided by Craig Smith, artist Mike Rothman (<http://www.soest.hawaii.edu/oceanography>).

the lipid-rich whale bones (a 40-t whale carcass can hold 2000-3000 kg of lipids) provide an extremely abundant energy and carbon source for sulphate reducers. As a consequence there is a net production of hydrogen sulfide which diffuses into the underlying sediment and into the surrounding seawater. This subsequently provides the energy source for chemoautotrophic sulfur-oxidizers and the habitat for invertebrates depending on sulfur-oxidizing chemoautotrophic symbionts (Fig. 10). Due to the abundance of hydrogen sulfide and sulfur-based bacteria-invertebrate symbioses this stage of whale bone decay has been termed *sulphophilic* [71] but methane is also released during whale tissue decay, presumably by methanogenic archaea, and accumulates in the sediments underneath the carcass [91] thus fostering free-living and endosymbiotic bacterial methanotrophs. Lucinid, thyasirid, and vesicomid clams are often abundant as are bathymodiolin mussels (excluding the genus *Bathymodiolus*). Large whale skeletons can support chemoautotrophic communities for decades [71]. As with cold seeps and hydrothermal vents there is almost no species overlap between vents and whale carcasses except for the vesicomid clam *Calyptogena pacifica* which is in fact the only species found at all three habitats [69]. However, on the higher phylogenetic level, several symbiont-containing taxa (e.g. families) are shared (Table 4).

Decomposing sunken wood, debris from marsh and mangrove plants, and kelp falls also provide sulfide-rich habitats which often host bathymodiolin mussels (excluding the genus *Bathymodiolus*) [22,48,66,71,76,77]. A rather recent and anthropogenic addition which contributes to the abundance of sulfide-rich habitats on the ocean floor are wooden shipwrecks which have been continuously lost to the oceans since humans started to sail the oceans. For example, between 1971 and 1990 alone an estimated 3,000 wooden ships were wrecked [66].

4.2.3 Marine sediments

Except for the sites of seafloor-spreading, i.e. at mid-ocean and back-arc spreading ridges the ocean seafloor is usually covered with sediments which typically increase in thickness towards the continental margins as a result of sedimentation processes over the tens of millions of years of seafloor spreading (Fig. 9). In coastal, intertidal, and subtidal sediments where input of organic matter is high, its decomposition by anaerobic sulfate reducing bacteria produces substantial amounts of hydrogen sulfide in areas where these sediments become anoxic [73,74]. The water overlying the sediment is generally well oxygenated as is the upper (oxic) sediment zone (which usually comprises only a few millimeters) before the sediment becomes suboxic and finally anoxic (and sulfidic). Invertebrates hosting sulfur-

oxidizing chemoautotrophic bacteria are frequently found in these sediments. They all use specialized behavioral, anatomical or physiological mechanisms to spatially or temporally bridge anoxic (sulfidic) and oxic zones [65].

Clams belonging to the families Solemyidae, Lucinidae, Thyasiridae, and Vesicomidae (Mollusca: Bivalvia) which have been reported from deep-sea hydrothermal vents, cold seeps, whale falls, and sunken wood can also be found in inter- and subtidal reducing sediments. Such sediments are also home to a group of annelid worms which have been termed gutless oligochaetes (Annelida: Oligochaeta: Tubificidae). Like siboglinid tubeworms (Annelida: "Polychaeta") gutless oligochaetes lack a mouth, gut, and anus but are unique among annelid worms in having a reduced nephridial excretory system [92]. Gutless oligochaetes have also been reported from muds in 100-400 m water depth indicating that they occur in many more environments than presently known [92] but are to date unknown from hydrothermal vents, cold seeps, whale falls or sunken woods. These worms are most dominant at 5-15 cm below the sediment surface, i.e. in anoxic (sulfidic), at best suboxic zones [92]. However, highly sulfidic conditions ($> 500 \mu\text{M}$) are usually avoided as are purely oxic zones [93]. The preference of gutless oligochaetes for these conditions is due to a symbiosis with gammaproteobacterial sulfur-oxidizing chemoautotrophic bacteria and at least two other phylogenetically distinct bacteria belonging to either the Alpha-, Gamma- or Deltaproteobacteria or the spirochaetes [92,93]. As many as six different co-occurring bacterial symbionts have been reported. The symbiotic bacteria reside extracellularly in a multicellular layer just below the thin cuticle of the worms, referred to as the symbiotic region [92]. The extracellular location of these bacterial endosymbionts distinguishes the oligochaete-bacteria association from most other invertebrate-bacteria associations from chemosynthetic environments in which the bacteria occur usually intracellularly [65].

Reducing sediments are also inhabited by two morphologically and phylogenetically distinct groups of symbiont-bearing nematode worms: the Stilbonematinae (Nemata: Desmodorida: Desmodoridae) hosting episympiotic chemoautotrophic bacteria and the mouthless Siphonolaimidae (Nemata: Monhysterida) hosting endosymbiotic chemoautotrophic bacteria [72-74]. Both host groups frequently share the same habitats and occur in high abundance in shallow intertidal and subtidal sediments. Ciliates (Chromalveolata: Alveolata: Ciliophora) belonging to the genus *Kentrophoros* and inhabiting sheltered marine sands several centimeter beneath the surface have been reported to host sulfur-oxidizing chemoautotrophic episympiotic bacteria [74].

4.3 Phylogeny of marine chemosynthetic symbionts

In contrast to the wide diversity of host taxa, chemosynthetic symbionts exhibit a relatively narrow phylogenetic range. Based on 16S rRNA sequences, endosymbiotic bacteria fall primarily in the Gammaproteobacteria while episymbiotic bacteria consistently cluster within the Epsilonproteobacteria [64,65]. Chemosynthetic symbionts of several higher-ranking host taxa fall within several well-supported monophyletic clades (Fig. 11). Distinct clades comprise the endosymbionts of siboglinid tubeworms (Annelida: “Polychaeta”: Siboglinidae), endosymbionts of vesicomylid clams (Mollusca: Bivalvia: Vesicomylidae), chemoautotrophic endosymbionts of bathymodiolin mussels, methanotrophic endosymbionts of bathymodiolin mussels (Mollusca: Bivalvia: Mytilidae), and most endosymbionts of lucinid clams (Mollusca: Bivalvia: Lucinidae). gammaproteobacterial endosymbionts of the gutless oligochaetes (Annelida: Oligochaeta) as well as endo- and episymbionts of the phylogenetically distinct nematode worms also form a monophyletic clade [64,65,72]. Another monophyletic clade comprising symbionts of phylogenetically distinct host taxa is formed by epsilonproteobacterial ectosymbionts of alvinellid polychaetes (Annelida: “Polychaeta”) and alvinocarid shrimp (Arthropoda: Chrustacea: Decapoda). In contrast, symbionts of solemyid and thyasirid clams appear to be paraphyletic as they are scattered throughout the tree. Some symbionts of lucinid clams also do not cluster with their otherwise monophyletic relatives.

4.4 Energy sources, energy conservation, and carbon assimilation

The only energy and electron sources that have to date been recognized to fuel chemosynthetic marine symbioses are reduced sulfur compounds (H_2S , S^0 , and $\text{S}_2\text{O}_3^{2-}$) and methane. The free energy stored in these compounds is conserved by electron transport along a respiratory chain thereby creating a proton-motive force by proton translocation across the membrane which ultimately drives ATP synthesis and other crucial functions such as reverse electron transport for the generation of reducing equivalents. Electrons transported along the respiratory chain are eventually transferred to a terminal acceptor, usually oxygen although alternative electron acceptors such as nitrite are used by some sulfur-oxidizing symbionts under anaerobic conditions [64,65]. ATP and NAD(P)H generated as a result of energy conservation are subsequently used for carbon assimilation and other biosynthetic pathways. Sulfur-oxidizing symbionts build up biomass by fixing inorganic CO_2 , i.e. they are chemoautotrophs whereas methane-oxidizing symbionts assimilate organic formaldehyde derived from the oxidation of methane and are thus in *sensu stricto* chemoheterotrophs.

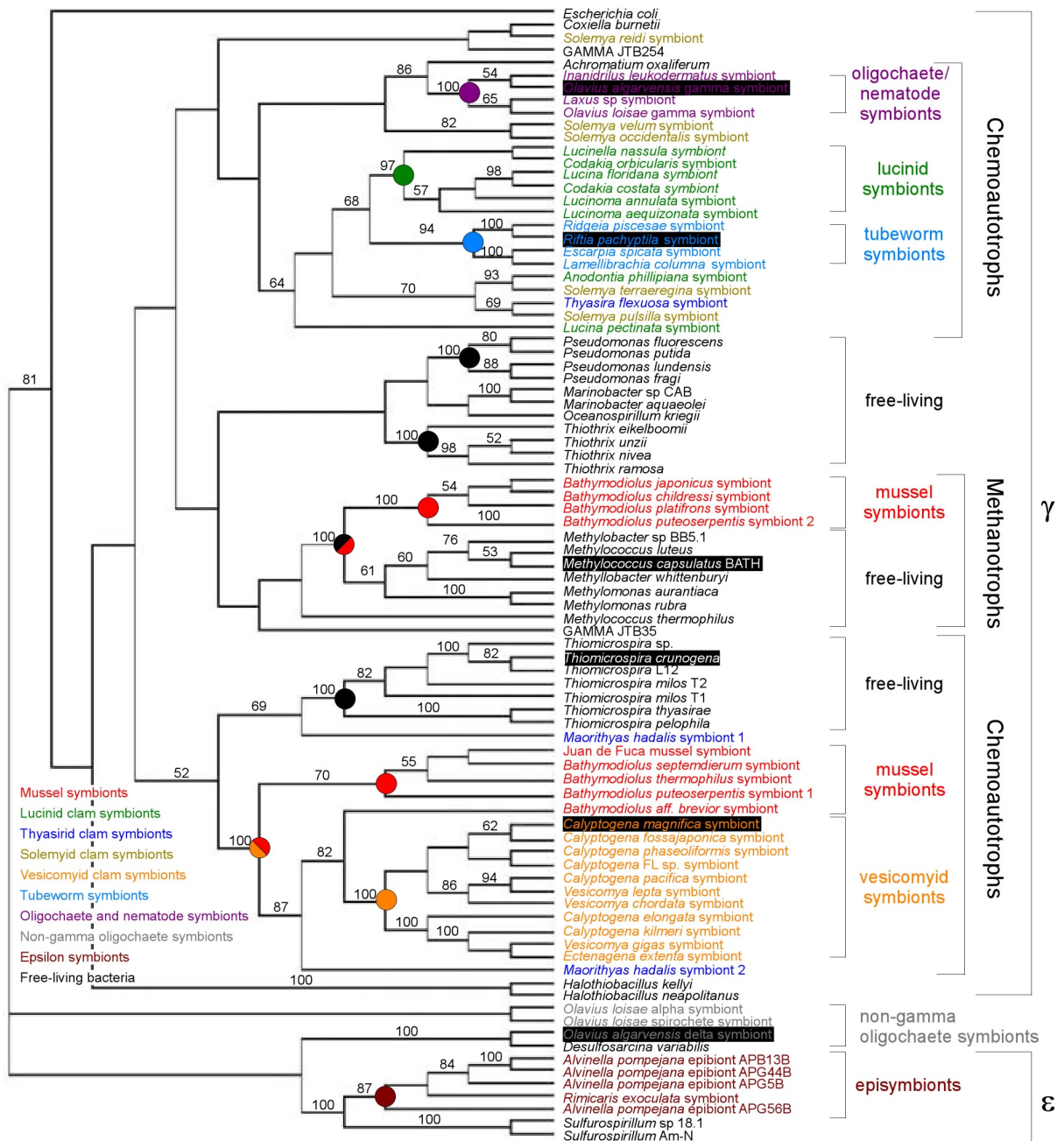


Fig. 11. Phylogenetic tree of chemosynthetic symbiotic and free-living bacteria. The tree is based on nearly full length 16S rRNA sequences (1456 bp). The figure shows a consensus of 46 most parsimonious trees using the maximum parsimony algorithm. Bootstrap values < 50% are not shown. Colored nodes indicate well-supported monophyletic clades. Bacteria whose genomes have been sequenced are indicated by black boxes (*R. pachyptila* symbiont = “*Candidatus* Endoriftia persephone”; *C. magnifica* symbiont = “*Candidatus* Ruthia magnifica”). From [65], modified including information from [94-98].

4.4.1 Sulfur-oxidizing chemoautotrophs

Recently, the genomes of several sulfur-oxidizing chemoautotrophic symbionts have become available (Fig. 11) from the deep-sea hydrothermal vent invertebrate hosts *Calyptogena magnifica* [96], *Calyptogena okutanii* [99], and *Riftia pachyptila* [98,100], as well as the symbionts of the sediment-dwelling gutless oligochaete *Olavius algarvensis* [94]. Furthermore the free-living sulfur-oxidizer *Thiomicrospira crunogena* XCL-2, originally

isolated from a deep-sea hydrothermal vent and a close relative of the *Calyptogenia/Bathymodiolus* symbiont cluster (Fig. 11) has also been sequenced [95]. These genomes yielded important insights into the pathways of symbiotic sulfur oxidation, energy conservation, and carbon assimilation which had only incompletely been understood up to this point.

Even though all sulfur-oxidizing endosymbionts fall within the Gammaproteobacteria they do not use a common pathway of sulfur oxidation most likely as a result of horizontal gene transfer. This is consistent with the fact that similar pathways are also used by phylogenetically unrelated sulfur-oxidizing bacteria. In fact, the group of sulfur-oxidizing bacteria, formerly referred to as the “colorless sulfur bacteria” is extremely heterogeneous [101-103]. Yet, all sulfur-oxidizing symbionts sequenced to date possess the key enzyme of the Calvin-Benson-Bassham cycle for CO₂ assimilation, ribulose-1,5-phosphate carboxylase/oxygenase (RuBisCO) which is not surprising as their chemoautotrophic potential was inferred from previous RuBisCO enzyme activity assays [65]. However, both the *R. pachyptila* endosymbiont “*Ca. Endoriftia persephone*” and the *C. magnifica* endosymbiont “*Ca. Ruthia magnifica*” lack two genes of the Calvin cycle [96,98,100]. Surprisingly, the “*Ca. E. persephone*” metagenome and proteome uncovered that this symbiont uses the reductive tricarboxylic acid cycle for CO₂ fixation in addition to the Calvin cycle [98,100]. The genes and enzymes involved in sulfur metabolism and carbon fixation of as yet sequenced chemoautotrophic sulfur-oxidizing endosymbionts are listed in Table 5. Fig. 12 gives a schematic overview of the different sulfur oxidation pathways in both symbiotic and free-living bacteria.

The free-living chemolithoautotroph *Thiomicrospira crunogena* XCL-2 for example possesses a full set of *sox* genes coding for the fully functional **Sox (sulfur oxidation) system** (Fig. 7). This system completely oxidizes H₂S, S⁰, SO₃²⁻, and S₂O₃²⁻ to sulfate [95]. This system is only partially present in the symbiont genomes, all of which lack the essential sulfur dehydrogenase (Sox[CD]₂) [96,99,100,104]. Without Sox(CD)₂ only two electrons are transferred to the respiratory chain, thus H₂S and S₂O₃²⁻ are only oxidized to S⁰ while the oxidation of SO₃²⁻ to SO₄²⁻ is unaffected [105,106].

Instead of the Sox system the *R. pachyptila* and the *C. okutanii* endosymbionts “*Ca. Endoriftia persephone*” and “*Ca. Vesicomysocius okutanii*”, respectively, possesses a full set of *dsr* genes coding for the fully functional **Dsr (dissimilatory sulfite reduction) system** (Fig. 12). This system was first described from sulfate reducing bacteria but is now known to operate in both the reductive and oxidative direction, i.e. it catalyzes both H₂S oxidation and SO₃²⁻ reduction. The Dsr system is also present in the *C. magnifica* endosymbiont “*Ca. R. magnifica*” and appears to be present in the gamma symbionts of *O. algarvensis* although some of the genes are missing in the former and some may be missing in the latter. Clearly, because sulfur dehydrogenase (Sox[CD]₂) is missing in these symbionts an alternative pathway is necessary for the oxidation of elemental sulfur. This is accomplished by dissimilatory sulfite reductase (DsrAB) which oxidizes H₂S to SO₃²⁻ and perhaps by an

Table 5. Predicted sulfur oxidation and carbon fixation pathways in chemoautotrophic symbionts

Gene	Enzyme	Reaction	Location	“R.m”	“V.o”	“E.p”	O.a γ1 & γ3	T.c
Sulfur oxidation								
sox gene cluster		S _{red} →SO ₄ ²⁻	membrane	partial ^a	partial ^a	partial ^{a,b,d,g}	partial ^{a,c,d}	+
<i>soxCD</i>	sulfur dehydrogenase	S _{red} →S _{ox} +2e ^{-c}	membrane	-	-	-	-	+
dsr gene cluster				partial ^f	+	+	+ ^d	-
<i>dsrAB</i>	dissimilatory sulfite reductase	H ₂ S→SO ₃ ²⁻	cytoplasm	+	+	+ ^g	+	-
<i>dsrC</i>	intracellular sulfur oxidation protein	S _{red} [?] →S _{ox} [?]	cytoplasm	+	+	+	?	-
<i>dsrK</i>	heterodisulfide reductase-like	S ₂ ²⁻ →S ²⁻	membrane-associated	+	+	+	+	-
<i>dsrP</i>	polysulfide reductase-like	S _n ²⁻ →S ²⁻	membrane	+	+	+	?	-
<i>hdrA</i>	heterodisulfide reductase	S ₂ ²⁻ →S ²⁻	membrane	-	-	+	-	-
apr gene cluster								
<i>aprBA</i>	dissimilatory APS reductase	SO ₃ ²⁻ →APS	cytoplasm	+	+	+	+	-
<i>sat</i>	ATP sulfurylase	APS→SO ₄ ²⁻	cytoplasm	+	+	+ ^h	+	-
other genes								
<i>sqr</i>	sulfide:quinone (oxido)reductase	H ₂ S→S ⁰	membrane	+	+	-	-	+
<i>fccAB</i>	flavocytochr. c / sulfide dehydrog.	H ₂ S→S ⁰	?	-	-	+ ^g	+	-
<i>sorAB</i>	sulfite:acceptor oxidoreductase	SO ₃ ²⁻ →SO ₄ ²⁻	cytoplasm	-	-	-	-	-
Carbon assimilation								
Calvin Cycle				partial ^{i,j}	+	partial ^{i,k}	+	+
<i>ccb</i>	RuBisCO		cytoplasm	II	II	II	I	I, II
Reductive TCA cycle						+		

Abbreviations: R.m, “*Ca. Ruthia magnifica*”; V.o, “*Ca. Vesicomysocius okutanii*”; E.p, “*Ca. Endoriftia persephone*”; O.a, *Olavius algarvensis* symbiont; T.c, *Thiomicrospira crunogena*; ^a sulfur dehydrogenase SoxCD missing; ^b SoxY missing; ^c SoxXA missing; ^d according to [104]; ^e without sulfur dehydrogenase (SoxCD) only two electrons can be transferred (H₂S→S⁰, S₂O₃²⁻→S⁰, SO₃²⁻→SO₄²⁻); ^f *dsrJNRS* are missing; ^g not found in the *Riftia* proteome; ^h referred to as *sopT*; ⁱ sedoheptulose-1,7-bisphosphatase missing; ^j ribose 5-phosphate isomerase missing; ^k fructose-1,6-bisphosphatase missing. Table compiled using information provided in [94-100,104]

intracellular sulfur oxidation protein (DsrC) which has, however, not yet been sufficiently characterized [100]. The *dsr* gene cluster also codes for proteins similar to a heterodisulfide reductase (DsrK) and a polysulfide reductase (DsrP) which catalyze the conversion of these sulfur compounds to hydrogen sulfide. These genes are present in the symbiont genomes [96,99,100,104]. Noticeably, the fact that sulfur-oxidizing symbionts simultaneously harbor a Dsr system and a Sox[CD]₂ lacking Sox system contradicts the formerly generalized observation that chemoautotrophic bacteria that lack *soxCD* genes do not harbor *dsr* genes [106].

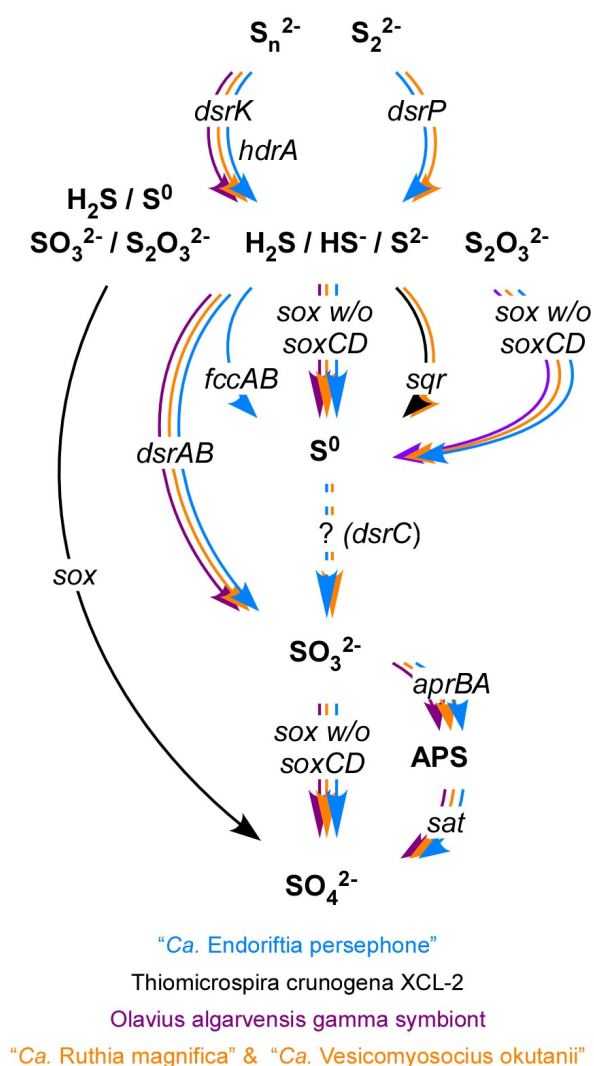


Fig. 12. Predicted sulfur oxidation pathways in symbiotic and free-living chemoautotrophic bacteria. Endosymbiotic bacteria use diverse sulfur oxidation systems. In contrast, their closest free-living relative uses essentially just one system for the complete oxidation of different sulfur species. For enzyme designation refer to **Table 5**. Figure inspired by [107] and based on information provided in [95-100,104-106].

All symbionts use the **Apr (adenosine-5'-phosphosulfate reductase) system** to oxidize SO_3^{2-} to SO_4^{2-} (Fig. 12). Like the Dsr system the Apr system also operates in reductive and oxidative directions and was initially described from sulfate reducing bacteria. In the oxidative Apr pathway APS reductase (AprBA) catalyzes the AMP-dependent oxidation of sulfite to adenosine-5'-phosphosulfate (APS) which is further oxidized by ATP sulfurylase (Sat) to sulfate thereby yielding ATP by substrate-level phosphorylation [107,108]. Besides these three well characterized sulfur oxidation systems additional enzymes are present which are involved in the oxidation of H_2S to S^0 (Fig. 12). Whereas "*Ca. E. persephone*" possesses a flavocytochrome c / sulfide dehydrogenase (FccAB), "*Ca. R. magnifica*" and "*Ca. V. okutanii*" employ a sulfide:quinone (oxido)reductase (Sqr) which is also present in the free-living *T. crunogena* XCL-2.

4.4.2 Methane-oxidizing chemoheterotrophs

In contrast to sulfur-oxidizing symbionts no methane-oxidizing symbiont has been sequenced to date. Nevertheless, the genomes of several free-living methylotrophs have recently become available comprising representatives of the Alpha-, Beta-, and Gammaproteobacteria and including the type X methanotroph *Methylococcus capsulatus* (Bath) [97,109-111]. *M. capsulatus* is a close relative of free-living and symbiotic type I methanotrophs (Fig. 11). Even though the genomes of sulfur oxidizers have shown that free-

Table 6. Predicted methane oxidation and carbon fixation pathways in free-living methanotrophs

Gene	Enzyme	Reaction	Location	M.c	M.e	M.p	M.f
				γ	α	β	β
Methane oxidation		$\text{CH}_4 \rightarrow \text{CH}_3\text{OH}$		+	-	-	-
<i>pmo</i> gene cluster				+	-	-	-
<i>pmoCAB</i>	particulate methane monooxygenase		membrane	+	-	-	-
<i>mmo</i> gene cluster				+	-	-	-
<i>mmo</i>	soluble methane monooxygenase		cytoplasm	+	-	-	-
Methanol oxidation		$\text{CH}_3\text{OH} \rightarrow \text{HCHO}$		+	+	+	+
<i>mx</i> gene cluster				+	+	+	+
<i>mx</i> <i>FI</i>	Methanol dehydrogenase		cytoplasm	+	+	- ^a	+
<i>pqq</i> gene cluster				+ ^b	+	-	+
<i>pqqFG</i>	PQQ synthesis			+ ^b	+	-	+
Formaldehyde oxidation^c		$\text{HCHO} \rightarrow \text{HCOOH}$		+	+	-	
	PQQ-linked oxidation		cytoplasm	+	-	-	-
	H ₄ F-linked oxidation		cytoplasm	+	+	+	-
	H ₄ MPT-linked oxidation		cytoplasm	+	+	+	+
	dissimilatory (oxid.) RuMP cycle	$\text{HCHO} \rightarrow \text{CO}_2$	cytoplasm	+	-	-	+
Formate oxidation		$\text{HCOOH} \rightarrow \text{CO}_2$		+	+	+	
<i>fdh</i> gene cluster				- ^d	+	+	
<i>fdh1AB</i>	Tungsten-dependent formate dehydrogenase		cytoplasm	- ^d	+	+	- ^d
<i>fdh2ABCD</i>	Molybdenum-dependent formate dehydrogenase		cytoplasm	- ^d	+	+ ^e	- ^d
<i>fdh3ABC</i>	Cytochrome-linked formate dehydrogenase		cytoplasm	- ^d	+	+	- ^d
Carbon assimilation							
<i>Ribulose monophosphate cycle^f</i>				+	-	-	+
	KDPGA/TA version			+	-	-	+
	KDPGA/SBP version			-	-	-	-
	FBPA/TA version			+	-	-	-
	FBPA/SBP version			-	-	-	-
<i>Serin cycle</i>			cytoplasm	partial ^g	+	+	-
<i>Calvin Cycle</i>			cytoplasm	partial ^h	-	+	-
<i>ccb</i>	RuBisCO		cytoplasm	type ?	-	I	-

Abbreviations: M.c *Methylococcus capsulatus* (Bath); M.e, *Methylobacterium extorquens* (AM1); M.p, *Methylobium petroleiphilum* (PM1); M.f, *Methylobacillus flagellatus* (KT); ^a true homologs missing; ^b presence not explicitly stated but assumed to be present as MxaFI-type methanol dehydrogenase requires PQQ as a co-factor and because PQQ-linked formaldehyde oxidation is employed; ^c PQQ, pyrroloquinoline quinone; H₄F, tetrahydrofolate; H₄MPT, tetrahydromethanopterin; RuMP, ribulose monophosphate; ^d homologs of formate dehydrogenase are present instead; ^e *fdh2D* not present; ^f FBPA, fructose-1,6-bisphosphate aldolase; KDPGA, 2-keto-3-deoxy-6-phosphogluconate aldolase; SBP, sedoheptulose-1,7-bisphosphatase; TA, transaldolase; ^g phosphoenolpyruvate carboxylase missing ^h sedoheptulose-1,7-bisphosphatase missing. Table compiled using information provided in [97,109-111].

living relatives of symbiotic sulfur-oxidizers may use entirely different pathways of sulfur oxidation indicating that there is substantial variety in energy metabolism even among close relatives, the *M. capsulatus* genome still provides insights into the versatility of methanotrophy and will provide the basis for comparative genomics once symbiotic methanotrophs have been sequenced. In fact, a proposal to sequence the endosymbionts of the hydrothermal vent mussel *B. azoricus* and thus the first symbiotic methanotroph has been funded (N. Dubilier, personal communication). The genes and enzymes involved in methane metabolism and carbon fixation of as yet sequenced free-living methane-oxidizing are listed in Table 6. Fig. 13 gives a schematic overview over the methane oxidation and carbon assimilation pathways in *Methylococcus capsulatus* (Bath).

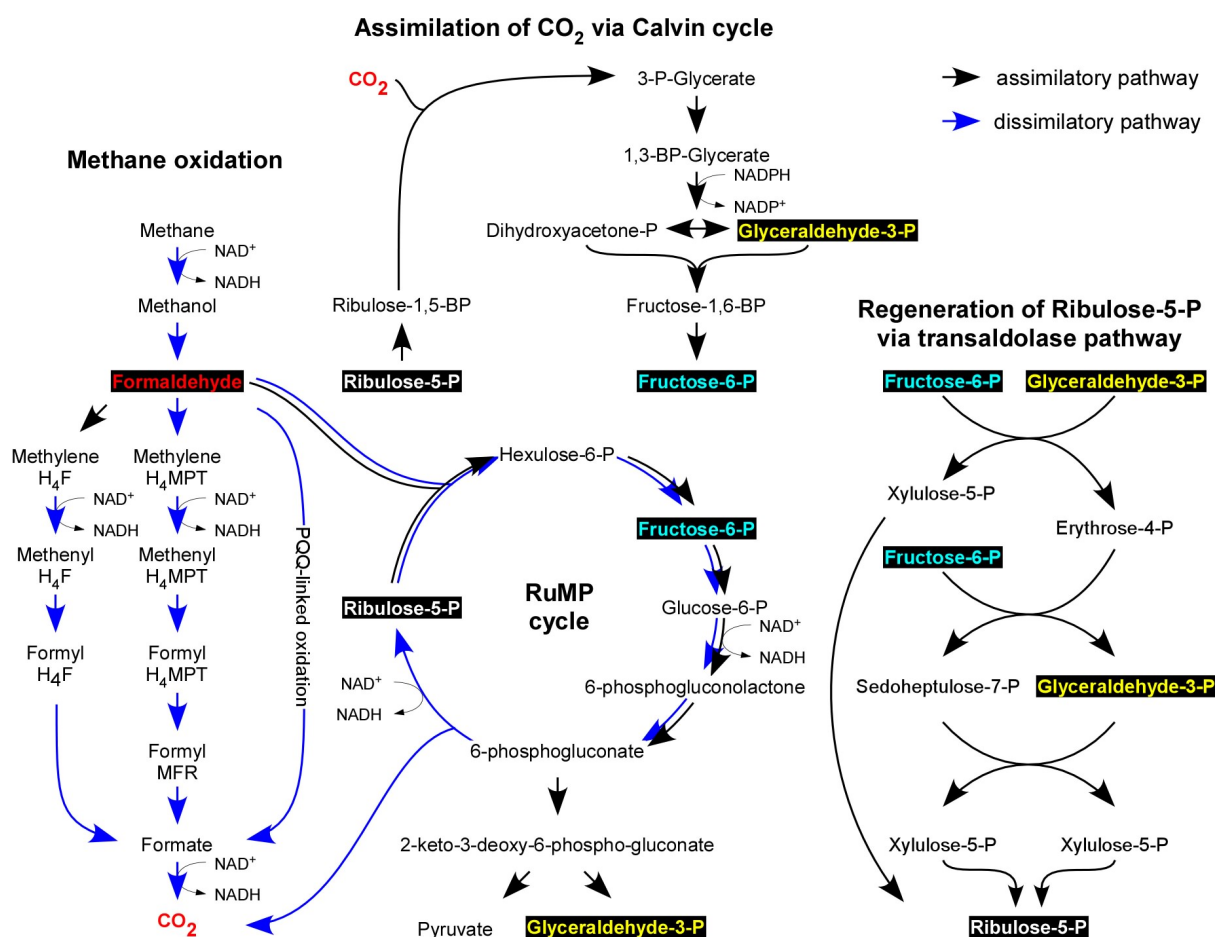


Fig. 13. Methane oxidation and carbon assimilation pathways in *Methylococcus capsulatus* (Bath). Abbreviations: BP, bisphosphate; H₄F, tetrahydrofolate; H₄MPT, tetrahydromethanopterin; RuMP, ribulose monophosphate; P, phosphate; PQQ, pyrroloquinoline quinone. Figure based on information provided in [97,110,112,113].

Methanotrophy is a special case of methylotrophy characterized by the capability to utilize methane as a sole energy and carbon source. According to morphological and physiological characteristics methane-oxidizing bacteria are classified as type I, type II, and

type X methanotrophs [114-116]. All methanotrophs oxidize methane sequentially to CO₂ via the intermediates methanol, formaldehyde, and formate [115-117]. The oxidation step from formaldehyde to formate may involve further intermediates depending on the co-factor used by the enzyme formaldehyde dehydrogenase [116]. Noticeably, out of six described formaldehyde oxidation pathways *M. capsulatus* uses three: the tetrahydromethanopterin (H₄MPT)-, the tetrahydrofolate (H₄F)-, and pyrroloquinoline quinone (PQQ)-linked pathways. Furthermore, *M. capsulatus* oxidizes formaldehyde completely to CO₂ (bypassing formate) by the dissimilatory (oxidative) Ribulose-5-monophosphate (RuMP) cycle [97,112]. The main function of the RuMP cycle in type I and type X methanotrophs is, however, assimilatory, i.e. the fixation of formaldehyde to build up biomass. Besides the assimilatory RuMP cycle *M. capsulatus* may also employ the serine cycle for formaldehyde assimilation which usually operates exclusively in type II methanotrophs [114,115]. A characteristic thus far unique to type X methanotrophs is the utilization of the Calvin-Benson-Bassham cycle for the assimilation of CO₂ [114,115]. The only enzyme lacking in *M. capsulatus* is sedoheptulose-1,7-bisphosphatase, yet alternative enzymes for the regeneration of ribulose-5-phosphate (enzymes of the pentose phosphate pathway) are present [97]. Thus, the regeneration of ribulose-5-phosphate does not proceed via the sedoheptulose-1,7-bisphosphate-aldolase pathway but the transaldolase pathway. The potential to operate the RuMP-cycle, the serine cycle, and the Calvin cycle for the assimilation of single carbon compounds makes *M. capsulatus* unique among methylotrophs [112].

5 Deep-sea bathymodiolin mussels - chemosymbiotic bivalves

5.1.1 Phylogeny of chemosymbiotic bivalves

Where ever hydrogen sulfide and methane occur in elevated concentrations in marine habitats be it at hydrothermal vents, cold seeps, whale carcasses, sunken wood, or reducing sediments, bivalves hosting chemosynthetic symbionts have been found. Long disregarded, bivalve phylogeny has recently entered a phase of renewed vigour, and is currently much debated and subject to frequent changes [118-121]. The currently accepted (but not universally agreed-upon) basis of the higher level bivalve phylogeny is shown in Fig. 14. Endosymbiotic chemosynthetic bacteria have been acquired independently in nearly all higher ranking bivalve taxa, i.e. in protobranch, pteriomorph, and heterodont bivalves. Yet, symbiosis with chemosynthetic bacteria appears to be restricted to only a few genera. In protobranch bivalves, chemoautotrophic endosymbionts have been reported from the solemyid genera *Solemya* and *Acharax* [122]. In pteriomorph bivalves both chemoautotrophic

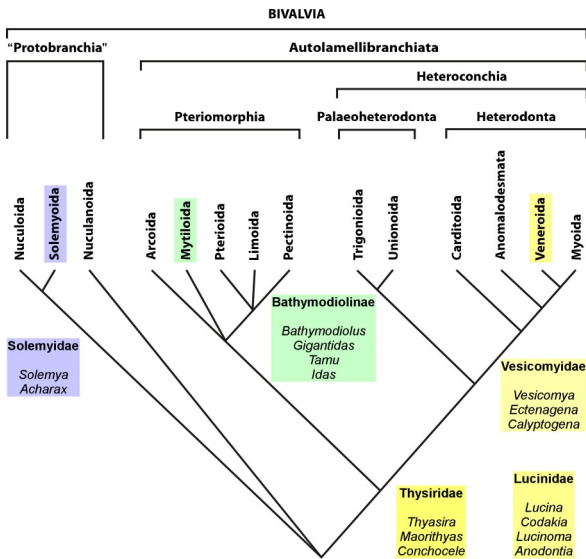


Fig. 14. Current bivalve phylogeny. Taxa and genera which have acquired chemosynthetic bacterial endosymbionts are highlighted. For species level symbioses see Fig. 11. Tree from [118], modified.

In heterodont bivalves chemoautotrophs occur in the vesicomomyid genera *Vesicomomya*, *Ectenagena*, and *Calyptogena*, the lucinid genera *Lucina*, *Codakia*, *Lucinoma*, and *Anodontia*, and the thyasirid genera *Thyasira*, *Maorithyas*, and *Conchocele* [65,70]. Except for thyasirid clams symbiosis with chemosynthetic bacteria appears to be obligate in these bivalve taxa [80,123,126,127].

5.1.2 The genus *Bathymodiolus*

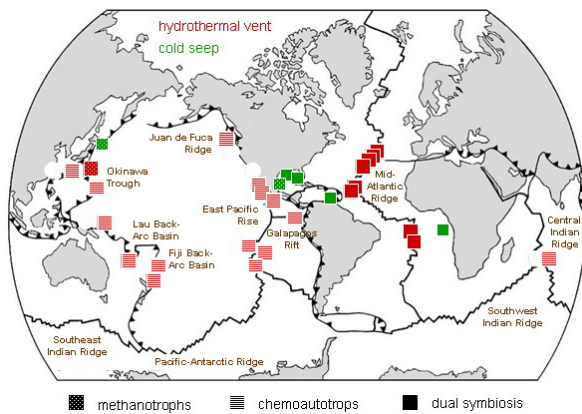


Fig. 15. World-wide distribution of the genus *Bathymodiolus*. After [46,123], modified.

Bathymodiolin mussels of the genus *Bathymodiolus* occur world-wide at deep-sea hydrothermal vents on mid-ocean and back-arc spreading ridges as well as cold seeps on continental margins (Fig. 15) [6,46,69,70,123]. Thus far, the genus has not been reported from whale carcasses or sunken wood, habitats which appear to be restricted to the bathymodiolin genera *Idas*, *Adipicola*, *Myrina*, and *Benthomodiolus* [71,128]. 16 *Bathymodiolus* species were known by 2006 [123]. Since then the list has been expanded to include at least 24 species of which four are undescribed and two hold an *affinis* status. However, recent phylogenetic analyses suggest that several species should be excluded from the genus *Bathymodiolus* as they are closer related to the genera *Tamu* and *Gigantidas* [129-131]. As they can to date not explicitly be assigned to one of these two genera these species are designated “*Bathymodiolus*” with double quotation marks and are referred to as the “childressi” group after the first species named. Species belonging to the “aduloides”

and methanotrophic endosymbionts are known to occur in bathymodiolin mussels of the genera *Bathymodiolus*, *Gigantidas*, *Tamu*, and *Idas* [82,123,124]. Chemosynthetic symbionts likely also occur in the other bathymodiolin genera *Adipicola*, *Myrina*, *Idasolas*, and *Benthomodiolus* which have, however, to date not been well investigated for their symbiotic state [125].

group are designated '*Bathymodiolus*' with single quotation marks [131]. With the exception of a mussel reported from the Juan de Fuca Ridge all remaining *Bathymodiolus* species are referred to as the "thermophilus" group and are true members of the genus *Bathymodiolus* [129-131]. A composite tree reflecting the current understanding of the phylogenetic relationship among mussels of the genus *Bathymodiolus* is shown in Fig. 16. Molecular estimates suggest an origin of bathymodiolin mussels between 23.7 and 74.3 million years ago (mya) [129]. According to the geological record the genus *Bathymodiolus* appeared approximately 50 mya [132].

In the absence of light and thus photosynthetic primary production concurrent with an insufficient supply of organic particles in the deep-sea these mussels are nutritionally dependent on endosymbiotic bacteria capable of chemosynthesis [64,65,123]. The bacteria reside intracellularly in the mussel's gill tissue in the cytoplasm of bacteriocytes which regularly alternate with symbiont-free intercalary cells (Fig. 17) [137,138]. Mussels of the genus *Bathymodiolus* harbor two types of chemosynthetic bacteria: a chemoautotroph, capable of fixing CO₂ in the presence of sulfide and thiosulfate as sole energy sources or a methanotroph using both methane as carbon and energy source [123,139-144]. Most *Bathymodiolus* species described thus far host exclusively the chemoautotrophic endosymbiont while some host only methanotrophs. However, mussels endemic to vents along the Mid-Atlantic Ridge and seeps in the Gulf of Mexico as well as off Africa harbor both types simultaneously (Fig. 15) [123,125]. Up to four symbionts have recently been reported from *B. heckerae*. In addition to these two symbiont types this species also harbors a

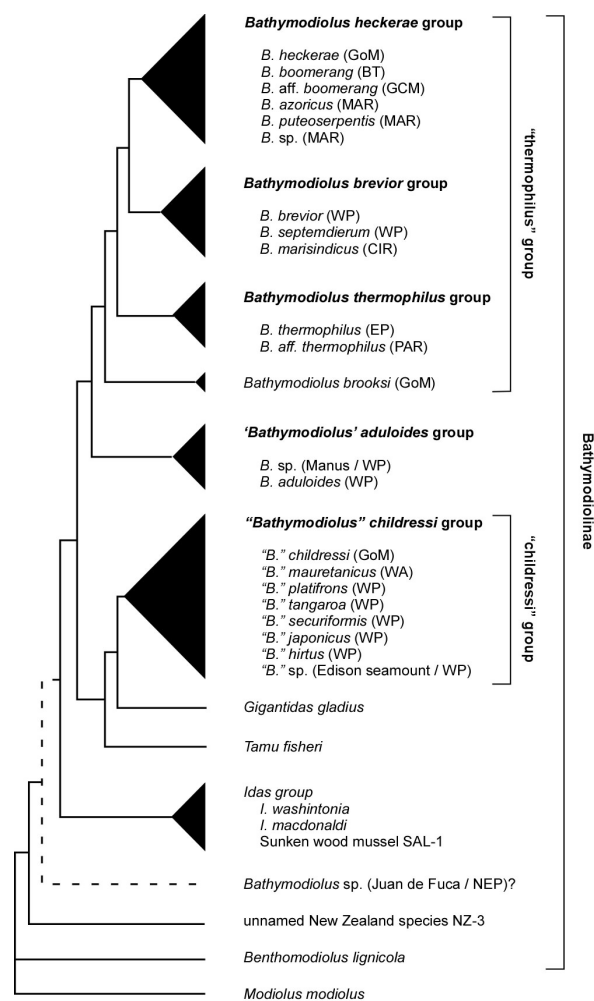


Fig. 16. Schematic phylogenetic tree of *Bathymodiolus* spp. The tree is a composite of several recently published trees on bathymodiolin mussels. The dashed line indicates an uncertain position. Abbreviations: BT, Barbados Trench; CIR, Central Indian Ridge; EP, East Pacific; GCM, Gabon-Congo Continental Margin; GoM, Gulf of Mexico; MAR, Mid-Atlantic Ridge; NEP, North East Pacific Ridges; PAR, Pacific-Antarctic Ridge; WA, West Africa; WP, West Pacific; Figure based on [129-131] and extended to include information provided in [125,133-136].

second sulfur-oxidizing chemoautotroph and a methylotroph [145]. Even though phylogenetically distinct all these symbionts belong to the Gammaproteobacteria. Clearly, mussels with dual or multiple chemosynthetic symbionts are environmentally more flexible than mussels relying on only one symbiont type. Sulfur-oxidizing chemoautotrophic symbionts are $\sim 0.3\text{-}0.5\ \mu\text{m}$ in diameter and often occur multiply within a single vacuole. Methanotrophic symbionts are bigger ($\sim 1.5\text{-}2.0\ \mu\text{m}$ in diameter), exhibit intracytoplasmic membranes typical of type I methanotrophs and are usually found individually within a vacuole. Though typically only one type of endosymbiont, either methanotroph or chemoautotroph, is found in a given vacuole, the symbionts can co-occur in the same vacuole [123,125].

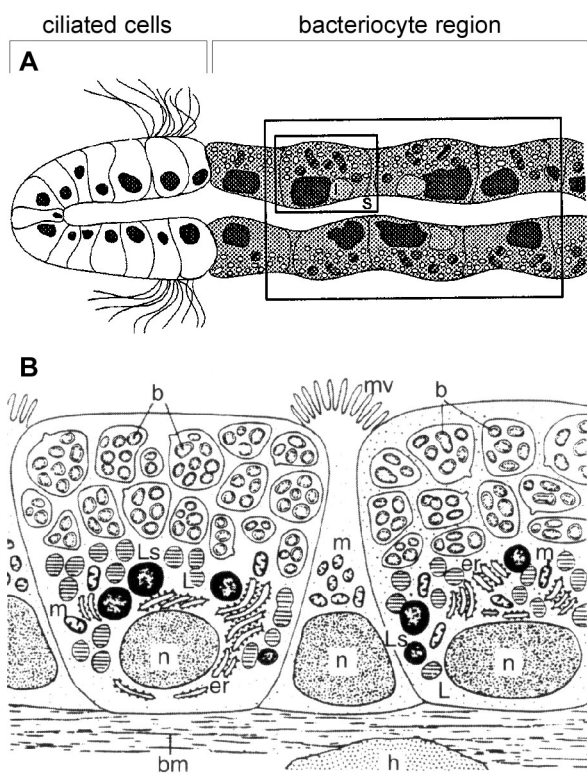


Fig. 17. Cell arrangement in gills of mussels belonging to the genus *Bathymodiolus*. (A) Single gill filament, (B) bacteriocyte region, shown are two bacteriocytes separated by an intercalary cell. Note that the bacteriocytes shown contain only chemoautotrophs. Abbreviations: b, bacteria; bm, basal membrane; er, endoplasmic reticulum; L, lipids; Ls, lysosomes; m, mitochondria; mv, microvilli; n, nucleus; h, hemocyte; s, blood sinus. From [137,138].

vesicomylid and lucinid clams, mussel symbionts do not store elemental sulfur [4,148].

Evidence for the use of methane as an energy source by methane-oxidizing symbionts comes from methane consumption experiments, the presence of methane monooxygenase and methanol dehydrogenase (the enzymes responsible for the first and second step of methane

Molecular evidence indicates that sulfur-oxidizing symbionts of bathymodiolin mussels possess and express the enzymes involved in the Aps pathway of SO_3^{2-} oxidation, i.e. APS reductase and ATP sulfurylase [146-148]. In contrast, the Sox pathway for the oxidation of thiosulfate and sulfide may not be present as the gene coding for the SoxB component could not be found [104]. This may either be a false-negative result as sulfide and thiosulfate have been shown to be energy sources [143,144] or these sulfur species may be oxidized by means of other pathways such as the Dsr pathway. Chemoautotrophy has been proven by the presence of RuBisCO for which there is enzymatic, immunological, and molecular evidence [141,142,147-149]. Unlike other sulfur-oxidizing symbionts such as those of siboglinid tubeworms,

oxidation, respectively), as well as the presence of the key enzyme of the RuMP cycle for the assimilation of formaldehyde (hexulose-phosphate synthase) [139,141,142,146,147,149-153]. Although type I methanotrophs typically rely on the RuMP cycle for formaldehyde assimilation RuBisCO has recently been reported from a methanotrophic symbiont indicating the presence of a functional CBB cycle in some methanotrophic symbionts [154].

6 Thesis goal

In contribution to the Priority Program SPP 1144 outlined on page 9 this PhD project aimed to (i) describe Logatchev mussel habitats in regard to *in situ* physico-chemical conditions, (ii) investigate the endosymbiotic diversity of *B. puteoserpentis* (Logatchev), and (iii) evaluate the activity of endosymbiotic bacteria in MAR bathymodiolin mussels from both the ultramafic-hosted Logatchev vent field and the basalt-hosted vent fields south of the equator. These goals were addressed in six research cruises, on board laboratory work, and subsequent analysis in the home laboratory. Table 7 gives an overview of these cruises. The results, a comprehensive discussion, and the background of each of these projects are provided in the manuscripts attached to this thesis (Zielinski *et al.*, manuscripts I-III) [155-157].

Table 7. Contributions to cruises prepared and/or participated in during this PhD project

Cruise	Destination	Date	Contribution	Chapter	Ref
Hydromar I	M60/3	Logatchev	14.1.-14.2.04	<i>in situ</i> measurements, sampling	II1, II2 [155,156,158,159]
Hydromar II	M64/2	Logatchev	6.5.-6.6.05	H ₂ consumption, transplantation, sampling	II1, II3 [157]
Hydromar III	MSM04/3	Logatchev	23.1.-14.2.07	preparation	II3 [160]
Suedmar I	M62/5B	4-11°S	1.-30.12.04	MAPR	- [161]
Suedmar II	M64/1	RL, TP, WA, LP	2.4.-3.5.05	preparation	- [1,47]
Suedmar III	M68/1	RL, CC, TP, WA, NL, LP	27.4.-2.6.06	H ₂ consumption, ¹⁴ CO ₂ fixation, sampling	II3 [1,2,47,161]

Abbreviations: RL, Red Lion; CC, Comfortless Cove; TP, Turtle Pits; WA, Wideawake (all 4°48'S); NL, Nibelungen (8°18'S); LP, Lilliput (9°33'S); MAPR – miniaturized autonomous plume recorder. Ref, references (publications in result of cruise).

The following three chapters, entitled ‘Habitat characterization’ (chapter II1), ‘Endosymbiont diversity’ (chapter II2), and ‘Endosymbiont activity’ (chapter II3), briefly present and discuss the results of above outlined working questions avoiding manuscript recurrences. The individual chapters first introduce the specific project and then briefly summarize the results which are provided in more detail in the manuscripts. The remaining sections discuss the data under different perspectives and in different contexts than is

discussed in the manuscripts. Furthermore they provide an outlook and give impulses for further research on the topic.

II Results and Discussion

1 Habitat characterization

1.1 Working question

The initial question of this PhD thesis was how gradients in vent fluids affect endosymbiont diversity and activity. Mussel beds of *B. puteoserpentis* at Logatchev had been described as 0.5 m thick near the base of the central chimney complex with the thickness gradually diminishing to just one layer of mussels at the edge of the bed [162]. Therefore, it was assumed that these mussels settle around a central source of hydrothermal diffuse flow where they form thick aggregations and that mussel aggregations become steadily thinner towards the edges of the bed in response to a gradually diminishing fluid flow. The idea was thus to measure the physico-chemical conditions along a transect from the center to the edge of the mussel bed followed by sampling specimens of *B. puteoserpentis* at the site of measurement and subsequent analysis.

The proposed horizontal gradient was to be resolved with regard to temperature, pH, sulfide, methane, hydrogen, and oxygen content. Temperature and pH are biologically meaningful parameters in general. Sulfide- and methane are important as electron donors for the sulfur- and methane-oxidizing endosymbionts, respectively whereas hydrogen is a potential electron source for both sulfur- and methane-oxidizing bacteria (Zielinski *et al.*, manuscript III) [157]. Oxygen is essential as it is the respiratory electron acceptor for the endosymbionts and the mussel host.

Temperature, dissolved sulfide (H_2S), and oxygen were measured *in situ* using a temperature sensor and electrochemical microsensors (Zielinski *et al.*, manuscript I) [155]. *In situ* pH measurements were attempted but failed due to interferences during calibration. Since sufficiently fast responding methane sensors have not yet been developed [163] and because hydrogen sensors were not available for this study, the methane and the hydrogen content of the water body overlaying the mussel beds were analyzed on board after discrete sampling (R. Seifert and S. Ertl, University of Hamburg, unpublished data).

1.2 Results of *in situ* microsensor measurements

The combined *in situ* sensor measurements of temperature, H₂S, and O₂ revealed high temporal fluctuations of all three parameters above the mussel beds. H₂S and O₂ co-occurred simultaneously with mean concentrations between 14 - 34 μM (H₂S) and 205 - 223 μM (O₂), showing the existence of free sulfide (H₂S/HS⁻) in diffuse fluids from the ultramafic-hosted Logatchev vent field (Fig. 18). Temperature maxima were generally concurrent with H₂S maxima and O₂ minima, with H₂S maxima of 79 μM and O₂ minima never below 142 μM. Despite temperature maxima up to 7.4°C, mean temperatures above mussel beds were generally only slightly above ambient sea water (2.6°C, Fig. 18). Dissolved oxygen concentrations consistently decreased as temperatures increased, resulting in a strongly negative and linear correlation of O₂ with temperature ($R^2 = 0.74-0.85$). While H₂S concentrations generally increased with temperature, a linear correlation could not be shown due to a slower response of the H₂S sensor over the temperature sensor. The Logatchev *in situ* measurements indicate that sulfide may also be present and bioavailable in diffuse fluids from similar high-temperature ultramafic-hosted vent systems which occur more often than previously recognized along slow- and ultraslow spreading ridges (Zielinski *et al.*, manuscript I) [155].

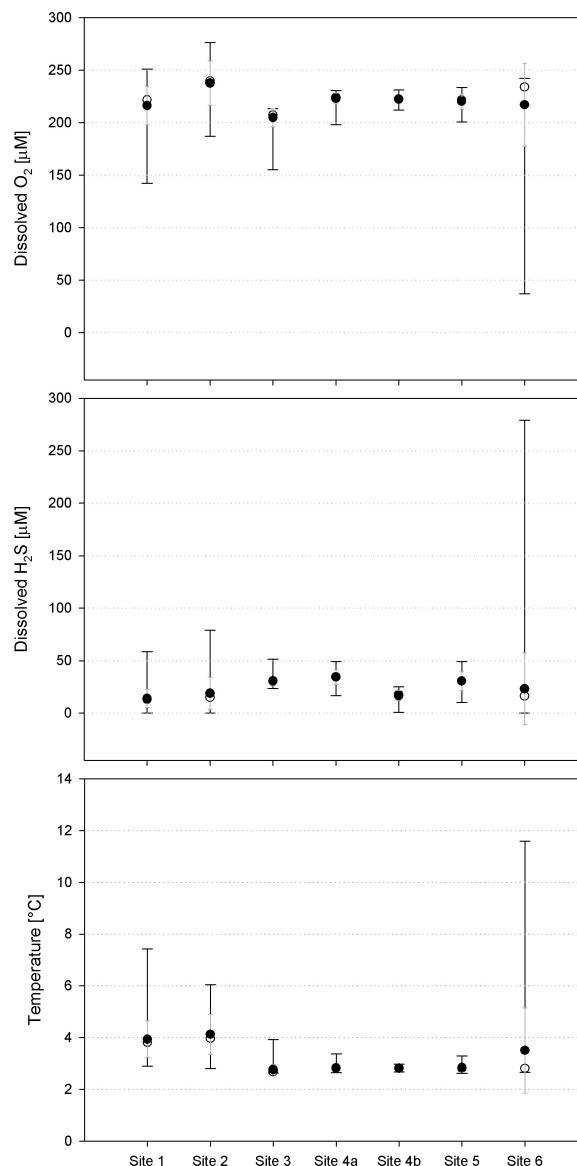


Fig. 18 Summary of *in situ* microsensor measurements. Dissolved O₂ (top), dissolved H₂S (middle), and temperature (bottom). Filled circles denote the mean value, whereas open circles denote the median value. The standard deviation is shown as a grey bar, whereas ranges are represented by the black bar. Site 1 – 4 were different mussel beds, Site 5 was a chimney wall populated with shrimp and Site 6 was a spot close to the rim of a smoking crater lacking the typical vent fauna.

1.3 *In situ* versus on board measurements

1.3.1 *Sulfide as a paradigm for discrepancies between in situ and on board measurements*

To compare *in situ* sulfide concentrations with sulfide values obtained from discrete sampling, sulfide was also analyzed on board (A. Koschinsky *et al.*, unpublished data). Table 8 gives a comparison of sulfide concentrations determined *in situ* and from discrete sampling.

Table 8. *In situ* sulfide concentrations versus sulfide analysis on board.

Location	<i>in situ</i> ^a			pH	discrete sampling ^b		
	∅ H ₂ S	Max H ₂ S	n		H ₂ S + HS ^{-c}	H ₂ S ^d	n
mussel patch	34	49	147	7.95	0.5	0.0	1
chimney base colonized by mussels	14	59	250	7.55	bd-1.3	bd-0.2	2
sulfide pillar overgrown with mussels	30	51	256	-	nd	-	-

Concentrations are given in μM . Data were obtained during the Hydromar I cruise (M60/3); ^a data from Zielinski *et al.*, manuscript I [155]; ^b A. Koschinsky, Jacobs University Bremen, unpublished data; ^c as measured by voltammetry; ^d calculated from voltammetric measurement according to [164,165] and an assumed habitat temperature of around 3.0°C; n, number of measurements; nd, not determined; bd, below detection

It is obvious that discrete sampling failed to detect the wealth of free sulfide in hydrothermal diffuse flow. This is not surprising because of the immense delay between sampling and analysis on board. It usually takes hours before water samples are recovered and additional time until analysis in the laboratory. This delay likely favors sulfide precipitation by reduced metal species such as Fe²⁺, Cu²⁺, and Zn²⁺ which are present in hydrothermal diffuse flow and thus in the samples [24]. Nevertheless, the lack of free sulfide in discrete samples prompted the suggestion that primary production at Logatchev is based on methane and hydrogen rather than on sulfide [159]. Clearly, this conclusion ignored the artifacts resulting from discrete sampling. The discrepancy between *in situ* and on board measurements after discrete sampling has also been pointed out in two recent studies [166,167].

Apart from redox processes during fluid transport another factor may account for the low sulfide concentrations measured by discrete sampling at Logatchev: the sampling mode. The easiest way to sample diffuse flow is to close a Niskin-type water sampler amidst hydrothermal diffuse flow. However, these water samplers usually hold at least 5 liters. Thus, the fluid sample is inevitably diluted with ambient seawater. To circumvent the dilution problem an actively pumping fluid sampling system, originally developed for sampling high temperature endmember fluids, has also been used for sampling diffuse fluids at Logatchev [24]. Briefly, a titanium sampling nozzle was inserted into a mussel bed and the fluid actively pumped into bottles made entirely of inert materials. Although sulfide concentrations reported from these samples are higher (0.4-6 μM) than those listed in Table 8 ([24] and Table 9) they

are clearly below *in situ* values. It should also be noted that active pumping changes the natural fluid flow within the mussel aggregations. Thus, any obtained sulfide value represents only an average value that fails to resolve the true conditions over space and time.

The low number of possible measurements is another evident disadvantage of discrete sampling (Table 8). Discrete sampling yields only one measurement per fluid sample, triplicates at best when time allows. In strong contrast, the number of *in situ* measurements at a given spot is theoretically unlimited. With a sampling resolution of one measurement per second, ten thousands of measurements can be recorded during one dive. In fact, when *in situ* techniques were first used at hydrothermal vents the number of measurements obtained during 30 minutes exceeded the total number of all earlier samples from this particular hydrothermal vent system [168].

1.3.2 *In situ techniques of sulfide detection*

Two basic principles have been used over the last two decades to measure sulfide *in situ* at deep-sea hydrothermal vents: colorimetry and electrochemistry. Conventional flow analysis (CFA) [168-170] and flow injection analysis (FIA) [171,172] relied on the colorimetric detection of sulfide. However, the colorimetric approach is limited to the detection of total sulfide ($\text{H}_2\text{S}/\text{HS}^- + \text{FeS}$) and does not distinguish between different sulfide species. Furthermore, the resolution depends on the time needed for the colorimetric reaction and measurement which is another limiting aspect. Besides, the need for actively pumping a sample for *in situ* analysis will inevitably disturb the natural fluid flow. On the other hand, flow injection devices have the advantage that the sampling inlet can be positioned arbitrarily.

Electrochemical sensors are a rather recent addition to the suite of *in situ* sulfide detection at deep-sea hydrothermal vents. Voltammetric (polarographic) electrochemical sensors use a solid-state gold-amalgam (Au/Hg) working electrode. By linear or cyclic voltammetric scanning these sensors relate an electrochemically induced change in electric current to the *in situ* concentrations of different sulfide species and are capable of detecting and distinguishing both free sulfide ($\text{H}_2\text{S}/\text{HS}^-$), soluble iron-sulfide clusters (FeS_{aq}), elemental sulfur (S^0), polysulfides (S_x^{2-}), thiosulfate ($\text{S}_2\text{O}_3^{2-}$), and tetrathionate ($\text{S}_4\text{O}_6^{2-}$) [83,173-177]. Another electrochemical approach relies on the amperometric detection of sulfide in its undissociated form as dissolved gaseous hydrogen sulfide (H_2S). Similar to the voltammetric approach amperometric microsensors relate an electrochemically induced change in electric current to the *in situ* concentrations of H_2S , the voltage is, however, kept constant and no other sulfide species can be detected [164,178]. Amperometric H_2S microsensors were deployed during

this PhD project and provided valuable *in situ* data (Zielinski *et al.*, manuscript I) [155]. In fact, H₂S microsensors were deployed for the first time at deep-sea hydrothermal vents in this PhD project.

1.3.3 Summary

Sulfide values from discrete measurements are erroneously low due to the sampling procedure and redox processes during fluid transport. Furthermore, they are extremely low in resolution. Therefore, discrete sampling fails to resolve physico-chemical conditions in hydrothermal diffuse flow over space and time. Thus, deducing *in situ* conditions from analysis of discrete water samples will likely result in underestimation of the real conditions. In contrast, *in situ* techniques are capable of resolving physico-chemical conditions in hydrothermal diffuse flow due to the virtually unlimited number of measurements and the absence of sampling artifacts. *In situ* techniques are closer to reality than discrete sampling and should be the method of choice whenever possible.

1.4 Gradients in hydrothermal diffuse flow

Measurements above the mussel beds suggested a wealth of dissolved H₂S and oxygen (Zielinski *et al.*, manuscript I) [155]. However, the physico-chemical properties above the beds were similar at all investigated sites with only slight variations (Fig. 18). This result casts doubt on the presence of a continuous horizontal gradient above mussel beds because if such a gradient existed, conditions at the source of hydrothermal diffuse flow should have differed considerably from the conditions away from the source. Apart from the fact that physico-chemical conditions outside the influence of hydrothermal diffuse flow were those of ambient seawater, conditions inside diffuse flow did not follow the expected pattern of a continuous horizontal gradient. Thus, *in situ* data obtained during this PhD project do not support the initial assumption of a “gradually diminishing” fluid flow.

The reasons for the lack of a horizontal gradient are probably manifold. First, Logatchev mussels are likely supplied by various sources of diffuse venting which may even differ in their endmember fraction as a result of stronger or lesser dilution with ambient seawater. In fact, the extended Logatchev mussel beds may be equally supplied by diffuse venting discharged from many small cracks in the ocean floor. Thus, neighboring fluid sources will mix and any potential gradient will be obliterated. Second, bathymodiolin mussels have been shown to laterally divert the fluid flow. This was revealed during clearance experiments with *B. thermophilus* on the Galapagos Rift [179,180]. Removal of mussels from spots with the highest sulfide concentrations did not necessarily reveal the fluid source but unexpectedly

bare ocean floor basalt [179]. In this way, mussels bridge areas that are not directly supplied with diffuse fluids and still thrive. These observations suggest that bathymodiolin mussels divert the fluid flow in all directions, not just laterally, and thus shape the fluid flow over space and time in response to their own energy needs. Third, deep ocean currents and tides will complicate the fluid flow through mussel beds as do local currents in response to the topography of the site. Furthermore, the discharge of diffuse fluids fluctuates over seconds with repeating patterns in response to tides what may additionally obliterate gradients [179,181-183].

In summary, different lines of evidence suggest that continuous gradients do not exist in Logatchev mussel beds – neither horizontally nor laterally. Thus, the initial question of this PhD project how gradients affect endosymbiont, diversity and activity remains open since gradients, a prerequisite of this question, do obviously not exist. Data obtained during this PhD project rather suggest that each individual mussel lives in a temporally changing microenvironment that is distinguished by its physico-chemical properties from the microenvironments of neighboring mussels. Direct *in situ* characterization of such a microhabitat is highly challenging.

Yet, microhabitats can indirectly be characterized *in situ*. Previous studies [166,184-186] and data obtained during this PhD project (Zielinski *et al.*, manuscript I) [155] suggest that temperature is positively correlated with sulfide and negatively correlated with oxygen in hydrothermal diffuse flow and can thus be used as an approximate estimate (proxy) of sulfide and oxygen concentrations. It is, however, crucial that the sulfide-temperature and oxygen-

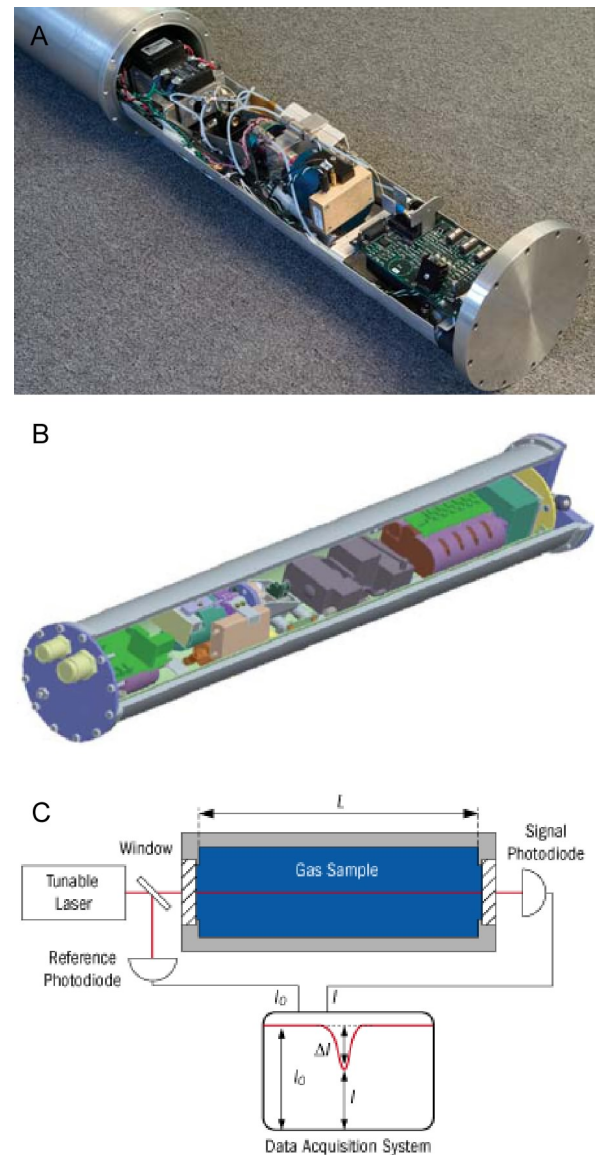


Fig. 19. The deep-sea gas analyzer. (A) Opened pressure cylinder showing internal electronics. (B) Graphical view. (C) Measuring principle.

temperature correlation is determined for each site of interest due to considerable inter- and intra-site variability [166,185,186].

1.5 Outlook

It appears reasonable to assume that other essential parameters in diffuse flow such as hydrogen and methane are potentially also positively correlated with temperature. As for hydrogen this correlation can be investigated since sufficiently fast responding hydrogen microsensors are available. Hydrogen and temperature sensors have been deployed *in situ* at Logatchev but still await final analysis (F. Wenzhöfer, MPI for Marine Microbiology, unpublished data). As for methane, this relationship must remain elusive until fast responding methane sensors become available. Nonetheless, the deployment of commercially available slow-responding methane sensors (> 10 min) *in situ* may be an alternative to discrete sampling. For example, a methane sensor developed by Capsum (Germany; www.capsum.de) and modified for deep-sea purposes has recently been tested [187].

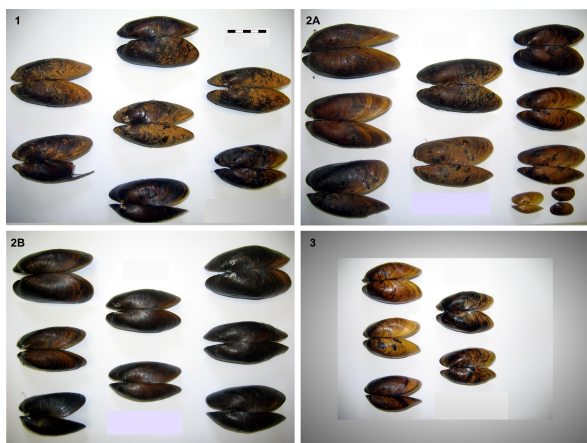


Fig. 20. Mussels sampled for the analysis of endosymbiont diversity, biomass, and activity in response to differing physico-chemical conditions. Note that mussel shells obtained from different locations visually differ from each other. **1** – mussel shells overall brown with “rusty” coating; **2A** – mussel shells overall shiny and only occasionally with “rusty” coating; shell color ranging from brown at hinge to amber at edge; **2B** – mussel shells shiny and overall dark brown to nearly black; **3** – mussels shell color inhomogeneous ranging from brown to almost yellow and shiny. Numbers correspond to sampling site (see Table 9 for further information). Scale bar is 5 cm.

As an alternative to *in situ* measurements with microsensors, a commercially available and self-calibrating deep-sea gas analyzer (Los Gatos Research, Mountain View, CA, USA) may be considered for *in situ* quantification of above mentioned parameters (Fig. 19). Next to oxygen, hydrogen, methane, and hydrogen sulfide this instrument measures a variety of gases including biologically important carbon dioxide, ammonia, nitrate, and nitrite. In addition even carbon isotopes are analyzed *in situ*. Gas detection and quantification is based on laser absorption spectroscopy which limits the response time to below 1 minute [188].

In response to the applicability of temperature as an estimate of *in situ* sulfide and oxygen conditions, the initial working question was modified and is currently: How do differing physico-chemical conditions in mussel microhabitats affect endosymbiont diversity, biomass, and activity? To answer this

question different sites within Logatchev mussel beds were selected which visually differed from each other (N. Dubilier, MPI for Marine Microbiology, personal communication) and which differed in their methane and hydrogen content as determined by discrete sampling (R. Seifert, University of Hamburg, unpublished data). These sites were subsequently further characterized in their physico-chemical properties by *in situ* measurements of temperature, pH, H₂S, hydrogen, and oxygen content (F. Wenzhöfer, MPI for Marine Microbiology, unpublished data). Subsequently, mussels were sampled, dissected for on-board experiments (Zielinski *et al.*, manuscript III) [157] or further analysis, and documented (Fig. 20). Respective sites were mined with long-term temperature loggers capable of measuring temperature above the mussel beds or vertically inside mussel beds at eight points (N. Dubilier and H.-H. Gennerich, University of Bremen, unpublished data). After 20 months of deployment, loggers were recovered and the mussels in their immediate surrounding sampled and fixed for further analysis (H.-H. Gennerich, J. M. Struck, and C. Borowski, MPI for Marine Microbiology, unpublished data). Temperature data, *in situ* measurements, and the diversity, biomass, and activity of the endosymbionts are currently being analyzed and correlated (H.-H. Gennerich, F. Wenzhöfer, and N. Dubilier *et al.*, unpublished data). Table 9 provides an overview of the data sampled to answer the question outlined above.

Table 9. Data sampled for the investigation of endosymbiont diversity, biomass, and activity in relation to differing physico-chemical properties of mussel microhabitats

site	<i>in situ</i> chemistry ^a	<i>in situ</i> temperature ^b [°C]	fluid chemistry ^c				mussel sample ^d station	temperature logger ^b	
			CH ₄ [μM]	H ₂ [μM]	ΣS [μM]	pH		station	logger #
1	Irina II 232ROV/4a 244ROV/1 in analysis	249ROV/1-4	232ROV/7				252ROV/6	249ROV/6	4143
		6-21	3.0	5.4	0.4	7.9	Fig. 20	257ROV/1 in analysis	0-9
2A	Irina II 232ROV/1 in analysis	232ROV/4	232ROV/3				232ROV/5	232ROV/6	4144
		22-47	1.6	1.4	0.2	7.9	Fig. 20	in analysis	
2B	Irina II 266ROV/1-5 277ROV/? in analysis	nd	266ROV/6				266ROV/7	nd	-
		-	15.0	5.9	6.0	7.6	Fig. 20	-	-
3	Quest nd	nd	281ROV/2				281ROV/3	281ROV/4	10-19
		-	63.7	4.2	70.0	7.0	Fig. 20	in analysis	295,298

Data were sampled during the Hydromar II cruise (M64/2); ^a *In situ* physico-chemical properties were measured by F. Wenzhöfer (MPI for Marine Microbiology). ^b Temperature loggers were constructed, built, and calibrated by H.-H. Gennerich (University of Bremen) and deployed by N. Dubilier (MPI for Marine Microbiology). The *in situ* temperature was measured with an eight channel temperature logger up to 28 cm inside mussel beds. ^c The fluid chemistry was analyzed on board after discrete sampling. Methane and hydrogen were analyzed by R. Seifert (University of Hamburg, unpublished data). Total sulfide content and pH were measured by K. Schmidt (Jacobs University Bremen) [24]; ^d Mussels were sampled by N. Dubilier and dissected / fixed / documented by F. Zielinski (MPI for Marine Microbiology). Station numbers of mussel samples after long-term deployment of temperature loggers are not given. nd – not determined

2 Endosymbiont diversity

2.1 Assessment of endosymbiotic diversity

Bacterial diversity in *B. puteoserpentis* (Logatchev) was assessed using universal bacterial primers, a moderate number of PCR cycles, and extended cloning and sequencing efforts (Zielinski *et al.*, manuscript II) [156]. Table 10 lists the number of partial and full sequences obtained from four mussel specimens which were sampled from different habitats at the Irina II site.

2.2 Chemoautotrophic and methanotrophic endosymbionts

Cloning and sequencing of the 16S rRNA gene in endosymbiont-containing gill tissue revealed three distinct phylotypes (Table 10). Two phylotypes originated from the sulfur-oxidizing chemoautotrophic and methanotrophic endosymbionts of bathymodiolin mussels living in a dual symbiosis. A comparison with 16S rRNA sequences of *B. puteoserpentis* from the Snake Pit vent field as well as *B. azoricus* from the Menez Gwen, Lucky Strike, and Rainbow vent fields along the Mid-Atlantic Ridge revealed that these two mussel species share highly similar to identical symbiont phylotypes [158]. Furthermore, FISH inspection of the relative abundances of the sulfur- and methane-oxidizing endosymbionts and comparison with sulfide and methane endmember concentrations suggested that the fluid chemistry of a particular vent field affects the relative abundances of the mussel endosymbionts. To which degree the relative abundances are shaped by the diffuse flow composition is currently under investigation and was discussed above (Table 9).

Table 10. Phylotypes obtained from sequencing the 16S rRNA gene pool of *B. puteoserpentis*

Phylotype Sample ID ^a	location	1		2		3		Total	
		partial	full	partial	full	partial	full	partial	full
35GTV	mussel bed	53	3	42	3	0	0	95	6
38ROV/6-5	sulfide-pillar	31	3	18	3	50	3	99	9
56ROV/6-j6	sulfide-pillar	63	3	7	3	3	3	73	9
66ROV/16-3	mussel patch	36	3	57	3	7	3	100	9
Total		183	12	124	12	60	9	367	33
closest relative		SOX <i>B. puteoserpentis</i> (MAR)		MOX <i>B. puteoserpentis</i> (Snake Pit)		"NIX" <i>S. patula</i> (non hydrothermal)			
phylogeny		Gamma		Gamma		Gamma			
identities		100%		99%		91%			
reference		[189]		[137]		[190]			

^a specimens were sampled during the Hydromar I cruise to the Logatchev vent field (M60/3); MAR, Mid-Atlantic Ridge; MOX, methane-oxidizing endosymbiont; NIX, Nuclear Inclusion X; SOX, sulfur-oxidizing endosymbiont

2.3 “*Candidatus Endonucleobacter bathymodioli*”

FISH inspection identified the third phylotype as a bacterial parasite that exclusively occurred inside mussel nuclei of all tissues although bacteriocyte nuclei appeared to be free of the infection (Zielinski *et al.*, manuscript II) [156]. Infected nuclei showed histo-pathological modifications and were ultimately lysed by the parasite. Different developmental stages could be observed and a developmental cycle of the parasite was proposed. As a result of extended molecular and morphological investigations the bacterium was given a “Candidatus” status and named “*Candidatus Endonucleobacter bathymodioli*” (Zielinski *et al.*, manuscript II) [156]. Eight other *Bathymodiolus* species from five hydrothermal vent fields and five cold seep sites located in the Atlantic and Pacific Ocean were specifically investigated for this parasite. Consequently, the parasite was confirmed in other hydrothermal vent mussels and was also found in cold seep mussels. All phylotypes were closely related to each other and formed a monophylum. It was suggested that “*Ca. E. bathymodioli*” is widespread in both hydrothermal vent and cold seep bathymodiolin mussels (Zielinski *et al.*, manuscript II) [156].

2.4 Conclusion

Using universal bacterial primers, three phylogenetically distinct bacterial populations were unveiled in *B. puteoserpentis* during this PhD project. However, the bacterial diversity of *B. puteoserpentis* may not fully have been revealed despite extensive cloning and sequencing efforts. For example, a recent assessment of the endobacterial diversity of *B. heckeræ* from a cold seep in the Gulf of Mexico using universal bacterial primers revealed four bacterial populations within gill bacteriocytes: one methanotroph dominating the bacterial population with ~80%, one methylotroph accounting for ~8% of all bacteria, and two distinct thiotrophs of which the predominant and minor type accounted for ~5% and 0.3%, respectively of the total bacterial population [145]. On the other hand, the four symbionts detected in *B. heckeræ* sum up to only 93% of the total bacterial population (based on rRNA slot blot hybridization) indicating a hidden diversity that has escaped detection. For example, the intranuclear parasite belonging to the “*Ca. E. bathymodioli*” group was not detected by Duperron *et al.* [145]. Using FISH this parasite was found in *B. heckeræ* during this study (Zielinski *et al.*, manuscript II) [156]. Although its abundance has not been quantified it appears reasonable to assume that this bacterium contributes substantially to the total bacterial population.

A recent investigation of the potential parasitic burden in *B. puteoserpentis* using light microscopy revealed bacterial inclusions which were described as *Rickettsia*-like on the basis

of their intracellular occurrence. However, neither immunological nor molecular proof was provided that the inclusions indeed contained Rickettsiae [191]. Rickettsiae belong to the Alphaproteobacteria, however, the assessment of bacterial diversity performed during this PhD project revealed exclusively Gammaproteobacteria. Therefore, the bacterial inclusions described by Ward *et al.* [191] are either not Rickettsiae or escaped detection during this PhD project. The true location of the *Rickettsia*-like bacteria may have been intranuclear rather than intracytoplasmic since a greatly enlarged nucleus containing intranuclear bacteria could easily be mistaken for an intracytoplasmic inclusion at the level of light microscopy (Zielinski *et al.*, manuscript II) [156].

In conclusion, assessing endosymbiotic diversity with universal bacterial primers may not completely resolve bacterial diversity even if PCR cycles are kept to a minimum. The effect of over-amplifying major bacterial phylotypes and thus preventing the detection of possible minor phylotypes is well known [192]. However, other factors may contribute to the difficulties in detecting minor populations. To detect these it may be worthwhile to use more specific primers targeting distinct groups of marine bacteria. For example, attempts to amplify intranuclear bacteria from *B. azoricus* (Menez Gwen – Mid-Atlantic Ridge) during this PhD project using primers specific to “*Ca. E. bathymodioli*” resulted in the amplification of additional phylotypes. Out of eight clones one clone contained the 16S rRNA gene of the intranuclear phylotype, the remaining seven carried 16S rRNA genes belonging to other groups of marine Gammaproteobacteria (Table 11). Notably, the closest relatives of these seven clones all shared one or two mismatches in position 11 and / or 12 of the specific primer for “*Ca. E. bathymodioli*” (bnix-64F) (18 bases).. FISH targeting these groups was not performed, therefore, it remains unclear whether these phylotypes occur intracellularly or rather represent free-living bacteria that were associated with the gill sample. Nevertheless, the amplification of these phylotypes suggests that there may be even greater endosymbiotic diversity in bathymodiolin mussels than is currently suggested by recent studies [145,156].

Table 11. Phylotypes obtained from sequencing the 16S rRNA gene pool of *B. azoricus* using primers for the detection of intranuclear bacteria

Phylotype	A	B	C	D	E	F	G
closest relatives	Gammaproteobacteria					unclassified	
	Alteromonadales						
	<i>Colwellia psychroerythraea</i>		PVB_OTU_12 ^a	<i>Alteromonas addita</i>		CAR-SF ^b	M92 ^c
Identity [%]	98.7	98.1	98.5	98.7	99.7	99.6	97.2
Acc. No.	AF173964		U15115	AY682202	AB086227	AY136116	

^a clone associated with a microbial mat from a Hawaiian hydrothermal vent system; ^b marine carbazole-degrading bacterium; ^c clone sequenced from an eastern Mediterranean offshore seawater sample

Table 12 lists all primers and probes used to assess the endosymbiotic diversity of *B. puteoserpentis* during this study.

Table 12. List of primers and probes used in this study

primer / probe	application	sequence	target site ^a	reference
GM3F	PCR	5' AGA GTT TGA TCM TGG C 3'	8-23	[193]
GM4R	PCR	5' TAC CTT GTT ACG ACT T 3'	1492-1507	[193]
bnix-64F	PCR	5' AGC GGT AAC AGG TCT AGC 3'	64-81	this study
bnix-1267R	PCR	5' GCA GCT TCG CGA CCG TCT 3'	1249-1267	this study
518F	Sequencing	5' CCA GCA GCC GCG GTA AT 3'	518-534	[194]
534R	Sequencing	5' ATT ACC GCG GCT GCT GG 3'	518-534	[195]
1099F	Sequencing	5' GCA ACG AGC GCA ACC C 3'	1099-1114	[194]
1193R	Sequencing	5' CGT CAT CCM CAC CTT CCT C 3'	1175-1193	[194]
Bnix64	FISH	5' GCT AGA CCT GTT ACC GCT 3'	64-81	this study
Bnix643	FISH	5' CCG TAC TCT AGC CAC CCA 3'	643-660	this study
Bnix1249	FISH	5' GCA GCT TCG CGA CCG TCT 3'	1249-1267	this study
BMARt-193	FISH	5' CGA AGG TCC TCC ACT TTA 3'	193-210	[158]
BMARm-845	FISH	5' GCT CCG CCA CTA AGC CTA 3'	845-862	[158]
EUK516	FISH	5' ACC AGA CTT GCC CTC C 3'	502-517	[196]

^a according to *E. coli*

2.5 Outlook

2.5.1 Re-assessment of endosymbiotic diversity of *B. puteoserpentis*

For reasons mentioned above it may be worthwhile to re-assess the endosymbiotic diversity of *B. puteoserpentis*. This may be most easily performed by applying the probes specifically targeting the newly discovered symbionts in *B. heckerae* [145]. Furthermore, an alphaproteobacterial or *Rickettsia*-specific probe may confirm or exclude the presence of such bacteria from *B. puteoserpentis*. In addition, *B. puteoserpentis* may be investigated for minor bacterial populations using probes specifically targeting subgroups of the Gammaproteobacteria such as Alteromonadales and Oceanospirillales.

2.5.2 Further research on “*Ca. E. bathymodioli*”

Species or strains? The 16S rRNA sequences of intranuclear bacteria of the “*Ca. E. bathymodioli*” clade share an average identity of 98.8% (min 98.1%, max 99.7%; Table 13). Whether these 16S rRNA's belong to different strains of one and the same species or rather represent different species of intranuclear bacteria can not be concluded from their sequence identity. According to Stackebrandt and Goebel [197], 16S rRNA sequence identities above 97% do not allow a final prediction if a new bacterium is a strain of a described species or a separate species. Forney *et al.* [198] have shown that even among type species of bacteria many have more than 97% identical 16S rRNA genes and the same holds true for bacterial species within a certain genus. Therefore, other phylogenetic approaches such as DNA-DNA

hybridization, multilocus sequence typing (MLST) of house-keeping genes or genomic sequence analysis would be needed to clarify the relationships between the discovered intranuclear bacteria [199-201]. Since DNA-DNA hybridizations are rather elaborate and cultivation-dependent and whole genome sequencing both elaborate and costly, MLST may be the method of choice for further characterization of the “*Ca. E. bathymodioli*” clade.

Table 13. Sequence identity matrix of the predominant “*Ca. E. bathymodioli*” 16S rRNA phylotypes from several *Bathymodiolus* species

	1	2	3	4	5	6	7
1 <i>B. puteoserpentis</i> (Logatchev – MAR)	ID	0.997	0.995	0.982	0.997	0.985	0.985
2 <i>B. sp.</i> (Lilliput – MAR)	0.997	ID	0.995	0.981	0.995	0.983	0.985
3 <i>B. sp.</i> (Turtle Pits 1 – MAR)	0.995	0.995	ID	0.981	0.992	0.983	0.982
4 <i>B. sp.</i> (Turtle Pits 2 – MAR)	0.982	0.981	0.981	ID	0.981	0.997	0.987
5 <i>B. azoricus</i> (Menez Gwen – MAR)	0.997	0.995	0.992	0.981	ID	0.983	0.983
6 <i>B. aff thermophilus</i> (PAR)	0.985	0.983	0.983	0.997	0.983	ID	0.989
7 <i>B. brooksii</i> & <i>B. heckerae</i> (GoM)	0.985	0.985	0.982	0.987	0.983	0.989	ID

GoM, Gulf of Mexico; MAR, Mid-Atlantic Ridge; PAR, Pacific-Antarctic Ridge; ID - identical

Developmental cycle. One obscure step in the developmental cycle of “*Ca. E. bathymodioli*” is the transition from a single filament to a filamentous coil (Stage 2 to Stage 3). Repetitive filament duplication by longitudinal (binary) fission has been suggested as one explanation for the formation of this filamentous assembly based on microscopic observations (Zielinski *et al.*, manuscript II) [156]. However, it has alternatively been hypothesized that the filamentous assembly results from a single filament which, during growth, frequently intertwines (Zielinski *et al.*, manuscript II) [156]. Future FISH investigations of intranuclear bacteria of the “*Ca. E. bathymodioli*” clade should especially focus on this developmental stage to ultimately clarify the transition from Stage 2 to 3. Longitudinal (binary) fission is rare among bacteria and has to date only been described in the sulfur-oxidizing symbionts of three marine host genera, the nematode *Laxus* sp. [74,202,203], the gutless oligochaete *Olavius* [93,204], and the sand-dwelling ciliates of the genus *Kentrophoros* [74,93,205-209]. Nothing is known about the molecular mechanisms controlling this unusual mode of bacterial cell division.

Other questions arising from the current research on “*Ca. E. bathymodioli*” are for example its infection mode, movement through the cytoplasm, and penetrations of the host nucleus both during infection and outbreak. The only model interactions, that could give clues on how “*Ca. E. bathymodioli*” may infect host cells and penetrate nuclei, are the symbiosis between obligate intranuclear bacteria of the genus *Holospora* (Alphaproteobacteria) and their ciliate hosts of the genus *Paramecium* (Ciliophora) as well as the interaction between

facultative intranuclear Rickettsiae (Alphaproteobacteria) and their arthropod / mammalian hosts.

Mode of infection. *Holospora* bacteria enter their host by using its endocytotic means of ingesting food particles (phagocytosis) [210,211]. Although bathymodiolin mussels rely on their endosymbionts for nutritional supply they still retain the ability to filter-feed and a functional albeit reduced gut [212,213]. Therefore, endocytosis of bacteria thriving in hydrothermal fluids may still be an additional even though insufficient nutritional source. Noteworthy, Johnson and Le Pennec [214] described endocytosis of bacterial inclusions in the littoral bivalve *Loripes lucinalis* which similar to bathymodiolin mussels harbors endosymbiotic bacteria within its gills. Endocytosis is also assumed to be the mode of environmental acquisition of symbionts in *Bathymodiolus* mussels [189,215,216]. Therefore, entry of “*Ca. E. bathymodioli*” by means of endocytosis is likely but remains to be clarified.

Movement through the cytoplasm. Movement of “*Ca. E. bathymodioli*” through the cytoplasm may likely rely on passive transport since flagella appear to be absent. For example, non-motile *Holospora* bacteria are transported passively. After ingestion, *Holosporae* are released from the phagosome (food or digestive vacuole) before it coalesces with a lysosome [211]. This way it effectively escapes digestion. Remaining encircled by a host membrane it is later surrounded by vesicles of endoplasmic reticulum which form a transport vesicle [210]. Cytoskeleton-based transportation has been suggested for the bacterium-bearing vesicle but could not be confirmed [217]. In contrast, *Rickettsia bellii* appears to reach the nucleus by actin polymerization-based motility [218]. If “*Ca. E. bathymodioli*” is transported in a fashion similar to *Holospora* or *R. bellii* or if it has a different transport mechanism must at this time remain elusive but is worthwhile being investigated.

Penetration of nuclei. Two modi of invading nuclei have been suggested – passive or active invasion. *Holospora* bacteria invade their host nucleus passively almost as a Trojan horse: the membrane originating from the endoplasmic reticulum fuses with the nuclear membrane resulting in the release of the bacterium into the nucleus [210]. Passive invasion has also been suggested for the facultative intranuclear spotted fever group (SFG) Rickettsiae. Todd *et al.* [219] hypothesized that nuclear invasion is rather accidental than on purpose resulting from the fact that cytoplasmic Rickettsiae are simply trapped inside a dividing nucleus with no mechanism of escape. However, Heinzen *et al.* [220] have observed cytoplasmic Rickettsiae perturbing the nuclear envelope that appeared to be in the process of

penetration and proposed that SFG Rickettsiae directly penetrate the nuclear membrane, aided by the propulsive force of actin tail assembly and possibly, phospholipase activity. This indicates active nuclear invasion and evokes that one and the same mechanism, namely actin polymerization, could be used both for intracellular movement and nuclear penetration. The nuclear invasion mechanism suggested by Heinzen *et al.* [220] seems an appealing scenario for “*Ca. E. bathymodioli*” even though this scenario must at this time remain hypothetical.

Protective mechanism of bacteriocytes. Thorough microscopic FISH observations of mussel gill filaments indicated that only intercalary cells were infected with intranuclear bacteria whereas the symbiont-containing gill bacteriocytes were apparently never infected (Zielinski *et al.*, manuscript II) [156]. This observation has intriguing implications for the role of the chemoautotrophic and methanotrophic endosymbionts, suggesting a protective function besides their nutritional role. Therefore, future research on “*Ca. E. bathymodioli*” should address this phenomenon in more detail: How do bacteriocytes differ from intercalary cells and what is the symbiont contribution to this difference? Are there perhaps differences in the glycolization of lipid membranes making bacteriocytes unsusceptible to the infection since certain receptors may be missing? Could the acquisition of endosymbionts give clues to why bacteriocytes are not prone to an infection with intranuclear bacteria? *Bathymodiolus* spp. are assumed to obtain their endosymbionts from the environment by means of endocytosis through the gill epithelium [189,215,216]. However, apart from pit-like structures on the apical surface of bacteriocytes - indicative of endocytosis - no other proof for environmental acquisition has to date been given for bathymodiolin mussels. Besides, on the molecular level nothing is known about how the bacteria induce a specific endocytosis in gill bacteriocytes or how the bacteriocyte distinguishes between its symbionts and “contaminants”. Elucidating the acquisition of symbionts in *Bathymodiolus* spp. on the molecular level may help understand the exclusion of “*Ca. E. bathymodioli*” from the gill bacteriocytes.

2.5.3 *Further research on intranuclear bacteria in marine metazoa*

Bivalves with intranuclear bacteria. The previous descriptions of intranuclear bacteria in the Pacific razor clam *Siliqua patula* [221] and the venerid clam *Ruditapes decussatus* [222] on the basis of electron microscopy open the opportunity for a re-investigation of these parasites to clarify their phylogenetic position and developmental cycles. A great advantage of these bivalves over *B. puteoserpentis* is that they inhabit shallow water and can thus easily be sampled without the need of time-consuming and costly research cruises. Moreover, these species can be kept in culture. This fortunate fact may allow answering details in the host-

parasite interaction which are currently unresolved such as the infection mode of intranuclear bacteria, their passage through the cytoplasm, and their penetration of the host nucleus (see above).

Shellfish consumed by humans. Following the discovery of “*Ca. E. bathymodioli*”, intranuclear bacteria were also found in the venerid clam *R. philippinarum*, a close relative of *R. decussatus* (Zielinski *et al.*, manuscript II) [156]. Other shellfish from aquaculture are currently investigated and intranuclear bacteria have indeed been found in diverse species (Luciana Raggi, MPI for Marine Microbiology, Bremen – unpublished data). The intranuclear bacterium described from *S. patula* may be especially interesting for further characterization since this parasite is unusual for a bacterium in many ways. Its morphology has been described as multilayered, membrane-rich, complexly folded, and partially cleaved at dimensions of 25 x 16 μm [221]. Furthermore, there may be a commercial interest in a more comprehensive characterization of this parasite since it has been suggested to be involved in massive mortalities of razor clams [221,223]. A collaboration on the molecular characterization of the “Nuclear Inclusion X” has recently been suggested and was in principle affirmed (Ralph Elston, AquaTechnics Inc. – personal communication).

Sponges. The morphological description of intranuclear bacteria in *Aplysina* sponges [224,225] should be followed up by cloning and sequencing these bacteria to infer their specific phylogenetic placement. Noticeably, these bacteria and “*Ca. E. bathymodioli*” are similar in their filamentous morphology.

Vent and seep invertebrates. Previous light-microscopical investigations of vesicomid clams from cold seeps and lepetodrilid limpets from hydrothermal vents revealed bacterial inclusions which were described as “*Rickettsia*-like” on the basis of their intracellular occurrence [226,227]. Similar to the inclusions reported from *B. puteoserpentis* [191], their intracytoplasmic nature was neither confirmed with electron microscopy nor was immunological, morphological, or molecular proof provided that the inclusions indeed contained Rickettsiae. Since greatly enlarged nuclei typical for an infection with intranuclear bacteria could easily be mistaken for intracytoplasmic inclusions at the level of light microscopy these inclusions should thus be re-investigated using fluorescent probes to reveal if they might be intracellular.

Future studies of deep-sea vent and seep bivalves as well as shallow water bivalves hosting chemosynthetic endosymbionts (solemyid, lucinid, thyasirid, and vesicomid clams) should generally consider the existence of intranuclear bacteria since it appears reasonable to

assume that these are not restricted to bathymodiolin mussels. Additionally, other endosymbiont-containing vent and seep invertebrates should be considered including siboglinid tubeworms and alvinellid polychaetes (Annelida) as well as provannid snails and lepetodrilid limpets (Mollusca).

3 Endosymbiont activity

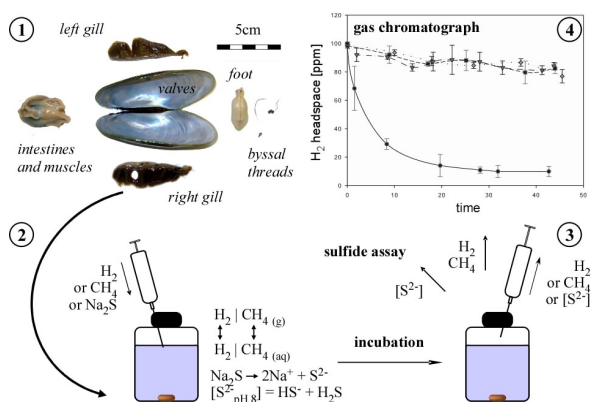


Fig. 21. Overview over on board incubation experiments. 1. Dissection. 2. Start of incubation by addition of inorganic energy source. Note that an equilibrium is established between aqueous and gaseous phases in case the electron donor is a gas. In contrast, sulfide completely dissolves in the aqueous phase and mainly speciates into free HS^- and dissolved H_2S . 3. Subsampling the gaseous (H_2 , CH_4) or aqueous ($\text{H}_2\text{S}/\text{HS}^-$) phase after discrete time points. 4. Results from gas chromatography. For more details see Zielinski *et al.*, manuscript III [157].

At the beginning of this PhD project the use of mRNA-FISH was proposed to evaluate the activity of the two chemosynthetic endosymbionts. A hybridization method targeting mRNA had just been developed [150,228]. The idea was to show the expression of functional genes coding for key enzymes involved in sulfur and methane oxidation pathways as well as in carbon fixation pathways. mRNA slot blot hybridization was proposed to quantify the expression of these functional genes to investigate how differing physico-chemical conditions affect the activity of the two chemosynthetic endosymbionts. mRNA-

FISH analyses of *B. puteoserpentis* symbionts indeed showed the expression of genes involved in sulfite (SO_3^{2-}) and methane oxidation and thus confirmed the sulfur- and methane oxidizing potential of the two mussel symbionts [146]. mRNA slot blot hybridizations have not yet been performed mainly because the characterization of mussel habitats turned out to be more complicated than expected and because *in situ* measurements performed during this PhD project suggested rather similar physico-chemical conditions (Zielinski *et al.*, manuscript I) [155]. The physico-chemical conditions of mussel microhabitats have been analyzed in more detail during the Hydromar II cruise (Table 9). Thus, the quantification of symbiont activity by means of mRNA slot blot hybridization is now meaningful and a correlation with physico-chemical data possible.

3.1 Evaluation of endosymbiotic activity by physiological experiments

Endosymbiotic activity can also be assessed by physiological experiments using symbiont-containing gill tissues of freshly collected mussels. This approach was developed in the course of this PhD project when it became apparent that the Logatchev hydrothermal fluids were extremely rich in hydrogen due to high and low temperature serpentinization processes. Hydrogen is a potential energy source for



Fig. 22. Mussel transplantation site.

chemolithotrophic bacteria but has never been shown to be utilized by any of the chemosynthetic symbionts from reducing environments. Thus, to get immediate evidence if hydrogen could be an energy source for the endosymbionts of *B. puteoserpentis*, hydrogen consumption experiments were performed on board the research vessel. And indeed, hydrogen was consumed by endosymbiotic bacteria (Zielinski *et al.*, manuscript III) [157]. The same approach was then applied in following cruises to evaluate hydrogen and sulfide consumption activities of mussel endosymbionts from Logatchev and the newly discovered vent fields south of the equator (Fig. 21). Consumption rates were compared with each other and with the abundance of hydrogen and sulfide at the sampling site (*in situ* concentration) allowing conclusions about whether or not differing concentrations of these electron donors affect symbiotic activity (Zielinski *et al.*, manuscript III) [157].

3.2 Results of H₂ and H₂S consumption experiments

Hydrogen was rapidly consumed by *B. puteoserpentis* (Logatchev) but only moderately by *B. sp.* (Comfortless Cove and Lilliput). However, consumption rates of *B. sp.* increased with elevated hydrogen partial pressures indicating that hydrogen uptake can be stimulated. In contrast, sulfide consumption rates did not differ in these mussels. Both hydrogen and sulfide stimulated carbon fixation in *B. puteoserpentis* gill tissues with similar CO₂ incorporation rates. Concurrent with hydrogen concentrations in high temperature and diffuse fluids our data indicate that chemoautotrophy in bathymodiolin mussels may be sulfur-based at basalt-hosted vent settings but hydrogen-based at ultramafic-hosted vents. At first approximation the Logatchev mussel population may oxidize 12-30 mol hydrogen per hour corresponding to 270-670 liters of hydrogen. Endosymbionts of *B. puteoserpentis* may therefore play an

appreciable role in hydrogen removal from diffuse fluids before hydrogen is issued into the open ocean (Zielinski *et al.*, manuscript III) [157].

3.3 Effect of mussel transplantation on hydrogen consumption rates

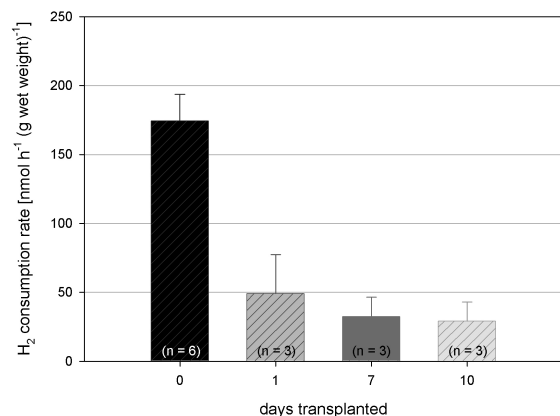


Fig. 23. Hydrogen consumption rates after removal of mussels from diffuse venting. Rates decreased substantially after only one day of transplantation and decreased only slightly more with longer transplantation intervals.

To examine if endobacterial hydrogen consumption is influenced by the presence or absence of hydrogen in the mussel environment, Logatchev mussels from the Irina II site were removed from diffuse venting using nets with a net-covered lid and deposited on bare ocean floor away from the active vent site, about 70 m northwest from the Irina II site and 110 m east of Quest, another active vent site (Fig. 22). The lid was closed to prevent predators from entering and mussels from escaping the nets. Nets were recovered 1, 2, 5, 7, and 10 days after

transplantation and gill tissues from mussels that had been transplanted for one, seven, and ten days were used for hydrogen consumption experiments. These gill tissues consumed hydrogen at 4 to 6-fold lower rates than mussels which had been sampled directly from diffuse venting (Table 14, Fig. 23).

Table 14. Hydrogen consumption rates for *B. puteoserpentis* (Logatchev) at 100 ppm partial pressure with fresh and transplanted gill tissue and various controls

tissue / control	site	Rate (Mean ± SD) ^a [nmol h ⁻¹ (g wet weight) ⁻¹]	n	H ₂ at site [μM]
gill	Irina II	174 ± 19	3	5.9 ^b
gill	Quest	169 ± 36	3	4.2 ^b
transplanted gill, 1 day	off diffuse venting	49 ± 28	3	nd
transplanted gill, 7 days	off diffuse venting	32 ± 14	3	nd
transplanted gill, 10 days	off diffuse venting	29 ± 14	3	nd
gill boiled	Irina II	0.4 ± 0.9*	3	5.4 ^b
foot	Irina II	0.2 ± 0.3*	2	5.4 ^a
seawater w/o tissue	-	0.5 ± 0.3*	10	-

^a Since the first measurement after the addition of hydrogen gas was made after eight to nine hours of incubation for transplanted gill tissues all consumption rates were calculated for this time interval. Thus, Irina II, Quest, and control consumption rates differ from the values given in Zielinski *et al.*, manuscript III [157] which were calculated for the first one to three hours. ^b T. Pape and R. Seifert, University of Hamburg, Institute for Biogeochemistry and Marine Chemistry, personal communication *rate in nmol h⁻¹, nd – not determined

There are at least two explanations for the decrease in hydrogen consumption rates: transcriptional regulation of genes involved in the hydrogen uptake machinery or symbiont digestion due to starvation. Two observations favor the regulation hypothesis: (i) hydrogen consumption rates of transplanted mussels were in the same range as consumption rates of Comfortless Cove and Lilliput mussels which inhabit diffuse-flow with only little dissolved hydrogen and (ii) hydrogen consumption was stimulated by increasing hydrogen partial pressures in Lilliput mussels (Zielinski *et al.*, manuscript III) [157]. Thus, the absence of hydrogen may inhibit the expression of genes involved in hydrogen uptake and the hydrogen

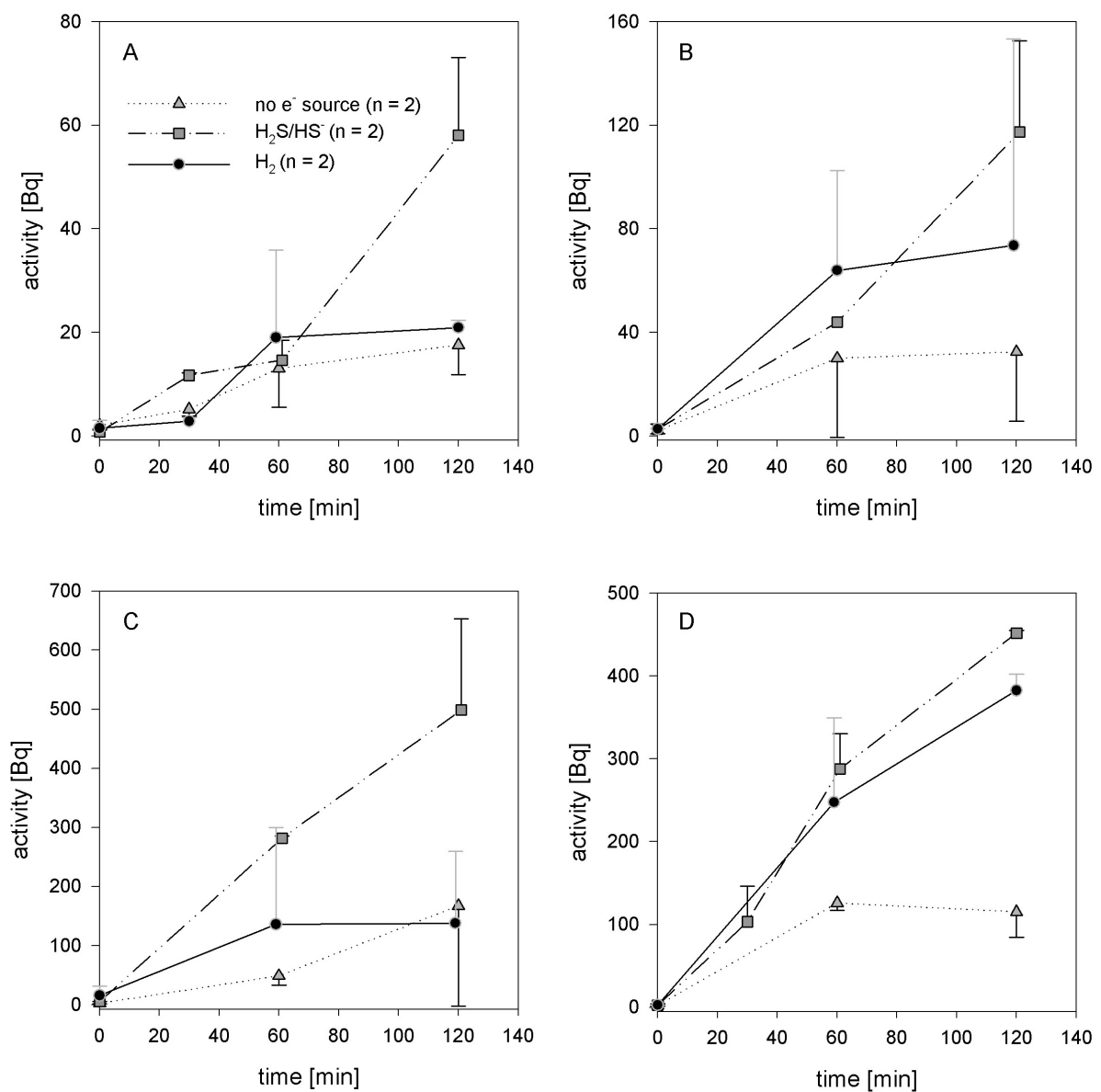


Fig. 24. $^{14}\text{CO}_2$ assimilation by endosymbiont-containing gill tissues of *B. puteoserpentis* (Logatchev). Hydrogen stimulated CO_2 fixation in 3 out of 8 individuals (1 out of 2 in B and 2 out of 2 in D) while sulfide had a stimulatory effect in all 8 investigated individuals. Error bars represent measurements of two individuals and are shown in only one direction. Diagrams A to C: Specimens from the Irina II site (different locations). Diagram D: Specimens from the Quest site. (Experiments were designed by F. Zielinski and performed by J. M. Struck and S. Wetzel.)

uptake machinery must first be synthesized and assembled under experimental conditions before hydrogen uptake can start. It appears reasonable to assume that the experimental conditions (0.08 μM dissolved hydrogen) may not have favored sufficient expression of hydrogen uptake genes in transplanted mussels to fully exploit the hydrogen uptake machinery.

Alternatively, due to the absence of not only hydrogen but alternative electron sources like sulfide and thiosulfate for the sulfur-oxidizing symbiont and methane for the methanotrophic endosymbiont, bacterial primary production may have fully ceased and the mussel may have started digesting its endosymbionts to survive the starvation period. In fact, FISH investigation of specimens that had been transplanted for ten days revealed that only 50% of the symbionts were left in the gill tissues (Dennis Fink, MPI for Marine Microbiology - MSc Thesis). Consumption rates after one and ten days of transplantation were not much different suggesting that symbiont digestion may proceed extremely fast. In fact, studies by Kochevar *et al.* [153] on “*Bathymodiolus*” *childressi*, a shallow water cold-seep mussel that hosts methanotrophic bacteria, have shown that mussels experienced a 90% reduction in symbiont numbers after placement for just 24 h in methane-free seawater in the laboratory.

FISH investigation of mussels that had been transplanted for only one day will certainly shed more light on the issue whether the low hydrogen consumption rates are due to gene regulation or endosymbiont digestion.

3.4 Carbon assimilation in the presence of hydrogen or sulfide

The discovery of hydrogen consumption in mussel symbionts suggested hydrogen oxidation with environmental oxygen and energy conservation via cyclic electron transport along a respiratory chain and the generation of a proton motive force to drive ATP synthesis. An indirect measure of energy conservation is CO_2 fixation which requires ATP. Thus, endosymbiont containing gill tissues of *B. sp.* (Comfortless Cove and Lilliput) and *B. puteoserpentis* (Logatchev) were incubated in the presence of $^{14}\text{CO}_2$ and hydrogen and for comparison in the presence of $^{14}\text{CO}_2$ and sulfide. Results from experiments with *B. sp.* gill tissues in the presence of hydrogen were ambiguous, presumably because experimental hydrogen concentrations were too low (0.08-2.3 μM) to account for energy conservation and thus carbon fixation. The experimental conditions were subsequently improved in experiments with *B. puteoserpentis* gill tissues (20 μM dissolved H_2) and hydrogen clearly stimulated carbon fixation in three out of eight individuals (Fig. 24). While these data indeed point to a stimulatory effect of hydrogen which is supported by molecular data (Zielinski *et*

al., manuscript III) [157] more experiments are clearly needed and have meanwhile been performed to corroborate this result.

In bathymodiolin mussels several studies have investigated if sulfide and thiosulfate stimulate carbon fixation in the chemoautotrophic endosymbiont of bathymodiolin mussels [141-144]. The stimulating effect of thiosulfate was shown in two studies with *B. thermophilus* from the East Pacific Rise [143,144]. However, only one study has thus far shown the stimulatory effect of sulfide [144]. Surprisingly, two independent studies on *B. puteoserpentis*

could not detect a stimulatory effect of sulfide or thiosulfate [141,142]. Data obtained during this PhD project clearly showed a stimulatory effect of sulfide in *B. puteoserpentis* gill tissues confirming that sulfide is an energy source for the chemoautotrophic symbiont (Fig. 24). One such experiment was also performed with *B. sp.* (Lilliput). Even though sulfide consumption rates were only low $^{14}\text{CO}_2$ was incorporated (Fig. 25).

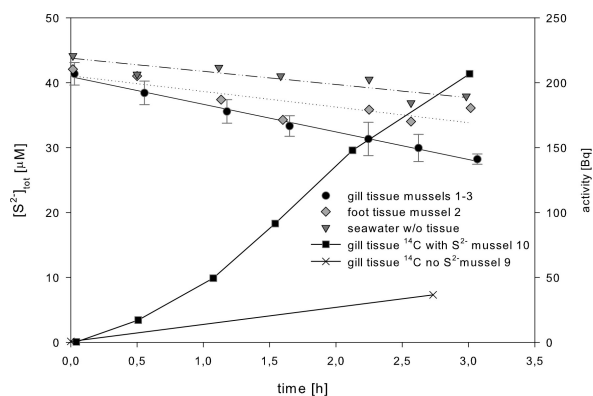


Fig. 25. Sulfide consumption and $^{14}\text{CO}_2$ assimilation by endosymbiont-containing gill tissue of Lilliput mussels. Upper three plots and left diagram axis: sulfide consumption over time. Lower two plots and right diagram axis: $^{14}\text{CO}_2$ assimilation over time.

3.5 Outlook / Experimental improvements

3.5.1 Consumption experiments

Hydrogen. Hydrogen consumption experiments with *B. puteoserpentis* gill tissues (Logatchev) were performed at very low dissolved hydrogen concentrations (77 nM) due to analytical constraints. However, hydrogen concentrations in Logatchev mussel habitats are in the micromolar range (4-6 μM minimum) and recent measurements even suggest concentrations up to 1 mM (R. Seifert, University of Hamburg, Institute for Biogeochemistry and Marine Chemistry, personal communication). Experiments with *B. sp.* gill tissues (Comfortless Cove and Lilliput) revealed that higher hydrogen partial pressures result in increased consumption rates (Zielinski *et al.*, manuscript III) [157]. Therefore, *B. puteoserpentis* hydrogen consumption rates at 77 nM dissolved hydrogen only provide a glimpse of the hydrogen consumption potential under *in situ* conditions. Indeed, careful extrapolation to 5 μM dissolved hydrogen suggested extraordinarily high hydrogen consumption rates (Zielinski *et al.*, manuscript III) [157].

Future experiments should attempt to determine hydrogen consumption rates of *B. puteoserpentis* gill tissues at *in situ* hydrogen concentrations. However, since hydrogen dissolves only poorly in aqueous solutions [229] high hydrogen partial pressures above this solution are necessary to achieve dissolved hydrogen concentrations in the micromolar range (Henry's law). Thus, due to the vast excess of hydrogen in the headspace as compared to the little amount of hydrogen in solution, gas chromatography may fail in resolving hydrogen consumption under these conditions. Nevertheless, a first step could be a series of consumption experiments at increasing hydrogen partial pressures as was done for *B. sp.* gill tissues (Zielinski *et al.*, manuscript III) [157]. Extrapolation through several data points (instead of just one) to *in situ* concentrations may then reveal if currently calculated consumption rates are underestimated.

To circumvent the constraints of gas chromatography these experiments could alternatively be done using Clark-type H₂ microsensors which are commercially available (www.unisense.com). A sealed incubation vial containing a gill tissue piece and fully filled with oxygen-saturated seawater can be supplemented with a hydrogen-saturated stock solution to the desired final concentration. The hydrogen content in the seawater can be monitored over time at any possible user-defined resolution. A sufficiently designed setup could simultaneously also monitor dissolved oxygen concentrations using Clark-type oxygen microsensors.

The advantage over gas chromatography is that hydrogen consumption can directly be measured in the seawater medium and that a headspace is not required. Furthermore, an almost unlimited number of data points can be recorded over time due to the high-resolution properties of this technique. With gas chromatography, hydrogen analysis is limited to a handful of measurements due to subsampling and manpower constraints and, with the focus on hydrogen analysis, the chromatographs used during this PhD project were also not set up for the analysis of oxygen. Another considerable advantage of microsensors is that they do not require as much equipment as gas chromatography and would allow performing hydrogen consumption experiments independent from gas chemists who, in collaboration with this PhD project, have thus far spent a considerable amount of their time on these experiments.

Sulfide / thiosulfate. A considerable drawback of sulfide consumption experiments using mussel tissues is the problem that endosymbiotic sulfide consumption can not reliably be distinguished from host mitochondrial sulfide consumption. Mitochondrial sulfide oxidation was first shown in the coastal clam *Solemya reidi* (Powell and Somero, 1986a) which like

bathymodiolin mussels hosts chemoautotrophic endosymbionts. Subsequently, this phenomenon was demonstrated in a wide range of organisms including polychaete worms, clams, fishes and chickens (Grieshaber and Volkel, 1998; Yong and Searcy, 2001). Obviously, mitochondrial sulfide oxidation is a means of sulfide detoxification, however, it may also be a means of energy conservation (Powell and Somero, 1986b; Yong and Searcy, 2001). Therefore, sulfide consumption of *Bathymodiolus* gill tissues is certainly the sum of endosymbiotic and mitochondrial sulfide oxidation. Even if the sulfide oxidation rate of foot tissue is subtracted from the gill tissue rate the resulting rate may not reliably be attributed to the chemoautotrophic endosymbionts. This is mainly because gill tissue which serves as an oxygen uptake organ is undeniably more efficient in gas and solute uptake than the structurally, morphologically, and physiologically differing foot tissue.

To reliably investigate the sulfur-oxidizing activity of the chemoautotrophic endosymbiont of bathymodiolin mussels from a physiological point of view thiosulfate consumption assays should be performed in addition to sulfide consumption assays. In fact, this non-toxic intermediate in sulfur oxidation is produced by many hydrothermal vent animals as a means of mitochondrial sulfide detoxification [230-232] and has been shown to serve as an energy source for the chemoautotrophic endosymbiont of *Bathymodiolus thermophilus* [143,144]. Even though thiosulfate accumulates in the blood of hydrothermal vent invertebrates (for example thiosulfate has been detected in the blood of *Calypptogena magnifica* at nearly millimolar levels [233]), blood concentrations should not interfere with experimental thiosulfate consumption assays due to the use of tissue pieces rather than whole mussels or whole gills. Thiosulfate can be analyzed by iodometric titration [234]. However, since this method also determines nitrite, care should be taken that the seawater incubation medium does not contain any nitrite or subsamples should simultaneously be analysed for nitrite which can be determined spectrophotometrically [235].

Methane. Methane consumption experiments were performed with mussels from southern MAR vents in collaboration with S. Weber (University of Hamburg, Institute for Biogeochemistry and Marine Chemistry) using gas chromatography but yielded no results due to analytical difficulties. Determining methane consumption rates of the methanotrophic endosymbionts would be useful for comparison with symbiotic hydrogen- and sulfur-oxidizing activities and also for the correlation to *in situ* methane concentrations. This could theoretically be accomplished with a methane microsensor. A microscale methane biosensor containing methanotrophic bacteria has been developed for use under normal pressure, however, oxygen interferes with the signal [236]. Besides, the methane sensor project has

been discontinued due to the lengthy production process and the difficulties involved in keeping the sensor functional (www.unisense.com). Thus, the methane biosensor is commercially unavailable (www.unisense.com). Therefore, future methane consumption experiments would have to rely on commercially available slow-responding methane sensors (response time > 10 min) or gas chromatography.

Combinations of electron donors. If research funding, ship time, board equipment, and manpower allows, incubation experiments could be extended to using combinations of the three electron donors (H_2/S_{red} , H_2/CH_4 , S_{red}/CH_4 , $H_2/S_{red}/CH_4$ [$S_{red} = H_2S$ or $S_2O_3^{2-}$]). This would show if one electron source is consumed preferentially over another. Especially interesting would be combining hydrogen with one of the two reduced sulfur compounds (H_2S , $S_2O_3^{2-}$) since both appear to be energy sources for the chemoautotrophic endosymbiont [143,144,157]. However, the energy yield from aerobic hydrogen oxidation is higher than from H_2S or thiosulfate oxidation (-528 kJ mol^{-1} versus $-378 / -384 \text{ kJ mol}^{-1}$, respectively per mol oxygen at 4°C) [237] indicating preferential growth on hydrogen. Another advantage of aerobic hydrogen oxidation is that it does not require reverse electron transport for the generation of reducing equivalents. However and most strikingly, hydrogen oxidation in the free-living sulfur- and ferrous iron oxidizing chemoautotroph *Acidithiobacillus ferrooxidans* appears to be repressed in the presence of sulfide and ferrous iron suggesting preferential growth on these substrates [238]. Further work is clearly needed to shed light on this issue.

In situ consumption experiments. Belkin *et al.* [143] showed that the chemoautotrophic symbiont of *B. thermophilus* consumed CO_2 at normal pressure at similar rates as under *in situ* pressure (250 atm). This indicates that consumption rates determined on board and under normal pressure may not significantly differ from *in situ* rates. Others, however have argued that experimental setups should mimic *in situ* conditions as closely as possible. Realistic consumption rates may thus only be acquired from incubation experiments performed *in situ* at 3000 m depth, within hydrothermal diffuse flow, in total darkness, and thus at true *in situ* physico-chemical conditions. In fact, *in situ* incubation experiments are technically possible using benthic respiration chambers equipped with sensors recording oxygen, hydrogen sulfide, hydrogen, and CO_2 concentrations as well as the pH and temperature. As an alternative to sensors a respiration chamber could also be coupled to a commercially available deep-sea gas analyzer (see chapter 0.1.5). With the help of an ROV such a respiration chamber could be placed on top of a mussel bed, individual mussels placed inside and the chamber tightly closed. Since *in situ* physico-chemical studies performed during this PhD project have shown that electron donor and acceptor concentrations ~ 10 cm above mussel

beds are sufficient to fuel aerobic sulfide oxidation (Zielinski *et al.*, manuscript I) [155] it can be assumed that hydrogen and methane are also sufficiently abundant above mussel beds. Thus, the respiration chamber can simply make use of the surrounding seawater without additional supplementation of electron donors or acceptors. For higher electron donor concentrations sulfide, hydrogen, and methane stock solutions could be injected into the respiration chamber via individual pre-filled gas-tight syringes connected to the chamber. After incubation the mussel can be anesthetized *in situ* using isotonic magnesium chloride upon which its muscles will relax and the shells open followed by *in situ* fixation with formaldehyde [239]. Both the relaxant and the preservative can be supplemented via pre-filled syringes connected to the respiration chamber.

The analysis of sensor or gas analyzer recordings would reveal simultaneous *in situ* oxygen, sulfide, hydrogen, CO₂, and methane consumption rates and would show how consumption rates respond to aerobic, microaerobic and anaerobic conditions. The fixed gill tissues could then be analyzed with available molecular tools for symbiont activity, abundance, and distribution.

3.5.2 Carbon fixation experiments

Hydrogen. Endosymbiotic CO₂ assimilation in the presence of hydrogen implies that it is the chemoautotrophic symbiont that derives energy from hydrogen oxidation which is supported by molecular data whereas the methanotroph may or may not conserve energy from this process (Zielinski *et al.*, manuscript III) [157]. Even though CO₂ fixation pathways have thus far not been described in type I methanotrophs [114] to which the methanotrophic endosymbiont is phylogenetically related, CO₂ fixation by the methanotrophic symbiont can also not firmly be ruled out at this point. To corroborate the stimulatory effect of hydrogen on carbon assimilation and to unambiguously assign hydrogen an energy source to the chemoautotrophic symbiont additional ¹⁴CO₂ assimilation experiments should be performed followed by microautoradiography in combination with FISH (MAR-FISH).

Sulfide and thiosulfate. Future experiments should also investigate the stimulatory effect of thiosulfate and calculate and compare the CO₂ incorporation rates in the presence of hydrogen, sulfide, or thiosulfate. Care should be taken that gill tissue pieces for all of these experiments and a negative control in the absence of an electron source come from the same individual since apparently there is a substantial variety in physiological activity even in individuals from the same location.

Methane. In contrast to chemoautotrophic assimilatory CO₂ fixation via the Calvin Cycle methanotrophs generally fix carbon from methane dissimilatorily. Only a small percentage is incorporated into biomolecules while the remainder is excreted as CO₂ and organic acids (formate and acetate) [142]. Dissimilatory carbon fixation experiments using ¹⁴CH₄ and unlabelled methane have been performed at Logatchev with *B. puteoserpentis* but still await analysis in the laboratory.

***In situ* carbon fixation experiments.** As with consumption experiments carbon fixation experiments could also be performed *in situ* using benthic incubation chambers. However, the instrument should be set up outside the influence of diffuse hydrothermal venting in ambient seawater to exclude the effect of multiple electron sources. A sole electron donor could be supplemented via a gas-tight syringe followed by the addition of the ¹⁴C-labelled inorganic carbon source (¹⁴CO₂ or ¹⁴CH₄). Consumption of electron donors and oxygen can be recorded during the experiment and the mussel subsequently anesthetized and fixed as described above. ¹⁴C activity in the mussel tissues would have to be analyzed on board or in the home laboratory.

3.5.3 *Cultivation*

To date chemosynthetic symbionts of invertebrates inhabiting reducing environments have consistently evaded culture [65]. While vertically transmitted endosymbionts which are passed from generation to generation may indeed be uncultivable outside their hosts, horizontally transmitted symbionts are in theory cultivable since they are acquired from the environment with each generation anew and thus their developmental cycle must include a free-living stage. Accumulating evidence indicates that bathymodiolin mussels transmit their chemoautotrophic and methanotrophic symbionts horizontally [146,189,215]. If the free-living stage of these symbionts is not just a resting stage but a physiologically active stage chances are that these chemoautotrophs can be cultivated outside their hosts. Cultivation attempts have likely been many since chemoautotrophic bacteria were discovered in *Riftia pachyptila* [240]. However, no paper documents any of these attempts. However, it appears reasonable to assume that most attempts to cultivate the chemoautotroph and the methanotroph were based on reduced sulfur compounds and methane, respectively as sole energy sources since these are the dominating inorganic chemicals in reducing habitats.

I suggest re-attempting cultivation of both the chemoautotrophic and methanotrophic endosymbionts of bathymodiolin mussels focusing on and including hydrogen as an energy source. Hydrogen consumption experiments using *B. sp.* gill tissues from the Lilliput diffuse

hydrothermal vent field have shown that hydrogen was consistently consumed over nine days whereupon the experiment had to be discontinued. This extended period of presumably endosymbiotic activity suggests that the endosymbionts may be kept in culture and perhaps isolated using hydrogen as sole or auxiliary energy source.

4 General conclusions

Bathymodiolus mussels with sulfur- and methane oxidizing endosymbionts from two hydrothermal settings on the slow-spreading Mid-Atlantic Ridge were investigated in this PhD thesis: *B. puteoserpentis* from the ultramafic-hosted Logatchev hydrothermal vent field at 14°45'N and *B. sp.* from the basalt-hosted hydrothermally active area at 4°48'S. *In situ* habitat characterization of Logatchev mussels using microsensors revealed abundant H₂S and O₂ in diffuse fluids emanating from the mussel beds. Thus, Logatchev mussel habitats, previously suggested to be deficient in free sulfide, comply with the requirements of aerobic sulfur-oxidation and support the sulfur-oxidizing symbiont. The Logatchev *in situ* measurements indicate that sulfide may also be present and bioavailable in diffuse fluids from similar high-temperature ultramafic-hosted vent systems which occur more often than previously recognized along slow- and ultraslow spreading ridges. Assessment of bacterial diversity in *B. puteoserpentis* revealed an intranuclear parasite, “*Candidatus* Endonucleobacter bathymodioli”, in addition to the beneficial sulfur- and a methane-oxidizing endosymbionts. This parasite exclusively occurred inside mussel nuclei of all tissues, however, bacteriocyte nuclei appeared to be free of the infection. Its cell cycle is the first to be reported from an intranuclear bacterium of metazoans. “*Ca. Endonucleobacter bathymodioli*” was subsequently also found in *B. sp.* from the hydrothermally active area at 4°48'S and in other *Bathymodiolus* species from both hydrothermal vents and cold seeps around the world. Accumulating evidence indicates that intranuclear bacteria are widespread in marine metazoans, including shellfish consumed by humans. Assessment of endosymbiotic activity by physiological experiments implied that endosymbiotic chemoautotrophy may be sulfur-based at the basalt-hosted vents at 4°48'S but hydrogen-based at the ultramafic-hosted Logatchev vent field. Indeed, the mussel population at Logatchev may oxidize 270-670 liters of hydrogen per hour. Endosymbionts of *B. puteoserpentis* may therefore play an appreciable role as H₂-oxidizing primary producers and thus in converting H₂-derived geochemical energy into biomass. In fact, H₂ has not been shown previously to be utilized by symbionts of invertebrates from reducing environments. This PhD thesis is an important contribution to the

research on deep-sea hydrothermal vents and may help improving our understanding of hydrothermal ecosystems in their complexity.

III References

1. Haase KM, Petersen S, Koschinsky A, Seifert R, Devey CW, et al. (2007) Young volcanism and related hydrothermal activity at 5°S on the slow-spreading southern Mid-Atlantic Ridge. *Geochem Geophys Geosyst* 8: Q11002, doi: 11010.11029 / 12006GC001509.
2. Koschinsky A, Billings A, Devey CW, Dubilier N, Duester A, et al. (2006) Discovery of new hydrothermal vent fields on the Southern Mid-Atlantic Ridge (4°S - 10°S) during Cruise M68/1. *InterRidge News* 15: 9-15.
3. Bird P (2003) An updated digital model of plate boundaries. *Geochem Geophys Geosyst* 4: 1027, doi: 1010.1029 / 2001GC000252.
4. Van Dover CL (2000) *The ecology of deep-sea hydrothermal vents*. Princeton, New Jersey: Princeton University Press. 424 p.
5. Snow JE, Edmonds HN (2007) Ultraslow-spreading ridges. *Oceanography* 20: 90-101.
6. Desbruyères D, Segonzac M, Bright M, (editors) (2006) *Handbook of Deep-Sea Hydrothermal Vent Fauna*. *Denisia* 18: 544 pp.
7. Ramirez-Llodra E, Shank TM, German CR (2007) Biodiversity and biogeography of hydrothermal vent species. *Oceanography* 20: 30-41.
8. Dick HJB, Lin J, Schouten H (2003) An ultraslow-spreading class of ocean ridge. *Nature* 426: 405-412.
9. Langmuir CH, Forsyth DW (2007) Mantle melting beneath mid-ocean ridges. *Oceanography* 20: 78-89.
10. Martinez F, Okino K, Ohara Y, Reysenbach A-L, Goffredi SK (2007) Back-arc basins. *Oceanography* 20: 116-127.
11. Baker ET, German CR (2004) On the global distribution of hydrothermal vent fields. In: German CR, Lin J, Parson LM, editors. *Mid-ocean ridges: hydrothermal interactions between the lithosphere and oceans*, *Geophysical Monograph Series* 148: American Geophysical Union. pp. 245-266.
12. Juniper SK, Escartin J, Cannat M (2007) Monitoring and observatories. *Oceanography* 20: 128-137.
13. Tunncliffe V (1991) The biology of hydrothermal vents: ecology and evolution. *Oceanogr Mar Biol Annu Rev* 29: 319-407.
14. Kelley DS, Baross JA, Delaney JR (2002) Volcanoes, fluids, and life at mid-ocean ridge spreading centers. *Annu Rev Earth Planet Sci* 30: 385-491.
15. German CR, Lin J (2004) The thermal structure of oceanic crust, ridge-spreading and hydrothermal circulation: how well do we understand their inter-connections. In: German CR, Lin J, Parson LM, editors. *Mid-ocean ridges: hydrothermal interactions between the lithosphere and oceans*, *Geophysical Monograph Series* 148: American Geophysical Union. pp. 1-18.
16. Stein CA, Stein S (1994) Constraints on hydrothermal heat flux through the oceanic lithosphere from global heat flow. *J Geophys Res* 99: 3081-3096.
17. Tivey MK (2007) Generation of seafloor hydrothermal vent fluids and associated mineral deposits. *Oceanography* 20: 50-65.
18. Kadko D, Baross J, Alt J (1995) The magnitude and global implications of hydrothermal flux. In: Humphris SE, Zierenberg RA, Mullineaux LS, Thomson RE, editors. *Seafloor hydrothermal systems: physical, chemical, biological, and geological interactions* *Geophysical Monograph* 91. Washington, DC: American Geophysical Union. pp. 446-466.
19. German CR, Von Damm KL (2006) Hydrothermal Processes, pp. 181-222. In *The Oceans and Marine Geochemistry* (ed H Elderfield) Vol 6 *Treatise on Geochemistry* (eds HD Holland and KK Turekian) 1ed. Oxford, UK: Elsevier-Pergamon.
20. Tolstoy M, Waldhauser F, Bohnenstiehl DR, Weekly RT, Kim WY (2008) Seismic identification of along-axis hydrothermal flow on the East Pacific Rise. *Nature* 451: 181-184.
21. Cannat M, Lagabriele Y, Bougault H, Casey J, deCoutures N, et al. (1997) Ultramafic and gabbroic exposures at the Mid-Atlantic Ridge: geological mapping in the 15°N region. *Tectonophysics* 279: 193-213.
22. Tunncliffe V, McArthur AG, McHugh D (1998) A biogeographical perspective of the deep-sea hydrothermal vent fauna. In: Blaxter JHS, Douglas B, Tyler PA, editors. *Advances in Marine Biology*, Vol 34. San Diego: Academic Press. pp. 353-442.
23. Wetzel LR, Shock EL (2000) Distinguishing ultramafic- from basalt-hosted submarine hydrothermal systems by comparing calculated vent fluid compositions. *J Geophys Res* 105: 8319-8340.
24. Schmidt K, Koschinsky A, Garbe-Schönberg D, de Carvalho LM, Seifert R (2007) Geochemistry of hydrothermal fluids from the ultramafic-hosted Logatchev hydrothermal field, 15°N on the Mid-Atlantic Ridge: Temporal and spatial investigation. *Chem Geol* 242: 1-21.
25. Douville E, Charlou JL, Oelkers EH, Bienvenu P, Colon CFJ, et al. (2002) The rainbow vent fluids (36°14'N, MAR): the influence of ultramafic rocks and phase separation on trace metal content in Mid-

- Atlantic Ridge hydrothermal fluids. *Chem Geol* 184: 37-48.
26. Charlou JL, Donval JP, Fouquet Y, Jean-Baptiste P, Holm N (2002) Geochemistry of high H₂ and CH₄ vent fluids issuing from ultramafic rocks at the Rainbow hydrothermal field (36°14'N, MAR). *Chem Geol* 191: 345-359.
27. Charlou JL, Donval JP, Jean-Baptiste P, Dapoigny A (1996) Gases and helium isotopes in high temperature solutions sampled before and after ODP Leg 158 drilling at TAG hydrothermal field (26°N, MAR). *Geophys Res Lett* 23: 3491-3494.
28. Allen DE, Seyfried WE (2003) Compositional controls on vent fluids from ultramafic-hosted hydrothermal systems at mid-ocean ridges: An experimental study at 400°C, 500 bars. *Geochim Cosmochim Acta* 67: 1531-1542.
29. Sleep NH, Meibom A, Fridriksson T, Coleman RG, Bird DK (2004) H₂-rich fluids from serpentinization: geochemical and biotic implications. *Proc Natl Acad Sci USA* 101: 12818-12823.
30. Bach W, Paulick H, Garrido CJ, Ildefonse B, Meurer WP, et al. (2006) Unraveling the sequence of serpentinization reactions: petrography, mineral chemistry, and petrophysics of serpentinites from MAR 15°N (ODP Leg 209, Site 1274). *Geophys Res Lett* 33.
31. Allen DE, Seyfried WE (2004) Serpentinization and heat generation: Constraints from Lost City and Rainbow hydrothermal systems. *Geochim Cosmochim Acta* 68: 1347-1354.
32. Berndt ME, Allen DE, Seyfried WE (1996) Reduction of CO₂ during serpentinization of olivine at 300°C and 500 bar. *Geology* 24: 351-354.
33. Foustoukos DI, Seyfried WE (2004) Hydrocarbons in hydrothermal vent fluids: The role of chromium-bearing catalysts. *Science* 304: 1002-1005.
34. Proskurowski G, Lilley MD, Seewald JS, Früh-Green GL, Olson EJ, et al. (2008) Abiogenic hydrocarbon production at Lost City hydrothermal field. *Science* 319: 604-607.
35. Seyfried WE, Foustoukos DI, Allen DE (2004) Ultramafic-hosted hydrothermal systems at mid-ocean ridges: chemical and physical controls on pH, redox and carbon reduction reactions. In: German CR, Lin J, Parson LM, editors. *Mid-ocean ridges: hydrothermal interactions between the lithosphere and oceans*, Geophysical Monograph Series 148: American Geophysical Union. pp. 267-284.
36. Kelley DS, Karson JA, Blackman DK, Früh-Green GL, Butterfield DA, et al. (2001) An off-axis hydrothermal vent field near the Mid-Atlantic Ridge at 30°N. *Nature* 412: 145-149.
37. Kelley DS, Karson JA, Früh-Green GL, Yoerger DR, Shank TM, et al. (2005) A serpentinite-hosted ecosystem: The Lost City hydrothermal field. *Science* 307: 1428-1434.
38. Proskurowski G, Lilley MD, Kelley DS, Olson EJ (2006) Low temperature volatile production at the Lost City Hydrothermal Field, evidence from a hydrogen stable isotope geothermometer. *Chem Geol* 229: 331-343.
39. Von Damm KL, Edmond JM, Grant B, Measures CI (1985) Chemistry of submarine hydrothermal solutions at 21°N, East Pacific Rise. *Geochim Cosmochim Acta* 49: 2197-2220.
40. Welhan J, Craig H (1983) Methane, hydrogen, and helium in hydrothermal fluids at 21°N on the East Pacific Rise. In: Rona PA, Boström K, Laubier L, Smith KL, editors. *Hydrothermal Processes at Seafloor Spreading Centers*. New York, NY: NATO Conference Series IV:12, Plenum Publishing Corp. pp. 391-409.
41. German CR, Von Damm KL (2004) Hydrothermal Processes. In: Holland HD, Turekian KK, editors. *Treatise on geochemistry, volume 6: The oceans and marine geochemistry*: Elsevier, Oxford, UK. pp. 181-222.
42. Trefry JH, Butterfield DB, Metz S, Massoth GJ, Trocine RP, et al. (1994) Trace metals in hydrothermal solutions from cleft segment on the southern Juan de Fuca Ridge. *J Geophys Res* 99: 4925-4935.
43. Ishibashi J-I, Urabe T (1995) Hydrothermal activity related to arc-backarc magmatism in the western Pacific. In: Taylor B, editor. *Backarc Basins: Tectonics and Magmatism*. New York, NY: Plenum. pp. 451-495.
44. Kelley DS (2005) From mantle to microbes: The Lost City hydrothermal fields. *Oceanography* 18: 32-45.
45. Tao C, Lin J, Guo S, Chen YJ, Wu G, et al. (2007) Discovery of the first active hydrothermal vent field at the ultraslow spreading Southwest Indian Ridge: The Chinese DY115-19 cruise. *InterRidge News* 16: 25-26.
46. Tarasov VG, Gebruk AV, Mironov AN, Moskalev LI (2005) Deep-sea and shallow-water hydrothermal vent communities: two different phenomena? *Chem Geol* 224: 5-39.
47. Haase KM, Koschinsky A, Devey CW, Fretzdorff S, German C, et al. (2007) Diking, young volcanism and diffuse hydrothermal activity on the southern Mid-Atlantic Ridge. *Marine Geology*: submitted.
48. Jørgensen BB, Boetius A (2007) Feast and famine - microbial life in the deep-sea bed. *Nat Rev Microbiol* 5: 770-781.
49. Fisher CR, Takai K, Le Bris N (2007) Hydrothermal vent ecosystems. *Oceanography* 20: 14-23.
50. Jannasch HW, Mottl MJ (1985) Geomicrobiology of deep-sea hydrothermal vents. *Science* 229: 717-725.
51. Jannasch HW (1995) Microbial interactions with hydrothermal fluids. In: Humphris SE, Zierenberg

- RA, Mullineaux LS, Thomson RE, editors. Seafloor hydrothermal systems: physical, chemical, biological, and geological interactions Geophysical Monograph 91. Washington, DC: American Geophysical Union. pp. 273-296.
52. Kutschera U, Niklas KJ (2005) Endosymbiosis, cell evolution, and speciation. *Theory Biosci* 124: 1-24.
53. Sapp J (1994) Evolution by association: a history of symbiosis. New Oxford, Oxford: Oxford University Press. 272 p.
54. Schwendener S (1867) Über die wahre Natur der Flechten. *Verhandlungen der Schweizerischen Naturforschenden Gesellschaft in Rheinfelden* 51: 88-90.
55. Schwendener S (1868) Untersuchungen über den Flechtenthallus. *Beiträge zur wissenschaftlichen Botanik* 6: 195-207.
56. Schwendener S (1869) Die Algentypen der Flechtengonidien. Programm für die Rectorsfeier der Universität Basel 4.
57. Sapp J, Carrapiço F, Zolotonosov M (2002) Symbiogenesis: The hidden face of Constantin Merezhkowsky. *Hist Philos Life Sci* 24: 413-440.
58. Frank AB (1877) Über die biologischen Verhältnisse des Thallus einiger Krustenflechten. *Beiträge zur Biologie der Pflanzen* 2: 123-200.
59. de Bary A (1878) Vortrag: Über Symbiose. *Tagblatt der 51. Versammlung Deutscher Naturforscher und Aerzte in Cassel*. Kassel: Baier & Lewalter. pp. 121-126.
60. de Bary A (1879) 'Die Erscheinung der Symbiose', Vortrag auf der Versammlung der Deutschen Naturforscher und Aerzte zu Cassel. Strassburg: Verlag von Karl J. Trubner. pp. 1-30.
61. Wilkinson DM (2001) At cross purposes - how do we cope with scientific terms that have two different definitions? *Nature* 412: 485-485.
62. Smith DC (2001) Symbiosis research at the end of the millenium. *Hydrobiologia* 461: 49-54.
63. Hentschel U, Steinert M, Hacker J (2000) Common molecular mechanisms of symbiosis and pathogenesis. *Trends Microbiol* 8: 226-231.
64. Stewart FJ, Newton ILG, Cavanaugh CM (2005) Chemosynthetic endosymbioses: adaptations to oxic-anoxic interfaces. *Trends Microbiol* 13: 439-448.
65. Cavanaugh CM, McKiness ZP, Newton ILG, Stewart FJ (2006) Marine chemosynthetic symbioses. In: Dworkin M, Falkow S, Rosenberg E, Schleifer KH, Stackebrandt E, editors. *The Prokaryotes*. 3 ed. Berlin, Heidelberg: Springer-Verlag. pp. 473-507.
66. Shank T (2004) The evolutionary puzzle of seafloor life. *Oceanus* 42: 1-8.
67. Van Dover CL, German CR, Speer KG, Parson LM, Vrijenhoek RC (2002) Evolution and biogeography of deep-sea vent and seep invertebrates. *Science* 295: 1253-1257.
68. Desbruyères D, Segonzac M, Bright M, (editors) (2006) Handbook of Deep-Sea Hydrothermal Vent Fauna. *Denisia* 18: 544 pp. Supplement & Corrigendum, December 2006, web site: www.noc.soton.ac.uk/chess/handbook.php.
69. Sibuet M, Olu K (1998) Biogeography, biodiversity and fluid dependence of deep-sea cold-seep communities at active and passive margins. *Deep-Sea Res II* 45: 517-567.
70. Sibuet M, Olu-Le Roy K (2002) Cold seep communities on continental margins: Structure and quantitative distribution relative to geological and fluid venting patterns. In: Wefer G, Billett D, Hebbeln D, Jørgensen BB, Schlüter M et al., editors. *Ocean Margin Systems*. Berlin, Heidelberg: Springer-Verlag. pp. 235-251.
71. Smith CR, Baco AR (2003) Ecology of whale falls at the deep-sea floor. *Oceanogr Mar Biol Annu Rev*. pp. 311-354.
72. Musat N, Giere O, Gieseke A, Thiermann F, Amann R, et al. (2007) Molecular and morphological characterization of the association between bacterial endosymbionts and the marine nematode *Astomonema* sp from the Bahamas. *Environ Microbiol* 9: 1345-1353.
73. Ott J, Bright M, Bulgheresi S (2004) Symbioses between marine nematodes and sulfur-oxidizing chemoautotrophic bacteria. *Symbiosis* 36: 103-126.
74. Ott J, Bright M, Bulgheresi S (2005) Marine microbial thiotrophic ectosymbioses. *Oceanogr Mar Biol Annu Rev* 42: 95-118.
75. Palacios C, Zbinden M, Baco AR, Treude T, Smith CR, et al. (2006) Microbial ecology of deep-sea sunken wood: quantitative measurements of bacterial biomass and cellulolytic activities. *Cah Biol Mar* 47: 415-420.
76. Gros O, Guibert J, Gaill F (2007) Gill-symbiosis in Mytilidae associated with wood fall environments. *Zoomorphology* 126: 163-172.
77. Duperron S, Laurent MCZ, Gaill F, Gros O (2008) Sulphur-oxidizing extracellular bacteria in the gills of Mytilidae associated with wood falls. *FEMS Microbiol Ecol* 63: 338-349.
78. Wolff T (2005) Composition and endemism of the deep-sea hydrothermal vent fauna. *Cah Biol Mar* 46: 97-104.
79. Southward EC, Gebruk A, Kennedy H, Southward AJ, Chevaldonne P (2001) Different energy sources for three symbiont-dependent bivalve molluscs at the Logatchev hydrothermal site (Mid-Atlantic Ridge). *J Mar Biol Assoc UK* 81: 655-661.
80. Taylor JD, Glover EA (2006) Lucinidae (Bivalvia) - the most diverse group of chemosymbiotic molluscs. *Zool J Linn Soc* 148: 421-438.
81. Desbruyères D (2006) *Acharax alinae* Métevier & Cosel, 1993. *Denisia* 18: p149. Supplement &

- Corrigendum, December 2006, web site: www.noc.soton.ac.uk/chess/handbook.php.
82. von Cosel R (2006) *Gigantidas gladius* Cosel & Marshall, 2003. *Denisia* 18: p162. Supplement & Corrigendum, December 2006, web site: www.noc.soton.ac.uk/chess/handbook.php.
83. Luther III GW, Rozan TF, Taillefert M, Nuzzio DB, Di Meo C, et al. (2001) Chemical speciation drives hydrothermal vent ecology. *Nature* 410: 813-816.
84. Chevalloné P, Desbruyères D, Childress JJ (1992)...and some even hotter. *Nature* 359: 593-594.
85. Vacelet J, Boury-Esnault N, Fiala-Medioni A, Fisher CR (1995) A methanotrophic carnivorous sponge. *Nature* 377: 296-296.
86. Vacelet J, Fiala-Medioni A, Fisher CR, Boury-Esnault N (1996) Symbiosis between methane-oxidizing bacteria and a deep-sea carnivorous cladorhizid sponge. *Mar Ecol Prog Ser* 145: 77-85.
87. Vacelet J (2006) New carnivorous sponges (Porifera, Poecilosclerida) collected from manned submersibles in the deep Pacific. *Zool J Linn Soc* 148: 553-584.
88. Kouris A, Juniper SK, Frébourg G, Gaill F (2007) Protozoan-bacterial symbiosis in a deep-sea hydrothermal vent folliculinid ciliate (*Folliculinopsis* sp.) from the Juan de Fuca Ridge. *Mar Ecol* 28: 63-71.
89. Schmaljohann R, Flügel HJ (1987) Methane-oxidizing bacteria in pogonophora. *Sarsia* 72: 91-99.
90. Buck KR, Barry JP, Simpson AGB (2000) Monterey Bay cold seep biota: Euglenozoa with chemoautotrophic bacterial epibionts. *Eur J Protistol* 36: 117-126.
91. Goffredi SK, Wilpiseski R, Lee R, Orphan VJ (2008) Temporal evolution of methane cycling and phylogenetic diversity of archaea in sediments from a deep-sea whale-fall in Monterey Canyon, California. *ISME J* 2: 204-220.
92. Dubilier N, Blazejak A, Rühland C (2006) Symbioses between bacteria and gutless marine oligochaetes. In: Overmann J, editor. *Molecular Basis of Symbiosis*. Berlin, Heidelberg: Springer-Verlag. pp. 251-275.
93. Bright M, Giere O (2005) Microbial symbiosis in Annelida. *Symbiosis* 38: 1-45.
94. Woyke T, Teeling H, Ivanova NN, Huntemann M, Richter M, et al. (2006) Symbiosis insights through metagenomic analysis of a microbial consortium. *Nature* 443: 950-955.
95. Scott KM, Sievert SM, Abril FN, Ball LA, Barrett CJ, et al. (2006) The genome of deep-sea vent chemolithoautotroph *Thiomicrospira crunogena* XCL-2. *PLoS Biol* 4: 2196-2212.
96. Newton ILG, Woyke T, Auchtung TA, Dilly GF, Dutton RJ, et al. (2007) The *Calymene magnifica* chemoautotrophic symbiont genome. *Science* 315: 998-1000.
97. Ward N, Larsen O, Sakwa J, Bruseth L, Khouri H, et al. (2004) Genomic insights into methanotrophy: the complete genome sequence of *Methylococcus capsulatus* (Bath). *PLoS Biol* 2: 1616-1628.
98. Robidart JC, Bench SR, Feldman RA, Novoradovsky A, Podell SB, et al. (2008) Metabolic versatility of the *Riftia pachyptila* endosymbiont revealed through metagenomics. *Environ Microbiol* 10: 727-737.
99. Kuwahara H, Yoshida T, Takaki Y, Shimamura S, Nishi S, et al. (2007) Reduced genome of the thioautotrophic intracellular symbiont in a deep-sea clam, *Calymene okutanii*. *Curr Biol* 17: 881-886.
100. Markert S, Arndt C, Felbeck H, Becher D, Sievert SM, et al. (2007) Physiological proteomics of the uncultured endosymbiont of *Riftia pachyptila*. *Science* 315: 247-250.
101. Karavaiko GI, Dubinina GA, Kondrat'eva TF (2006) Lithotrophic microorganisms of the oxidative cycles of sulfur and iron. *Microbiology* 75: 512-545.
102. Robertson LA, Kuenen JG (2006) The colorless sulfur bacteria. In: Dworkin M, Falkow S, Rosenberg E, Schleifer KH, Stackebrandt E, editors. *The Prokaryotes*. 3 ed. Berlin, Heidelberg: Springer-Verlag. pp. 985-1011.
103. Robertson LA, Kuenen JG (2006) The genus *Thiobacillus*. In: Dworkin M, Falkow S, Rosenberg E, Schleifer KH, Stackebrandt E, editors. *The Prokaryotes*. 3 ed. Berlin, Heidelberg: Springer-Verlag. pp. 812-827.
104. Meyer B, Imhoff JF, Kuever J (2007) Molecular analysis of the distribution and phylogeny of the *soxB* gene among sulfur-oxidizing bacteria - evolution of the Sox sulfur oxidation enzyme system. *Environ Microbiol* 9: 2957-2977.
105. Friedrich CG, Rother D, Bardischewsky F, Quentmeier A, Fischer J (2001) Oxidation of reduced inorganic sulfur compounds by bacteria: emergence of a common mechanism? *Appl Environ Microbiol* 67: 2873-2882.
106. Friedrich CG, Bardischewsky F, Rother D, Quentmeier A, Fischer J (2005) Prokaryotic sulfur oxidation. *Curr Opin Microbiol* 8: 253-259.
107. Nelson DC, Hagen KD (1995) Physiology and biochemistry of symbiotic and free-living chemoautotrophic sulfur bacteria. *Am Zool* 35: 91-101.
108. Nelson DC, Fisher CR (1995) Chemoautotrophic and methanotrophic endosymbiotic bacteria at deep-sea vents and seeps. In: Karl DM, editor. *The microbiology of deep-sea hydrothermal vents*. Boca Raton, New York, London, Tokyo: CRC Press. pp. 125-167.
109. Chistoserdova L, Chen SW, Lapidus A, Lidstrom ME (2003) Methylophily in *Methylobacterium extorquens* AM1 from a genomic point of view. *J Bacteriol* 185: 2980-2987.

110. Chistoserdova L, Lapidus A, Han C, Goodwin L, Saunders L, et al. (2007) Genome of *Methylobacillus flagellatus*, molecular basis for obligate methylotrophy, and polyphyletic origin of methylotrophy. *J Bacteriol* 189: 4020-4027.
111. Kane SR, Chakicherla AY, Chain PSG, Schmidt R, Shin MW, et al. (2007) Whole-genome analysis of the methyl *tert*-butyl ether-degrading beta-proteobacterium *Methylibium petroleiphilum* PM1. *J Bacteriol* 189: 1931-1945.
112. Chistoserdova L, Vorholt JA, Lidstrom ME (2005) A genomic view of methane oxidation by aerobic bacteria and anaerobic archaea. *Genome Biol* 6.
113. White D (2000) The physiology and biochemistry of prokaryotes. New York, New York: Oxford University Press. 565 p.
114. Bowman J (2006) The methanotrophs - the families Methylococcaceae and Methylocystaceae. In: Dworkin M, Falkow S, Rosenberg E, Schleifer KH, Stackebrandt E, editors. *The Prokaryotes*. 3 ed. Berlin, Heidelberg: Springer-Verlag. pp. 266-289.
115. Hanson RS, Hanson TE (1996) Methanotrophic bacteria. *Microbiol Rev* 60: 439-471.
116. Lidstrom ME (2006) Aerobic methylotrophic prokaryotes. In: Dworkin M, Falkow S, Rosenberg E, Schleifer KH, Stackebrandt E, editors. *The Prokaryotes*. 3 ed. Berlin, Heidelberg: Springer-Verlag. pp. 618-634.
117. DiSpirito AA, Kunz RC, Choi D-W, Zahn JA (2004) Respiration in methanotrophs. In: Zannoni D, editor. *Respiration in archaea and bacteria Vol 2: Diversity of prokaryotic respiratory systems*. 1 ed. Dordrecht, The Netherlands: Springer. pp. 149-168.
118. Bieler R, Mikkelsen PM (2006) Bivalvia - a look at the branches. *Zool J Linn Soc* 148: 223-235.
119. Giribet G, Wheeler W (2002) On bivalve phylogeny: a high-level analysis of the Bivalvia (Mollusca) based on combined morphology and DNA sequence data. *Invertebr Biol* 121: 271-324.
120. Giribet G, Distel DL (2003) Bivalve phylogeny and molecular data. In: Lydeard C, Lindberg DR, editors. *Molecular systematics and phylogeography of mollusks*. Washington and London: Smithsonian Books. pp. 45-90.
121. Taylor JD, Williams ST, Glover EA, Dyal P (2007) A molecular phylogeny of heterodont bivalves (Mollusca: Bivalvia: Heterodonta): new analyses of 18S and 28S rRNA genes. *Zool Scr* 36: 587-606.
122. Neulinger SC, Sahling H, Süling J, Imhoff JF (2006) Presence of two phylogenetically distinct groups in the deep-sea mussel *Acharax* (Mollusca: Bivalvia: Solemyidae). *Mar Ecol Prog Ser* 312: 161-168.
123. DeChaine EG, Cavanaugh CM (2006) Symbioses of methanotrophs and deep-sea mussels (Mytilidae: Bathymodiolinae). In: Overmann J, editor. *Molecular Basis of Symbiosis*. Berlin, Heidelberg: Springer-Verlag. pp. 227-249.
124. Duperron S, Halary S, Lorion J, Sibuet M, Gaill F (2008) Unexpected co-occurrence of six bacterial symbionts in the gills of the cold seep mussel *Idas* sp. (Bivalvia: Mytilidae). *Environ Microbiol* 10: 433-445.
125. Duperron S, Lorion J, Lopez P, Samadi S, Gros O, et al. (2008) Symbioses between deep-sea mussels (Mytilidae: Bathymodiolinae) and chemosynthetic bacteria: diversity, function and evolution. submitted.
126. Taylor JD, Williams ST, Glover EA (2007) Evolutionary relationships of the bivalve family Thyasiridae (Mollusca: Bivalvia), monophyly and superfamily status. *J Mar Biol Assoc UK* 87: 565-574.
127. Fisher CR (1990) Chemoautotrophic and methanotrophic symbioses in marine invertebrates. *Rev Aquat Sci* 2: 399-436.
128. Distel DL, Baco AR, Chuang E, Morrill W, Cavanaugh C, et al. (2000) Do mussels take wooden steps to deep-sea vents? *Nature* 403: 725-726.
129. Jones WJ, Won YJ, Maas PAY, Smith PJ, Lutz RA, et al. (2006) Evolution of habitat use by deep-sea mussels. *Mar Biol* 148: 841-851.
130. Jones WJ, Vrijenhoek RC (2006) Evolutionary relationships within the "*Bathymodiolus*" *childressi* group. *Cah Biol Mar* 47: 403-407.
131. Won Y-J, Jones WJ, Vrijenhoek RC (2008) Absence of cospeciation between deep-sea mytilids and their thiotrophic endosymbiont. *J Shellfish Res* 27: 129-138.
132. Kiel S, Little CTS (2006) Cold-seep mollusks are older than the general marine mollusk fauna. *Science* 313: 1429-1431.
133. Iwasaki H, Kyuno A, Shintaku M, Fujita Y, Fujiwara Y, et al. (2006) Evolutionary relationships of deep-sea mussels inferred by mitochondrial DNA sequences. *Mar Biol* 149: 1111-1122.
134. Olu-Le Roy K, Caprais JC, Fifis A, Fabri MC, Galéron J, et al. (2007) Cold-seep assemblages on a giant pockmark off West Africa: spatial patterns and environmental control. *Mar Ecol* 28: 115-130.
135. Olu-Le Roy K, von Cosel R, Hourdez S, Carney SL, Jollivet D (2007) Amphi-Atlantic cold-seep *Bathymodiolus* species complexes across the equatorial belt. *Deep-Sea Res I* 54: 1890-1911.
136. Samadi S, Quémère E, Lorion J, Tillier A, von Cosel R, et al. (2007) Molecular phylogeny in mytilids supports wooden steps to deep-sea vents hypothesis. *C R Biol* 330: 446-456.
137. Distel DL, Lee HKW, Cavanaugh CM (1995) Intracellular coexistence of methanotrophic and thioautotrophic bacteria in a hydrothermal vent mussel. *Proc Natl Acad Sci USA* 92: 9598-9602.
138. Fiala-Médioni A, Le Pennec M (1987) Trophic structural adaptations in relation to the bacterial association of bivalve mollusks from hydrothermal vents and subduction zones. *Symbiosis* 4: 63-74.

139. Fisher CR, Childress JJ, Oremland RS, Bidigare RR (1987) The importance of methane and thiosulfate in the metabolism of the bacterial symbionts of two deep-sea mussels. *Mar Biol* 96: 59-71.
140. Fisher CR, Childress JJ (1992) Organic carbon transfer from methanotrophic symbionts to the host hydrocarbon-seep mussel. *Symbiosis* 12: 221-235.
141. Robinson JJ, Polz MF, Fiala-Medioni A, Cavanaugh CM (1998) Physiological and immunological evidence for two distinct C₁-utilizing pathways in *Bathymodiolus puteoserpentis* (Bivalvia: Mytilidae), a dual endosymbiotic mussel from the Mid-Atlantic Ridge. *Mar Biol* 132: 625-633.
142. Pimenov NV, Kalyuzhnaya MG, Khmelenina VN, Mityushina LL, Trotsenko YA (2002) Utilization of methane and carbon dioxide by symbiotrophic bacteria in gills of Mytilidae (*Bathymodiolus*) from the Rainbow and Logachev hydrothermal fields on the Mid-Atlantic Ridge. *Microbiology* 71: 587-594.
143. Belkin S, Nelson DC, Jannasch HW (1986) Symbiotic assimilation of CO₂ in two hydrothermal vent animals, the mussel *Bathymodiolus thermophilus* and the tube worm *Riftia pachyptila*. *Biol Bull* 170: 110-121.
144. Nelson DC, Hagen KD, Edwards DB (1995) The gill symbiont of the hydrothermal vent mussel *Bathymodiolus thermophilus* is a psychrophilic, chemoautotrophic, sulfur bacterium. *Mar Biol* 121: 487-495.
145. Duperron S, Sibuet M, MacGregor BJ, Kuypers MMM, Fisher CR, et al. (2007) Diversity, relative abundance and metabolic potential of bacterial endosymbionts in three *Bathymodiolus* mussel species from cold seeps in the Gulf of Mexico. *Environ Microbiol* 9: 1423-1438.
146. Pernthaler A, Ward JE, Zielinski F, Borowski C, Dubilier N (in prep.) Expression patterns of *pmoA* and *aprA* in symbionts of the hydrothermal vent mussel *Bathymodiolus puteoserpentis*.
147. Fiala-Médioni A, McKiness ZP, Dando P, Boulegue J, Mariotti A, et al. (2002) Ultrastructural, biochemical, and immunological characterization of two populations of the mytilid mussel *Bathymodiolus azoricus* from the Mid-Atlantic Ridge: evidence for a dual symbiosis. *Mar Biol* 141: 1035-1043.
148. Fisher CR, Childress JJ, Arp AJ, Brooks JM, Distel D, et al. (1988) Microhabitat variation in the hydrothermal vent mussel, *Bathymodiolus thermophilus*, at the Rose Garden vent on the Galapagos Rift. *Deep-Sea Res I* 35: 1769-1791.
149. Spiridonova EM, Kuznetsov BB, Pimenov NV, Tourova TP (2006) Phylogenetic characterization of endosymbionts of the hydrothermal vent mussel *Bathymodiolus azoricus* by analysis of the 16S rRNA, *cbbl*, and *pmoA* genes. *Microbiology* 75: 694-701.
150. Pernthaler A, Amann R (2004) Simultaneous fluorescence in situ hybridization of mRNA and rRNA in environmental bacteria. *Appl Environ Microbiol* 70: 5426-5433.
151. Childress JJ, Fisher CR, Brooks JM, Kennicutt MC, Bidigare R, et al. (1986) A methanotrophic marine molluscan (Bivalvia, Mytilidae) symbiosis: mussels fueled by gas. *Science* 233: 1306-1308.
152. Cary SC, Fisher CR, Felbeck H (1988) Mussel growth supported by methane as sole carbon and energy source. *Science* 240: 78-80.
153. Kochevar RE, Childress JJ, Fisher CR, Minnich E (1992) The methane mussel: roles of symbiont and host in the metabolic utilization of methane. *Mar Biol* 112: 389-401.
154. Elsaied HE, Kaneko R, Naganuma T (2006) Molecular characterization of a deep-sea methanotrophic mussel symbiont that carries a RuBisCO gene. *Mar Biotechnol* 8: 511-520.
155. Zielinski FU, Borowski C, Gennerich HH, Dubilier N, Wenzhöfer F (manuscript I) *In situ* measurements of hydrogen sulfide, oxygen, and temperature in diffuse fluids of the ultramafic-hosted Logatchev hydrothermal vent field (Mid-Atlantic Ridge): implications for symbiont-containing *Bathymodiolus* mussels. Intended as article in Deep-Sea Research I.
156. Zielinski FU, Pernthaler A, Duperron S, Raggi L, Giere O, et al. (manuscript II) Widespread occurrence of an intranuclear bacterial parasite in vent and seep mussels. Intended as article in Proceedings of the National Academy of Sciences of the United States of America.
157. Zielinski FU, Struck JM, Wetzel S, Pape T, Seifert R, et al. (manuscript III) The sulfur-oxidizing endosymbiont of the hydrothermal vent mussel *Bathymodiolus puteoserpentis* (Bivalvia: Mytilidae) uses hydrogen as an energy source. Intended as article in NN.
158. Duperron S, Bergin C, Zielinski F, Blazejak A, Pernthaler A, et al. (2006) A dual symbiosis shared by two mussel species, *Bathymodiolus azoricus* and *Bathymodiolus puteoserpentis* (Bivalvia: Mytilidae), from hydrothermal vents along the northern Mid-Atlantic Ridge. *Environ Microbiol* 8: 1441-1447.
159. Kuhn T, Alexander B, Augustin N, Birgel D, Borowski C, et al. (2004) The Logatchev hydrothermal field – revisited: preliminary results of the R/V METEOR Cruise HYDROMAR I (M60/3). *InterRidge News* 13: 1-4.
160. Borowski C, Asendorf V, Bürk D, Jr. AC, Elder R, et al. (2007) New coordinates for the hydrothermal structures in the Logatchev vent field at 14°45'N on the Mid-Atlantic Ridge. *InterRidge News* 16: 13-14.
161. Devey CW, Lackschewitz KS, Baker E, Bannert B, Bislich O, et al. (2005) Hydrothermal and volcanic activity found on the Southern Mid-Atlantic Ridge. *EOS Trans Am Geophys Union* 86: 209-216.
162. Gebruk AV, Chevaldonné P, Shank T, Lutz RA, Vrijenhoek RC (2000) Deep-sea hydrothermal vent communities of the Logatchev area (14°45'N, Mid-Atlantic Ridge): diverse biotopes and high biomass. *J Mar Biol Assoc UK* 80: 383-393.

163. Johnson KS, Needoba JA, Riser SC, Showers WJ (2007) Chemical sensor networks for the aquatic environment. *Chem Rev* 107: 623-640.
164. Jeroschewski P, Steuckart C, Kühl M (1996) An amperometric microsensor for the determination of H₂S in aquatic environments. *Anal Chem* 68: 4351-4357.
165. Millero FJ, Plese T, Fernandez M (1988) The Dissociation of Hydrogen Sulfide in Seawater. *Limnol Oceanogr* 33: 269-274.
166. Le Bris N, Rodier P, Sarradin PM, Le Gall C (2006) Is temperature a good proxy for sulfide in hydrothermal vent habitats? *Cah Biol Mar* 47: 465-470.
167. Schmidt C, Vuillemin R, Le Gall C, Gaill F, Le Bris N (2008) Geochemical energy sources for microbial primary production in the environment of hydrothermal vent shrimps. *Mar Chem* 108: 18-31.
168. Johnson KS, Beehler CL, Sakamoto-Arnold CM, Childress JJ (1986) In situ measurements of chemical distributions in a deep-sea hydrothermal vent field. *Science* 231: 1139-1141.
169. Sakamoto-Arnold CM, Johnson KS, Beehler CL (1986) Determination of hydrogen sulfide in seawater using flow injection analysis and flow analysis. *Limnol Oceanogr* 31: 894-900.
170. Johnson KS, Beehler CL, Sakamoto-Arnold CM (1986) A submersible flow analysis system. *Anal Chim Acta* 179: 245-257.
171. Sarradin PM, Le Bris N, Birot D, Caprais JC (1999) Laboratory adaptation of the methylene blue method to flow injection analysis: towards in situ sulfide analysis in hydrothermal seawater. *Anal Commun* 36: 157-160.
172. Le Bris N, Sarradin PM, Birot D, Alayse-Danet AM (2000) A new chemical analyzer for in situ measurement of nitrate and total sulfide over hydrothermal vent biological communities. *Mar Chem* 72: 1-15.
173. Rozan TF, Theberge SM, Luther III G (2000) Quantifying elemental sulfur (S⁰), bisulfide (HS⁻) and polysulfides (S_x²⁻) using a voltammetric method. *Anal Chim Acta* 415: 175-184.
174. Luther III GW, Glazer BT, Hohmann L, Popp JJ, Taillefert M, et al. (2001) Sulfur speciation monitored *in situ* with solid state gold amalgam voltammetric microelectrodes: polysulfides as a special case in sediments, microbial mats and hydrothermal vent waters. *J Environ Monit* 3: 61-66.
175. Luther III GW, Glazer BT, Ma SF, Trouwborst RE, Moore TS, et al. (2008) Use of voltammetric solid-state (micro)electrodes for studying biogeochemical processes: Laboratory measurements to real time measurements with an *in situ* electrochemical analyzer (ISEA). *Mar Chem* 108: 221-235.
176. Mullaugh KM, Luther III GW, Ma S, Moore TS, Yücel M, et al. (2008) Voltammetric (micro)electrodes for the in situ study of Fe²⁺ oxidation kinetics in hot springs and S₂O₃²⁻ production at hydrothermal vents. *Electroanalysis* 20: 280-290.
177. Waite TJ, Moore TS, Childress JJ, Hsu-Kim H, Mullaugh KM, et al. (2008) Variation in sulfur speciation with shellfish presence at a Lau Basin diffuse flow vent site. *J Shellfish Res* 27: 163-168.
178. Kühl M, Steuckart C, Eickert G, Jeroschewski P (1998) A H₂S microsensor for profiling biofilms and sediments: application in an acidic lake sediment. *Aquat Microb Ecol* 15: 201-209.
179. Johnson KS, Childress JJ, Beehler CL, Sakamoto CM (1994) Biogeochemistry of hydrothermal vent mussel communities: the deep-sea analogue to the intertidal zone. *Deep-Sea Res I* 41: 993-1011.
180. Johnson KS, Childress JJ, Hessler RR, Sakamoto-Arnold CM, Beehler CL (1988) Chemical and biological interactions in the Rose Garden hydrothermal vent field, Galapagos spreading center. *Deep-Sea Res A* 35: 1723-1744.
181. Chevalloné P, Desbruyères D, Le Haître M (1991) Time-series of temperature from three deep-sea hydrothermal vent sites. *Deep-Sea Res A* 38: 1417-1430.
182. Little SA, Stolzenbach KD, Grassle FJ (1988) Tidal current effects on temperature in diffuse hydrothermal flow: Guaymas basin. *Geophys Res Lett* 15: 1491-1494.
183. Johnson HP, Tunnicliffe V (1985) Time-series measurements of hydrothermal activity on northern Juan de Fuca Ridge. *Geophys Res Lett* 12: 685-688.
184. Johnson KS, Childress JJ, Beehler CL (1988) Short-term temperature variability in the Rose Garden hydrothermal vent field: an unstable deep-sea environment. *Deep-Sea Res A* 35: 1711-1721.
185. Le Bris N, Sarradin PM, Caprais JC (2003) Contrasted sulphide chemistries in the environment of 13°N EPR vent fauna. *Deep-Sea Res I* 50: 737-747.
186. Le Bris N, Govenar B, Le Gall C, Fisher CR (2006) Variability of physico-chemical conditions in 9°50'N EPR diffuse flow vent habitats. *Mar Chem* 98: 167-182.
187. Sarradin PM, Sarrazin J, Sauter E, Shillito B, Waldmann C, et al. (2007) **EXT**reme ecosystem studies in the deep **OCE**an: Technological Developments. *InterRidge News* 16: 17-21.
188. Los-Gatos-Research (2006) Ultrasensitive analyzers for real-world environments. Catalog. Mountain View, CA, USA: Los Gatos Research Incorporation. 1-23 p.
189. Won YJ, Hallam SJ, O'Mullan GD, Pan IL, Buck KR, et al. (2003) Environmental acquisition of thiotrophic endosymbionts by deep-sea mussels of the genus *Bathymodiolus*. *Appl Environ Microbiol* 69: 6785-6792.
190. Kerk D, Gee A, Dewhirst FE, Drum AS, Elston RA (1992) Phylogenetic placement of "Nuclear Inclusion X (NIX)" into the gamma subclass of

- proteobacteria on the basis of 16S ribosomal RNA sequence comparisons. *Syst Appl Microbiol* 15: 191-196.
191. Ward ME, Shields JD, Van Dover CL (2004) Parasitism in species of *Bathymodiolus* (Bivalvia: Mytilidae) mussels from deep-sea seep and hydrothermal vents. *Dis Aquat Org* 62: 1-16.
192. Kanagawa T (2003) Bias and artifacts in multitemplate polymerase chain reactions (PCR). *J Biosci Bioeng* 96: 317-323.
193. Muyzer G, Teske A, Wirsén CO, Jannasch HW (1995) Phylogenetic relationships of *Thiomicrospira* species and their identification in deep-sea hydrothermal vent samples by denaturing gradient gel electrophoresis of 16S rDNA fragments. *Arch Microbiol* 164: 165-172.
194. Buchholz-Cleven BEE, Rattunde B, Straub KL (1997) Screening for genetic diversity of isolates of anaerobic Fe(II)-oxidizing bacteria using DGGE and whole-cell hybridization. *Syst Appl Microbiol* 20: 301-309.
195. Muyzer G, Dewaal EC, Uitterlinden AG (1993) Profiling of complex microbial populations by denaturing gradient gel electrophoresis analysis of polymerase chain reaction-amplified genes coding for 16S rRNA. *Appl Environ Microbiol* 59: 695-700.
196. Amann RI, Binder BJ, Olson RJ, Chisholm SW, Devereux R, et al. (1990) Combination of 16S rRNA-targeted oligonucleotide probes with flow-cytometry for analyzing mixed microbial populations. *Appl Environ Microbiol* 56: 1919-1925.
197. Stackebrandt E, Goebel BM (1994) A place for DNA-DNA reassociation and 16S ribosomal RNA sequence analysis in the present species definition in bacteriology. *Int J Syst Bacteriol* 44: 846-849.
198. Forney LJ, Zhou X, Brown CJ (2004) Molecular microbial ecology: land of the one-eyed king. *Curr Opin Microbiol* 7: 210-220.
199. Staley JT (2006) The bacterial species dilemma and the genomic-phylogenetic species concept. *Philos Trans R Soc B Biol Sci* 361: 1899-1909.
200. Hanage WP, Fraser C, Spratt BG (2006) Sequences, sequence clusters and bacterial species. *Philos Trans R Soc B Biol Sci* 361: 1917-1927.
201. Medini D, Serruto D, Parkhill J, Relman DA, Donati C, et al. (2008) Microbiology in the post-genomic era. *Nat Rev Microbiol* 6: 419-430.
202. Polz MF, Distel DL, Zarda B, Amann R, Felbeck H, et al. (1994) Phylogenetic analysis of a highly specific association between ectosymbiotic, sulfur-oxidizing bacteria and a marine nematode. *Appl Environ Microbiol* 60: 4461-4467.
203. Polz MF, Felbeck H, Novak R, Nebelsick M, Ott JA (1992) Chemoautotrophic, sulfur-oxidizing symbiotic bacteria on marine nematodes - morphological and biochemical characterization. *Microb Ecol* 24: 313-329.
204. Giere O, Krieger J (2001) A triple bacterial endosymbiosis in a gutless oligochaete (Annelida): ultrastructural and immunocytochemical evidence. *Invertebr Biol* 120: 41-49.
205. Raikov IB (1974) Étude ultrastructurale des bactéries épizoïques et endozoïque de *Kentrophoros latum* Raikov, cilié holotriche mésopsammique. *Cah Biol Mar* 15: 379-393.
206. Raikov IB (1971) Bactéries épizoïque et mode de nutrition du cilié psammophile *Kentrophoros fistulosum* Fauré-Fremiet (étude au microscope électronique). *Protistologica* 7: 365-378.
207. Fauré-Fremiet E (1951) The marine sand-dwelling ciliates of Cape Cod. *Biol Bull* 100: 59-70.
208. Fauré-Fremiet E (1950) Caulobactéries épizoïque associées aux *Centropherella* (ciliés holotriches). *Bull Soc Zool France* 75: 134-137.
209. Fauré-Fremiet E (1950) Écologie des ciliés psammophiles littoraux. *Bull Biol France-Belgique* 84: 35-75.
210. Görtz H-D (2006) Symbiotic associations between ciliates and prokaryotes. In: Dworkin M, Falkow S, Rosenberg E, Schleifer KH, Stackebrandt E, editors. *The Prokaryotes*. 3 ed. Berlin, Heidelberg: Springer-Verlag. pp. 364-402.
211. Fokin SI (2004) Bacterial endocytobionts of Ciliophora and their interactions with the host cell. *Int Rev Cytol* 236: 181-249.
212. von Cosel R, Comtet T, Krylova EM (1999) *Bathymodiolus* (Bivalvia: Mytilidae) from hydrothermal vents on the Azores Triple Junction and the Logatchev hydrothermal field, Mid-Atlantic Ridge. *Veliger* 42: 218-248.
213. Kenk VC, Wilson BR (1985) A new mussel (Bivalvia, Mytilidae) from hydrothermal vents in the Galapagos Rift zone. *Malacologia* 26: 253-271.
214. Johnson MA, Le Pennec M (1995) Association between the mollusc bivalve *Loripes lucinalis* and a *Chlamydia*-like organism, with comments on its pathogenic impact, life cycle and possible mode of transmission. *Mar Biol* 123: 523-530.
215. Le Pennec M, Diouris M, Herry A (1988) Endocytosis and lysis of bacteria in gill epithelium of *Bathymodiolus thermophilus*, *Thyasira flexuosa* and *Lucinella divaricata* (bivalve, molluscs). *J Shellfish Res* 7: 483-489.
216. Kádár E, Bettencourt R, Costa V, Santos RS, Lobo-Da-Cunha A, et al. (2005) Experimentally induced endosymbiont loss and re-acquirement in the hydrothermal vent bivalve *Bathymodiolus azoricus*. *J Exp Mar Biol Ecol* 318: 99-110.
217. Sabaneyeva EV, Fokin SI, GavriloVA EV, Kornilova ES (2005) Nocodazole inhibits macronuclear infection with *Holospira obtusa* in *Paramecium caudatum*. *Protoplasma* 226: 147-153.
218. Ogata H, La Scola B, Audic S, Renesto P, Blanc G, et al. (2006) Genome sequence of *Rickettsia bellii* illuminates the role of amoebae in gene exchanges

- between intracellular pathogens. PLoS Genet 2: 733-744.
219. Todd WJ, Burgdorfer W, Mauro AJ, Grey GP (1981) Ultrastructural analysis of *Rickettsia rickettsii* in cultures of persistently infected vole cells. In: Burgdorfer W, Anacker RL, editors. Rickettsiae and rickettsial diseases. New York, NY: Academic Press. pp. 248-250.
220. Heinzen RA, Grieshaber SS, Van Kirk LS, Devin CJ (1999) Dynamics of actin-based movement by *Rickettsia rickettsii* in Vero cells. Infect Immun 67: 4201-4207.
221. Elston RA (1986) An intranuclear pathogen [Nuclear Inclusion X (NIX)] associated with massive mortalities of the Pacific razor clam, *Siliqua patula*. J Invertebr Pathol 47: 93-104.
222. Azevedo C (1989) Fine structure of endonucleobiotic bacteria in the gill epithelium of *Ruditapes decussatus*. Mar Biol 100: 339-341.
223. Ayres DL, Schumaker EJ, Elston RA (2004) Recent mortality event of Pacific razor clams, *Siliqua patula*, along the Pacific coast of Washington state associated with record infection intensity of the gills by Nuclear Inclusion X (NIX). J Shellfish Res 23: 651-651.
224. Vacelet J (1970) Description de cellules a bactéries intranucléaires chez des éponges *Verongia*. J Microsc 9: 333-346.
225. Friedrich AB, Merkert H, Fendert T, Hacker J, Proksch P, et al. (1999) Microbial diversity in the marine sponge *Aplysina cavernicola* (formerly *Verongia cavernicola*) analyzed by fluorescence in situ hybridization (FISH). Mar Biol 134: 461-470.
226. Mills AM, Ward ME, Heyl TP, Van Dover CL (2005) Parasitism as a potential contributor to massive clam mortality at the Blake Ridge Diapir methane-hydrate seep. J Mar Biol Assoc UK 85: 1489-1497.
227. Terlizzi CM, Ward ME, Van Dover CL (2004) Observations on parasitism in deep-sea hydrothermal vent and seep limpets. Dis Aquat Org 62: 17-26.
228. Pernthaler A, Pernthaler J (2005) Simultaneous fluorescence in situ hybridization of mRNA and rRNA for the detection of gene expression in environmental microbes. In: Leadbetter JR, editor. Methods Enzymol. San Diego, CA, USA: Elsevier. pp. 352-371.
229. Crozier TE, Yamamoto S (1974) Solubility of hydrogen in water, seawater, and NaCl solutions. J Chem Eng Data 19: 242-244.
230. O'Brien J, Vetter RD (1990) Production of thiosulfate during sulfide oxidation by mitochondria of the symbiont-containing bivalve *Solemya reidi*. J Exp Biol 149: 133-148.
231. Grieshaber MK, Volkel S (1998) Animal adaptations for tolerance and exploitation of poisonous sulfide. Annu Rev Physiol 60: 33-53.
232. Yong R, Searcy DG (2001) Sulfide oxidation coupled to ATP synthesis in chicken liver mitochondria. Comp Biochem Physiol B Biochem Mol Biol 129: 129-137.
233. Childress JJ, Fisher CR, Favuzzi JA, Sanders NK (1991) Sulfide and carbon dioxide uptake by the hydrothermal vent clam *Calymene magnifica* and its chemoautotrophic symbionts. Physiol Zool 64: 1444-1470.
234. Dyrssen D, Fonselius S, Yhlen B (1999) Determination of thiosulphate and sulphur. In: Klaus Grasshoff, Klaus Kremling, Ehrhardt M, editors. Methods of Seawater Analysis. 3 ed. Weinheim: Wiley-VCH. pp. 101-108.
235. Hansen HP, Koroleff F (1999) Determination of nitrite. In: Klaus Grasshoff, Klaus Kremling, Ehrhardt M, editors. Methods of Seawater Analysis. 3 ed. Weinheim: Wiley-VCH. pp. 177-180.
236. Damgaard LR, Revsbech NP (1997) A microscale biosensor for methane containing methanotrophic bacteria and an internal oxygen reservoir. Anal Chem 69: 2262-2267.
237. Amend JP, Shock EL (2001) Energetics of overall metabolic reactions of thermophilic and hyperthermophilic Archaea and Bacteria. FEMS Microbiol Rev 25: 175-243.
238. Drobner E, Huber H, Stetter KO (1990) *Thiobacillus ferrooxidans*, a facultative hydrogen oxidizer. Appl Environ Microbiol 56: 2922-2923.
239. Cohen WD (2002) Anesthetic, relaxant, and narcotizing agents for aquatic invertebrates. Biol Bull Compendia [Online] Cited Dec 12, 2007: Available from <http://www.mbl.edu/BiologicalBulletin/ANESCOMP/AnesComp-Intro.html>.
240. Cavanaugh CM, Gardiner SL, Jones ML, Jannasch HW, Waterbury JB (1981) Prokaryotic cells in the hydrothermal vent tube worm *Riftia pachyptila* Jones: possible chemoautotrophic symbionts. Science 213: 340-342.

Acknowledgements

I would like to thank the many people who have supported me in the last four years be it scientifically or psychologically. I owe particular respect to my family and longstanding friends who were with me both in good times and periods of major trouble. Many frank (!) thanks to:

Nicole Dubilier first of all for giving me the opportunity to do a PhD in the field of deep-sea hydrothermal vent research (one of the most fascinating research projects I can think of) and the opportunity to move with my family to California to continue my PhD at Caltech, the confidence that I can finish this PhD without the unique scientific support by the MPI team, the constant scientific enthusiasm, and for sharing beers and gossip not only on our research cruises.

Rudi Amann for the reassuring calmness, the laissez-faire, valuable contributions in thesis committee meetings, social intelligence, and the confidence that this project can be accomplished 9100 km away from Bremen.

Antje Boetius for the scientific input in several thesis committees, always fast responses to emails, and the general overarching reliability.

Christian Borowski for the great time on Meteor M60/3, helpful information in scientific and non-scientific issues, plenty of shared beers and mutual discussions between dusk and dawn on board Meteor at the the railing or next to the well-stocked fridge.

Bernd Stickfort for finding and providing any paper I asked for and thus saving a lot of effort and time.

Christiane Glöckner for the tea and the willing help with regulations, formalities, and paperwork in order to graduate.

The **Molecular Ecology group** in general and **Silke Wetzel, Jörg Wulf, Dagmar Wöbken, Elke Allers** and **Andreas Ellrott** in particular for being around whenever needed, the help in the lab, with computer issues, or just socializing, and for being great office companions.

The **shipboard scientific parties** of **M60/3, M62/5b, M64/2, and M68/1** for extraordinary research cruises in terms of scientific exchange and social events and the **shipboard technical and nautical crews** for the routine, expertise, and reliability thus assuring that scientific work could be done at a high level under the oddest circumstances and for extinguishing the machine room fire during M62/5b preventing us from stranding at the infamous skeleton coast (Namibia). Special thanks to the always good-tempered stewards **Jan Hoppe** and **Andreas Wege**.

Sébastien Duperron for fruitful, productive, and valuable email exchange and mutual discussion regarding bathymodiolin mussels and symbionts, and for providing his review paper prior to acception.

Victoria Orphan and **Shana Goffredi** for hosting me at Caltech, providing office and lab space, their optimistic attitude towards life, great house concerts with excellent food, and the honest attention whenever I got scientifically or personally stuck. Thanks for listening to me when I was in major trouble. I am certain it prevented a major crisis.

Hauke Harms for hiring me though not yet graduated, the leap of faith, and giving me the time and space to finish this PhD at the Helmholtz Centre for Environmental Research in Leipzig.

My family but especially my **mother** for listening to stories of any kind, helping out during research cruises, taking care of Béla whenever possible and simply for being a wonderful mother and grandmother.

Annelie Pernthaler for Béla, the good times, the plenty of spaghetti, taking care for Béla during my many and long research cruises, and for proof-reading this thesis.

Deborah and **Clair Laux** for hanging out with me in California and reminding me that there is a life beyond science.

Moritz Brauer, Anke Jordan, Ulrike Louis, and Robert Klose for being true and good friends over many, many years, for being available and reliable in any moment, and for not resenting my long absences and temporary silence while focusing on this project.

IV List of publications and manuscripts

1 Publications and manuscripts presented in this thesis

- (1) **Zielinski, F. U.**, C. Borowski, H. H. Gennerich, N. Dubilier, and F. Wenzhöfer. *In situ* measurements of hydrogen sulfide, oxygen, and temperature in diffuse fluids of the ultramafic-hosted Logatchev hydrothermal vent field (Mid-Atlantic Ridge): implications for symbiont-containing *Bathymodiolus* mussels. In prep. Intended as article in Deep-Sea Research I.

Experimental design: F. U. Zielinski, C. Borowski, N. Dubilier

Microsensor measurements and data analysis: F. U. Zielinski

Temperature logger measurements and data analysis: F. U. Zielinski, H. H. Gennerich

Writing: F. U. Zielinski, F. Wenzhöfer, N. Dubilier

- (2) **Zielinski, F. U.**, A. Pernthaler, S. Duperron, L. Raggi, S. Wetzel, O. Giere, C. Borowski, and N. Dubilier. Widespread occurrence of an intranuclear bacterial parasite in vent and seep mussels. In prep. Intended as article in Proceedings of the National Academy of Sciences of the United States of America.

Experimental design: F. U. Zielinski, N. Dubilier

Sampling: F. U. Zielinski, C. Borowski, S. Duperron, O. Giere

Cloning and Sequencing: F. U. Zielinski, S. Wetzel, L. Raggi

Sequence assembly: F. U. Zielinski

Phylogenetic reconstruction: S. Duperron, F. U. Zielinski

Probe design: S. Duperron

FISH: A. Pernthaler

Microscopy and image analysis: F. U. Zielinski

TEM: O. Giere

Writing: F.U. Zielinski and N. Dubilier

- (3) **Zielinski, F. U.**, J. M. Struck, S. Wetzel, T. Pape, R. Seifert, F. Wenzhöfer, and N. Dubilier. The sulfur-oxidizing endosymbiont of the hydrothermal vent mussel *Bathymodiolus puteoserpentis* (Bivalvia: Mytilidae) uses hydrogen as an energy source. In prep. Intended as article in N.N.

Experimental design: F.U. Zielinski, T. Pape, N. Dubilier

Sampling and incubation experiments: F.U. Zielinski, N. Dubilier, J.M. Struck, S. Wetzel

Hydrogen measurements: T. Pape, R. Seifert

Data analysis: F.U. Zielinski

Writing: F.U. Zielinski, N. Dubilier

- (4) Duperron, S., C. Bergin, **F. Zielinski**, A. Blazejak, A. Pernthaler, Z. P. McKiness, E. DeChaine, C. M. Cavanaugh, and N. Dubilier. 2006. A dual symbiosis shared by two mussel species, *Bathymodiolus azoricus* and *Bathymodiolus puteoserpentis* (Bivalvia: Mytilidae), from hydrothermal vents along the northern Mid-Atlantic Ridge. *Environmental Microbiology* 8: 1441-1447.

Experimental design: S. Duperron, C. Bergin, F. U. Zielinski, A. Blazejak, A. Pernthaler, Z. P. McKiness, C. M. Cavanaugh, N. Dubilier

Cloning, sequencing, and sequence assembly: C. Bergin, F. Zielinski, Z.P. McKiness, E. DeChaine

Phylogenetic reconstruction: S. Duperron

Probe design: C. Bergin, S. Duperron

FISH: S. Duperron, A. Blazejak, A. Pernthaler

Writing: S. Duperron, C.M. Cavanaugh, N. Dubilier

2 Contributions to other publications

- (5) Pernthaler, A., J. E. Ward, **F. Zielinski**, C. Borowski, and N. Dubilier. Expression patterns of *pmoA* and *aprA* in symbionts of the hydrothermal vent mussel *Bathymodiolus puteoserpentis*. In prep. Intended as article in *Environmental Microbiology*.
- (6) Devey, C. W., K. S. Lackschewitz, and E. Baker (as well as B. Bannert, O. Bislich, G. Engemann, L. Fowler, P. Günnewig, D. Hüttig, Y.-G. Kim, A. Klügel, A. Knee, A. Koschinsky, A. Ksienzyk, B. Kührig, T. Kuhn, D. Matthew, C. Mertens, T. Mosch, B. Murton, N. Nowald, H. Paulick, V. Ratmeyer, M. Reuter, I. Rouse, O. Schmale, W. Schmidt, F. Schubotz, M. Schröder, C. Seiter, K. Stange, J. Stecher, U. Stöber, S. Storm, J. Sültenfuss, T. Teichgräber, P. O. Thierer, S. Tille, S. Tyler, W. Walter, P. Wefers, and **F. Zielinski**). 2005. Hydrothermal and volcanic activity found on the Southern Mid-Atlantic Ridge. *EOS* 86: 209-216.

This article publishes the results of cruise M62/5, leg A and B, (SUEDMAR I). The task of this cruise was to discover hydrothermal vents on the Mid-Atlantic Ridge south of the equator (between 4 and 10°S). During leg M62/5B I deployed miniaturized autonomous plume recorders (MAPR) and analyzed the data. These instruments measure turbidity in the water column as an indicator of hydrothermal plumes. Together with other measurements the MAPR data led to the discovery of the Nibelungen vent field at 8°17.85'S. To above cited publication I contributed a diagram summarizing turbidity, methane, and manganese data. All MAPR measurements (117 datasets) are stored in the Pangaea database (www.pangaea.de) and can be searched for using my name.

3 Publications as a result of research cruises

The preparation of a research cruise is quite elaborate and the success depends to a great extent on its participants, i.e. the shipboard scientific party, their will to communicate and collaborate.

Therefore, the whole shipboard scientific party is appreciated as co-authors on the following papers although not every single person has necessarily contributed data to the manuscript.

- (7) Haase, K.M., Petersen, S., Koschinsky, A., Seifert, R., Devey, C.W., Keir, R., Lackschewitz, K.S., Melchert, B., Perner, M., Schmale, O., Süling, J., Dubilier, N., **Zielinski, F.**, Fretzdorff, S., Garbe-Schönberg, D., Westernströer, U., German, C.R., Shank, T.M., Yoerger, D., Giere, O., Kuever, J., Marbler, H., Mawick, J., Mertens, C., Stöber, U., Ostertag-Henning, C., Paulick, H., Peters, M., Strauss, H., Sander, S., Stecher, J., Warmuth, M., Weber, S., 2007. Young volcanism and related hydrothermal activity at 5°S on the slow-spreading southern Mid-Atlantic Ridge. *Geochemistry Geophysics Geosystems* 8 (11), Q11002, doi:10.1029/2006GC001509

This article publishes the discovery of three hydrothermal vent fields on the Mid-Atlantic Ridge south of the equator which were found during the cruises M64/1 (SUEDMAR II) and M68/1 (SUEDMAR III).

- (8) Haase, K. M., A. Koschinsky, C. W. Devey, S. Fretzdorff, C. German, K. S. Lackschewitz, B. Melchert, S. Petersen, R. Seifert, J. Stecher, O. Giere, H. Paulick, D. Yoerger, M64/1, and **M68/1**. 2007. Diking, young volcanism and diffuse hydrothermal activity on the southern Mid-Atlantic Ridge. *Marine Geology*: submitted.

This article publishes the discovery of diffuse flow hydrothermal vent fields on the Mid-Atlantic Ridge south of the equator which were found during the cruises M64/1 (SUEDMAR II) and M68/1 (SUEDMAR III).

- (9) Koschinsky, A., A. Billings, C. W. Devey, N. Dubilier, A. Duester, D. Edge, D. Garbe-Schönberg, C. R. German, O. Giere, R. Keir, K. S. Lackschewitz, H. A. Mai, H. Marbler, J. Mawick, B. Melchert, C. Mertens, M. Peters, S. Sandler, O. Schmale, W. Schmidt, R. Seifert, C. Seiter, U. Stöber, I. Suck, M. Walter, S. Weber, D. Yoerger, M. Zarrouk, and **F. Zielinski**. 2006. Discovery of new hydrothermal vent fields on the Southern Mid-Atlantic Ridge (4°S - 10°S) during Cruise M68/1. *InterRidge News* 15: 9-15.

This article publishes the results of cruise M68/1 (SUEDMAR III).

- (10) Kuhn, T., B. Alexander, N. Augustin, D. Birgel, C. Borowski, L. de Carvalho, G. Engemann, S. Ertl, L. Franz, C. Grech, P. Herzig, R. Hekinian, J. Imhoff, T. Jellinek, S. Klar, A. Koschinsky, J. Kuever, F. Kulescha, K. Lackschewitz, S. Petersen, V. Ratmeyer, J. Renken, G. Ruhland, J. Scholten, K. Schreiber, R. Seifert, J. Süling, M. Türkay, U. Westernströer, and **F. Zielinski**. 2004. The Logatchev hydrothermal field – revisited: preliminary results of the R/V METEOR Cruise HYDROMAR I (M60/3). *InterRidge News* 13: 1-4.

This article publishes the results of cruise M60/3 (HYDROMAR I).

***In situ* measurements of hydrogen sulfide, oxygen, and temperature in diffuse fluids of the ultramafic-hosted Logatchev hydrothermal vent field (Mid-Atlantic Ridge): implications for symbiont-containing *Bathymodiolus* mussels**

Frank U. Zielinski^{a,b,*}, Christian Borowski^a, Hans-Hermann Gennerich^c,
Nicole Dubilier^a, Frank Wenzhöfer^d

^a Max Planck Institute for Marine Microbiology, Symbiosis Group, Celsiusstr. 1, 28359 Bremen, Germany; Email: fzielins@mpi-bremen.de, cborowsk@mpi-bremen.de, ndubilie@mpi-bremen.de

^b Helmholtz-Center for Environmental Research – UFZ, Department of Environmental Microbiology, Permoserstraße 15, 04318 Leipzig, Germany; Email: frank.zielinski@ufz.de

^c University of Bremen, Department of Geosciences, Section Marine Technology – Sensors, Klagenfurter Str., 28334 Bremen, Germany; Email: hherm@uni-bremen.de

^d Max Planck Institute for Marine Microbiology, Department of Biogeochemistry, Celsiusstr. 1, 28359 Bremen, Germany; Email: fwenzhoe@mpi-bremen.de

* Corresponding author: Phone: 0049 (0)341 235 1373; Fax: 0049 (0)341 235 2247; Email: frank.zielinski@ufz.de

Abstract

At the slow-spreading Mid-Atlantic Ridge, two high temperature hydrothermal vent fields are influenced by mantle-derived ultramafic rocks, Rainbow (36°14'N) and Logatchev (14°45'N). The focused, high temperature fluids of these vents are relatively low in sulfide compared to basalt-hosted vents indicating that even less sulfide may be available in the diffuse, low temperature fluids of these ultramafic-hosted vents. However, the occurrence of bathymodiolin mussels with sulfur-oxidizing bacterial endosymbionts at Rainbow and Logatchev indicates the existence of bioavailable sulfide at these vents. To characterize the composition of diffuse fluids above mussel beds of *Bathymodiolus puteoserpentis* at Logatchev and to clarify if these habitats provide the reductants and oxidants needed for endobacterial aerobic sulfide oxidation, *in situ* microsensor measurements of H₂S, O₂ and temperature were performed. The combined sensor measurements revealed high temporal fluctuations of all three parameters above the mussel beds. H₂S and O₂ co-occurred simultaneously with mean concentrations between 14 - 34 μM (H₂S) and 205 - 223 μM (O₂), showing the existence of free sulfide in diffuse fluids from this ultramafic-hosted vent system. Temperature maxima were generally concurrent with H₂S maxima and O₂ minima, with H₂S maxima of 79 μM and O₂ minima never below 142 μM. Despite temperature maxima up to 7.4°C, mean temperatures above mussel beds were generally only slightly above ambient sea water (2.6°C). Dissolved oxygen concentrations consistently decreased as temperatures increased, resulting in a strongly negative and linear correlation of O₂ with temperature ($R^2 = 0.74-0.85$). While H₂S concentrations generally increased with temperature, a linear correlation could not be shown due to a slower response of the H₂S sensor over the temperature sensor. *In situ* measurements at Logatchev indicate that sulfide may also be present and bioavailable in diffuse fluids from similar high-temperature ultramafic-hosted vent systems which occur more often than previously recognized along slow- and ultraslow spreading ridges.

Keywords: *in situ* measurements, ultramafic-hosted, hydrothermal vents, Mid Atlantic Ridge, Logatchev, *Bathymodiolus puteoserpentis*, mussels

1 Introduction

Hydrothermal vents along mid-ocean ridge spreading systems occur in two different settings. Vents on ultra-fast, fast- and intermediate spreading ridges occur exclusively in basalt-hosted settings where the upper oceanic crust is composed entirely of basaltic rocks (Wetzel and Shock, 2000). In contrast, vents on slow- and ultra-slow spreading ridges are either basalt- or ultramafic-hosted. In ultramafic-hosted settings the upper oceanic crust is composed mainly of mantle-derived peridotite (Wetzel and Shock, 2000). Basalt and peridotite react differently with subsurface seawater leading to differences in the fluid composition of basalt- and ultramafic-hosted systems. High temperature hydrothermal fluids discharged from basalt-hosted systems are dominated by sulfide whereas high temperature fluids from ultramafic-hosted systems such as Rainbow (36°14'N) and Logatchev (14°45'N) on the Mid-Atlantic Ridge contain large quantities of dissolved hydrogen and methane but are relatively low in sulfide (Charlou *et al.*, 2002; Douville *et al.*, 2002; Schmidt *et al.*, 2007). Concurrently, discrete sampling of Rainbow and Logatchev low temperature diffuse fluids followed by analysis on board also indicated only low sulfide concentrations (Geret *et al.*, 2002; Schmidt *et al.*, 2007). *In situ* measurements confirmed the low sulfide content in Rainbow diffuse fluids (Schmidt *et al.*, 2008), suggesting that free sulfide ($\text{H}_2\text{S}/\text{HS}^-$) may be depleted in diffuse fluids discharged from ultramafic-hosted vent systems, however, only shrimp habitats were investigated and few measurements were performed. To date, no *in situ* measurements have been recorded for the Logatchev vent field or other ultramafic-hosted hydrothermal vent system, despite the fact that these systems are now known to occur more often than previously recognized along slow- and ultra-slow spreading ridges (Bach *et al.*, 2002; Edmonds *et al.*, 2003; Dias and Barriga, 2006; Davydov *et al.*, 2007; Snow and Edmonds, 2007).

In contrast, sulfide has frequently been measured *in situ* in diffuse fluids discharged

from basalt-hosted hydrothermal systems at the fast-spreading East-Pacific Rise (Rozaan *et al.*, 2000; Luther III *et al.*, 2001a; Luther III *et al.*, 2001b; Le Bris *et al.*, 2003; Alain, 2004; Di Meo-Savoie *et al.*, 2004; Le Bris *et al.*, 2005; Le Bris *et al.*, 2006a; Luther III *et al.*, 2008; Lutz *et al.*, 2008; Nees *et al.*, 2008) and the intermediate-spreading Galapagos Rift (Johnson *et al.*, 1986b; Fisher *et al.*, 1988; Johnson *et al.*, 1988b; Johnson *et al.*, 1994). Only few *in situ* sulfide measurements have been performed at basalt-hosted vent fields on the slow-spreading Mid-Atlantic Ridge (Le Bris *et al.*, 2000; Desbruyères *et al.*, 2001). Recently, *in situ* sulfide data have also become available for the intermediate-spreading East Lau Spreading Center in the West Pacific (Mullaugh *et al.*, 2008; Waite *et al.*, 2008).

Two methods have been used to determine *in situ* sulfide concentrations in hydrothermal diffuse flow, colorimetry and electrochemistry. Colorimetric detection was initially based on conventional flow analysis (Johnson *et al.*, 1986a; Johnson *et al.*, 1986b; Sakamoto-Arnold *et al.*, 1986; Johnson *et al.*, 1988a; Johnson *et al.*, 1988b; Johnson *et al.*, 1994; Tunnicliffe *et al.*, 1997) and was later displaced by flow injection analysis (Sarradin *et al.*, 1999; Le Bris *et al.*, 2000; Desbruyères *et al.*, 2001; Le Bris *et al.*, 2003; Le Bris *et al.*, 2005; Le Bris *et al.*, 2006a; Schmidt *et al.*, 2008). The disadvantage of this method is that the total sulfide concentration is measured, which is the sum of several different sulfide species such as dissolved H_2S , HS^- , and soluble and suspended metal sulfides. While the relative contribution of metal sulfides to the total sulfide concentration is difficult to assess with this method, dissolved H_2S and HS^- can be determined if the pH is measured in parallel and if metal sulfides are ignored. However, soluble and suspended metal sulfides are common at vents, of which FeS is particularly abundant. Metal sulfides, however, can not be easily used by many sulfur-oxidizing microorganisms. Thus, total sulfide values do not correctly reflect the sulfide species that are biologically relevant to most sulfur-oxidizing microorganisms, H_2S and HS^- .

Voltammetric electrochemical sensors can detect and distinguish between free sulfide ($\text{H}_2\text{S}/\text{HS}^-$), soluble iron-sulfide clusters (FeS_{aq}), elemental sulfur (S^0), polysulfides (S_x^{2-}), thiosulfate ($\text{S}_2\text{O}_3^{2-}$), and tetrathionate ($\text{S}_4\text{O}_6^{2-}$) (Roazan *et al.*, 2000; Luther III *et al.*, 2001a; Luther III *et al.*, 2001b; Di Meo-Savoie *et al.*, 2004; Luther III *et al.*, 2008; Mullaugh *et al.*, 2008; Waite *et al.*, 2008). Voltammetric measurements of sulfide species in diffuse fluids of a basalt-hosted vent field on the East Pacific Rise showed that the distribution of the hydrothermal vent tube worm, *Riftia pachyptila*, was limited to habitats in which sufficient quantities of free sulfide were available to support its endosymbiotic community of sulfur-oxidizing bacteria (Luther III *et al.*, 2001b).

At the Logatchev hydrothermal vent field, dense beds of the deep-sea mussel *Bathymodiolus puteoserpentis* cover areas where diffuse fluids emerge from the subsurface. These mussels harbor two types of bacterial symbionts in their gills, a methane oxidizer or methanotroph, and a sulfur oxidizer or thiotroph (Duperron *et al.*, 2006). The high methane concentrations in the endmember fluids of this ultramafic-hosted vent (Charlou *et al.*, 2002; Schmidt *et al.*, 2007) indicate sufficient quantities of methane for endosymbiotic methanotrophy. However, the lack of data on *in situ* concentrations of sulfide at ultramafic-hosted vents raises the question if enough free sulfide ($\text{H}_2\text{S}/\text{HS}^-$) is available to support the thiotrophic symbionts of *B. puteoserpentis*. In this study, we conducted combined *in situ* measurements of dissolved hydrogen sulfide (H_2S), oxygen, and temperature over *B. puteoserpentis* mussel beds. The results are compared to data from the ultramafic-hosted Rainbow field and basalt-hosted hydrothermal vent systems and their implications for the *Bathymodiolus* symbiosis are discussed.

2 Material and Methods

2.1 Study site

The geological setting of the ultramafic-hosted Logatchev vent field has been described in detail elsewhere (Bogdanov *et al.*,

1997; Gebruk *et al.*, 2000; Schmidt *et al.*, 2007; Kuhn *et al.*, 2008). Here we provide a short summary of the sites relevant to this study. The Logatchev field is located at $14^\circ 45' \text{N}$ and $44^\circ 58' \text{W}$ on the Mid-Atlantic Ridge at a water depth of 3060 m to 2910 m (Figure 1). Areas of diffuse hydrothermal flow are found at the IRINA II and QUEST sites and are densely populated by the mussel *Bathymodiolus puteoserpentis* (Maas *et al.*, 1999; von Cosel *et al.*, 1999).

IRINA II consists of an elongate mound structure with steep slopes rising about 15 m above the surrounding seafloor with a basal diameter of about 50×25 m. Five vertical chimneys, emanating black smoke, mark the top of the mound (Schmidt *et al.*, 2007; Kuhn *et al.*, 2008) (Figure 1). Active venting of grey smoke is restricted to one of the chimneys but was also observed at small cracks at the basis of so-called pillar-like sulfide structures that are densely overgrown with mussels. The chimneys are surrounded by dense mussel beds up to 20 m in diameter, smaller mussel beds (e.g. 3×4 m) and mussel patches of 20-30 cm in diameter (Gebruk *et al.*, 2000; Schmidt *et al.*, 2007; Kuhn *et al.*, 2008). These mussel beds are inhabited by polychaetes, gastropods (snails and limpets), alvinocarid shrimps, crabs, and tremendously abundant brittle stars (*Ophioctenella acies*) (Gebruk *et al.*, 2000; Van Dover and Doerries, 2005). A single black smoker at the southeastern end of the mound emanates vigorous black smoke (Schmidt *et al.*, 2007; Kuhn *et al.*, 2008).

IRINA I and QUEST are characterized by high-temperature smoking craters, structures that are thus far unique to the Logatchev vent field. Small chimneys occur on the crater rims at IRINA I but are absent on crater rims at QUEST. Black smoke is intensively vented at both sites, either from the chimneys on the crater rim or from holes in the ground within the craters (Schmidt *et al.*, 2007; Kuhn *et al.*, 2008). At IRINA I, fauna is scarce and mainly comprises actinians and hydrozoans (Kuhn *et al.*, 2004). The fauna at QUEST is similar but additionally consists of small mussel beds. These mussel beds are smaller than those of IRINA

II (e.g. 3 x 1 m) but comprise more frequently juvenile mussels.

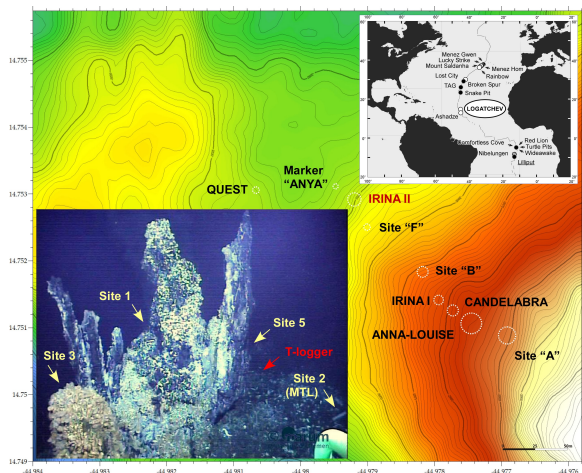


Figure 1. Map of the Logatchev hydrothermal vent field depicting currently known vent sites. The IRINA II site where measurements were performed is highlighted in red. Map courtesy of Nico Augustin (IfM Geomar, Kiel, Germany). **Lower inset:** View on the IRINA II hydrothermal main structure from NW (copyright: MARUM University of Bremen). The yellow arrows indicate where *in situ* measurements were performed. Site 1: chimney base colonized by mussels, Site 2: mussel bed submontane main structure, Site 3: pillar-like structure densely overgrown with mussels, Site 5: wall of chimney structure populated with swarms of shrimp. Red arrow: site of long-term temperature measurement inside the mussel bed. **Upper inset:** Map showing the Logatchev hydrothermal vent field in relation to known hydrothermal vent fields along the Mid-Atlantic Ridge. White and black circles denote ultramafic-hosted and basalt-hosted vent fields, respectively.

2.2 *In situ* measurements

In situ measurements of dissolved hydrogen sulfide, dissolved oxygen, and temperature were performed in 2004 during the Hydromar I cruise with the R/V Meteor (M60/3; (Kuhn *et al.*, 2004) using H₂S and O₂ electrochemical microsensors as well as a temperature sensor connected to a custom-built titanium electronic-cylinder which in the following is referred to as the In Situ Instrument (ISI). The ISI is similar to the *in situ* microprofiler used previously in sedimented environments (Wenzhöfer *et al.*, 2000; Wenzhöfer and Glud, 2002; de Beer *et al.*, 2006). Measurements were conducted

semi-autonomously on four dives using the ROV Quest (Marum, Bremen, Germany; Table 1). The ISI was fastened horizontally on an extendable drawer underneath the ROV, with the sensor tips protruding from the drawer (Figure 2 A). To prevent damage, the sensors were surrounded by a protective cage but allowing the bottom water to pass the sensors without disturbance. To permit power supply and data exchange the instrument was directly connected to the ROV via the SeaNet Cable/Connector System (Schilling Robotics, Davis, CA, USA). Data were sampled every second during the whole dive. For specific measurements at mussel populations, the ROV stopped moving and the instrument was horizontally extended on its drawer so that the sensor tips were positioned as close as possible to the mussel beds (Figure 2 B). Due to the technical setup and the horizontal ISI deployment mode, H₂S and O₂ microsensors were positioned between 5 and 13 cm above the beds while the temperature sensor was located between 7 and 11 cm above the mussels. All data were stored in the ISI internal memory as well as in the central ROV database and downloaded for analysis at the end of the dive.

Specific measurements at mussel beds were performed for 2 to 5 minute intervals approximately 10 cm above mussel beds at or around the IRINA II site (Figure 1, Table 1). Four different mussel habitats were chosen to investigate the chemical energy supply from diffuse venting: the base of a colonized chimney on the IRINA II main structure (Site 1), the lower end of the IRINA II main mussel bed extending downhill from the western slope of the IRINA II mound (Site 2), an overgrown sulfide pillar on the IRINA II main structure (Site 3), and a small mussel patch downhill from the IRINA II main structure (Site 4). Additionally, two sites without mussels were investigated for a more general comparison of the diffuse fluid composition: a chimney wall (IRINA II main structure) covered with alvinocarid shrimp but without mussels (Site 5) and the rim of a smoking crater at the IRINA I site (Site 6).

Table 1. Location of *in situ* measurements

Location	Designation	Latitude*	Longitude*	Dive	Date	Time [UTC]	Depth [m]	Figure 5
chimney base colonized by mussels	Site 1	14°45.1629'N	44°58.7478'W	9 (38ROV)	26 Jan 04	17:11-17:16	3034	A
mussel bed	Site 2	"	"	"	"	15:41-15:45	3035	B
sulfide pillar overgrown with mussels	Site 3	"	"	"	"	16:33-16:38	3035	C
mussel patch	Site 4a	"	"	14 (66ROV)	03 Feb 04	18:50-18:53	3052	D
"	Site 4b	"	"	"	"	20:02-20:04	3053	not shown
chimney wall populated with shrimp	Site 5	"	"	8 (29ROV)	24 Jan 04	16:52-16:55	3033	E
rim of smoking crater	Site 6	14°45.0776'N	44°58.6684'W	14 (66ROV)	03 Feb 04	17:00-17:05	2961	Figure 3

* due to inaccurate positioning in the course of the Hydromar I cruise, during which *in situ* measurements were performed, coordinates given are based on highly accurate data obtained during a recent revisit of the Logatchev vent field (Kuhn *et al.*, 2008).

2.3 Sensors and calibration

Dissolved H₂S was measured with amperometric H₂S microelectrodes as described by Jeroschewski *et al.* (1996) and Kühl *et al.* (1998). The sensors were calibrated in an anoxic phosphate buffer solution (pH 7.5, 200 mM) by stepwise addition of discrete amounts of a 1.3 M Na₂S stock solution. To determine the respective concentrations of total dissolved sulfide [S²⁻_{tot}] subsamples were taken, fixed in acidic 5% (w/v) zinc acetate solution, and stored at 4°C in the dark until further analysis. The resulting ZnS precipitate concentration was subsequently measured spectrophotometrically at 670 nm using the methylene blue method according to Cline (1969). The H₂S concentrations in the subsamples were calculated as described by Jeroschewski *et al.* (1996) using the equation $[H_2S] = [S^{2-}_{tot}] / 1 + 10^{(pH - pK_1)}$ where pK₁ is the negative decadal logarithm of the first dissociation constant of the sulfide equilibrium K₁. The pK₁ was corrected for temperature and salinity according to Millero *et al.* (1988). To account for the varying *in situ* temperatures at the hydrothermal vent, the calibration procedure was performed for at least two temperature points.

Dissolved O₂ was measured with Clark type microelectrodes (Revsbech, 1989). The sensors were calibrated in seawater which was bubbled with nitrogen gas and air to create an anoxic or oxygen-saturated environment, respectively. The respective O₂ concentrations for saturation were calculated according to (Weiss, 1970). To account for *in situ* temperature variations, the sensors were calibrated at two to three different temperatures.

Temperature was measured with a Pt100 stainless steel sensor (UST Umweltsensortechnik Geschwenda, Germany). For A/D converting a 16 bit chip was used allowing a resolution of 0.01°C. The sensor was calibrated against a commercial digital thermometer for a temperature range from 1 to 78°C based on eight calibration points (10 mV/°C, R² 0.9999).

All sensors were calibrated before each dive on board. The O₂ concentration of the non-hydrothermal bottom water was determined by Winkler titration on a ROV recovered water sample.

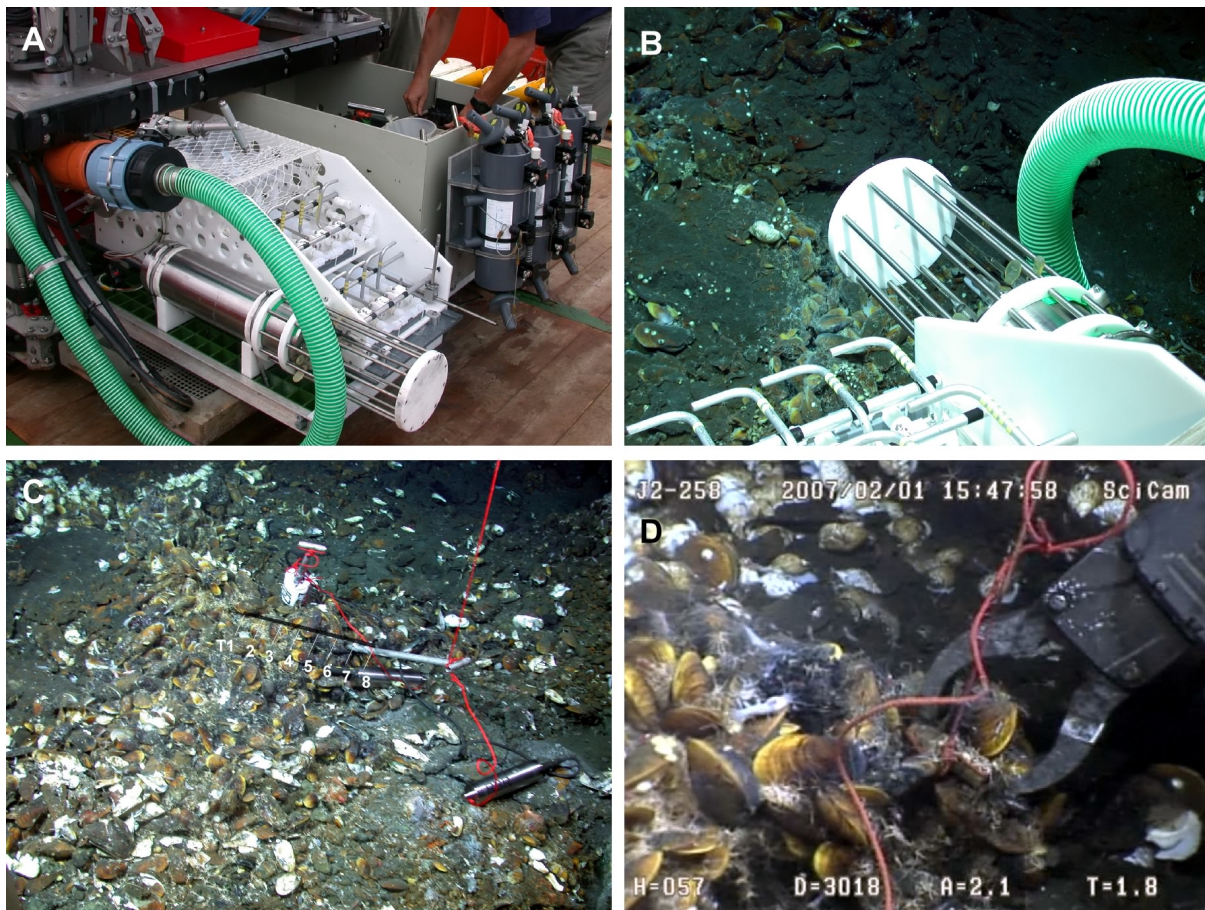


Figure 2. In Situ Instrument (ISI) and 8-channel temperature logger. (A) ISI setup on the extendable drawer of the ROV Quest (bottom left). (B) ISI measuring on top of a small mussel patch. (C) 8-channel temperature loggers on their first day of deployment. While one logger was pushed vertically into the mussel bed the other was deployed horizontally. The black line outlines the position of the horizontal temperature lance inside the mussel bed while T1-8 indicate the position of the sensors on the lance. (D) Horizontal temperature logger on day of recovery. (B & C) Copyright: MARUM University of Bremen, (D) Copyright: Woods Hole Oceanographic Institute.

2.4 Long-term temperature measurements

To monitor the temperature above mussel beds (~1 cm) independently from the ISI and immediately following the ISI measurement, a miniaturized temperature data logger (MTL) previously described by (Pfender and Villinger, 2002) was deployed for 130 hours (5.5 days) at Site 2 (Figure 1) at a temporal resolution of 10 seconds. The MTL temperature range comprised -5 to 60°C with an absolute accuracy of $\pm 0.1^\circ\text{C}$.

To monitor the temperature inside mussel beds with high spatial and temporal resolution 8-channel temperature loggers capable of long-term measurements were designed. Eight temperature sensors were equidistantly distributed at 4 cm intervals over a

total length of 28 cm inside a steel tube (sensory lance) and connected to a data logger. Each sensor was calibrated for a total precision of $\pm 0.005^\circ\text{C}$. The loggers were deployed in 2005 during the Hydromar II cruise (R/V Meteor, M64/2) using the ROV Quest (Lackschewitz *et al.*, 2005). At IRINA II, two loggers were vertically or horizontally placed inside a mussel bed at the southeastern end of the mound in close proximity to the small active black smoker and not far from the earlier ISI measurement at Site 2 (Figure 1, Figure 2 C). While the sensory lance of the vertical logger was pushed deep into the sediment underlying the mussel bed, the horizontal logger lance was inserted ap-

proximately 10 cm underneath the top of the mussel bed. Temperatures were measured every minute by all 8 sensors simultaneously and monitored over 250 days resulting in a total of 2.8 million data points. All data were stored inside the data logger. After 20 months on the seafloor the loggers were recovered in 2007 during the Hydromar III cruise (R/V Maria S. Merian, MSM 04/3, Borowski *et al.* 2007) using the ROV Jason II (Woods Hole Oceanographic Institute, Figure 2 D).

3 Results

3.1 Recordings of the *In situ* Instrument

During four ROV dives, each of which explored the Logatchev vent field for approximately 6 hours, data from 6 sites were collected with a temporal resolution of one second (Table 1). The bottom water temperature at approximately 3000 m depth in non-hydrothermally influenced water was 2.62°C with a corresponding mean dissolved oxygen concentration of 232 µM. The highest temperature concurrent with an H₂S maximum and O₂ minimum was recorded at the mussel-free IRINA I site close to the rim of a smoking crater (Site 6). At this site the temperature maximum of 11.6°C corresponded to concentrations of dissolved H₂S as high as 279 µM and O₂ concentrations as low as 37 µM (Figure 3).

Compared to ambient seawater, physico-chemical conditions approximately 10 cm above mussel beds at IRINA II were generally characterized by elevated temperatures, with slightly lower oxygen concentrations and increased hydrogen sulfide concentrations (Figure 4, Table 2). A temperature maximum of 7.4°C was recorded at Site 1 over mussel beds at a chimney base concurrent with a maximum of dissolved H₂S (59 µM) and a minimum of dissolved O₂ (142 µM) (Figure 5 A). Similar conditions were found at Site 2 at the lower edge of an extended mussel bed with temperature and H₂S maxima of 6.0°C and 79 µM, respectively (Figure 5 B). Amplitudes of physico-chemical conditions were smaller at the two

other mussel beds investigated. Above a pillar-like structure densely overgrown with

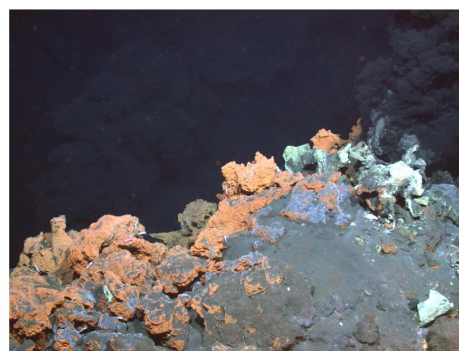
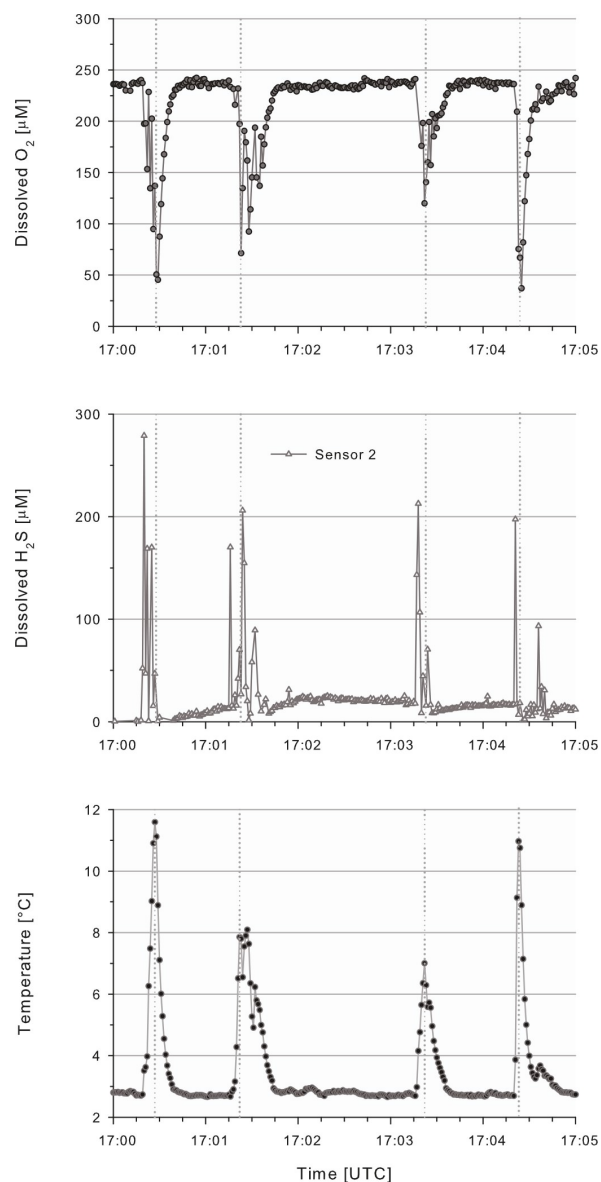


Figure 3. ISI recordings at the rim of a smoking crater. (Copyright: MARUM University of Bremen). Note that temperature peaks are concurrent with H₂S maxima and O₂ minima (dotted line).

mussels (Site 3) and a small mussel patch (Site 4) temperatures did not exceed 3.9°C and 3.4°C respectively, while the highest recorded dissolved H₂S concentrations were 51 μM and 49 μM respectively (Figure 5 C & D). In comparison, at a chimney wall populated with alvinocarid shrimp but free of mussels (Site 5) the ISI recorded 3.3°C and 49 μM dissolved H₂S (Figure 5 E).

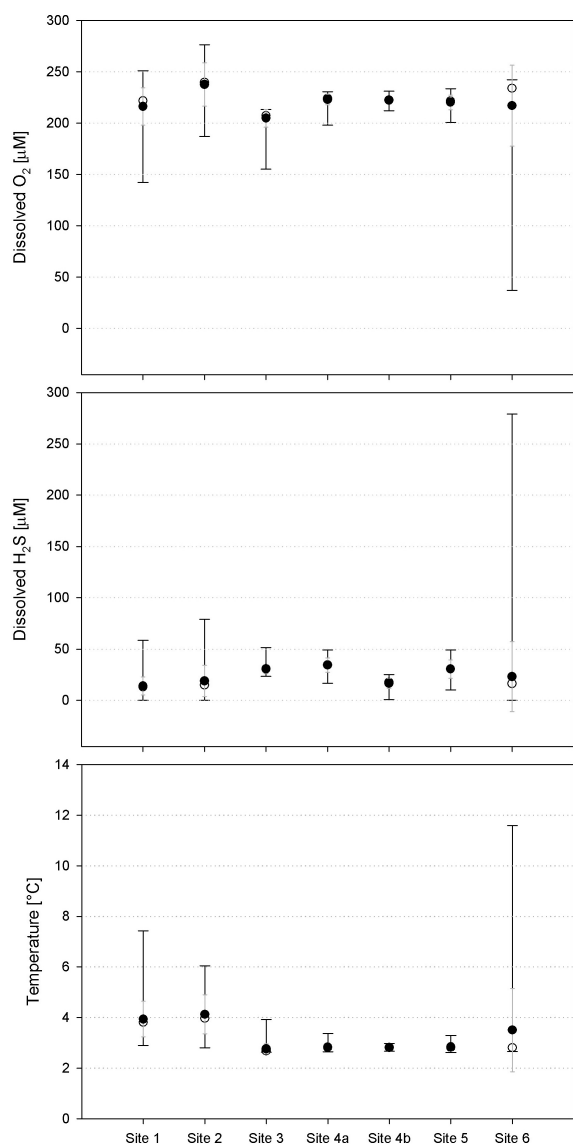


Figure 4. Summary of ISI recordings. Dissolved O₂ (top), dissolved H₂S (middle), and temperature (bottom). Filled circles denote the mean value, whereas open circles denote the median value. The standard deviation is shown as a grey bar, whereas ranges are represented by the black bar.

The temperature generally fluctuated noticeably within seconds at all investigated sites (Figure 5) with local minima close to ambient seawater. Mean temperatures did

not exceed $4.1 \pm 0.8^\circ\text{C}$ (mussel bed at Site 2) and $3.9 \pm 0.7^\circ\text{C}$ (chimney base at Site 1) and were only $2.8 \pm 0.1/0.2^\circ\text{C}$ at Sites 3 - 5. These latter sites also had comparable mean dissolved H₂S concentrations ($29 \pm 5 \mu\text{M}$ to $34 \pm 7 \mu\text{M}$). In contrast, Sites 1 and 2 had lower mean H₂S concentrations at $14 \pm 9 \mu\text{M}$ and $19 \pm 15 \mu\text{M}$, respectively. The mean O₂ concentrations at all sites were between $205 \pm 9 \mu\text{M}$ and $223 \pm 5 \mu\text{M}$ (Figure 4, Table 2).

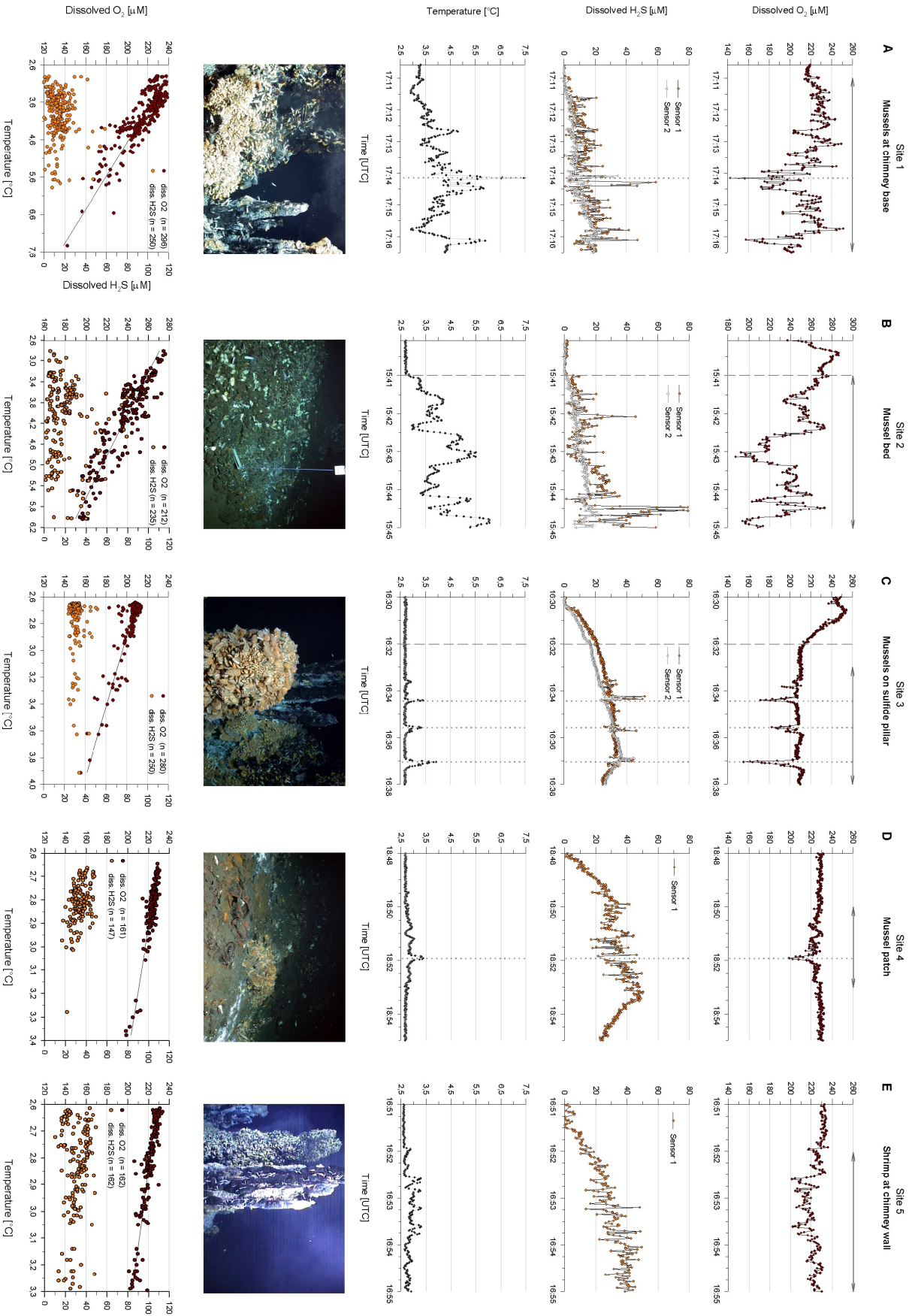
3.2 Correlation of temperature with H₂S and O₂ based on ISI microhabitat measurements

H₂S microsensors used in this study were relatively slow responding to H₂S changes, yet, if hit by sudden effluxes of hydrothermal diffuse-flow (as judged from sudden temperature peaks) they generally reacted instantly to the increased H₂S content. These H₂S peaks may be regarded as qualitative rather than quantitative H₂S maxima. Occasionally, the H₂S sensors recorded such effluxes even a few seconds prior to the temperature sensor (Figure 3, Figure 5 C) which resulted from the spatial separation of these sensors on the ISI and the consequence that the H₂S sensor actually experienced the efflux prior to the temperature sensor. Because of the characteristics of the H₂S microsensors used, dissolved H₂S concentrations did not show a direct correlation with temperature. In contrast, the O₂ profile consistently mirrored the temperature profile, resulting in a strongly negative and linear correlation of O₂ with temperature ($R^2 = 0.74-0.85$) (Figure 5). However, the ratio of this correlation (slope) was variable and depended on the recorded temperature range: the narrower the temperature range, the steeper the slope (Figure 6). For the sulfide pillar at Site 3 (2.6-3.9°C), the mussel patch at Site 4 (2.6-3.4°C), and the chimney wall at Site 5 (2.6-3.3°C) slopes were comparable and in the range of -38 to $-35 \mu\text{M}/^\circ\text{C}$. The slopes for the chimney base at Site 1 (2.9-7.4°C), the mussel bed at Site 2 (2.8-6.0°C), and the rim of the smoking crater at Site 6 (2.7 -11.6°C) were less steep ranging from -25 to $-20 \mu\text{M}/^\circ\text{C}$ (Table 2).

Table 2. Median, mean, minima, and maxima of distinct *in situ* measurements at mussel populations

Site	time	Temperature ^a					Dissolved O ₂ ^b					Dissolved H ₂ S					Figure 5		
		Med	Mean	Min	Max	n	Med	Mean	Min	n	slope	R ²	Med	Mean	Max	n			
		[°C]	[°C]	[°C]	[°C]		[°C]	[µM]	[µM]		[µM/°C]		[°C]	[µM]	[µM]				
1	chimney base colonized by mussels	5.5	3.8	3.9 ± 0.7	2.9	7.4	331	222	217 ± 16	142	296	-22	0.748	<i>SI</i>	13	14 ± 9	59	250	A
														<i>S2</i>	7	9 ± 6	34	290	
2	mussel bed	4	4.0	4.1 ± 0.8	2.8	6.0	241	240	237 ± 21	187	212	-25	0.820	<i>SI</i>	15	19 ± 15	79	235	B
														<i>S2</i>	11	10 ± 5	29	241	
3	sulfide pillar overgrown with mussels	5	2.7	2.8 ± 0.2	2.6	3.9	301	207	205 ± 9	155	280	-38	0.795	<i>SI</i>	31	30 ± 4	51	256	C
														<i>S2</i>	30	29 ± 5	45	274	
4a	mussel patch	3	2.8	2.8 ± 0.1	2.6	3.4	181	224	223 ± 5	198	161	-37	0.808	<i>SI</i>	34	34 ± 7	49	147	D
														<i>S2</i>	f	f	f		
4b	"	2	2.8	2.8 ± 0.1	2.7	3.0	121	222	222 ± 4	212	105	-50	0.849	<i>SI</i>	18	17 ± 5	25	109	not shown
														<i>S2</i>	f	f	f		
5	chimney wall populated with shrimp	3	2.8	2.8 ± 0.2	2.6	3.3	181	222	220 ± 7	201	162	-35	0.785	<i>SI</i>	31	31 ± 9	49	162	E
														<i>S2</i>	f	f	f		
6	rim of smoking crater	5	2.8	3.5 ± 1.6	2.7	11.6	301	234	217 ± 40	37	266	-20	0.748	<i>SI</i>	f	f	f	Figure 3	
														<i>S2</i>	16	23 ± 34	279	268	

^a ambient seawater temperature was 2.62°C; ^b ambient mean seawater oxygen concentration was 232 µM; *SI* and *S2* – H₂S sensors 1 and 2, respectively; f – sensor failure; Med – median; mean is given ± standard deviation



◀ **Figure 5. ISI recordings above mussel beds inhabiting areas of hydrothermal diffuse flow.** (A) mussels inhabiting chimney base, (B) mussel bed submontane main structure, (C) mussels overgrowing sulfide pillar, (D) small mussel patch downhill from main structure, (E) mussel-free chimney wall. The ISI was moved vertically toward the investigated structure. Dashed lines indicate the time point when moving from ambient seawater to the mussel habitat. Arrows denote the time interval of which data were used for correlation. Dotted lines indicate the simultaneous sensing of prominent temperature and oxygen changes in diffuse fluids (peaks) along with slightly offset H₂S amplitudes. **Photographs:** Copyright, MARUM University of Bremen.

Long-term temperature measurements

Following the ISI deployment at Site 2, a miniaturized temperature logger (MTL) was placed on top of the mussel bed at the same site (see photograph in Figure 5 B). During the first 96 hours (4 days) of the measurement the mean temperature was $4.1^{\circ}\text{C} \pm 0.5^{\circ}\text{C}$ with a maximum of 6.3°C and a minimum of 2.8°C . This is consistent with the ISI temperature recordings of only 4 minutes. After the fourth day of deployment the temperature suddenly dropped off to a mean of $3.0^{\circ}\text{C} \pm 0.1^{\circ}\text{C}$ with a maximum of 3.4°C and a minimum of 2.7°C and remained on this level until the end of the recording. Based on the ISI dataset from Site 2 and the resulting temperature to oxygen ratio, the oxygen concentration above the mussels at this site could be deduced from the MTL temperature recordings. Accordingly, the mean oxygen concentration was $202 \pm 16 \mu\text{M}$ with a minimum of $140 \mu\text{M}$ at 6.3°C and a maximum of $230 \mu\text{M}$ at 2.7°C (Figure 7).

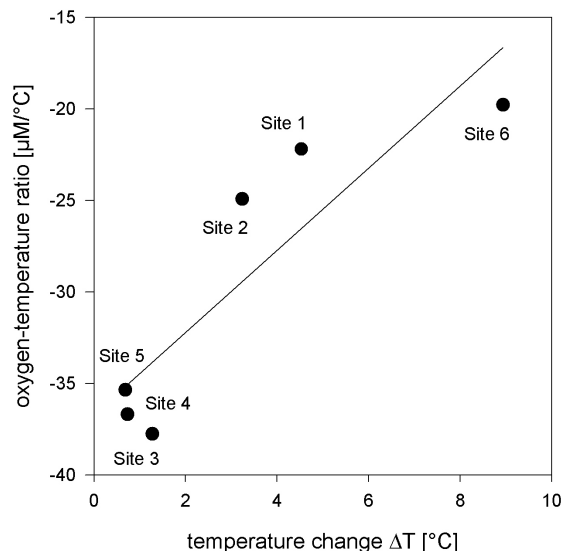


Figure 6. Correlation between the oxygen-temperature ratio and the recorded temperature change.

Following the ISI deployment in 2004, two 8-channel temperature loggers were deployed in 2005 at the IRINA II site and placed into a mussel bed in close proximity to the earlier ISI measurement at Site 2 (Figure 1, Figure 2 C). Over a distance of 28 cm the horizontal 8-channel temperature logger recorded temperature fluctuations between $2.7 - 18.2^{\circ}\text{C}$. Temperature maxima exceeding 10°C occurred consistently at 24 and 28 cm deep inside the mussel bed but were rare single events within the first 20 cm (Figure 8). This is reflected in the temperature means which were in the range of $3.8 \pm 0.6^{\circ}\text{C}$ to $5.5 \pm 1.5^{\circ}\text{C}$ over the first 20 cm and $8.3 \pm 2.6^{\circ}\text{C}$ and $10.9 \pm 3.4^{\circ}\text{C}$ at 24 and 28 cm, respectively (Table 3).

Table 3. Mean, minima, and maxima of long-term temperature measurements 10 cm inside a mussel bed over a horizontal distance of 28 cm

Horizontal depth [cm]	0	4	8	12	16	20	24	28
Channel	T8	T7	T6	T5	T4	T3	T2	T1
Median [°C]	4.1	3.7	3.7	3.6	4.0	5.4	8.6	11.6
Mean ± SD [°C]	4.4 ± 1.1	3.9 ± 0.7	3.8 ± 0.6	3.8 ± 0.9	4.3 ± 1.0	5.5 ± 1.5	8.3 ± 2.6	10.9 ± 3.4
Maximum [°C]	15.8	11.1	9.6	14.7	11.3	11.2	15.9	18.2
Minimum [°C]	2.7	2.7	2.7	2.7	2.8	2.7	2.8	2.7

SD – standard deviation

4 Discussion

4.1 Sulfide above mussel beds

The ISI recordings revealed mean dissolved H_2S concentrations between $14\ \mu\text{M}$ and $34\ \mu\text{M}$, mean dissolved O_2 concentrations between $205\ \mu\text{M}$ and $223\ \mu\text{M}$, and mean temperatures between 2.8 and 4.1°C approximately $10\ \text{cm}$ above mussel beds (Figure 4, Table 2). These data show that the Logatchev mussels have simultaneous access to both dissolved H_2S and oxygen and indicate that their diffuse-flow habitats do com-

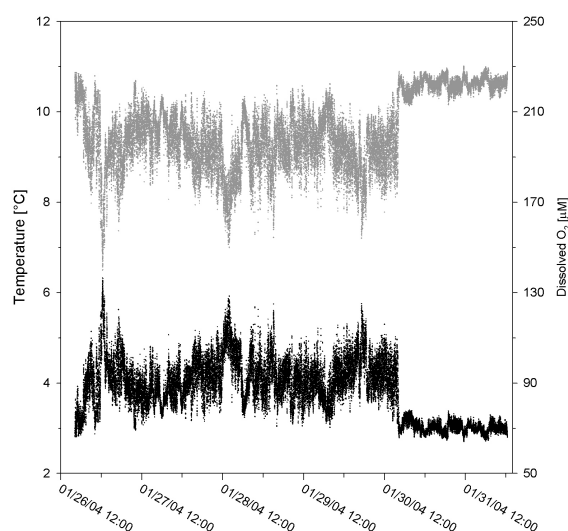


Figure 7. Long-term oxygen conditions above mussels at Site 2. Using a miniaturized temperature logger (MTL) the temperature was monitored over 128 hours with a temporal resolution of 10 seconds ($n = 46,158$). On the basis of the temperature to oxygen ratio resulting from the ISI measurements preceding the MTL deployment, the oxygen conditions (grey) were deduced from the MTL recordings (black).

ply with the requirements of endobacterial aerobic sulfide oxidation. The co-occurrence of H_2S and oxygen in diffuse-flow areas is in agreement with previous observations (Johnson *et al.*, 1986b; Johnson *et al.*, 1988b; Luther III *et al.*, 2008; Mullaugh *et al.*, 2008; Nees *et al.*, 2008) and does not contradict sulfide oxidation kinetics. The half-life for the oxidation of free sulfide ($\text{H}_2\text{S}/\text{HS}^-$) in air saturated seawater is about 26 h at 25°C , pH 8.0 (Millero *et al.*, 1987)

and increases at lower temperatures and lower oxygen concentrations (about 380 h at 2°C , pH 7.8, and $110\ \mu\text{M}\ \text{O}_2$ (Johnson *et al.*, 1994). Johnson *et al.* (1988b) have also shown that the spontaneous oxidation rate of free sulfide ($60\ \text{nmol}\ \text{l}^{-1}\ \text{s}^{-1}$ at 2°C , pH 7.8, $110\ \mu\text{M}\ \text{O}_2$, $10\ \mu\text{M}\ \text{H}_2\text{S}/\text{HS}^-$) does not account for sulfide and oxygen removal in diffuse-flow habitats.

The wealth of dissolved H_2S in Logatchev diffuse-flow habitats is in contrast to the extremely low free sulfide concentrations at Rainbow. At Rainbow *in situ* measurements in diffuse fluids dominated by the shrimp *Rimicaris exoculata* revealed total sulfide concentrations ($\text{H}_2\text{S}/\text{HS}^- + \text{FeS}$) below $5\ \mu\text{M}$ (Schmidt *et al.*, 2008). This may not be surprising for Rainbow as this ultramafic-hosted hydrothermal system is extremely rich in ferrous iron (Fe^{2+}) eventually precipitating most of the sulfide (FeS) or forming soluble FeS_{aq} clusters (FeS_{aq}). Indeed, Rainbow high temperature fluids have an $\text{Fe}/\text{H}_2\text{S}$ ratio of 24 (Charlou *et al.*, 2002; Douville *et al.*, 2002) and the $\text{Fe}/\text{H}_2\text{S}$ ratio exceeds 30 in the shrimp environment (Schmidt *et al.*, 2008). Contrary to Rainbow, ferrous iron concentrations at Logatchev are in the range of those reported from basalt-hosted vent systems on the MAR and the $\text{Fe}/\text{H}_2\text{S}$ ratio is about 1 (Schmidt *et al.*, 2007). This indicates that sulfide ($\text{H}_2\text{S}/\text{HS}^-$) may not fully be precipitated by Fe^{2+} . Furthermore, Luther III *et al.* (2001b) have argued that soluble FeS_{aq} clusters are not stable below 30°C . This means that their formation does not play a role for the removal of dissolved H_2S from low temperature diffuse flow mussel habitats. Our data clearly show that dissolved H_2S is abundant in Logatchev diffuse fluids and imply that neither is H_2S fully precipitated nor otherwise completely removed by ferrous iron.

Figure 8. Horizontal temperature distribution in a mussel bed monitored over 250 days. The temperature was measured about $10\ \text{cm}$ inside the mussel bed with 8 sensors (T1-T8) distributed over a distance of $28\ \text{cm}$. The grey plot shows the complete data set with a resolution of 1 minute ($n = 360,000$ / channel). The overlying black plot shows the mean temperature distribution with a resolution of 12 hours (averaged from 720 data points each). ▶

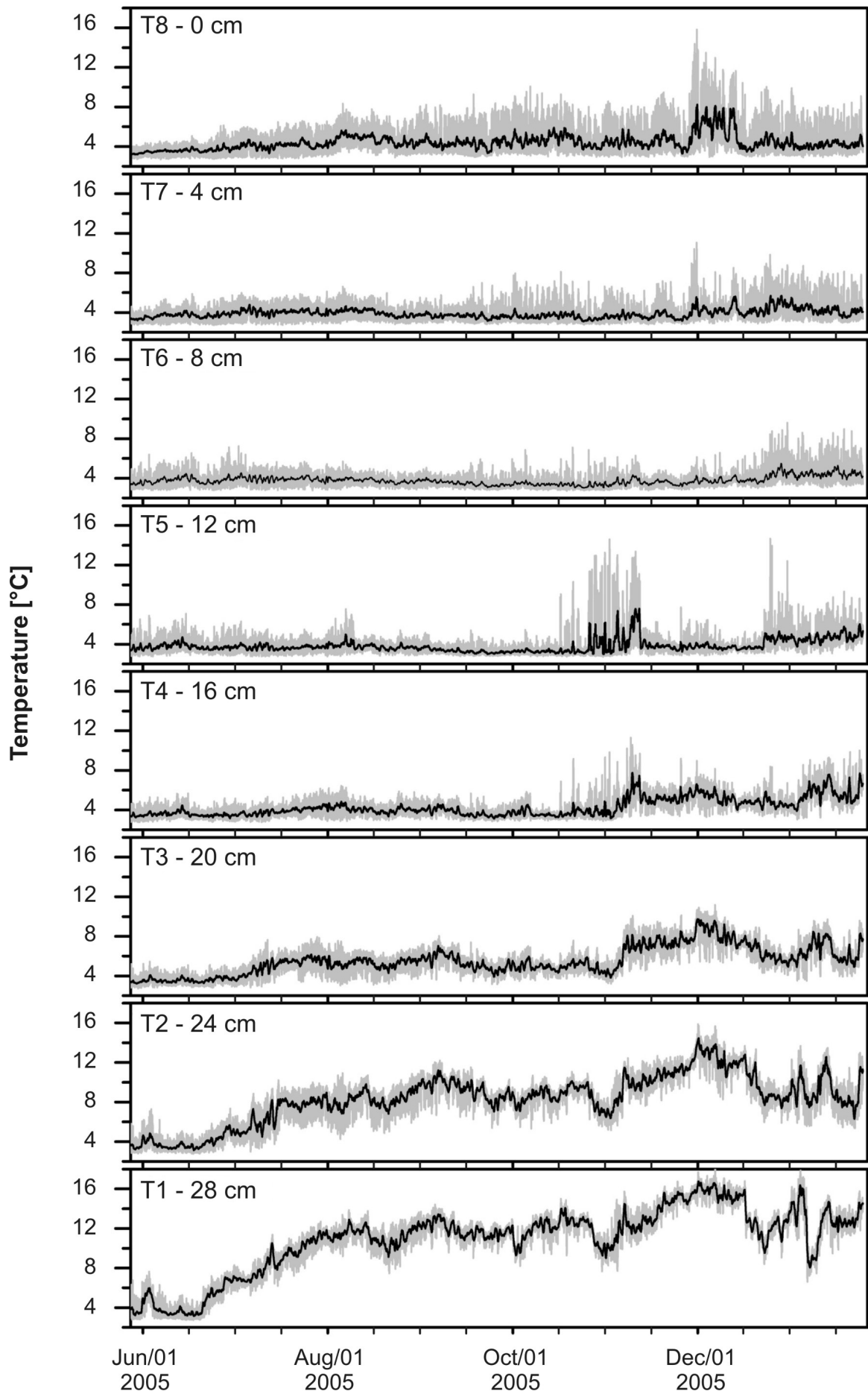


Table 4. *In situ* sulfide, oxygen, and temperature conditions of various hydrothermal diffuse flow habitats in comparison

Reference	This study	[1]	[2]	[3]	[4]	[5]	[6]	[7]	[8]	[9]	[10]	[11]	[12]	[13]
Field	Logatchev	Rainbow	Lucky Strike	9°50'N	9°50'N	9°50'N	9°50'N	13°N	9°50'N	Kilo Moana	Kilo Moana	Rose Garden	Rose Garden	Rose Garden
Ridge	MAR	MAR	MAR	EPR	EPR	EPR	EPR	EPR	EPR	ELSC	ELSC	GR	GR	GR
Habitat of	mussels	shrimp	mussels	mussels	mussels	tubeworms	mussels	tubeworms	tubeworms	mussels	mussels	mussels	mussels	mussels
H₂S	[μ M]	range 0-79 mean 14-34	na	na	na	na	na	na	na	na	na	na	na	na
H₂S/HS⁻	[μ M]	range na mean na	na	na	23-43	0-87	0-130	na	na	5-40	na	na	na	na
H₂S/HS⁻ + Fes	[μ M]	range na mean na	< 5	-	na	na	na	na	na	na	na	na	na	na
O₂	[μ M]	range 142-276 mean 205-223	nd	nd	nd	3-187	40-150	nd	nd	nd	nd	nd	nd	nd
T	[°C]	range 2.6-7.4 mean 2.8-4.1	5.3-18.2	-	7.6-7.9	2.0-16.5	2-9	≤15	2-8	nd	ca. 5	4-13	2.1-8.1	2.1-14

[1] (Schmidt *et al.*, 2008), [2] (Desbruyères *et al.*, 2001), [3] (Lutz *et al.*, 2008), [4] (Nees *et al.*, 2008), [5] (Luther III *et al.*, 2008), [6] (Le Bris *et al.*, 2006a), [7] (Le Bris *et al.*, 2003), [8] (Luther III *et al.*, 2001b), [9] (Mullaugh *et al.*, 2008), [10] (Waite *et al.*, 2008), [11] (Johnson *et al.*, 1994), [12] (Fisher *et al.*, 1988), [13] (Johnson *et al.*, 1988b); Abbreviations: na – not applicable, nd – not determined, dash – data not given, GR – Galapagos Rift, ELSC – East Lau Spreading Center, EPR – East Pacific Rise, MAR – Mid-Atlantic Ridge;

In contrast to our *in situ* measurements, on board analysis of diffuse fluids after discrete sampling implied only extremely low H₂S concentrations in IRINA II diffuse fluids. Schmidt *et al.* (2007) reported a maximum of 6.0 μM free sulfide (H₂S/HS⁻) which corresponds to 2.7 μM dissolved H₂S at their reported pH (7.0) and an assumed habitat temperature of around 3.0°C (Millero *et al.*, 1988; Jeroschewski *et al.*, 1996). The discrepancy between *in situ* and on board measurements after discrete sampling has already been pointed out in earlier studies (Le Bris *et al.*, 2006b; Schmidt *et al.*, 2008). In the absence of *in situ* techniques discrete samples may provide an approximate clue of sulfide concentrations in diffuse fluids, however as sulfide may be lost during sample recovery (Schmidt *et al.*, 2007; Schmidt *et al.*, 2008) such samples may have little to do with the actual *in situ* conditions and may thus be misleading in our understanding of diffuse-flow habitats.

As the measured sulfide species in this study was dissolved H₂S our data are not directly comparable to free sulfide (H₂S/HS⁻) or total sulfide (H₂S/HS⁻ + FeS) concentrations reported from basalt-hosted systems. The free sulfide (H₂S/HS⁻) concentrations can be calculated from dissolved H₂S if the pH, salinity, and temperature are also known (Millero *et al.*, 1988; Jeroschewski *et al.*, 1996). *In situ* measurements of pH and salinity were attempted in this study using pH microsensors and a conductivity sensor but these measurements failed. Thus, with two unknowns our data set does not allow computing the proportion of HS⁻ and the free sulfide concentrations can therefore only be estimated. At basalt-hosted systems free sulfide (H₂S/HS⁻) concentrations in diffuse fluids are in the range from non-detectable to 130 μM with mean concentrations up to 27 μM (Table 4). Total sulfide concentrations (H₂S/HS⁻ + FeS) can reach 330 μM (Table 4).

4.2 Temperature above and inside mussel beds

The calculated mean temperatures ranged from 2.8 ± 0.1°C to 4.1 ± 0.8°C over

and from 3.8 ± 0.6°C to 10.9 ± 3.4°C inside the mussel beds and are thus in agreement with temperature means reported from other hydrothermal vent fields. Mean temperatures between 3.7°C and 14.4°C have been reported for *B. azoricus* from the Rainbow, Lucky Strike and Menez Gwen fields on the slow-spreading MAR (Desbruyères *et al.*, 2001). Johnson *et al.* (1988a; 1994) reported mean temperatures between 3.0°C and 5.5°C above and inside clumps of *B. thermophilus* from the basalt-hosted Rosen Garden vent field on the intermediate-spreading GR. Mean values between 7.7°C and 17.0°C have been reported from mussel beds in the Lau Back-Arc Basin (Chevaldonné *et al.*, 1991). The maximum temperatures with 7.4°C and 18.2°C being the highest record above and inside Logatchev mussel beds, respectively are also consistent with reported maxima from other vent fields. Temperature maxima of around 20°C inside mussel beds have frequently been measured (Chevaldonné *et al.*, 1991; Johnson *et al.*, 1994; Shank *et al.*, 1998; Desbruyères *et al.*, 2001). Temperature fluctuations with minima close to ambient as we report here are in agreement with previous studies from intermediate- (Fisher *et al.*, 1988; Johnson *et al.*, 1988a; Johnson *et al.*, 1988b; Johnson *et al.*, 1994), and slow-spreading ridges (Desbruyères *et al.*, 2001) as well as Back-Arc Basins (Chevaldonné *et al.*, 1991).

It has been argued that the mean of physico-chemical conditions in diffuse-flow habitats is not meaningful because of the variability of conditions and extreme short-term fluctuations. However, for extended periods the mean does reflect whether mussels are generally exposed to lower or higher temperatures, have more or less access to oxygen-rich ambient water, and experience lower or higher sulfide concentrations. Yet, mean values must not exceed a critical point. Values beyond this point would be lethal due to oxygen limitation, sulfide overexposure (failure of sulfide detoxification processes), thermal disruption of mitochondrial membranes and thus respiration activity (O'Brien *et al.*, 1991) or a combination of these factors. For example, the respiration activity of

B. thermophilus drops off at 33°C (Arrhenius break point, Dahlhoff *et al.*, 1991). However, fluids at these temperatures are already anoxic and sulfide-rich. For example, Johnson *et al.* (1988a; 1994) have shown that fluids at Rose Garden (GR) become anoxic above 11°C and can likely contain 1 mM sulfide at approximately 20°C. Thus, from a physiological point of view, mussels of the genus *Bathymodiolus* are unlikely to survive extended periods at mean temperatures exceeding a critical value which depending on the physico-chemical conditions at a given vent field (ambient temperature, ambient oxygen concentration, sulfide content of diffuse-flow) may range between 11°C and 17°C. At Logatchev a critical long-term temperature mean of 13°C was estimated as diffuse fluids become anoxic at around this temperature (see below). The long-term temperature means inside Logatchev mussel beds were generally far below this value (Figure 8, Table 3) indicating that over the monitored period of 250 days the mussels were neither oxygen-limited nor overexposed to free sulfide ($\text{H}_2\text{S}/\text{HS}^-$).

4.3 Correlation of temperature with H_2S and O_2 based on micro-habitat measurements

Johnson *et al.* (1988a) have demonstrated that temperature can be used to estimate sulfide and oxygen concentrations in diffuse-flow vent habitats. In the range of 2 to 11°C temperature correlated positively with total sulfide ($\text{H}_2\text{S}/\text{HS}^- + \text{FeS}$) and negatively with oxygen although the relationship was not always linear due to biological consumption of these compounds (Johnson *et al.*, 1988a). Le Bris and co-workers have confirmed the linear sulfide to temperature relation, but pointed out that sulfide to temperature ratios are all but constant between sites but highly variable (Le Bris *et al.*, 2003; Le Bris *et al.*, 2006a; Le Bris *et al.*, 2006b). Due to this inter-site variability it is inevitable to assess the sulfide to temperature ratio for each site of interest. Deducing sulfide concentrations from temperature recordings are then justified but only for this particular site (Le Bris *et al.*, 2003; Le Bris

et al., 2006a; Le Bris *et al.*, 2006b). Temporal variability of sulfide-temperature ratios has recently been demonstrated using *in situ* voltammetry (Nees *et al.*, 2008). Because the H_2S microsensors available for our study were rather slow responding to H_2S changes, dissolved H_2S concentrations did not show an apparent correlation pattern with temperature. However, the conservative mixing model predicts that the relation of the H_2S concentration to temperature should be close to linear in the diffuse flow areas, with only a slight curvature at temperatures close to ambient (Le Bris *et al.*, 2006a).

The O_2 profile consistently mirrored the temperature profile in all fluctuations resulting in a strongly negative and linear correlation of O_2 with temperature. This is in agreement with previous observations (Johnson *et al.*, 1988a; Nees *et al.*, 2008). However, the ratio of this correlation (slope) was variable ranging from -22 to -38 $\mu\text{M}/^\circ\text{C}$. Apparently, there is a correlation between the recorded temperature range and the steepness of the oxygen-temperature slope: the narrower the temperature range the steeper the slope. Extrapolation from data comprising a wider temperature range to zero oxygen fluid content indicates that diffuse-flow habitats at Logatchev become anoxic at temperatures around 13°C.

4.4 Conclusion and outlook

Our study shows that changes in temperature are correlated to changes in O_2 and that elevated temperatures are indicative of dissolved H_2S at the Logatchev mussel beds. The oxygen-temperature correlation is consistent with earlier *in situ* investigations (Johnson *et al.*, 1988a; Nees *et al.*, 2008) and complements previous findings of sulfide-temperature correlations in diffuse-flow vent habitats (Le Bris *et al.*, 2003; Le Bris *et al.*, 2006a; Le Bris *et al.*, 2006b; Nees *et al.*, 2008; Waite *et al.*, 2008). Thus, previous studies and this investigation indicate that temperature loggers could be used as indicators of oxygen and sulfide fluctuations in diffuse-flow habitats over longer time periods allowing the estimation of long-term oxygen (as demonstrated in Figure 7) and

sulfide concentrations in these habitats. However, as has been pointed out earlier, estimations of sulfide and oxygen from temperature recordings are justified only for those sites for which the oxygen- and sulfide-temperature ratios have been determined beforehand with high-resolution *in situ* techniques. Long term measurements may be more representative of the energy flow from the vent fluids to the mussels and its chemosynthetic bacterial endosymbionts than those that can be recorded during a single dive.

Bathymodiolin mussels from vent fields along the MAR harbor two types of chemosynthetic endosymbionts. One is related to type I methanotrophs and the other to chemoautotrophic symbionts of other *Bathymodiolus* hosts (Duperron *et al.*, 2006). Additionally, a bacterial parasite is widely distributed in these mussels infecting and destroying host nuclei (Zielinski *et al.*). It can be assumed that the abundance and activity of these bacteria is determined by the physico-chemical conditions surrounding their hosts, i.e. by the availability of H₂S and CH₄ as electron donors and O₂ as terminal electron acceptor during respiration and thus energy conservation. Differing long- and short term physico-chemical conditions in different habitats may result in differences in endobacterial abundances and activities. Long-term physico-chemical conditions of the habitat (i.e. weeks and months) may shape the relative abundance of the two chemosynthetic endosymbionts and perhaps the abundance of the intranuclear bacterial parasite (i.e. their mutual proportion) whereas short-term fluctuations (i.e. hours and less) in diffuse fluids may influence their relative activity. Long-term temperature recordings which permit the estimation of chemical conditions in mussel habitats could certainly help to shed more light on this question.

Acknowledgements

We acknowledge the chief scientists Thomas Kuhn, Klas Lackschewitz, and Christian Borowski of the involved research cruises as well as the captains and crews of

the vessels Meteor and Maria S. Merian and the chief engineers and crews of the ROV's Quest and Jason II for their best support to deploy the In Situ Instrument and temperature loggers. We thank Volker Meyer, Paul Färber, and Harald Osmer for their engagement in last minute adaptation of the In Situ Instrument for use with the ROV Quest. Ursula Werner and Eva Walpersdorf are acknowledged for their introduction into working with microsensors. We appreciate Gabriele Eickert who skillfully constructed the microelectrodes and gave indispensable comments for their deployment in the field. This work was supported by grants from the priority program 1144 of the German Science Foundation (DFG). This is publication number XY of the priority program 1144 "From Mantle to Ocean: Energy-, Material- and Life cycles a Spreading Axes" of DFG.

References

- Alain, K., 2004. Early steps in microbial colonization processes at deep-sea hydrothermal vents. *Environ. Microbiol.* 6 (3), 227-241.
- Bach, W., Banerjee, N.R., Dick, H.J.B., Baker, E.T., 2002. Discovery of ancient and active hydrothermal systems along the ultra-slow spreading Southwest Indian Ridge 10 degrees-16 degrees E. *Geochem. Geophys. Geosyst.* 3.
- Bogdanov, Y.A., Bortnikov, N.S., Vikent'ev, I.V., Gurvich, E.G., Sagalevich, A.M., 1997. A new type of modern mineral-forming system: Black smokers of the hydrothermal field at 14°45'N latitude, Mid-Atlantic Ridge. *Geology of Ore Deposits* 39 (1), 58-78.
- Charlou, J.L., Donval, J.P., Fouquet, Y., Jean-Baptiste, P., Holm, N., 2002. Geochemistry of high H₂ and CH₄ vent fluids issuing from ultramafic rocks at the Rainbow hydrothermal field (36°14'N, MAR). *Chem. Geol.* 191 (4), 345-359.
- Chevaldonné, P., Desbruyères, D., Le Haître, M., 1991. Time-series of temperature from three deep-sea hydrothermal vent sites. *Deep-Sea Res. A* 38 (11), 1417-1430.
- Cline, J.D., 1969. Spectrophotometric Determination of Hydrogen Sulfide in Natural Waters. *Limnol. Oceanogr.* 14 (3), 454-458.
- Dahlhoff, E., O'Brien, J., Somero, G.N., Vetter, R.D., 1991. Temperature effects on mitochondria from hydrothermal vent invertebrates: evidence for adaptation to elevated and variable habitat temperatures. *Physiol. Zool.* 64 (6), 1490-1508.

- Davydov, M.P., Aleksandrov, P.A., Perova, E.N., Semkova, T.A., 2007. Ferromanganese deposits in the Ashadze-1 hydrothermal field (Mid-Atlantic Ridge, 12°58'N). *Dokl. Earth Sci.* 415 (6), 954-960.
- de Beer, D., Sauter, E., Niemann, H., Kaul, N., Foucher, J.P., Witte, U., Schlüter, M., Boetius, A., 2006. In situ fluxes and zonation of microbial activity in surface sediments of the Håkon Mosby Mud Volcano. *Limnol. Oceanogr.* 51 (3), 1315-1331.
- Desbruyères, D., Biscoito, M., Caprais, J.-C., Colaço, A., Comtet, T., Crassous, P., Fouquet, Y., Khripounoff, A., Le Bris, N., Olu, K., Riso, R., Sarradin, P.M., Segonzac, M., Vangriesheim, A., 2001. Variations in deep-sea hydrothermal vent communities on the Mid-Atlantic Ridge near the Azores plateau. *Deep-Sea Res. I* 48 (5), 1325-1346.
- Di Meo-Savoie, C.A., Luther III, G.W., Cary, S.C., 2004. Physicochemical characterization of the microhabitat of the epibionts associated with *Alvinella pompejana*, a hydrothermal vent annelid. *Geochim. Cosmochim. Acta* 68 (9), 2055-2066.
- Dias, Á.S., Barriga, F.J.A.S., 2006. Mineralogy and geochemistry of hydrothermal sediments from the serpentinite-hosted Saldanha hydrothermal field (36°34'N; 33°26' W) at MAR. *Mar. Geol.* 225 (1-4), 157-175.
- Douville, E., Charlou, J.L., Oelkers, E.H., Bienvenu, P., Colon, C.F.J., Donval, J.P., Fouquet, Y., Prieur, D., Appriou, P., 2002. The rainbow vent fluids (36°14'N, MAR): the influence of ultramafic rocks and phase separation on trace metal content in Mid-Atlantic Ridge hydrothermal fluids. *Chem. Geol.* 184 (1-2), 37-48.
- Duperron, S., Bergin, C., Zielinski, F., Blazejak, A., Pernthaler, A., McKiness, Z.P., DeChaine, E., Cavanaugh, C.M., Dubilier, N., 2006. A dual symbiosis shared by two mussel species, *Bathymodiolus azoricus* and *Bathymodiolus puteoserpentis* (Bivalvia: Mytilidae), from hydrothermal vents along the northern Mid-Atlantic Ridge. *Environ. Microbiol.* 8 (8), 1441-1447.
- Edmonds, H.N., Michael, P.J., Baker, E.T., Connelly, D.P., Snow, J.E., Langmuir, C.H., Dick, H.J.B., Muhe, R., German, C.R., Graham, D.W., 2003. Discovery of abundant hydrothermal venting on the ultraslow-spreading Gakkel ridge in the Arctic. *Nature* 421 (6920), 252-256.
- Fisher, C.R., Childress, J.J., Arp, A.J., Brooks, J.M., Distel, D., Favuzzi, J.A., Felbeck, H., Hessler, R., Johnson, K.S., II, M.C.K., Macko, S.A., Newton, A., Powell, M.A., Somero, G.N., Soto, T., 1988. Microhabitat variation in the hydrothermal vent mussel, *Bathymodiolus thermophilus*, at the Rose Garden vent on the Galapagos Rift. *Deep-Sea Res. I* 35 (10/11), 1769-1791.
- Gebbruk, A.V., Chevaldonné, P., Shank, T., Lutz, R.A., Vrijenhoek, R.C., 2000. Deep-sea hydrothermal vent communities of the Logatchev area (14°45'N, Mid-Atlantic Ridge): diverse biotopes and high biomass. *J. Mar. Biol. Assoc. U.K.* 80 (3), 383-393.
- Geret, F., Riso, R., Sarradin, P.M., Caprais, J.C., Cosson, R.P., 2002. Metal bioaccumulation and storage forms in the shrimp, *Rimicaris exoculata*, from the Rainbow hydrothermal field (Mid-Atlantic Ridge); preliminary approach to the fluid-organism relationship. *Cahiers De Biologie Marine* 43 (1), 43-52.
- Jeroschewski, P., Steuckart, C., Kühl, M., 1996. An amperometric microsensor for the determination of H₂S in aquatic environments. *Anal. Chem.* 68 (24), 4351-4357.
- Johnson, K.S., Beehler, C.L., Sakamoto-Arnold, C.M., 1986a. A submersible flow analysis system. *Anal. Chim. Acta* 179, 245-257.
- Johnson, K.S., Beehler, C.L., Sakamoto-Arnold, C.M., Childress, J.J., 1986b. In situ measurements of chemical distributions in a deep-sea hydrothermal vent field. *Science* 231 (4742), 1139-1141.
- Johnson, K.S., Childress, J.J., Beehler, C.L., 1988a. Short-term temperature variability in the Rose Garden hydrothermal vent field: an unstable deep-sea environment. *Deep-Sea Res. A* 35 (10-11), 1711-1721.
- Johnson, K.S., Childress, J.J., Beehler, C.L., Sakamoto, C.M., 1994. Biogeochemistry of hydrothermal vent mussel communities: the deep-sea analogue to the intertidal zone. *Deep-Sea Res. I* 41 (7), 993-1011.
- Johnson, K.S., Childress, J.J., Hessler, R.R., Sakamoto-Arnold, C.M., Beehler, C.L., 1988b. Chemical and biological interactions in the Rose Garden hydrothermal vent field, Galapagos spreading center. *Deep-Sea Res. A* 35 (10-11), 1723-1744.
- Kühl, M., Steuckart, C., Eickert, G., Jeroschewski, P., 1998. A H₂S microsensor for profiling biofilms and sediments: application in an acidic lake sediment. *Aquat. Microb. Ecol.* 15 (2), 201-209.
- Kuhn, K., Kuhn, T., Hékinian, R., Franz, L., Augustin, N., Petersen, S., Borowski, C., 2008. The geological setting of the ultramafic-hosted Logatchev hydrothermal field (14°45'N, MAR) and its influence on massive sulfide formation. Submitted to *Lithos*.
- Kuhn, T., Alexander, B., Augustin, N., Birgel, D., Borowski, C., de Carvalho, L., Engemann, G., Ertl, S., Franz, L., Grech, C., Herzig, P., Hékinian, R., Imhoff, J., Jellinek, T., Klar, S., Koschinsky, A., Kuever, J., Kulescha, F., Lackschewitz, K., Petersen, S., Ratmeyer, V., Renken, J., Ruhland, G., Scholten, J., Schreiber, K., Seifert, R., Süling, J., Türkay, M., Westernströer, U., Zielinski, F., 2004. The Logatchev hydrothermal field – revisited: preliminary results of the R/V METEOR Cruise HYDROMAR I (M60/3). *InterRidge News* 13, 1-4.

- Lackschewitz, K.S., Armini, M., Augustin, N., Dubilier, N., Edge, D., Engemann, G., Fabian, M., Felden, J., Franke, P., Gärtner, A., Garbe-Schönberg, D., Gennerich, H.H., Hüttig, D., Marbler, H., Meyerdirks, A., Pape, T., Perner, M., Reuter, M., Ruhland, G., Schmidt, K., Schott, T., Schroeder, M., Schroll, G., Seiter, C., Stecher, J., Strauss, H., Viehweger, M., Weber, S., Wenzhöfer, F., Zielinski, F., 2005. Longterm study of hydrothermalism and biology at the Logatchev field, Mid-Atlantic Ridge at 14°45'N (revisit 2005; HYDROMAR II). Cruise Report. Meteor Berichte 05. Mid-Atlantic Expedition 2005. Cruise No. 64, Leg 2. Leitstelle Meteor - Institut für Meereskunde der Universität Hamburg, pp. 1-61.
- Le Bris, N., Govenar, B., Le Gall, C., Fisher, C.R., 2006a. Variability of physico-chemical conditions in 9°50'N EPR diffuse flow vent habitats. *Mar. Chem.* 98 (2-4), 167-182.
- Le Bris, N., Rodier, P., Sarradin, P.M., Le Gall, C., 2006b. Is temperature a good proxy for sulfide in hydrothermal vent habitats? *Cah. Biol. Mar.* 47 (4), 465-470.
- Le Bris, N., Sarradin, P.M., Birot, D., Alayse-Danet, A.M., 2000. A new chemical analyzer for *in situ* measurement of nitrate and total sulfide over hydrothermal vent biological communities. *Mar. Chem.* 72 (1), 1-15.
- Le Bris, N., Sarradin, P.M., Caprais, J.C., 2003. Contrasted sulphide chemistries in the environment of 13°N EPR vent fauna. *Deep-Sea Res. I* 50 (6), 737-747.
- Le Bris, N., Zbinden, M., Gaill, F., 2005. Processes controlling the physico-chemical micro-environments associated with Pompeii worms. *Deep-Sea Res. I* 52 (6), 1071-1083.
- Luther III, G.W., Glazer, B.T., Hohmann, L., Popp, J.I., Taillefert, M., Rozan, T.F., Brendel, P.J., Theberge, S.M., Nuzzio, D.B., 2001a. Sulfur speciation monitored *in situ* with solid state gold amalgam voltammetric microelectrodes: polysulfides as a special case in sediments, microbial mats and hydrothermal vent waters. *J. Environ. Monit.* 3 (1), 61-66.
- Luther III, G.W., Glazer, B.T., Ma, S.F., Trouwborst, R.E., Moore, T.S., Metzger, E., Kraiya, C., Waite, T.J., Druschel, G., Sundby, B., Taillefert, M., Nuzzio, D.B., Shank, T.M., Lewis, B.L., Brendel, P.J., 2008. Use of voltammetric solid-state (micro)electrodes for studying biogeochemical processes: Laboratory measurements to real time measurements with an *in situ* electrochemical analyzer (ISEA). *Mar. Chem.* 108, 221-235.
- Luther III, G.W., Rozan, T.F., Taillefert, M., Nuzzio, D.B., Di Meo, C., Shank, T.M., Lutz, R.A., Cary, S.C., 2001b. Chemical speciation drives hydrothermal vent ecology. *Nature* 410 (6830), 813-816.
- Lutz, R.A., Shank, T.M., Luther III, G.W., Vetriani, C., Tolstoy, M., Nuzzio, D.B., Moore, T.S., Waldhauser, F., Crespo-Medina, M., Chatziefthimiou, A.D., Annis, E.R., Reed, A.J., 2008. Interrelationships between vent fluid chemistry, temperature, seismic activity, and biological community structure at a mussel-dominated, deep-sea hydrothermal vent along the East Pacific Rise. *J. Shellfish Res.* 27 (1), 177-190.
- Maas, P.A.Y., O'Mullan, G.D., Lutz, R.A., Vrijenhoek, R.C., 1999. Genetic and morphometric characterization of mussels (*Bivalvia: Mytilidae*) from Mid-Atlantic hydrothermal vents. *Biol. Bull.* 196 (3), 265-272.
- Millero, F.J., Hubinger, S., Fernandez, M., Garnett, S., 1987. Oxidation of H₂S in seawater as a function of temperature, pH, and ionic strength. *Environ. Sci. Technol.* 21 (5), 439-443.
- Millero, F.J., Plese, T., Fernandez, M., 1988. The Dissociation of Hydrogen Sulfide in Seawater. *Limnol. Oceanogr.* 33 (2), 269-274.
- Mullaugh, K.M., Luther III, G.W., Ma, S., Moore, T.S., Yücel, M., Becker, E.L., Podowski, E.L., Fisher, C.R., Trouwborst, R.E., Pierson, B.K., 2008. Voltammetric (micro)electrodes for the *in situ* study of Fe²⁺ oxidation kinetics in hot springs and S₂O₃²⁻ production at hydrothermal vents. *Electroanalysis* 20, 280-290.
- Nees, H.A., Moore, T.S., Mullaugh, K.M., Holyoke, R.R., Janzen, C.P., Ma, S., Metzger, E., Waite, T.J., Yücel, M., Lutz, R.A., Shank, T.M., Vetriani, C., Nuzzio, D.B., Luther III, G.W., 2008. Hydrothermal vent mussel habitat chemistry, pre- and post-eruption at 9°50' North on the East Pacific Rise. *J. Shellfish Res.* 27 (1), 169-175.
- O'Brien, J., Dahlhoff, E., Somero, G.N., 1991. Thermal resistance of mitochondrial respiration - hydrophobic interactions of membrane proteins may limit thermal resistance. *Physiol. Zool.* 64 (6), 1509-1526.
- Pfender, M., Villinger, H., 2002. Miniaturized data loggers for deep sea sediment temperature gradient measurements. *Mar. Geol.* 186 (3-4), 557-570.
- Revsbech, N.P., 1989. An oxygen microsensor with a guard cathode. *Limnol. Oceanogr.* 34 (2), 474-478.
- Rozan, T.F., Theberge, S.M., Luther III, G., 2000. Quantifying elemental sulfur (S⁰), bisulfide (HS⁻) and polysulfides (S_x²⁻) using a voltammetric method. *Anal. Chim. Acta* 415 (1-2), 175-184.
- Sakamoto-Arnold, C.M., Johnson, K.S., Beehler, C.L., 1986. Determination of hydrogen sulfide in seawater using flow injection analysis and flow analysis. *Limnol. Oceanogr.* 31 (4), 894-900.
- Sarradin, P.M., Le Bris, N., Birot, D., Caprais, J.C., 1999. Laboratory adaptation of the methylene blue method to flow injection analysis: towards *in situ*

- sulfide analysis in hydrothermal seawater. *Anal. Commun.* 36 (4), 157-160.
- Schmidt, C., Vuillemin, R., Le Gall, C., Gaill, F., Le Bris, N., 2008. Geochemical energy sources for microbial primary production in the environment of hydrothermal vent shrimps. *Mar. Chem.* 108, 18-31.
- Schmidt, K., Koschinsky, A., Garbe-Schönberg, D., de Carvalho, L.M., Seifert, R., 2007. Geochemistry of hydrothermal fluids from the ultramafic-hosted Logatchev hydrothermal field, 15°N on the Mid-Atlantic Ridge: Temporal and spatial investigation. *Chem. Geol.* 242 (1-2), 1-21.
- Shank, T.M., Fornari, D.J., Von Damm, K.L., Lilley, M.D., Haymon, R.M., Lutz, R.A., 1998. Temporal and spatial patterns of biological community development at nascent deep-sea hydrothermal vents (9°50'N, East Pacific Rise). *Deep-Sea Res. II* 45 (1-3), 465-515.
- Snow, J.E., Edmonds, H.N., 2007. Ultraslow-spreading ridges. *Oceanography* 20 (1), 90-101.
- Tunnicliffe, V., Embley, R.W., Holden, J.F., Butterfield, D.A., Massoth, G.J., Juniper, S.K., 1997. Biological colonization of new hydrothermal vents following an eruption on Juan de Fuca Ridge. *Deep-Sea Res. I* 44 (9-10), 1627-1644.
- Van Dover, C.L., Doerries, M.B., 2005. Community structure in mussel beds at Logatchev hydrothermal vents and a comparison of macrofaunal species richness on slow- and fast-spreading mid-ocean ridges. *Mar. Ecol.* 26 (2), 110-120.
- von Cosel, R., Comtet, T., Krylova, E.M., 1999. *Bathymodiolus* (Bivalvia: Mytilidae) from hydrothermal vents on the Azores Triple Junction and the Logatchev hydrothermal field, Mid-Atlantic Ridge. *Veliger* 42 (3), 218-248.
- Waite, T.J., Moore, T.S., Childress, J.J., Hsu-Kim, H., Mullaugh, K.M., Nuzzio, D.B., Paschal, A.N., Tsang, J., Fishers, C.R., Luther III, G.W., 2008. Variation in sulfur speciation with shellfish presence at a Lau Basin diffuse flow vent site. *J. Shellfish Res.* 27 (1), 163-168.
- Weiss, R.F., 1970. Solubility of Nitrogen, Oxygen and Argon in Water and Seawater. *Deep-Sea Res. Oceanogr. Abstr.* 17 (4), 721-735.
- Wenzhöfer, F., Glud, R.N., 2002. Benthic carbon mineralization in the Atlantic: a synthesis based on in situ data from the last decade. *Deep-Sea Research Part I-Oceanographic Research Papers* 49 (7), 1255-1279.
- Wenzhöfer, F., Holby, O., Glud, R.N., Nielsen, H.K., Gundersen, J.K., 2000. In situ microsensor studies of a shallow water hydrothermal vent at Milos, Greece. *Mar. Chem.* 69 (1-2), 43-54.
- Wetzel, L.R., Shock, E.L., 2000. Distinguishing ultramafic- from basalt-hosted submarine hydrothermal systems by comparing calculated vent fluid compositions. *J. Geophys. Res.* 105 (B4), 8319-8340.
- Zielinski, F.U., Pernthaler, A., Duperron, S., Raggi, L., Giere, O., Borowski, C., Dubilier, N., Widespread occurrence of an intranuclear bacterial parasite in vent and seep mussels. *PLoS Biol.* submitted.

Widespread Occurrence of an Intranuclear Bacterial Parasite in Vent and Seep Mussels

Frank U. Zielinski^{1,2}, Annelie Pernthaler³, Sébastien Duperron⁴, Luciana Raggi¹,
Olav Giere⁵, Christian Borowski¹, and Nicole Dubilier^{1*}

¹ Max Planck Institute for Marine Microbiology, Department of Molecular Ecology
Celsiusstr. 1, 28359 Bremen, Germany

² Helmholtz Centre for Environmental Research – UFZ, Department of Environmental Microbiology,
Permoser Str. 15, 04318 Leipzig, Germany

³ California Institute of Technology, Division of Geological and Planetary Sciences,
1200 E California Blvd, Pasadena CA, 91125, USA

⁴ Université Pierre et Marie Curie, Équipe Adaptation aux Milieux Extrêmes,
7 Quai St Bernard, 75005 Paris, France

⁵ University of Hamburg, Biozentrum Grindel und Zoologisches Museum,
Martin-Luther-King Platz 3, 20146 Hamburg, Germany

* Corresponding author:

Phone: +49 (0)421 2028 932; Fax: +49 (0)421 2028 580; Email: ndubilie@mpi-bremen.de

Abstract

Many parasitic bacteria live in the cytoplasm of multicellular animals, but only a few are known to regularly invade their nuclei. In this study, we describe the novel bacterial parasite “*Candidatus Endonucleobacter bathymodioli*” that invades the nuclei of deep-sea bathymodiolin mussels from hydrothermal vents and cold seeps. Bathymodiolin mussels are well known for their symbiotic associations with sulfur- and methane-oxidizing bacteria. In contrast, the parasitic bacteria of vent and seep animals have received comparatively little attention despite their potential importance for vent and seep ecosystems. We first discovered the intranuclear parasite “*Ca. E. bathymodioli*” in *Bathymodiolus puteoserpentis* mussels from the Logatchev hydrothermal vent field on the Mid-Atlantic Ridge. Using primers and probes specific to the 16S rRNA sequence of “*Ca. E. bathymodioli*” we found this intranuclear parasite in at least seven bathymodiolin mussel species from vents and seeps around the world. Fluorescence *in situ* hybridization and transmission electron microscopy analyses of the developmental cycle of “*Ca. E. bathymodioli*” showed that the infection of a nucleus begins with a single rod-shaped bacterium which grows to an unseptated filament of up to 20 µm length and eventually divides repeatedly until the nucleus is filled with up to 80,000 bacteria. The greatly swollen nucleus ruptures the cytoplasmic membrane of its host cell and the bacteria are released after the nuclear membrane is disrupted. Intriguingly, we found infected nuclei in the cells of all mussel tissues with only one exception: the gill bacteriocytes. These cells contain the symbiotic sulfur- and methane-oxidizing bacteria, suggesting that the mussel symbionts can protect their host nuclei from infection with “*Ca. E. bathymodioli*”. Phylogenetic analyses showed that the “*Ca. E. bathymodioli*” 16S rRNA gene sequence belongs to a monophyletic clade of Gammaproteobacteria associated with marine metazoans as diverse as sponges, corals, bivalves, ascidians, and fish. The location of these bacteria in their hosts is unknown for all but two. The bacteria of these two host species have been identified as intranuclear parasites, one in a previous study in the razor clam *Siliqua patula*, and one in this study in the venerid clam *Ruditapes philippinarum*, a commercially important species for both the wild fishery and aquaculture industry worldwide. We propose that many of the sequences from this clade originated from intranuclear bacteria, and that these are widespread in marine invertebrates.

Abbreviations

FISH, fluorescence *in situ* hybridization; GCM, Gabon-Continental Margin; GoM, Gulf of Mexico; MAR, Mid-Atlantic Ridge; NIX, "Nuclear Inclusion X"; PAR, Pacific-Antarctic Ridge; TEM, Transmission Electron Microscopy

Introduction

Bacteria inhabit every imaginable place on earth. With the evolution of the eukaryotes, numerous bacteria have established a symbiotic or parasitic relationship inside eukaryotic cells. Most of these bacteria live in the cytoplasm, but some have found their way into eukaryotic cell compartments, including mitochondria [1-3], chloroplasts [4-6], the perinuclear space [7], and nuclei [7-11]. Although eukaryotic cell compartments have been investigated for decades with light and electron microscopy, little is known about intracompartimental bacteria, particularly those that live in the nuclei of eukaryotes. Most commonly described from protists [7,11-13], almost nothing is known about intranuclear bacteria of metazoans. Rickettsial Alphaproteobacteria occasionally invade nuclei of their arthropod or mammalian hosts but occur mainly in the cytoplasm [14-19]. Apart from these facultative intranuclear *Rickettsia*, reports of intranuclear bacteria that are morphologically or phylogenetically distinct from the Rickettsiales are rare in metazoans. Only a single 16S rRNA sequence is currently known from an intranuclear bacterium that does not belong to the Rickettsiales [20]. This Gammaproteobacterium, called "Nuclear Inclusion X" (NIX), causes mass mortalities in the Pacific razor clam *Siliqua patula* [21,22]. A few morphological observations of non-Rickettsiales-like intranuclear bacteria have been described from the venerid clam *Ruditapes decussatus* [23], and two marine *Aplysina* sponges (formerly *Verongia*) [24,25].

Deep-sea hydrothermal vents and cold seeps have been studied extensively since their discovery 25 – 30 years, ago. Given the high diversity of metazoans currently described from vents and seeps [26-30],

remarkably little is known about their parasites [31]. To date about a dozen metazoan macroparasites have been described [32,33]. A few studies, using 18S rRNA based molecular techniques, have suggested that there may be a high abundance of parasitic protist at vents [34-38], and the morphology of fungal, protist, bacterial, and viral parasites has been described in more detail in some vent and seep mussels, clams, and limpets [39-43]. These studies suggest the potential importance of parasites for vent and seep ecosystems, yet comprehensive investigations of the taxonomy, phylogeny, and life cycle of vent and seep parasites are still lacking.

Mussels of the genus *Bathymodiolus* (Bivalvia: Mytilidae) occur worldwide at deep-sea hydrothermal vents and cold seeps [44-47]. In the absence of light and thus, photosynthetic carbon fixation, these mussels depend on chemosynthetic bacterial symbionts for their nutrition [48,49]. These endosymbionts occur in the mussel's gill tissue, in the cytoplasm of bacteriocytes that regularly alternate with symbiont-free intercalary cells [50,51]. Bathymodiolin mussels can harbor two types of chemosynthetic bacteria: a chemoautotrophic sulfur-oxidizer, capable of fixing CO₂ in the presence of sulfide or thiosulfate as energy sources, and a methane-oxidizer that uses methane both as a carbon and an energy source [52-57]. Some mussel species harbor only thiotrophic or only methanotrophic symbionts, while other mussel species harbor both types and thus live in a dual symbiosis [45]. The energy sources for the bacterial symbionts, reduced sulfur compounds and methane, are provided by the hydrothermal fluids at vents and through hydrocarbon seepage at cold seeps. Both the mussels and their chemosynthetic bacteria mutually benefit from their symbiosis: the mussel facilitates access to the reductants and oxidants that are necessary for energy production (such as sulfide, methane, and oxygen) by supplying its symbionts with a constant fluid flow. In exchange, the bacterial symbionts provide carbon compounds that support the growth and maintenance of host biomass [48,49]. In

addition to their symbiotic bacteria, some vent and seep mussels have recently been described that are colonized by parasitic microbes, but beyond their morphology, almost nothing is known about these parasites [39,40,43].

This study describes a novel bacterial parasite of bathymodiolin mussels. Using comparative 16S rRNA sequence analysis, fluorescence *in situ* hybridization (FISH) and transmission electron microscopy we show that this parasite lives in the nuclei of mussels from vents and seeps around the world. We describe the life cycle of this intranuclear parasite through reconstruction of its developmental cycle from a solitary cell to the proliferation of up to 80,000 bacteria within a single greatly enlarged nucleus. We propose the name “*Candidatus Endonucleobacter bathymodioli*” for this bacterium. The genus name “*Endonucleobacter*” translates freely into ‘bacterium living inside the nucleus’ and the species name “*bathymodioli*” refers to the host genus of vent and seep mussels, *Bathymodiolus*, in which we discovered this parasite.

Results

Discovery of intranuclear bacteria in *Bathymodiolus puteoserpentis*. Three gammaproteobacterial 16S rRNA phylotypes were found in gill tissues of *B. puteoserpentis* from the Logatchev hydrothermal vent field on the Mid-Atlantic Ridge (Figure 2 A). In addition to the sequences already known from the sulfur- and methane-oxidizing symbionts [58], a novel 16S rRNA sequence was discovered (“*Candidatus Endonucleobacter bathymodioli*” in Figure 2 A). This novel sequence fell in a clade consisting of 16S rRNA sequences from bacteria associated with marine animals including sponges, corals, a sea slug, an ascidian, a sea urchin, and a fish (93-97% identity, Table S1). This clade also included the sequence from the “Nuclear Inclusion X” parasite of the Pacific razor clam *Siliqua patula* [20]. The monophyly of this clade was well supported in both maximum likelihood and Bayesian analyses (support values: 60 and 1.00). The cultivated species within this clade were all heterotrophic: *Endozoicomonas elysicola*, a strictly aerobic and mesophilic bacterium from the gastrointestinal tract of the sea slug *Elysia ornata* [59], and three species from marine sponges, one rod-shaped (H425) and one spirillum-like (H262) bacterium [60], and *Spongiobacter nickelotolerans* (unpublished information from GenBank). The closest relatives to the clade containing “*Ca. E. bathymodioli*” were *Zooshikella gangwhensis*, a chemoorganotrophic, aerobic, and halophilic isolate from sediments of a Korean tidal flat [61] (91% identity to the “*Ca. E. bathymodioli*” sequence from *B. puteoserpentis*) and two sequences from *Rickettsia*-like bacteria causing mass mortality in the oyster *Crassostrea ariakensis* (unpublished information in Genbank under accession numbers DQ118733 und DQ123914).

FISH analyses with probes specific to the “*Ca. E. bathymodioli*” phylotype showed that it originated from bacteria that occurred exclusively in the nuclei of *B. puteoserpentis* cells (Figure 3). Transmission electron microscopy (TEM) confirmed that the bacteria

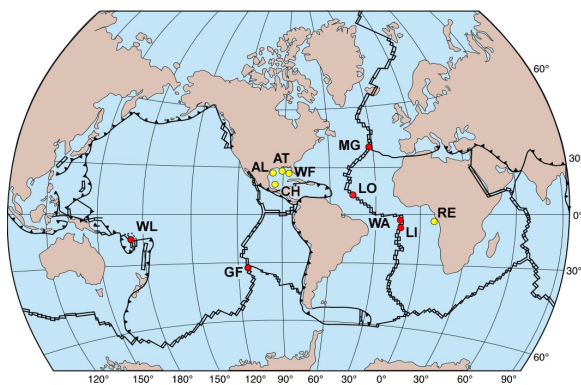
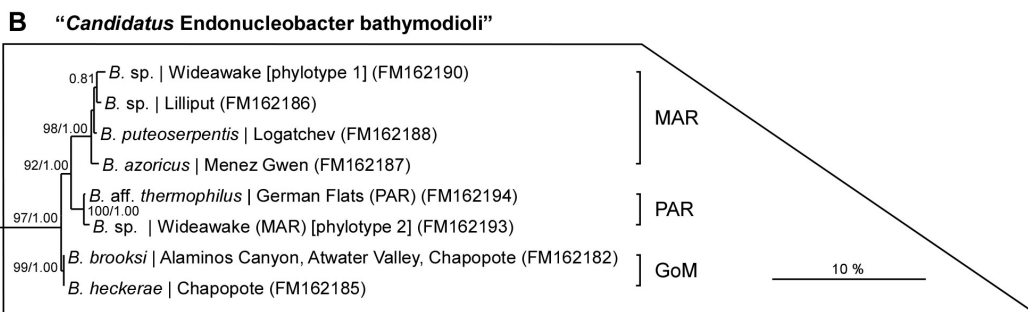
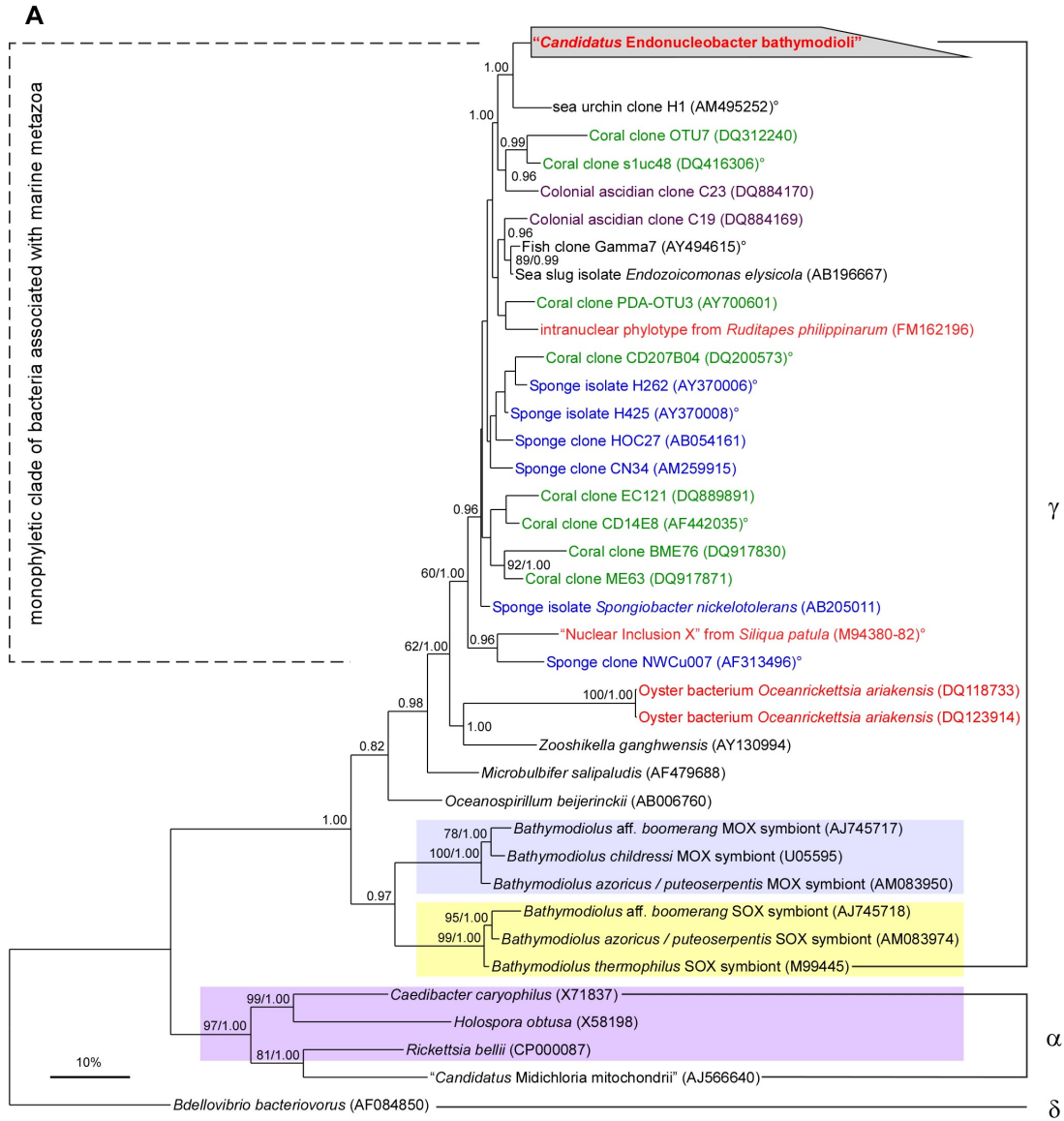


Figure 1. Sampling sites of bathymodiolin species investigated in this study. Circles show hydrothermal vents (red) and cold seeps (yellow). Abbreviations: MG – Menez Gwen, LO – Logatchev, WA – Wideawake, LI – Lilliput (Mid-Atlantic Ridge); AL – Alaminos Canyon, AT – Atwater Valley, CH – Chapopote, WF – West Florida Escarpment (Gulf of Mexico); RE – Regab (Gabon Continental Margin); GF – German Flats (Pacific-Antarctic Ridge); WL – White Lady (North Fiji Back-Arc Basin).

were inside the host nuclei (Figure 4). Gill tissues were most heavily colonized (Figure 3 A-D, F), but the bacteria were also occasionally observed in nuclei of the gut (Figure 3 E), digestive gland, labial palp, mantle, and foot (data not shown). In the gill tissues, only

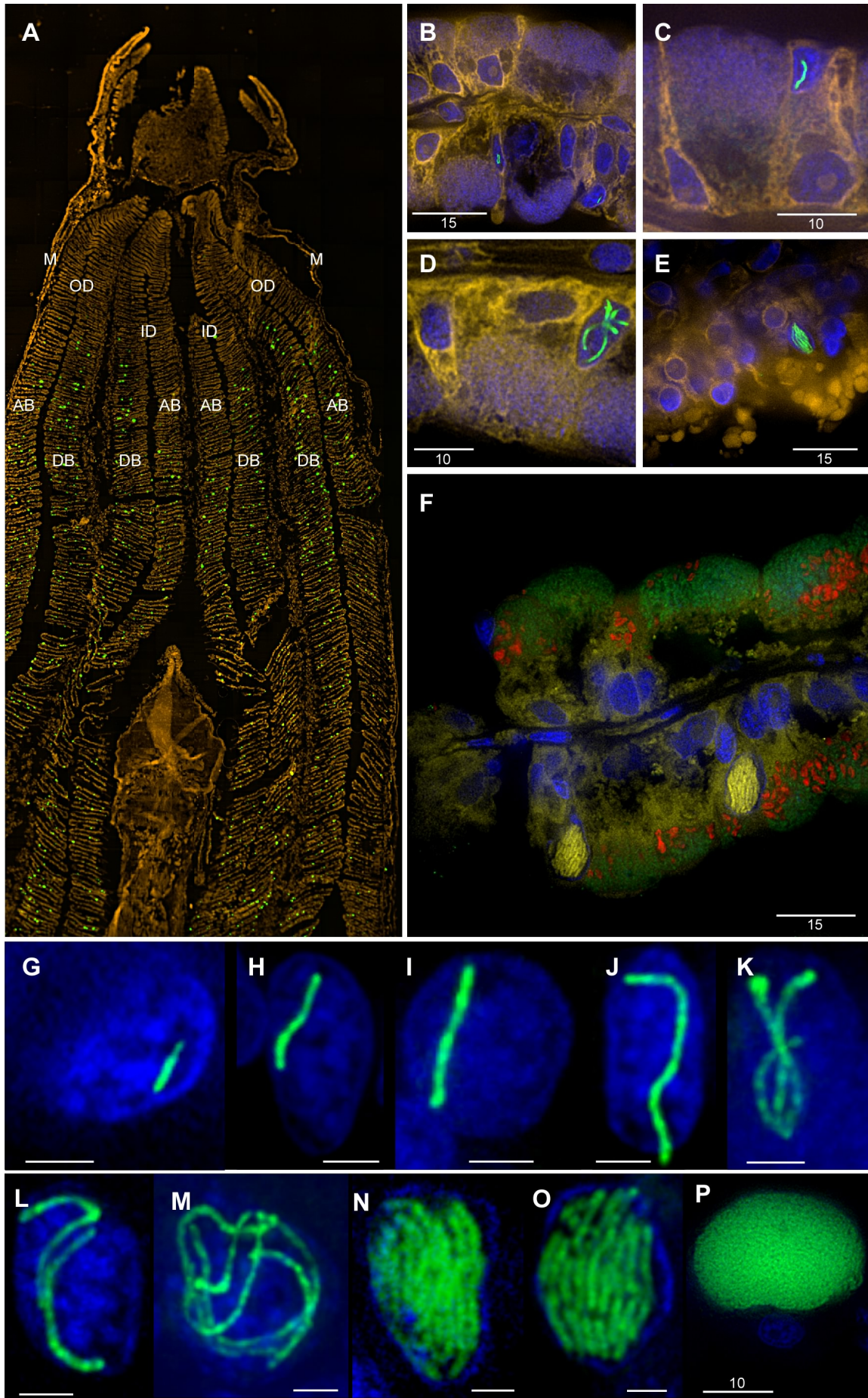
nuclei of the symbiont-free intercalary cells were infected, whereas intranuclear bacteria were never observed in the bacteriocytes containing the thiotrophic and methanotrophic symbionts (Figure 3 B-D, F).



Developmental cycle of “*Ca. E. bathymodioli*”. FISH and TEM analyses of “*Ca. E. bathymodioli*” revealed six distinct developmental stages in *B. puteoserpentis* gill tissues (Figure 3, Figure 4, Figure 5). In Stage 1, a single rod-shaped bacterium (1.8 x 0.4 μm) is present inside the nucleus (Figure 3 B, G). In Stage 2, the bacterium has grown to an unseptated filament of up to 18-20 μm length (Figure 3 H-J). In Stage 3, a loosely wrapped filamentous coil is visible inside the host nucleus (Figure 3 M). We could not clearly discern if this coil consists of several separate filaments or one long unseptated filament. However, on rare occasions we observed two filaments of equal length (Figure 3 L) and filaments that appeared to be in the process of longitudinal division in some nuclei (Figure 3 K), suggesting that the Stage 3 coil consists of several filaments. The host nuclei in Stage 3 have become more irregular in shape and chromatin is reduced to a thin layer along the nuclear membrane (Figure 4 A, D). Transverse binary fission of the filamentous coils leads to Stage 4 in which stacks of shorter filaments of up to 8-10 μm

length fill the host nucleus (Figure 3 E, N). At this stage, host nuclei are at least 2-3 times the volume of uninfected nuclei. Repeated transverse binary fissions lead to the formation of numerous rods in Stage 5 with the nuclei further enlarged to about five times the volume of uninfected nuclei. Chromatin is nearly completely reduced and barely visible along some parts of the nuclear membrane (Figure 4 E). In Stage 6, the bacteria have reproduced massively forming a “bubble” of up to 30 μm in diameter that is still surrounded by a membrane (Figure 3 P). At this stage, the infected nuclei are no longer visible within structurally intact host cells, but occur extracellularly within the gill epithelium. At average bacterial sizes of 1.8 x 0.4 μm , Stage 6 nuclei can contain up to 80,000 bacteria. These “bubbles” are eventually disrupted and the bacteria released into the fluids surrounding the mussel gills. Three-dimensional examples of the developmental Stages 2, 3, 4, and 6 can be viewed as supporting animations (VideoS1-VideoS4).

◀ **Figure 2. 16S rRNA phylogenetic tree inferred from Bayesian and maximum likelihood analysis. (A)** The tree shows the “*Candidatus* Endonucleobacter bathymodioli” clade (grey trapezoid) together with its closest relatives. Colors of sequences from marine invertebrates were assigned according to host phylogeny, with bacteria from bivalves shown in red, from sponges in blue, and from ascidians in purple (sea slug, sea urchin, and fish bacteria shown in black). Also included in the tree are (i) the closest free living relatives within the Oceanospirillales and Alteromonadales, (ii) the methane-oxidizing endosymbionts of bathymodiolin mussels (blue box), (iii) the sulfur-oxidizing endosymbionts of bathymodiolin mussels (yellow box), as well as (iv) intranuclear bacteria belonging to the Rickettsiales from ciliates and ticks (purple box). *Bdellovibrio bacteriovorus* was used as an outgroup. The phylogenetic reconstruction is based primarily on nearly full sequences. Partial sequences (508-983 bp) are marked (°). Methane- and sulfur-oxidizing symbionts of bathymodiolin mussels are labelled MOX and SOX, respectively. Values at nodes represent maximum likelihood bootstrap values in % (first value) and posterior probabilities (second value). Scale bar represents 10% estimated base substitution. Only bootstrap values ≥ 60 and posterior probabilities > 0.80 are shown. (Abbreviations: MAR – Mid-Atlantic Ridge, PAR – Pacific-Antarctic Ridge, GoM – Gulf of Mexico). **(B)** Tree of “*Ca. E. bathymodioli*” sequences from vent and seep mussels (collection sites of mussels are shown). The “*Ca. E. bathymodioli*” sequences form a monophyletic clade.



◀ **Figure 3. “*Ca. E. bathymodioli*” in various mussel tissues and developmental stages.** (A) Cross-section through a juvenile mussel showing the distribution of the intranuclear bacterium throughout the gill tissue. Intranuclear bacteria are shown in green and mussel tissue appears in orange. The morphology results from staining nuclei and bacterial endosymbiotic DNA with DAPI which was assigned an orange color. Abbreviations: AB – ascending gill branch; DB – descending gill branch; ID – inner demibranch; M – mantle; OD – outer demibranch; (B-D) Non-ciliated gill tissue with intranuclear bacterium in intercalary cells which alternate with bacteriocytes; (E) Gut tissue; (B-E) Intranuclear bacteria are shown in green and eukaryotic tissue is represented in yellow. Nuclei and bacterial endosymbiotic DNA in bacteriocytes appear in blue. (F) Non-ciliated gill tissue with intranuclear bacteria; Intranuclear bacteria appear in bright yellow, whereas eukaryotic tissue is represented by a yellowish to brownish color. Chemoautotrophic and methanotrophic bacterial endosymbionts in bacteriocytes are shown in green and red, respectively. Nuclei were stained with DAPI and appear in blue. (G-P) Developmental stages of “*Ca. E. bathymodioli*”. The intranuclear bacterium appears in green, the nucleus in blue. The scale bar represents 2 μm unless otherwise shown. (G-J) Series showing growth from a single short rod to a single filament in Stages 1 and 2; (K) Two overlapping filaments or filament in the process of longitudinal binary fission in transition from Stage 2 to 3; (L) Two separate filaments (Stages 2 to 3); (M) Filamentous assembly consisting of either one single long coiled filament or several filaments (Stage 3); (N) Stacks of shorter filaments (Stage 4) resulting from transverse fissions of coiled filaments; (O) Long rods resulting from division of Stage 4 filaments; (P) Bacterial “bubble” released from the destroyed host cell (Stage 6). Bacteria are retained inside the nuclear membrane. Images H-M result from projection of a stack of several two-dimensional layers onto one single layer reflecting the overall 3-dimensional structure on a 2-dimensional plane.

Widespread occurrence of “*Ca. E. bathymodioli*” in deep-sea mussels. Using PCR primers and FISH probes specific to the “*Ca. E. bathymodioli*” phylotype found in *B. puteoserpentis*, we searched for these bacteria in other bathymodiolin hosts from hydrothermal vents and cold seeps in the Atlantic Ocean, the Gulf of Mexico, and the Pacific Ocean (Figure 1, Table 1). We found “*Ca. E. bathymodioli*” in the nuclei of all host species except “*B.*” *childressi* (Gulf of Mexico), *B. aff. boomerang* (South East Atlantic), and *B. brevior* (West Pacific). All “*Ca. E. bathymodioli*” sequences were very closely related to each other with 98.8% identity between sequences on average and 98.1% identity between the two most distant phylotypes (Figure 2 B). In most host species, a single 16S rRNA phylotype dominated the clone libraries. Less dominant

phylotypes that differed by at most 2 bp from the dominant phylotypes were also found in several host species. These phylotypes often co-occurred in the same host individuals and were shared between individuals (Table S2). In *B. sp.* from Wideawake (Mid-Atlantic Ridge), a single 16S rRNA clone was found with a sequence that differed distinctly by 1.9% (26 bp) from all other “*Ca. E. bathymodioli*” phylotypes found in this species (called “minor phylotype III” in Table S2). This phylotype was most closely related to the sequence from *B. aff. thermophilus* (Pacific-Antarctic Ridge) (Figure 2 A). With the exception of this minor phylotype III, all other “*Ca. E. bathymodioli*” sequences fell into three clusters reflecting their geographic origins from the Mid-Atlantic Ridge, the Pacific-Antarctic Ridge, and the Gulf of Mexico (Figure 2 B).

Table 1. Bathymodioliin species investigated in this study and sampling sites

Bathymodioliin species	Location	Cruise name Sample ID	recovery ^d	month and year		chief scientist Latitude	Reference Longitude	
				Depth	Year			
<i>B. azoricus</i> ^a	Menez Gwen	ATOS MG3, 5, and 10	Victor	Jun/Jul 2001	850 m	P. M. Sarradin 37°51'N	[102] 31°31'W	
<i>B. puteoserpentis</i> ^a	Logatchev / Irina 2	Hydromar I	Quest	Jan/Feb 2004	3016 m	T. Kuhn 14°45.1629'N	[103] 44°58.7478'W	
		35GTV-3			3035 m			
		38ROV/6-5			3035 m			
		56ROV/6-6			3035 m			
		66ROV/16-3			3053 m			
<i>B. sp.</i> ^a	Widawake	Marsued II	Quest	Apr 2005	2998 m	K. Haase 4°48.64'S	[104] 12°22.36'W	
		109GTV/A-3			2998 m			
		125ROV/1B-2			2987 m		4°48.6293'S	12°22.3524'W
		125ROV/7-4			2986 m		4°48.6275'S	12°22.3503'W
		125ROV/12-6			2987 m	4°48.6231'S	12°22.3515'W	
<i>B. sp.</i> ^a	Liliput / Main Liliput	Marsued II 200ROV/9-3	Quest	Apr 2005	1496 m	K. Haase 9°33.1783'S	[105] 13°11.8462'W	
<i>B. brevior</i> ^a	White Lady / LHOS	Hyflux II	TV-grab	Aug/Sep 1998	1976 m	P. Halbach 16°59.348'S	[106] 173°55.029'E	
		39GTV-6			2009 m	16°59.449'S	173°54.940'E	
		66GTV-12			2000 m	16°59.486'S	173°54.911'E	
		99GTV-9						
<i>B. aff. thermophilus</i> ^a	German Flats (38°S) ^c	Foundation 3	TV-grab	Jun/Jul 2001	2212 m	P. Stoffers 37°47.4673'S	[107,108] 110°54.8675'W	
		30GTV-1 to 4						
<i>B. aff. boomerang</i> ^b	Gabon-Cont. Margin (GCM)	Biozair 2	Victor	Nov 2001	3150 m	M. Sibuet 5°52.8134'S	[82,109] 9°37.9419'E	
		GCM / Regab						
<i>B. heckerae</i> ^b	West Florida Escarpment	Deep Seeps III/I	Alvin	Oct 2003	3284 m	C. R. Fisher and B. Carney 26°02.00'N	84°55.03'W	
		GoM M6						
<i>B. heckerae</i> ^b	Campeche Knolls (CK)	Meteor M67/2	Quest	Apr 2006	2915 m	G. Bohrmann 21°53.98'N	93°26.12'W	
		CK / Chapopote						
<i>B. brooksi</i> ^b	Louisiana Cont. Slope (LCS)	Sp2.1 & Sp2.2			2915 m			
		Deep Seeps III/I	Alvin	Oct 2003	1893 m	C. R. Fisher and B. Carney 27°34.1'N	88°29.8'W	
<i>B. brooksi</i> ^b	LCS / Alamos Canyon	GoM M24			2226 m	26°21.32'N	94°30.12'W	
<i>B. brooksi</i> ^b	LCS / Alaminos Canyon	GoM M29			2226 m			
<i>B. brooksi</i> ^b	LCS / Alaminos Canyon	GoM M34			2226 m			

^a species from hydrothermal vents; ^b species from cold seeps; ^c vent field name according to [27]; ^d Samples were recovered using the remotely-operated vehicles Quest (Marum, University of Bremen, Germany) and Victor (Ifremer, France), the manned submersible Alvin (Woods Hole Oceanographic Institution, USA), and a TV-controlled grab (Oktopus GmbH Kiel, Germany).

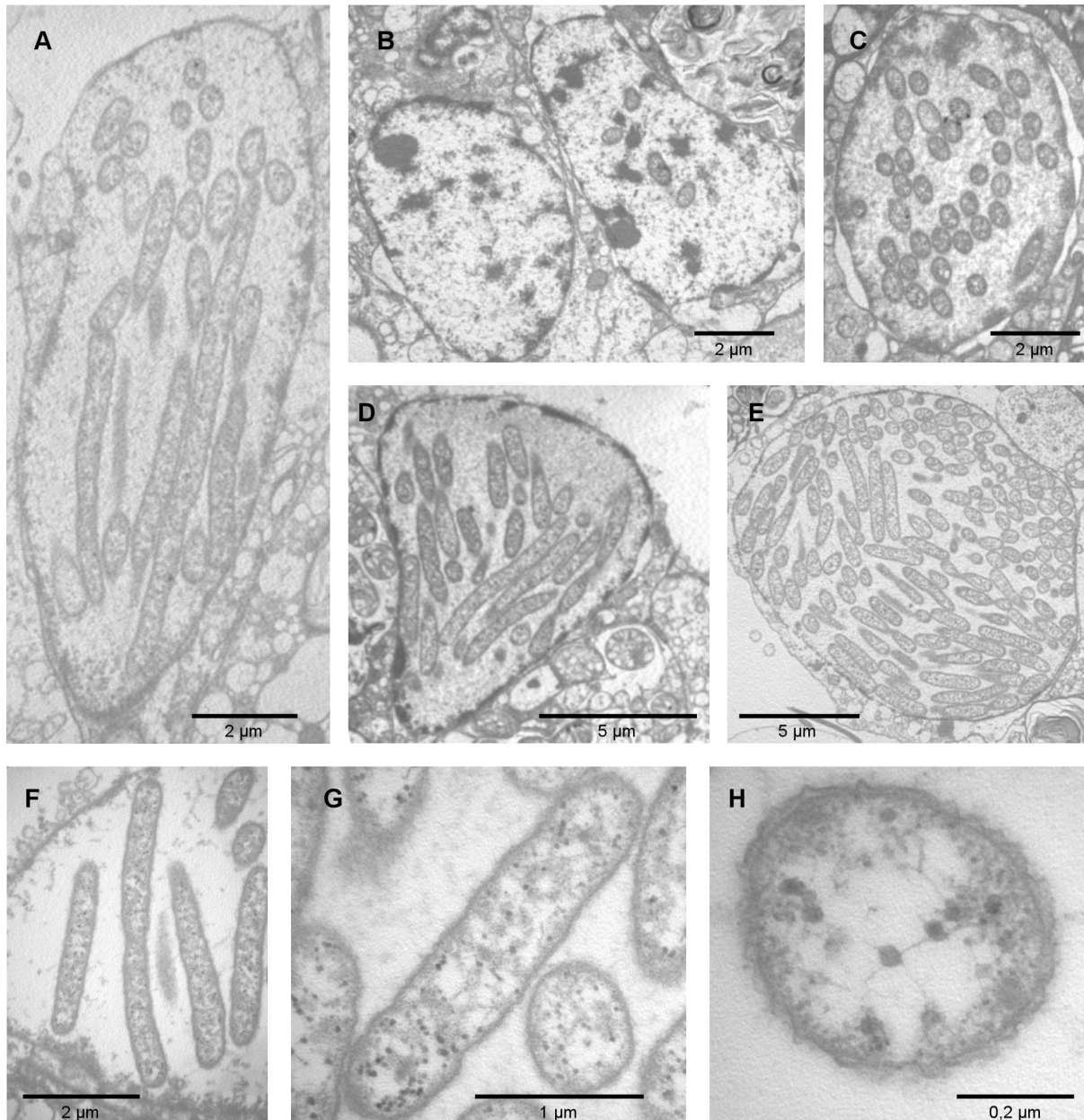


Figure 4. Transmission electron microscopy images showing different stages in the development of “*Ca. E. bathymodioli*”. (A) Oval elongated nucleus with intranuclear bacteria in longitudinal, transversal, and cross section most likely representing the filamentous assembly of Stage 3. Note the filamentous appearance of bacteria in this stage and that the filaments are unseptated. (B) Uninfected nucleus (left) and infected nucleus (right). The infected nucleus represents a cross-section of either a twisted Stage 2 filament or an early Stage 3 filamentous coil. (C) Stage 4 nucleus showing a stack of shorter filaments in cross section. (D) Pear-shaped nucleus with intranuclear bacteria in longitudinal, transversal and cross section most likely representing the multi-filamentous coil of Stage 3. The nucleus, normally at the basal end of the cell when uninfected, is now at the apical end. (E) Swollen Stage 5 nucleus with bacteria in longitudinal and cross section. Note the reduced length of each single bacterium as compared to the elongated form in Stage 3. Also notice the absence of chromatin except for narrow remnants along the nuclear membrane. (F) Dividing filament (middle) showing transverse binary fission. (G) Single bacterium showing electron dense particles distributed throughout the cell. (H) One single bacterium in cross section. Note the inner and outer membrane characteristic of Gram-negative bacteria.

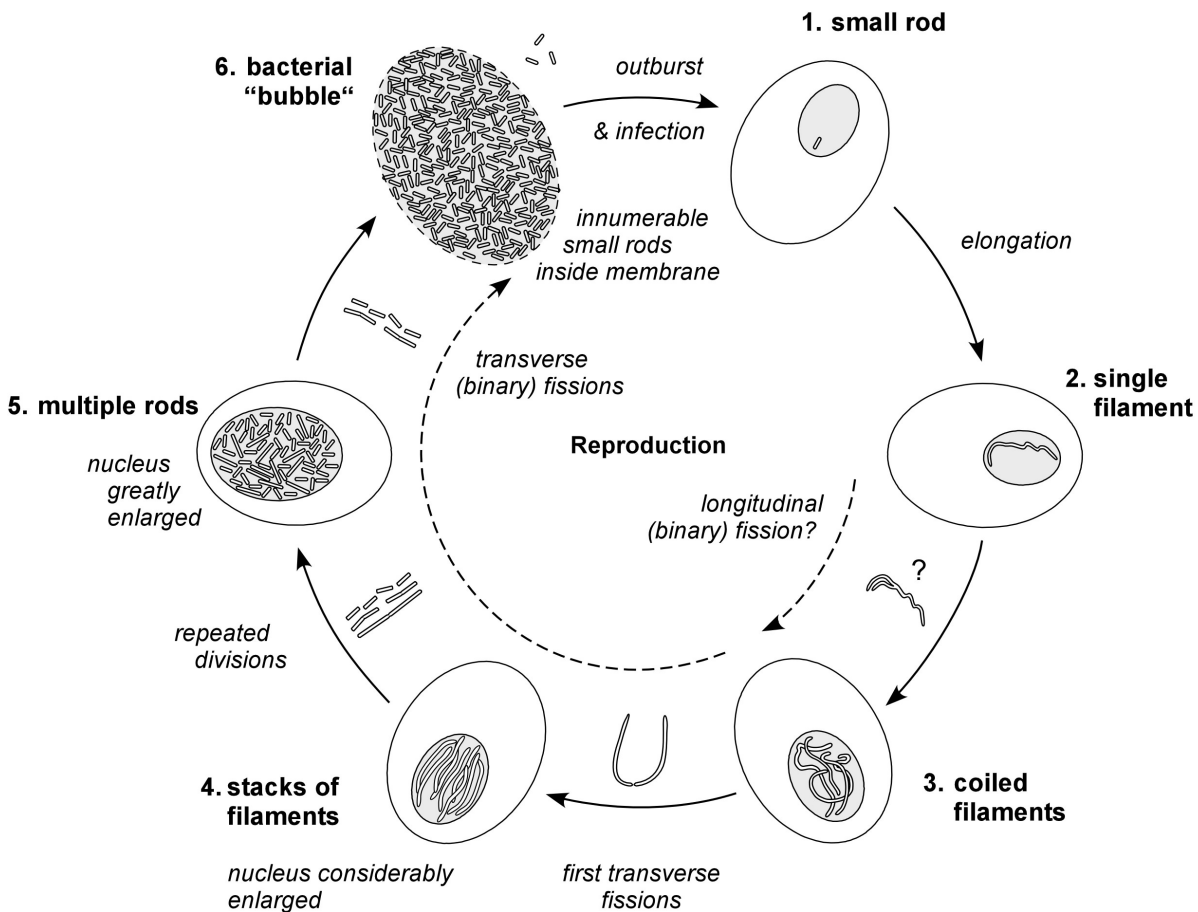


Figure 5. Proposed developmental cycle of “*Candidatus Endonucleobacter bathymodioli*”. The infection begins with a single rod-shaped bacterium inside the nucleus (Stage 1) that grows into an unseptated filament of up to 18-20 μm in length (Stage 2). Multiplication, possibly by longitudinal fission, yields several such filaments that are loosely wrapped in a filamentous coil (Stage 3). These subsequently form stacks of shorter filaments of up to 8-10 μm in length (Stage 4). Repeated transverse binary fissions lead to numerous rod-shaped bacteria (Stage 5). Further multiplication results in a voluminous membrane-surrounded bacterial “bubble” containing up to 80,000 rod-shaped bacteria and the destruction of the host cell (Stage 6). These “bubbles” are eventually disrupted and the bacteria released.

Occurrence of intranuclear bacteria in a shallow-water clam. The close phylogenetic relationship of “*Ca. E. bathymodioli*” with 16S rRNA sequences from bacteria associated with marine metazoans, including the “Nuclear Inclusion X” (“NIX”) parasite of the Pacific razor clam *Siliqua patula* suggests that many if not all sequences within this clade originated from intranuclear bacteria (Figure 2 A). Given morphological descriptions of an intranuclear bacterium in the venerid clam *Ruditapes decussatus* [23] we wanted to know if these bacteria fall in the same clade as “*Ca. E. bathymodioli*” and “NIX”. Using univer-

sal bacterial PCR primers we found a single 16S rRNA sequence in the congeneric venerid clam *Ruditapes philippinarum* (this was the only *Ruditapes* species available at the local fish store). This sequence belongs to the same monophyletic clade as “*Ca. E. bathymodioli*” and “NIX” (Figure 2 A) with 95% identity to the “*Ca. E. bathymodioli*” sequence from *B. puteoserpentis* and 93% identity to the NIX sequence from *Siliqua patula*. FISH of *R. philippinarum* gill tissues with the general bacterial probe EUB338I-III revealed greatly enlarged nuclei infected with bacteria (Raggi *et al.* in preparation).

Discussion

Developmental cycle. The colonization of a nucleus requires several steps: the infection of the host cell, passage through the cytoplasm, and penetration of the nuclear membrane. None of these stages were observed in this study, presumably because these events occur on very short time scales and are therefore only rarely visible. The first discernible infection stage in our study was the presence of a single rod-shaped bacterium in the mussel nuclei that grows to an unseptated filament of about 20 μm and possibly longer (Stage 1 and 2 in Figure 3 G-J). This may be a characteristic feature of intranuclear bacteria. In the marine sponge *Aplysina*, intranuclear bacteria can form filaments up to 350 μm in length [24,25], and infectious forms of *Holospora obtusa* can reach 20 μm in length in the macronucleus of the ciliate *Paramecium caudatum* [11]. Unseptated filamentous growth has also been observed in *Bdellovibrio bacteriovorus*, a deltaproteobacterial predator of Gram-negative bacteria [62,63]. The transition from Stage 2 to 3 appears to take place through longitudinal fission (Figure 3 K). Longitudinal division is rare among bacteria and has only been described in the sulfur-oxidizing symbionts of three marine host genera, the nematode *Laxus* sp. [64-66], the gutless oligochaete *Olavius* [67,68], and the sand-dwelling ciliates of the genus *Kentrophoros* [66,67,69-73].

The shift from filamentous growth to massive reproduction through transverse fission may be triggered by nutrient limitation. The chromatin of Stage 3 nuclei is greatly reduced to a thin layer along the nuclear membrane (Figure 4 A, D). Given that this reduction does not appear to be physically induced because the bacteria do not completely fill out the nucleus at this stage, it is likely that the bacteria have used the chromatin for nutrition (see below). In *B. bacteriovorus*, transition to the multiple fission phase occurs when the cytoplasm is consumed and the host's resources are exhausted [62].

Multiple rounds of transverse binary fission between Stages 3 to 6 lead to massive swelling of the host nuclei. Greatly enlarged nuclei are typical for protists infected with intranuclear bacteria (Table S3) and have also been described in the Pacific razor clam *Siliqua patula* infected with the intranuclear pathogen "NIX" [21]. It is intriguing that in two of the host species shown to be infected with "*Ca. E. bathymodioli*" in this study (*B. heckerae* and *B. puteoserpentis*), previous light microscopical analyses indicated the presence of hypertrophied nuclei in some tissues [39]. Transmission electron microscopy and FISH analyses are needed to clarify if these nuclear distortions were caused by viruses, as suggested by Ward *et al.* [39], or by intranuclear bacteria. Similarly, bacteria described as *Rickettsia*-like and *Chlamydia*-like based on light microscopical analyses of gill tissues of vent and seep mollusks might well be bacteria belonging to the "*Ca. E. bathymodioli*" group [39-42].

The completion of the "*Ca. E. bathymodioli*" cell cycle requires the release of the infected nuclei from the host cell. This most likely occurs through the destruction of the host cell and rupture of the host cytoplasmic membrane. In "NIX"-infected *Siliqua patula*, the host cells are ruptured by the greatly enlarged nuclei, indicating a greater resiliency of the nuclear over the cytoplasmic membrane [21]. When the "*Ca. E. bathymodioli*" infected nuclei become extracellular, they are still surrounded by a membrane (Figure 3 P). This membrane is most likely of nuclear origin, because it stained positively with DAPI, suggesting remnants of nuclear DNA along the inside of the membrane. Finally, the bacteria must escape from the membrane-surrounded Stage 6 nuclei. Not unexpectedly, we only very rarely saw single extracellular "*Ca. E. bathymodioli*", as the washing procedure for the fixation of gill tissues would have removed most loosely attached cells. It remains unclear if the bacteria escape from the "bubble" actively by penetrating the membrane or through mechanical disruption of the membrane. Little is known about how other intranuclear bacteria escape their hosts. In

the ciliate *Paramecium caudatum*, infectious forms of the intranuclear bacterium *Holospora obtusa* make use of the division apparatus of the host nucleus to escape from the nucleus [7,11]. In the bacterial predator *B. bacteriovorus*, 15 lipases have been identified that dissolve the outer membrane of its hosts and enable its release [74].

Chromatin as a nutritional source.

The disappearance of chromatin during the development of “*Ca. E. bathymodioli*” suggests that the host DNA with its surrounding chromosomal proteins provides the nutrition for the growing and reproducing parasites. Chromatin reduction has also been observed in protists infected with intranuclear bacteria (Table S3). Clearly, DNA provides a rich source of sugar, nitrogen, and phosphorus. ATP for biomass synthesis could be acquired by breaking down host DNA or host nucleotides could be used for DNA synthesis. Recent studies have shown the importance of extracellular DNA for free-living bacteria [75,76], but nothing is known about the metabolism of intranuclear bacteria and their genomes have not yet been sequenced. Although not an intranuclear bacterium but rather a bacterial parasite, *B. bacteriovorus* efficiently consumes its prey’s cellular contents including nucleic material. It has been studied extensively [reviewed in 77] and its genome sequenced [74]. *B. bacteriovorus* has the genes for 20 different deoxyribonucleases (DNases) for DNA hydrolysis and is able to obtain ATP and phosphorylated nucleosides directly from its prey’s cytosol [63,74] although the mechanism for ATP transport remains unknown [74]. A further source of nutrition for “*Ca. E. bathymodioli*” may also be cytosolic substrates, particularly during later developmental stages in which the extreme enlargement of the nuclear membrane might enable the leakage of substrates from the cytosol to the nucleus.

Within the monophyletic clade containing “*Ca. E. bathymodioli*” four bacteria have been cultivated, *Endozoicomonas elysicola* (isolated from a sea slug), and *Spongiobacter nickelotolerans*, H262 and H425 (isolated from marine sponges). Published information is only available for *E. elysicola* which is an

aerobic, mesophilic heterotroph but details for growth substrates of *E. elysicola* were not described and it is not clear if this species can grow on DNA alone [59].

Symbiont – parasite interactions. Both our FISH and TEM analyses showed that only symbiont-free intercalary gill cells were infected by “*Ca. E. bathymodioli*” whereas the nuclei of bacteriocytes containing the thiotrophic and methanotrophic endosymbionts were never infected. This suggests that the *Bathymodiolus* symbionts can protect their host nuclei from infection. How this protection is afforded is not clear but the consequences are substantial. As the bacteriocyte nuclei are not infected, it is likely that chemosynthetic energy production and carbon fixation by the endosymbiotic primary producers remains fully functional, thus assuring the nutritional supply of the host. While the infection may be deleterious to the intercalary cells, the overall health of the host does not appear to be significantly affected because its power plants, the bacteriocytes, are not infected. This assumption is supported by the fact that we have not observed mass mortality of the *B. puteoserpentis* population at the Logatchev hydrothermal vent field during the four research cruises we have had to this field between 2004 and 2007, despite the regular presence of “*Ca. E. bathymodioli*” within the population throughout this period. This is in contrast to the mass mortality caused by the intranuclear bacteria of the clam *Siliqua patula* and the *Rickettsia*-like bacteria of the oyster *Crassostrea ariakensis* that do not have symbiotic bacteria in their gills [21,22, unpublished information in Genbank under accession numbers DQ118733 und DQ123914].

What is not currently known is if chemosynthetic symbionts protect their hosts against other parasites besides “*Ca. E. bathymodioli*”. Mass mortality of symbiont-containing mussels and clams was observed at the Blake Ridge seep off the southeastern coast of the USA and morphological analyses of the clams and mussels showed that both were infested with eukaryotic and prokaryotic parasites [39,41]. However, mortal-

ity could not be clearly linked to parasitism as shifts in seepage might also have caused mussel and clam deaths [39,41].

Global occurrence. Our studies show that “*Ca. E. bathymodioli*” occurs in seep and vent mussels from around the world. We were not able to find the intranuclear parasite in only three species: “*B.*” *childressi* from the Gulf of Mexico, *B. aff. boomerang* from the Gabon continental margin, and *B. brevior* from the West Pacific. It is possible that some bathymodiolin species are not infected by “*Ca. E. bathymodioli*”. However, there are no shared characteristics between the three mussel species lacking “*Ca. E. bathymodioli*” that would explain why these hosts would not be infected with this global intranuclear parasite: Neither are they closely related to each other, nor do they occur in the same geographic region. An alternative explanation is that these species contained intranuclear bacteria at levels too low to be detected with PCR and FISH. Although we did not quantify infestation levels, we did observe differences in the abundances of “*Ca. E. bathymodioli*” both between hosts from different fields as well as between individuals of the same species (Table S2).

Biogeographical clusters. In the Gulf of Mexico, *B. brooksi* and *B. heckerae* share the same “*Ca. E. bathymodioli*” 16S rRNA phylotype despite the fact that these hosts are not closely related to each other [78,79]. Together with the fact that the “*Ca. E. bathymodioli*” phylotypes fall into three regional clusters that reflect the origin of their hosts, this suggests that host geography and not co-speciation played a role in the establishment of these associations. However, the investigation of more host species from different geographic regions, particularly the West Pacific, is needed before this hypothesis can be substantiated.

One mussel species, *B. sp.* from the Wideawake vent field on the southern Mid-Atlantic Ridge, harbored two “*Ca. E. bathymodioli*” phylotypes that differed distinctly

from each other by 1.9%. One falls into the Mid-Atlantic Ridge cluster whereas the other one falls in the Pacific-Antarctic Ridge cluster (Figure 2 B). This indicates that although most “*Ca. E. bathymodioli*” bacteria cluster according to their geography, there may have been transoceanic crossing in the past, in this case from vent sites on the Pacific-Antarctic Ridge to the southern Mid-Atlantic Ridge. Historical dispersal across ocean basins has been suggested for some bathymodiolin host species [78,80], and there is no reason to assume that it would not have occurred in their intranuclear bacteria. Extensive comparative analyses of the phylogeny of bathymodiolin hosts, their symbionts and their intranuclear bacteria will provide an ideal data set for a better understanding of historical dispersal patterns in these deep-sea associations.

Conclusions. This study shows that intranuclear bacteria are widespread in bathymodiolin mussels from hydrothermal vents and cold seeps. The 16S rRNA sequences of “*Ca. E. bathymodioli*” belong to a monophyletic clade that consists of sequences from bacteria associated with marine metazoans as diverse as sponges, corals, sea slugs, clams, ascidians, sea urchins, and fish. Two further sequences within this clade also originate from intranuclear bacteria, the previously described “NIX” parasite from the razor clam *Siliqua patula* [20-22] and the novel intranuclear bacterium found in this study in the venerid clam *Ruditapes philippinarum*. In addition, morphological descriptions of intranuclear bacteria exist for other animal hosts within this clade, for example from two species of *Aplysina* sponges [24,25] and the venerid clam *Ruditapes decussatus* [23] (Table 2). We postulate that many of the sequences within this clade originate from intranuclear bacteria, and that these parasites are widespread in marine animals, including clams and other shellfish consumed by humans.

Table 2. Intranuclear bacteria described to date in Metazoa (excluding facultative intranuclear Rickettsiae)

Metazoa taxon	Higher-ranking taxon	Shape	Size [μm]	Phylogeny	Reference
<i>Host species</i>	Designation of bacteria inside nuclei				
Demospongia	Porifera				
<i>Aplysina cavernicola</i> <i>A. aerophoba</i> ;	intranuclear bacteria	filamentous	150-350; at least 4.5	Gamma ^a	[24,25]
Bivalvia	Mollusca				
<i>Siliqua patula</i>	“Nuclear Inclusion X” (NIX)	multilayered, membrane rich, complexly folded, partially cleaved	25 x 16	Gamma	[20,21]
<i>Ruditapes decussatus</i>	endonucleobiotic bacteria	spherical to ellipsoidal	\varnothing 1.3	nd	[23]
<i>Ruditapes philippinarum</i>	intranuclear phylotype	nd	nd	Gamma	this study
<i>Bathymodiolus</i> spp	“ <i>Ca. Endonucleobacter bathymodioli</i> ”	rod-shaped to filamentous	1.8 x 0.4; up to 20	Gamma	this study

nd – not determined; ^a Phylogeny based on FISH with general gammaproteobacterial probe, no 16S rRNA sequence available

Material and Methods

Sampling sites and processing. Nine *Bathymodiolus* species from six deep-sea hydrothermal vent fields and five cold seep sites located in the Atlantic and Pacific Ocean were investigated (Figure 1, Table 1). One to four individuals of each species were examined (Table 1). Upon recovery mussels were immediately transferred into chilled bottom sea water and processed as previously described [58,81,82]. Briefly, gill tissue was frozen and stored at -20°C for DNA extraction as well as fixed for fluorescence *in situ* hybridization (FISH) and transmission electron microscopy (TEM) investigations. *Ruditapes philippinarum* (= *Tapes semidecussatus*) was bought live at a local fish store in Bremen, Germany and was prepared for analyses as described above.

Cloning and sequencing “*Ca. E. bathymodioli*” from *B. puteoserpentis* (Logatchev). Genomic DNA was extracted from gill tissue according to Zhou et al. [83]. PCR was performed using the universal bacterial primers GM3F and GM4R [84]. Amplification products were purified and ligated into pGEM-T Easy vectors (Promega). One Shot TOP10 competent *E. coli* cells (Invitrogen) were subsequently transformed. 96 clones per individual (total 384) with the right sized insert (determined by PCR screening using

the M13F/M13R primer pair [85]) were partially sequenced. PCR products were purified in MultiScreen-HV plates (Millipore) using Sephadex G50 Superfine resin (Amersham Biosciences) and sequenced using the Big-Dye Terminator v2.0 Cycle Sequencing Kit along with the Genetic Analyzer Abiprism 3100 (Applied Biosystems). The GM3F oligonucleotide [84] was used as sequencing primer. The resulting partial sequences were analyzed with BioEdit Sequence Alignment Editor version 7.0 [86] using the ClustalW implementation [87]. Uniquely occurring sequences were ignored. Repetitive sequences were grouped. 3 clones per group and individual were fully sequenced by sequencing both the coding and non-coding DNA strands with the sequencing primers M13F, M13R [85], 534R [88], 518F, 1099F, and 1193R [89]. Cycle sequencing accessories, equipment, and conditions were as described for partial sequencing. Sequences were assembled using Sequencher (Gene Codes Corporation, www.genecodes.com). The vectorial remnants and the primer sites were discarded.

Cloning and sequencing “*Ca. E. bathymodioli*” from other bathymodiolin mussels. Primers specifically targeting the 16S rRNA gene of “*Ca. E. bathymodioli*”

(Logatchev) were designed using the reverse and complementary sequence of probe Bnix64 as a forward primer (bnix-64F: AGCGGTAACAGGTCTAGC) and the sequence of probe Bnix1249 as a reverse primer (bnix-1267R: GCAGCTTCGCGACCGTCT) resulting in a 1203 bp amplification product (for probe design see below). A combination of the bnix-64F primer together with the universal bacterial reverse primer GM4R was eventually chosen to cover 1409 bp of the 16S rRNA gene. Steps for cloning, sequencing, and analyzing intranuclear bacteria belonging to “*Ca. E. bathymodioli*” were as described above for *B. puteoserpentis*. The annealing temperatures for the bnix-64F/bnix-1267R and bnix-64F/GM4R primer pairs were 56°C and 45°C, respectively. Sequencing was performed using the BigDye Terminator v3.1 Cycle Sequencing Kit along with the Genetic Analyzer Abiprism 3130 (Applied Biosystems).

Cloning and sequencing the intranuclear phylotype from *Ruditapes philippinarum*. The bnix-64F/bnix-1267R primer pair described above failed to amplify a 16S rRNA gene from *R. philippinarum* gills, but the universal bacterial primers GM3F and GM4R [84] amplified the gene shown in Figure 2 A. PCR amplification and sequencing were performed as described above for *B. puteoserpentis*. The nearly complete 16S rRNA gene sequence from the *R. philippinarum* intranuclear phylotype revealed 3 mismatches each to the bnix-64F and bnix-1267R primers, explaining why these did not yield a PCR product.

Phylogenetic reconstruction. Sequences were analyzed using ARB [90] and compared with the NCBI nucleotide database using nucleotide BLAST [91], the RDP-II database using the Sequence Match tool [92], and the Silva rRNA database using the SINA webaligner [93]. Highly similar sequences were included in the analysis and aligned using ClustalX. Positions displaying more than 25% gaps as well as positions ambiguously aligned were removed from the analysis. The final alignment comprised 1416 positions. Phylogenetic analyses were per-

formed using Bayesian as well as maximum likelihood (ML) analysis. The former was run using MrBayes 3 (v3.1.2) [94] under a General Time Reversible (GTR) model along with Gamma-distributed rates of evolution and a proportion of invariant sites. Analyses were performed for 2,000,000 generations using 4 parallel Monte Carlo Markov chains. Sample trees were taken every 1,000 generations. Posterior probabilities calculated over 5,000 best trees were used as support values for nodes in the tree. The ML analysis was performed using PHYLIP. To assess the robustness of nodes, 1,000 ML bootstrap replicates were run.

Design of probes targeting “*Ca. E. bathymodioli*”. Based on the 16S rRNA full sequence (1468 bp) of “*Ca. E. bathymodioli*” from *B. puteoserpentis* (Logatchev) three probes were designed using the probe design tool of ARB [90]. To verify their specificity, probes Bnix64 (GCTAGACCTGTTACCGCT), Bnix643 (CCGTACTCTAGCCACCCA), and Bnix1249 (GCAGCTTCGCGACCGTCT) were checked against the 16S dataset of the Ribosomal Database Project II using the online Probe Match tool [92]. The most recent probe match against the RDP-II dataset 9.60 (April 2008) revealed that probe Bnix64 targeted also 10 gammaproteobacterial sequences belonging to the Oceanospirillales and Alteromonadales. Probe Bnix643 targeted also 11 cyanobacterial sequences, 5 unclassified gammaproteobacterial sequences, and 1 deltaproteobacterial sequence. However, probe Bnix1249 was confirmed to specifically target “*Ca. E. bathymodioli*” (Logatchev). With the amplification of more “*Ca. E. bathymodioli*” phylotypes from other bathymodiolin species it became evident that the probes Bnix1249 and Bnix643 had one mismatch each to some of the other intranuclear phylotypes (Table S2).

All probes were fluorescently labeled (biomers.net, Ulm, Germany). Specific hybridization conditions for all three probes were determined by varying the formamide concentration in the hybridization buffer [95]. All probes hybridized equally well with

the target organism at 35% formamide concentration. Probe EUB338 [96] covering most bacteria was used as a positive control and the NON338 probe [97] as a control for background autofluorescence.

Fluorescence *in situ* hybridization. Subsamples of *B. puteoserpentis* gill tissue were fixed in 1 x phosphate buffered saline (PBS: 137 mM NaCl, 2.7 mM KCl, 10 mM Na₂HPO₄, 2 mM KH₂PO₄) containing 2% paraformaldehyde at 4°C for 9 to 18 hours. Samples were washed three times by placing them in fresh 1 x PBS for 10 minutes each time and subsequently transferred into cold PBS/ethanol solution containing 1 x PBS and pure ethanol in equal parts. Samples were kept at 4°C on board the research vessel, air-freighted back to the laboratory at 4°C and finally stored at -20°C. Fixed specimens were embedded in Steedman's Wax [98] and sectioned with a microtome into 10 µm thick sections. The sections were placed onto SuperFrost slides (Fisher Scientific), dewaxed in three successive baths of absolute ethanol for 5 min each and air dried. Sections were then covered with 200 µl of hybridization buffer [95] containing fluorescently labelled oligonucleotide probes (5 ng·µl⁻¹ final concentration), covered with a glass coverslip and hybridized at 46°C for 10 min in a histological microwave oven (Microwave Research & Applications, Inc., Laurel, MD, USA) with the power output set to 20%. The slides were rinsed in 1 x PBS, MQwater, and absolute ethanol for one minute each. Single hybridizations targeting specifically “*Ca. E. bathymodioli*” (Logatchev) were performed using probe Bnix1249 labeled with Cy3. For visualization of all bacteria in *B. puteoserpentis*, Cy3-labeled EUB338 was used [96]. Double hybridizations targeting eukaryotic 18S rRNA were performed using Cy5-labeled EUK516 [96]. Triple hybridizations targeting the chemoautotrophic endosymbiont, the methanotrophic endosymbiont, and the eukaryotic 18S rRNA were performed using the probes BMARt-193 (Cy3), BMARm-845 (Cy5) [58], and EUK516 (Fluos). For quadruple hybridizations targeting additionally “*Ca. E.*

bathymodioli” (Logatchev) Fluos-labeled Bnix1249 was used.

Deconvolution (restoration) microscopy. The air dried slides were embedded in a DAPI amended mountant and evaluated on a DeltaVision RT Restoration Microscopy System (Applied Precision, Issaquah, Washington, USA) using an Olympus IX71 (Olympus, Center Valley, PA, USA) equipped with appropriate filter sets for Cy3, Cy5, DAPI, and fluorescein. For image capture and deconvolution the SoftWorx image analysis software was used (Applied Precision, Issaquah, Washington, USA). Images were further processed and analyzed using the Imaris software package (www.bitplane.com) that was also used to assign colors to the different wavelengths.

Transmission Electron Microscopy. Gill filaments of *B. puteoserpentis* from Logatchev were fixed in a modified Trump's fixative [99] (0.05 M sodium cacodylate solution containing 2% glutaraldehyde and 2% paraformaldehyde, pH 7.3) and stored therein for several months. The tissues were dehydrated in an ethanol series and embedded in the acrylic resin LR White (Sigma). Ultrathin sections were stained with uranyl acetate and lead citrate, and examined with a Zeiss EM 109-S2. TEM was performed on five adult specimens. 57 gill filaments were investigated in total.

Supporting Information

VideoS1. Developmental Stage 2

VideoS2. Developmental Stage 3

VideoS3. Developmental Stage 4

VideoS4. Developmental Stage 6

Accession Numbers

The 16S rRNA gene sequences belonging to “*Candidatus* Endonucleobacter bathymodioli” have been registered at the EMBL database [100] under accession numbers FM162182 to FM162195. The intranuclear phylotype from *Ruditapes philippinarum* has accession number FM162196. (Table S2). The alignment used for the phylogenetic analysis can be obtained from the EMBL database (accession number:

Align_001264). The probes targeting “*Ca. E. bathymodioli*” from *B. puteoserpentis* are deposited in the oligonucleotide probe database ‘probeBase’ [101] under accession numbers pB-01516 to pB-01518.

Acknowledgements

We acknowledge the chief scientists and the captains and crews of the involved research vessels (Table 1) as well as the chief engineers and crews of the ROV’s Quest 4000 and Victor 6000 and the manned submersible Alvin for providing excellent support to obtain deep-sea hydrothermal vent and cold seep samples. We appreciate our laboratory assistants Silke Wetzel and Sabine Gaude and their indispensable skills. We are grateful to Victoria Orphan for letting us use her DeltaVision RT Restoration Microscopy System along with the SoftWorx deconvolution and image analysis software as well as the Imaris image analysis software package. The author (FUZ) is particularly thankful to Victoria Orphan for hosting him in her lab at the California Institute of Technology during parts of this study and Shana Goffredi for

helpful comments and suggestions for the improvement of this manuscript.

Author contribution

FUZ and ND conceived and designed the experiments. FUZ, AP, SD, LR, and OG performed the experiments. FUZ and SD analyzed the phylogenetic data. FUZ, SD, OG, CB, and ND contributed reagents/materials/analysis tools. FUZ and ND wrote the paper.

Funding

This work was supported by grants from the Priority Program 1144 of the German Science Foundation (DFG). This is publication number 24 of the priority program 1144 “From Mantle to Ocean: Energy-, Material- and Life cycles at Spreading Axes” of the DFG.

Competing interests

The authors have declared that no competing interests exist.

Table S1. Closest relatives of “*Candidatus Endonucleobacter bathymodiolii*” (Logatchev)

Uncultured gamma proteobacterium or isolate	Identities [%]	Sequence length [bp]	Associated with	Taxon or species	Accession Number
clone B6F4	98.8	415	-	-	AMD68617
clone D4-spf-A85	97.2	389	marine sponge	<i>Discodermia dissoluta</i> ^a	AY897105
clone CD14B9 and 46 other clones	95-97	212-616	coral	<i>Diploria strigosa</i> ^a	AF442025
clone Hjj17-A3	95.4	479	-	-	DQ670587
clone C19; clone CRNA5	94.5; 95.1	1489; 413	colonial ascidian	<i>Cystodites dellechiaiei</i> ^b	DQ884169; DQ884160
intranuclear phylotype	95.0	1467	clan	<i>Rudisapes philippinarum</i>	this study; FM162196
<i>Spongiobacter nickelotolerans</i> ^a	94.9	1492	marine sponge	-	AB205011
<i>Endozoaionomus elysicola</i> ^a	94.4	1437	sea slug	<i>Elysia ornata</i> ^b	AB196667
clone H1	94.4	531	sea urchin	<i>Tripanistes gratilla</i>	AM495252
clone <i>Spongiobacter</i> sp. ME19 and 5 other clones	92-94	1502-1527	<i>coral</i>	<i>Muricea elongata</i> ^b	DQ917863
clone HOC27; clone HOC2	94.0	1473	marine sponge	<i>Halicchontrida okadae</i> ^b	AB054161; AB054136
clone PDA-OUT2; clone PDA-OUT3	93.6; 94.0	1500; 1503	coral	<i>Pocillopora damicornis</i> ^b	AY700600; AY700601
clone CN34	93.9	1448	marine sponge	<i>Chondrilla nucula</i>	AMD59915
clone sluc48	93.9	682	coral	<i>Oculina patagonica</i> ^b	DQ416306
clone H262 ^a	93.9	703	marine sponge; sea slug	Dictyoceratida, Theoretidae ^b , Pleurobranchidae ^b	AY370006
clone H425 ^a	93.9	740	marine sponge	Halicchontrida, Axinellidae ^b , Halicchontrida, Halicchontridae ^b	AY370008
clone C23	93.4	1486	colonial ascidian	<i>Cystodites dellechiaiei</i> ^b	DQ884170
clone H1sp1_A3	93.4	1024	sea grass	<i>Halophila stipulacea</i> ^b	AF159674
clone Gamma7	93.2	919	fish	<i>Salmo salar</i> ^c	AY494615
clone CD207E01 and 8 other clones	89.3-92.7	865-983	coral	<i>Monasteria annularis</i> ^b	DQ200605
clone NWCu007	92.2	895	marine sponge	<i>Rhopileoides odorabile</i> ^b	AF313496
clone <i>Spongiobacter</i> sp. EC22; clone <i>Spongiobacter</i> sp. EC121	92.0; 91.8	1504; 1507	octocoral	<i>Erythropodium caribaeorum</i> ^b	DQ889931; DQ889891
nuclear inclusion X (NIX)	91.1	695	clan	<i>Siliqua patula</i> ^d	M94380-82
clone <i>Spongiobacter</i> sp. BME76	90.9	1512	coral	<i>Muricea elongata</i> ^b	DQ917830
clone OTU 6 and 7 other clones	88.1-90.8	1296-1298	coral	<i>Alcyonium antarcticum</i> ^b	DQ312244
<i>Zooskellia ganghwensis</i> ^a	90.6	1441	-	-	AY130994
<i>Ocearrhenkista ariakensis</i> ; R6; <i>O. ariakensis</i> ; R54	87.8	1300; 1304	oyster	<i>Cassiopea ariakensis</i>	DQ118733; DQ123914

^a Clones obtained from Ssm healthy specimens; ^b Condition of specimens not stated; ^c Clone obtained from specimen infected with amoebic gill disease; ^d bacterium involved in massive mortalities of the Pacific razor clam *Siliqua patula*; * isolates

Table S2. Nucleotide differences of dominant and minor “*Ca. E. bathymodiolii*” 16S rRNA sequences from bathymodiolin species

Specimen	Location		# examined ^a	# infected ^b	# full sequences ^c				nucleotide position ^d	Probe ^e	Acc. No
					I	II	III	IV			
<i>B. brooksi</i>	AT, AL, CH	GoM	4	4	8	8	5	6	27	0	FM162182-FM162184
	WF, CH	GoM	3	1	5	-	-	na	5	0	FM162185
<i>B. heckerae</i>	Lilliput	MAR	1	1	4	na	na	na	4	y	FM162186
<i>B. azoricus</i>	Menez Gwen	MAR	3	1	1	-	-	na	1	0	FM162187
<i>B. puteoserpentis</i>	Logatchev	MAR	4	3	-	3	3	3	9	474	
	dominant phylotype				-	1	2	3	6	G	FM162188
	minor phylotype				-	2	1	-	3	A	FM162189
<i>B. sp.</i>	Wideawake	MAR	4	4	8	6	8	8	30	474	1023
	dominant phylotype				8	4	5	-	17	A	A
	minor phylotype I				-	-	1	8	9	G	A
minor phylotype II					-	2	1	-	3	G	G
minor phylotype III					-	-	1	-	1		
<i>B. aff. thermophilus</i>	German Flats	PAR	4	3	6	8	8	-	22	137	184
	dominant phylotype				5	7	7	-	19	C	C
	minor phylotype				1	1	1	-	3	T	T
<i>Ruditapes philippinarum</i>	local store	-	1	1	5	na	na	na	5		
										/	FM162196

^a number of examined individuals; ^b number of infected individuals; ^c number of full sequences per individual (I-IV); ^d position based on *Escherichia coli* numbering; ^e probe specificity: x,y,z – probes Bnix64 (x), Bnix643 (y), and Bnix1249 (z) match their target specifically (no mismatches), probe Bnix64 is applicable only to “*Ca. E. bathymodiolii*” from *B. puteoserpentis* (Logatchev) as this part of the 16S rRNA sequence is not known from the other phylotypes, o – either one of the probes y and z has one single mismatch, / - not covered by either one of the probes (2-3 mismatches); Abbreviations: AT – Atwater Valley, AL – Alaminos Canyon, CH – Chapopote, WF – West Florida Escarpment, GoM – Gulf of Mexico, MAR – Mid-Atlantic Ridge, PAR – Pacific-Antarctic Ridge; na – not applicable

Table S3. Intranuclear bacteria described from protists

Protist taxon ^a Host species	Protist super group and higher ranking taxa ^a Designation of bacteria inside nuclei	Shape	Phylogeny	Reference
Ciliophora	Chromalveolata: Alveolata			
<i>Paramecium</i> spp. and numerous other ciliate genera	endonuclear bacteria; (<i>Holospora</i> spp. [9 species] ^{b, d} , <i>Credibacter caryophilus</i> ^e , <i>C. macronucleorum</i> ^d , <i>Nonospora macronucleata</i> ^d , and several other but unnamed endonuclear bacteria)	rods	Alpha	[7,11-13,110,111]
Dinoflagellata	Chromalveolata: Alveolata: Dinozoa			
<i>Gyrodinium instriatum</i>	endonucleoplasmic bacteria (unnamed) ^{b, e}	rods	Beta	[112-114]
<i>Gymnodinium splendens: Glenodinium foliaceum</i>	endonuclear bacteria (unnamed) ^{b, d}	rods	nd	[114,115]
Euglenida	Excavata: Euglenozoa			
<i>Euglena spirogyra: Strombomonas conspersa;</i> <i>Trachelomonas oblonga: Lepocnelis ovum;</i> <i>Euglena hemichromata</i>	endonuclear bacteria (unnamed) ^e	rods	nd	[116]
<i>Euglena deses</i>	endonuclear bacteria (unnamed) ^{b, c, d}	rods	nd	[117]
<i>Trachelomonas</i> sp.	<i>Caryococcus hypertrophicus</i> ^b	cocci	nd	[118-121]
<i>Peranema trichophorum</i>	electron dense bodies ^f	rods	nd	[122]
	rod-shaped bodies ^{b, f}	rods	nd	[123]
Trichonymphida	Excavata: Parabasalia			
<i>Trichonympha seapiculatae</i>	nuclear parasites	spherical bodies	nd	[120]
<i>Trichonympha corbula</i>	<i>Caryococcus nucleophilus</i> ^d ; <i>Caryococcus cretus</i> ^d	cocci	nd	[121]
<i>Trichonympha pepliphora</i>	<i>Caryococcus invadens</i> ^d	cocci	nd	[121]
<i>Trichonympha chlatoni</i>	<i>Caryococcus dilatator</i> ^{b, c, d}	cocci	nd	[121]
<i>Staurioenitha assimilis</i>	intranuclear symbionts ^{b, d}	cocci	nd	[124]
Cristamonadida	Excavata: Parabasalia			
<i>Caduceia versatilis</i>	intranuclear bacteria ^{b, f}	cocci	nd	[125,126]
Spirotrichonymphida	Excavata: Parabasalia			
<i>Holomastixgoides henrygymnum</i>	bactéries dans le noyau ^f	rods	nd	[127]

^a The designation of the protist taxon and the super group follows the taxonomy proposed by Adl et al. [128]; b bacteria cause hypertrophy of nuclei; c intranuclear bacteria are associated with the disappearance of chromatin; d obligate intranuclear; e facultative intranuclear; f unclear if obligate or facultative in the nucleus; nd – not determined

References

1. Beninati T, Lo N, Sacchi L, Genchi C, Noda H, et al. (2004) A novel alpha-proteobacterium resides in the mitochondria of ovarian cells of the tick *Ixodes ricinus*. *Appl Environ Microbiol* 70: 2596-2602.
2. Lo N, Beninati T, Sasseria D, Bouman EAP, Santagati S, et al. (2006) Widespread distribution and high prevalence of an alpha-proteobacterial symbiont in the tick *Ixodes ricinus*. *Environ Microbiol* 8: 1280-1287.
3. Chang KP, Musgrave AJ (1970) Ultrastructure of rickettsia-like microorganisms in midgut of a plant bug, *Stenotus binotatus* Jak. (Heteroptera: Miridae). *Can J Microbiol* 16: 621-622.
4. Wilcox LW (1986) Prokaryotic endosymbionts in the chloroplast stroma of the dinoflagellate *Woloszynskia pascheri*. *Protoplasma* 135: 71-79.
5. Schmid AMM (2003) Endobacteria in the diatom *Pinnularia* (Bacillariophyceae). I. "Scattered ct-nucleoids" explained: DAPI-DNA complexes stem from exoplastidial bacteria boring into the chloroplasts. *J Phycol* 39: 122-138.
6. Schmid AMM (2003) Endobacteria in the diatom *Pinnularia* (Bacillariophyceae). II. Host cell cycle-dependent translocation and transient chloroplast scars. *J Phycol* 39: 139-153.
7. Fokin SI (2004) Bacterial endocytobionts of Ciliophora and their interactions with the host cell. *Int Rev Cytol* 236: 181-249.
8. Maillet PL, Folliot R (1967) Nouvelles observations sur le transport de microorganismes intranucléaires appelés particules Phi par les spermatozoïdes chez des insectes Homoptères. *C R Hebd Seances Acad Sci D* 264: 965-968.
9. Grandi G, Guidi L, Chicca M (1997) Endonuclear bacterial symbionts in two termite species: An ultrastructural study. *J Submicrosc Cytol Pathol* 29: 281-292.
10. Arneodo JD, Bressan A, Lherminier J, Michel J, Boudon-Padiou E (2008) Ultrastructural detection of an unusual intranuclear bacterium in *Pentastiridius leporinus* (Hemiptera: Cixiidae). *J Invertebr Pathol* 97: 310-313.
11. Görtz H-D (2006) Symbiotic associations between ciliates and prokaryotes. In: Dworkin M, Falkow S, Rosenberg E, Schleifer KH, Stackebrandt E, editors. *The Prokaryotes*. 3 ed. Berlin, Heidelberg: Springer-Verlag. pp. 364-402.
12. Görtz HD (1983) Endonuclear symbionts in ciliates. *Int Rev Cytol*: 145-176.
13. Görtz HD (1986) Endonucleobiosis in ciliates. *Int Rev Cytol* 102: 169-213.
14. Burgdorfer W, Anacker RL, Bird RG, Bertram DS (1968) Intranuclear Growth of *Rickettsia rickettsii*. *J Bacteriol* 96: 1415-1418.
15. Brinton LP, Burgdorfer W (1971) Fine Structure of *Rickettsia canada* in tissues of *Dermacentor andersoni* Stiles. *J Bacteriol* 105: 1149-1159.
16. Ogata H, La Scola B, Audic S, Renesto P, Blanc G, et al. (2006) Genome sequence of *Rickettsia bellii* illuminates the role of amoebae in gene exchanges between intracellular pathogens. *PLoS Genet* 2: 733-744.
17. Perotti MA, Clarke HK, Turner BD, Braig HR (2006) *Rickettsia* as obligate and mycetomic bacteria. *FASEB J* 20: E1646-1656.
18. Urakami H, Tsuruhara T, Tamura A (1982) Intranuclear *Rickettsia tsutsugamushi* in cultured mouse fibroblasts (L-cells). *Microbiol Immunol* 26: 445-447.
19. Pongponratn E, Maneerat Y, Chaisri U, Wilairatana P, Punpoowong B, et al. (1998) Electron-microscopic examination of *Rickettsia tsutsugamushi* infected human liver. *Trop Med Int Health* 3: 242-248.
20. Kerk D, Gee A, Dewhirst FE, Drum AS, Elston RA (1992) Phylogenetic placement of "Nuclear Inclusion X (NIX)" into the gamma subclass of proteobacteria on the basis of 16S ribosomal RNA sequence comparisons. *Syst Appl Microbiol* 15: 191-196.
21. Elston RA (1986) An intranuclear pathogen [Nuclear Inclusion X (NIX)] associated with massive mortalities of the Pacific razor clam, *Siliqua patula*. *J Invertebr Pathol* 47: 93-104.
22. Ayres DL, Schumaker EJ, Elston RA (2004) Recent mortality event of Pacific razor clams, *Siliqua patula*, along the Pacific coast of Washington state associated with record infection intensity of the gills by Nuclear Inclusion X (NIX). *J Shellfish Res* 23: 651-651.
23. Azevedo C (1989) Fine structure of endonucleobiotic bacteria in the gill epithelium of *Ruditapes decussatus*. *Mar Biol* 100: 339-341.
24. Vacelet J (1970) Description de cellules a bactéries intranucléaires chez des éponges *Verongia*. *J Microsc* 9: 333-346.
25. Friedrich AB, Merkert H, Fendert T, Hacker J, Proksch P, et al. (1999) Microbial diversity in the marine sponge *Aplysina cavernicola* (formerly *Verongia cavernicola*) analyzed by fluorescence in situ hybridization (FISH). *Mar Biol* 134: 461-470.
26. Wolff T (2005) Composition and endemism of the deep-sea hydrothermal vent fauna. *Cah Biol Mar* 46: 97-104.

27. Desbruyères D, Segonzac M, Bright M, (editors) (2006) Handbook of Deep-Sea Hydrothermal Vent Fauna. *Denisia* 18: 544 pp.
28. Desbruyères D, Segonzac M, Bright M, (editors) (2006) Handbook of Deep-Sea Hydrothermal Vent Fauna. *Denisia* 18: 544 pp. Supplement & Corrigendum, December 2006, web site: www.noc.soton.ac.uk/chess/handbook.php.
29. Sibuet M, Olu K (1998) Biogeography, biodiversity and fluid dependence of deep-sea cold-seep communities at active and passive margins. *Deep-Sea Res II* 45: 517-567.
30. Sibuet M, Olu-Le Roy K (2002) Cold seep communities on continental margins: Structure and quantitative distribution relative to geological and fluid venting patterns. In: Wefer G, Billett D, Hebbeln D, Jørgensen BB, Schlüter M et al., editors. *Ocean Margin Systems*. Berlin, Heidelberg: Springer-Verlag. pp. 235-251.
31. de Buron I, Morand S (2004) Deep-sea hydrothermal vent parasites: why do we not find more? *Parasitology* 128: 1-6.
32. de Buron I, Segonzac M (2006) Hydrothermal vent parasites. *Denisia* 18: 29-30.
33. de Buron I, Segonzac M (2006) Hydrothermal vent parasites. *Denisia* 18: 29-30 Supplement & Corrigendum, November 2006, web site: www.noc.soton.ac.uk/chess/handbook.php.
34. López-García P, Philippe H, Gail F, Moreira D (2003) Autochthonous eukaryotic diversity in hydrothermal sediment and experimental microcolonizers at the Mid-Atlantic Ridge. *Proc Natl Acad Sci USA* 100: 697-702.
35. López-García P, Vereshchaka A, Moreira D (2007) Eukaryotic diversity associated with carbonates and fluid-seawater interface in Lost City hydrothermal field. *Environ Microbiol* 9: 546-554.
36. Atkins MS, Teske AP, Anderson OR (2000) A survey of flagellate diversity at four deep-sea hydrothermal vents in the Eastern Pacific Ocean using structural and molecular approaches. *J Eukaryot Microbiol* 47: 400-411.
37. Edgcomb VP, Kysela DT, Teske A, Gomez AD, Sogin ML (2002) Benthic eukaryotic diversity in the Guaymas Basin hydrothermal vent environment. *Proc Natl Acad Sci USA* 99: 7658-7662.
38. Moreira D, López-García P (2003) Are hydrothermal vents oases for parasitic protists? *Trends Parasitol* 19: 556-558.
39. Ward ME, Shields JD, Van Dover CL (2004) Parasitism in species of *Bathymodiolus* (Bivalvia: Mytilidae) mussels from deep-sea seep and hydrothermal vents. *Dis Aquat Org* 62: 1-16.
40. Powell EN, Barber RD, Kennicutt MC, Ford SE (1999) Influence of parasitism in controlling the health, reproduction and PAH body burden of petroleum seep mussels. *Deep-Sea Res I* 46: 2053-2078.
41. Mills AM, Ward ME, Heyl TP, Van Dover CL (2005) Parasitism as a potential contributor to massive clam mortality at the Blake Ridge Diapir methane-hydrate seep. *J Mar Biol Assoc UK* 85: 1489-1497.
42. Terlizzi CM, Ward ME, Van Dover CL (2004) Observations on parasitism in deep-sea hydrothermal vent and seep limpets. *Dis Aquat Org* 62: 17-26.
43. Van Dover CL, Ward ME, Scott JL, Underdown J, Anderson B, et al. (2007) A fungal epizootic in mussels at a deep-sea hydrothermal vent. pp. 54-62.
44. Tarasov VG, Gebruk AV, Mironov AN, Moskalev LI (2005) Deep-sea and shallow-water hydrothermal vent communities: two different phenomena? *Chem Geol* 224: 5-39.
45. DeChaine EG, Cavanaugh CM (2006) Symbioses of methanotrophs and deep-sea mussels (Mytilidae: Bathymodiolinae). In: Overmann J, editor. *Molecular Basis of Symbiosis*. Berlin, Heidelberg: Springer-Verlag. pp. 227-249.
46. Won Y-J, Jones WJ, Vrijenhoek RC (2008) Absence of cospeciation between deep-sea mytilids and their thiotrophic endosymbiont. *J Shellfish Res* 27: 129-138.
47. Génio L, Johnson SB, Vrijenhoek RC, Cunha MR, Tyler PA, et al. (2008) New record of "*Bathymodiolus*" *mauritanicus* Cosel 2002 from the Gulf of Cadiz (NE Atlantic) mud volcanoes. *J Shellfish Res* 27: 53-61.
48. Stewart FJ, Newton ILG, Cavanaugh CM (2005) Chemosynthetic endosymbioses: adaptations to oxic-anoxic interfaces. *Trends Microbiol* 13: 439-448.
49. Cavanaugh CM, McKiness ZP, Newton ILG, Stewart FJ (2006) Marine chemosynthetic symbioses. In: Dworkin M, Falkow S, Rosenberg E, Schleifer KH, Stackebrandt E, editors. *The Prokaryotes*. 3 ed. Berlin, Heidelberg: Springer-Verlag. pp. 473-507.
50. Distel DL, Lee HKW, Cavanaugh CM (1995) Intracellular coexistence of methanotrophic and thioautotrophic bacteria in a hydrothermal vent mussel. *Proc Natl Acad Sci USA* 92: 9598-9602.
51. Fiala-Médioni A, Le Pennec M (1987) Trophic structural adaptations in relation to the bacterial association of bivalve mollusks from hydrothermal vents and subduction zones. *Symbiosis* 4: 63-74.
52. Pimenov NV, Kalyuzhnaya MG, Khmelenina VN, Mityushina LL, Trotsenko YA (2002) Utilization of methane and carbon dioxide by symbiotrophic bacteria in gills of Mytilidae (*Bathymodiolus*) from the Rainbow and Logachev hydrothermal fields on the Mid-Atlantic Ridge. *Microbiology* 71: 587-594.
53. Robinson JJ, Polz MF, Fiala-Medioni A, Cavanaugh CM (1998) Physiological and

- immunological evidence for two distinct C₁-utilizing pathways in *Bathymodiolus puteoserpentis* (Bivalvia: Mytilidae), a dual endosymbiotic mussel from the Mid-Atlantic Ridge. *Mar Biol* 132: 625-633.
54. Belkin S, Nelson DC, Jannasch HW (1986) Symbiotic assimilation of CO₂ in two hydrothermal vent animals, the mussel *Bathymodiolus thermophilus* and the tube worm *Riftia pachyptila*. *Biol Bull* 170: 110-121.
55. Nelson DC, Hagen KD, Edwards DB (1995) The gill symbiont of the hydrothermal vent mussel *Bathymodiolus thermophilus* is a psychrophilic, chemoautotrophic, sulfur bacterium. *Mar Biol* 121: 487-495.
56. Fisher CR, Childress JJ, Oremland RS, Bidigare RR (1987) The importance of methane and thiosulfate in the metabolism of the bacterial symbionts of two deep-sea mussels. *Mar Biol* 96: 59-71.
57. Fisher CR, Childress JJ (1992) Organic carbon transfer from methanotrophic symbionts to the host hydrocarbon-seep mussel. *Symbiosis* 12: 221-235.
58. Duperron S, Bergin C, Zielinski F, Blazejak A, Pernthaler A, et al. (2006) A dual symbiosis shared by two mussel species, *Bathymodiolus azoricus* and *Bathymodiolus puteoserpentis* (Bivalvia: Mytilidae), from hydrothermal vents along the northern Mid-Atlantic Ridge. *Environ Microbiol* 8: 1441-1447.
59. Kurahashi M, Yokota A (2007) *Endozoicomonas elysicola* gen. nov., sp. nov., a γ -proteobacterium isolated from the sea slug *Elysia ornata*. *Syst Appl Microbiol* 30: 202-206.
60. Sfanos K, Harmody D, Dang P, Ledger A, Pomponi S, et al. (2005) A molecular systematic survey of cultured microbial associates of deep-water marine invertebrates. *Syst Appl Microbiol* 28: 242-264.
61. Yi H, Chang YH, Oh HW, Bae KS, Chun J (2003) *Zooshikella ganghwensis* gen. nov., sp. nov., isolated from tidal flat sediments. *Int J Syst Evol Microbiol* 53: 1013-1018.
62. Angert ER (2005) Alternatives to binary fission in bacteria. *Nat Rev Microbiol* 3: 214-224.
63. Dworkin M (2006) Prokaryotic life cycles. In: Dworkin M, Falkow S, Rosenberg E, Schleifer KH, Stackebrandt E, editors. *The Prokaryotes*. 3 ed. Berlin, Heidelberg: Springer-Verlag. pp. 140-166.
64. Polz MF, Felbeck H, Novak R, Nebelsick M, Ott JA (1992) Chemoautotrophic, sulfur-oxidizing symbiotic bacteria on marine nematodes - morphological and biochemical characterization. *Microb Ecol* 24: 313-329.
65. Polz MF, Distel DL, Zarda B, Amann R, Felbeck H, et al. (1994) Phylogenetic analysis of a highly specific association between ectosymbiotic, sulfur-oxidizing bacteria and a marine nematode. *Appl Environ Microbiol* 60: 4461-4467.
66. Ott J, Bright M, Bulgheresi S (2005) Marine microbial thiotrophic ectosymbioses. *Oceanogr Mar Biol Annu Rev* 42: 95-118.
67. Bright M, Giere O (2005) Microbial symbiosis in Annelida. *Symbiosis* 38: 1-45.
68. Giere O, Krieger J (2001) A triple bacterial endosymbiosis in a gutless oligochaete (Annelida): ultrastructural and immunocytochemical evidence. *Invertebr Biol* 120: 41-49.
69. Raikov IB (1974) Étude ultrastructurale des bactéries épizoïques et endozoïque de *Kentrophoros latum* Raikov, cilié holotriche mésopsammique. *Cah Biol Mar* 15: 379-393.
70. Fauré-Fremiet E (1951) The marine sand-dwelling ciliates of Cape Cod. *Biol Bull* 100: 59-70.
71. Fauré-Fremiet E (1950) Caulobactéries épizoïque associées aux *Centropherella* (ciliés holotriches). *Bull Soc Zool France* 75: 134-137.
72. Raikov IB (1971) Bactéries épizoïque et mode de nutrition du cilié psammophile *Kentrophoros fistulosum* Fauré-Fremiet (étude au microscope électronique). *Protistologica* 7: 365-378.
73. Fauré-Fremiet E (1950) Écologie des ciliés psammophiles littoraux. *Bull Biol France-Belgique* 84: 35-75.
74. Rendulic S, Jagtap P, Rosinus A, Eppinger M, Baar C, et al. (2004) A predator unmasked: Life cycle of *Bdellovibrio bacteriovorus* from a genomic perspective. *Science* 303: 689-692.
75. Lennon JT (2007) Diversity and metabolism of marine bacteria cultivated on dissolved DNA. *Appl Environ Microbiol* 73: 2799-2805.
76. Pinchuk GE, Ammons C, Culley DE, Li SMW, McLean JS, et al. (2008) Utilization of DNA as a sole source of phosphorus, carbon, and energy by *Shewanella* spp.: Ecological and physiological implications for dissimilatory metal reduction. *Appl Environ Microbiol* 74: 1198-1208.
77. Jurkevitch E (2006) The genus *Bdellovibrio*. In: Dworkin M, Falkow S, Rosenberg E, Schleifer KH, Stackebrandt E, editors. *The Prokaryotes*. 3 ed. Berlin, Heidelberg: Springer-Verlag. pp. 12-30.
78. Jones WJ, Won YJ, Maas PAY, Smith PJ, Lutz RA, et al. (2006) Evolution of habitat use by deep-sea mussels. *Mar Biol* 148: 841-851.
79. Cordes EE, Carney SL, Hourdez S, Carney RS, Brooks JM, et al. (2007) Cold seeps of the deep Gulf of Mexico: Community structure and biogeographic comparisons to Atlantic equatorial belt seep communities. *Deep-Sea Res I* 54: 637-653.
80. Olu-Le Roy K, von Cosel R, Hourdez S, Carney SL, Jollivet D (2007) Amphi-Atlantic cold-seep

- Bathymodiolus* species complexes across the equatorial belt. *Deep-Sea Res I* 54: 1890-1911.
81. Duperron S, Sibuet M, MacGregor BJ, Kuypers MMM, Fisher CR, et al. (2007) Diversity, relative abundance and metabolic potential of bacterial endosymbionts in three *Bathymodiolus* mussel species from cold seeps in the Gulf of Mexico. *Environ Microbiol* 9: 1423-1438.
82. Duperron S, Nadalig T, Caprais JC, Sibuet M, Fiala-Medioni A, et al. (2005) Dual symbiosis in a *Bathymodiolus* sp. mussel from a methane seep on the Gabon continental margin (southeast Atlantic): 16S rRNA phylogeny and distribution of the symbionts in gills. *Appl Environ Microbiol* 71: 1694-1700.
83. Zhou JZ, Bruns MA, Tiedje JM (1996) DNA recovery from soils of diverse composition. *Appl Environ Microbiol* 62: 316-322.
84. Muyzer G, Teske A, Wirsen CO, Jannasch HW (1995) Phylogenetic relationships of *Thiomicrospira* species and their identification in deep-sea hydrothermal vent samples by denaturing gradient gel electrophoresis of 16S rDNA fragments. *Arch Microbiol* 164: 165-172.
85. Yanisch-Perron C, Vieira J, Messing J (1985) Improved M13 phage cloning vectors and host strains: nucleotide sequences of the M13mp18 and pUC19 vectors. *Gene* 33: 103-119.
86. Hall TA (1999) BioEdit: a user-friendly biological sequence alignment editor and analysis program for Windows 95/98/NT. *Nucleic Acids Symp Ser* 41.
87. Thompson JD, Higgins DG, Gibson TJ (1994) Clustal W: improving the sensitivity of progressive multiple sequence alignment through sequence weighting, position-specific gap penalties and weight matrix choice. *Nucleic Acids Res* 22: 4673-4680.
88. Muyzer G, Dewaal EC, Uitterlinden AG (1993) Profiling of complex microbial populations by denaturing gradient gel electrophoresis analysis of polymerase chain reaction-amplified genes coding for 16S rRNA. *Appl Environ Microbiol* 59: 695-700.
89. Buchholz-Cleven BEE, Rattunde B, Straub KL (1997) Screening for genetic diversity of isolates of anaerobic Fe(II)-oxidizing bacteria using DGGE and whole-cell hybridization. *Syst Appl Microbiol* 20: 301-309.
90. Ludwig W, Strunk O, Westram R, Richter L, Meier H, et al. (2004) ARB: a software environment for sequence data. *Nucleic Acids Res* 32: 1363-1371.
91. McGinnis S, Madden TL (2004) BLAST: at the core of a powerful and diverse set of sequence analysis tools. *Nucleic Acids Res* 32: W20-W25.
92. Cole JR, Chai B, Farris RJ, Wang Q, Kulam-Syed-Mohideen AS, et al. (2007) The ribosomal database project (RDP-II): introducing myRDP space and quality controlled public data. *Nucleic Acids Res* 35: D169-D172.
93. Pruesse E, Quast C, Knittel K, Fuchs BM, Ludwig W, et al. (2007) SILVA: a comprehensive online resource for quality checked and aligned ribosomal RNA sequence data compatible with ARB. *Nucl Acids Res* 35: 7188-7196.
94. Ronquist F, Huelsenbeck JP (2003) MrBayes 3: Bayesian phylogenetic inference under mixed models. *Bioinformatics* 19: 1572-1574.
95. Pernthaler A, Pernthaler J, Amann R (2002) Fluorescence in situ hybridization and catalyzed reporter deposition for the identification of marine bacteria. *Appl Environ Microbiol* 68: 3094-3101.
96. Amann RI, Binder BJ, Olson RJ, Chisholm SW, Devereux R, et al. (1990) Combination of 16S rRNA-targeted oligonucleotide probes with flow-cytometry for analyzing mixed microbial populations. *Appl Environ Microbiol* 56: 1919-1925.
97. Wallner G, Amann R, Beisker W (1993) Optimizing fluorescent in situ hybridization with rRNA-targeted oligonucleotide probes for flow cytometric identification of microorganisms. *Cytometry* 14: 136-143.
98. Steedman HF (1957) Polyester Wax - New Ribbing Embedding Medium for Histology. *Nature* 179: 1345-1345.
99. McDowell EM, Trump BF (1976) Histologic fixatives suitable for diagnostic light and electron microscopy. *Arch Pathol Lab Med* 100: 405-414.
100. Kulikova T, Akhtar R, Aldebert P, Althorpe N, Andersson M, et al. (2007) EMBL Nucleotide Sequence Database in 2006. *Nucl Acids Res* 35: D16-D20.
101. Loy A, Maixner F, Wagner M, Horn M (2007) probeBase - an online resource for rRNA-targeted oligonucleotide probes: new features 2007. *Nucleic Acids Res* 35: D800-D804.
102. Sarradin PM, Desbruyères D, Dixon D, Almeida A, Briand P, et al. (2001) ATOS cruise R/V L'Atalante, ROV Victor, June 22nd - July 21st 2001. *InterRidge News* 10: 18-20.
103. Kuhn T, Alexander B, Augustin N, Birgel D, Borowski C, et al. (2004) The Logatchev hydrothermal field - revisited: preliminary results of the R/V METEOR Cruise HYDROMAR I (M60/3). *InterRidge News* 13: 1-4.
104. Haase KM, Petersen S, Koschinsky A, Seifert R, Devey CW, et al. (2007) Young volcanism and related hydrothermal activity at 5°S on the slow-spreading southern Mid-Atlantic Ridge. *Geochem Geophys Geosyst* 8: Q11002, doi:10.1029/2006GC001509.
105. Haase KM, Koschinsky A, Devey CW, Fretzdorff S, German C, et al. (in prep.) Diking,

young volcanism and diffuse hydrothermal activity on the southern Mid-Atlantic Ridge.

106. Halbach P, Koschinsky A, Seifert R, Giere O, Kuhn T, et al. (1999) Diffuse hydrothermal fluid activity, biological communities, and mineral formation in the North Fiji Basin (SW Pacific): Preliminary results of the R/V Sonne Cruise SO-134. *InterRidge News* 8: 38-44.

107. Stoffers P, Worthington T, Hekinian R, Petersen S, Hannington M, et al. (2002) Silicic volcanism and hydrothermal activity documented at the Pacific-Antarctic Ridge. *EOS Trans Am Geophys Union* 83: 301-304.

108. Stecher J, Turkay M, Borowski C (2002) Faunal assemblages on the Pacific-Antarctic Ridge near the Foundation Seamount Chain (37 degrees 30 ' S, 110 degrees 30 ' W). *Cah Biol Mar* 43: 271-274.

109. Ondreas H, Olu K, Fouquet Y, Charlou JL, Gay A, et al. (2005) ROV study of a giant pockmark on the Gabon continental margin. *Geo-Mar Lett* 25: 281-292.

110. Görtz HD, Brigge T (1998) Intracellular bacteria in protozoa. *Naturwissenschaften* 85: 359-368.

111. Görtz H-D (2001) Intracellular bacteria in ciliates. *Int Microbiol* 4: 143-150.

112. Alverca E, Biegala IC, Kennaway GM, Lewis J, Franca S (2002) *In situ* identification and localization of bacteria associated with *Gyrodinium instriatum* (Gymnodiniales, Dinophyceae) by electron and confocal microscopy. *Eur J Phycol* 37: 523-530.

113. Biegala IC, Kennaway G, Alverca E, Lennon JF, Vaultot D, et al. (2002) Identification of bacteria associated with dinoflagellates (Dinophyceae) *Alexandrium* spp. using tyramide signal amplification-fluorescent *in situ* hybridization and confocal microscopy. *J Phycol* 38: 404-411.

114. Silva ES, Franca S (1985) The association dinoflagellate-bacteria: Their ultrastructural relationship in two species of dinoflagellates. *Protistologica* 21: 429-446.

115. Silva ES (1978) Endonuclear bacteria in two species of dinoflagellates. *Protistologica* 14: 113-119.

116. Leedale GF (1969) Observations on endonuclear bacteria in euglenoid flagellates. *Österreichische Botanische Zeitschrift* 116: 279-294.

117. Shin W, Sung MB, Fritz L (2003) Endonuclear bacteria in *Euglena hemichromata* (Euglenophyceae): a proposed pathway to endonucleobiosis. *Phycologia* 42: 198-203.

118. Dangeard P (1902) Sur les caryophysème des Eugléniens. *C R Hebd Seances Acad Sci* 134: 1365-1366.

119. Dangeard P (1933) Nouvelles observations sur les parasites des *Euglenes*. *Le Botaniste* 24: 1-45.

120. Kirby H (1941) Organisms living on and in Protozoa. In: Calkins GN, Summers FM, editors. *Protozoa in biological research*. New York, NY: Columbia University Press. pp. 1009-1113.

121. Kirby H (1944) The structural characteristics and nuclear parasites of some species of *Trichonympha* in termites. *Univ Calif Publ Zool* 49: 185-282.

122. Ueda K (1960) Structure of plant cells with special reference to lower plants: IV. Structure of *Trachelomonas* sp. *Cytologia* 25: 8-16.

123. Roth LE (1959) An electron-microscope study of the cytology of the protozoan *Peranema trichophorum*. *J Protozool* 6: 107-116.

124. Dolan MF, Wier AM, Melnitsky H, Whiteside JH, Margulis L (2004) Cysts and symbionts of *Staurojoenina assimilis* Kirby from *Neotermes*. *Eur J Protistol* 40: 257-264.

125. d'Ambrosio U, Dolan M, Wier AM, Margulis L (1999) Devescovinid trichomonad with axostyle-based rotary motor ("Rubberneckia"): Taxonomic assignment as *Caduceia versatilis* sp. nov. *Eur J Protistol* 35: 327-337.

126. Tamm SL, Tamm S (1974) Direct Evidence for Fluid Membranes. *Proc Natl Acad Sci USA* 71: 4589-4593.

127. Hollande A, Carruette-Valentin J (1971) Les atractophores, l'induction du fuseau et la division cellulaire chez les hypermastigines: Étude infrastructurale et révision systématique des trichonymphines et des spirotrichonymphines. *Protistologica* 7: 5-100.

128. Adl SM, Simpson AGB, Farmer MA, Andersen RA, Anderson OR, et al. (2005) The new higher level classification of eukaryotes with emphasis on the taxonomy of protists. *J Eukaryot Microbiol* 52: 399-451.

The sulfur-oxidizing endosymbiont of the hydrothermal vent mussel
***Bathymodiolus puteoserpentis* (Bivalvia: Mytilidae)**
uses hydrogen as an energy source

Frank U. Zielinski^{1,2}, Jillian M. Struck¹, Silke Wetzel¹, Thomas Pape^{3‡}, Richard Seifert³,
Frank Wenzhöfer⁴, Nicole Dubilier^{1*}

¹ Max Planck Institute for Marine Microbiology, Department of Molecular Ecology
Celsiusstr. 1, 28359 Bremen, Germany

² Helmholtz-Center for Environmental Research – UFZ, Department of Environmental Microbiology,
Permoserstraße 15, 04318 Leipzig, Germany

³ University of Hamburg, Institute for Biogeochemistry and Marine Chemistry, Bundesstr. 55, 20146
Hamburg, Germany

⁴ Max Planck Institute for Marine Microbiology, Department of Biogeochemistry
Celsiusstr. 1, 28359 Bremen, Germany

[‡] present adress: University of Bremen, Research Center Ocean Margins, Department of General and
Marine Geology, Leobener Str., 28359 Bremen, Germany

* Corresponding author:

Phone: 0049 (0)421 2028 932; Fax: 0049 (0)421 2028 580; Email: ndubilie@mpi-bremen.de

Abstract

Hydrothermal vents along the slow-spreading Mid-Atlantic Ridge (MAR) occur in both ultramafic and basaltic settings and differ prominently in their fluid composition. High temperature fluids discharged from the ultramafic-hosted Logatchev vent field at the northern MAR (14°45'N) contain hydrogen up to 19 mM due to a geochemical process known as serpentinization. In contrast, fluids emanating from the basalt-hosted Comfortless Cove field at the southern MAR (4°48'S) hold hydrogen concentrations of only 61 µM. Only nanomolar concentrations are present in the basalt-hosted Lilliput diffuse fluids (9°33'S). Deep-sea hydrothermal vent mussels belonging to the genus *Bathymodiolus* are found at all three vent fields and dominate the invertebrate community. They thrive in areas supplied by diffuse fluids as a result of a dual symbiosis with sulfur- and methane-oxidizing bacterial endosymbionts. To date, reduced sulfur compounds and methane are the only two energy sources known to fuel chemosynthetic symbioses. However, hydrogen is a potential energy source for chemolithotrophic bacteria but has never been shown to be utilized by any of the chemosynthetic symbionts nourishing invertebrates in reducing environments. We incubated endosymbiont containing gill tissues of *B. puteoserpentis* (Logatchev) and *B. sp.* (Comfortless Cove and Lilliput) in the presence of hydrogen and sulfide. Hydrogen was rapidly consumed by *B. puteoserpentis* but only moderately by *B. sp.* However, consumption rates of *B. sp.* increased with elevated hydrogen partial pressures indicating that hydrogen uptake can be stimulated. In contrast, sulfide consumption rates did not differ in these mussels. Both hydrogen and sulfide stimulated carbon fixation in *B. puteoserpentis* gill tissues with similar CO₂ incorporation rates. Furthermore, the *hynL* gene coding for the large subunit of a membrane-bound respiratory hydrogen uptake [NiFe]-hydrogenase and indicative of energy conservation across the bacterial respiratory chain was found in *B. puteoserpentis* and *B. sp.* gill DNA extracts. The *hynL* gene was also amplified from *B. cf. thermophilus* which solely hosts chemoautotrophic symbionts whereas methanotrophs are absent. This implies that hydrogen may be an energy source for the sulfur-oxidizing symbiont of bathymodiolin vent mussels. Attempts to amplify this gene from cold-seep bathymodiolin mussels have so far been unsuccessful indicating that hydrogen is not recruited for energy conservation in seep mussels. While hydrogen-based energy

conservation by chemoautotrophic symbionts of bathymodiolin vent mussels is strongly supported for *B. puteoserpentis* by physiological evidence we can not exclude at this point that the methanotrophic endosymbiont may also contribute to hydrogen consumption with or without conserving energy from this process. Concurrent with hydrogen concentrations in high temperature and diffuse fluids our data indicate that chemoautotrophy in bathymodiolin mussels may be sulfur-based at basalt-hosted vent settings and cold seeps but hydrogen-based at ultramafic-hosted vents. Accordingly, the chemoautotrophic strains of Rainbow and Lost City mussels may also rely on hydrogen rather than on sulfide for energy conservation. Meanwhile and at first approximation the Logatchev mussel population may oxidize 12-30 mol hydrogen per hour corresponding to 270-670 liters of hydrogen. Endosymbionts of *B. puteoserpentis* may therefore play an appreciable role in hydrogen removal from diffuse fluids before hydrogen is issued into the open ocean.

Keywords: hydrothermal vents, Mid-Ocean Ridges, Mid Atlantic Ridge, Serpentinization, Logatchev, *Bathymodiolus puteoserpentis*, mussels, bivalvia, endosymbiosis, chemoautotrophic bacteria

Introduction

The Logatchev hydrothermal vent fauna is dominated by the mussel *Bathymodiolus puteoserpentis* that forms dense aggregates in areas of diffuse hydrothermal fluid-flow. Mussel biomass at Logatchev has been estimated to exceed 70 kg m⁻² (Gebruk *et al.*, 2000). In the absence of light and thus photosynthetic primary production, the abundance of *B. puteoserpentis* is the result of a symbiotic association with chemosynthetic bacteria that reside intracellularly in specialized gill bacteriocytes. *B. puteoserpentis* hosts two types of gammaproteobacterial endosymbionts: one is related to free-living and symbiotic type I methanotrophs and the other to chemoautotrophic symbionts of other *Bathymodiolus* hosts (Duperron *et al.*, 2006). It is generally assumed that bacterial symbionts that fall within the methanotrophic and chemoautotrophic clades of mussel symbionts use methane and reduced sulfur compounds as an energy source. However, even very closely related bacteria may have very different metabolic repertoires as a result of horizontal gene transfer enabling them to occupy very different ecological niches (Suen *et al.*, 2007). Furthermore, for the chemoautotrophic clade of bathymodiolin symbioses, clear evidence for the use of reduced sulfur compounds as an electron donor has only been presented for a single host species, *B. thermophilus*. In this mussel, both sulfide and thiosulfate stimulated CO₂ fixation (Belkin *et al.*, 1986; Nelson *et al.*, 1995).

In *B. puteoserpentis*, evidence for the use of methane as an energy source is based on ¹⁴CH₄ oxidation experiments, immunodetection of methanol dehydrogenase (a key enzyme in methane oxidation), hexulose-phosphate synthase assays (key enzyme of the ribulose monophosphate cycle of formaldehyde assimilation), amplification of genes coding for key enzymes in the oxidation of methane (methane monooxygenase (*pmoA*) and methanol dehydrogenase (*mxoA*) (Pimenov *et al.*, 2002; Robinson *et al.*, 1998), and the expression of the *pmoA* gene (Pernthaler *et al.*, in prep.).

In contrast, it has been more difficult to prove chemoautotrophy based on reduced sulfur compounds for the second endosymbiont of *B. puteoserpentis*. Both sulfide and thiosulfate did not stimulate ¹⁴CO₂ fixation and enzyme assays with the key enzyme for the assimilation of CO₂ via the Calvin Cycle (RubisCO - ribulose 1,5-bisphosphate carboxylase) were either negative or showed only low activities in two independent studies (Pimenov *et al.*, 2002; Robinson *et al.*, 1998). However, immunodetection indicated the presence of RubisCO in *B. puteoserpentis* gill tissues (Robinson *et al.*, 1998). Recently, (Pernthaler *et al.*, in prep.) showed that the *aprA* gene is expressed in the chemoautotrophic endosymbiont of *B. puteoserpentis*. This gene codes for the alpha subunit of adenosine-5'-phosphosulfate reductase (APS reductase) and is used by sulfur-oxidizing bacteria to oxidize sulfite (Hipp *et*

al., 1997; Sánchez *et al.*, 2001). This suggests that the chemoautotrophic endosymbiont of *B. puteoserpentis* is able to use reduced sulfur compounds as an energy source.

To date methane and reduced sulfur compounds are the only two energy sources known to fuel chemosynthetic symbioses (Cavanaugh *et al.*, 2006; Stewart *et al.*, 2005). In theory, however, other reduced compounds such as hydrogen, ammonium, nitrite, ferrous iron, and manganese could also be used as electron donors (Amend and Shock, 2001; Fisher *et al.*, 2007; Jannasch and Mottl, 1985; Jørgensen and Boetius, 2007). Hydrogen is a particularly favorable energy source as the energy yield from hydrogen oxidation is higher than from methane or sulfur oxidation and much higher than the energy yield from the oxidation of all other potential inorganic electron donors. For example, the standard molal Gibbs free energy (ΔG^0) yielded from the aerobic oxidation of hydrogen at 4°C (-528 kJ mol⁻¹ per mol oxygen) exceeds the energy yield from aerobic methane oxidation (-412 kJ mol⁻¹) and aerobic sulfide oxidation at the same conditions (-378 kJ mol⁻¹) (Amend and Shock, 2001).

A wide range of phylogenetically diverse bacteria use hydrogen as an energy source including free-living aerobic methane- and sulfur-oxidizing bacteria. *Acidithiobacillus ferrooxidans* which was initially characterized as a sulfur- and ferrous iron-oxidizing aerobic chemolithoautotroph also grows aerobically on hydrogen (Drobner *et al.*, 1990; Ohmura *et al.*, 2002). Besides, the potential to grow on hydrogen has been inferred from the complete genome sequences of the sulfide-oxidizing chemolithoautotrophs *Thiobacillus denitrificans* and *Thiomicrospira crunogena* (Beller *et al.*, 2006; Scott *et al.*, 2006) and the methanotroph *Methylococcus capsulatus* (Bath) (Ward *et al.*, 2004).

Hydrothermal vent fields along the slow-spreading Mid-Atlantic Ridge (MAR) can be grouped into basalt-hosted and ultramafic-hosted systems. Whereas in basalt-hosted systems the upper oceanic crust is entirely composed of basaltic rocks, in ultrama-

fic-hosted systems the upper oceanic crust is primarily composed of mantle-derived peridotite (one type of ultramafic rocks) (Wetzel and Shock, 2000). Thus, these two systems differ in their fluid composition as a result of basalt-seawater or peridotite-seawater reactions (Wetzel and Shock, 2000). Hydrothermal fluids discharged from ultramafic-hosted vent fields along the MAR such as Logatchev (14°45'N) and Rainbow (36°14'N) contain large quantities of dissolved hydrogen while the hydrogen content of fluids discharged from basaltic-hosted systems is comparably low (Charlou *et al.*, 2002; Charlou *et al.*, 1996; Douville *et al.*, 2002; Schmidt *et al.*, 2007). The wealth of hydrogen in in ultramafic-hosted hydrothermal systems results from a geochemical process known as serpentinization (Allen and Seyfried, 2003, 2004; Bach *et al.*, 2004; Bach *et al.*, 2006; Berndt *et al.*, 1996; Charlou *et al.*, 2002; Paulick *et al.*, 2006; Schmidt *et al.*, 2007; Sleep *et al.*, 2004; Wetzel and Shock, 2000).

In this study, we examined if hydrogen could be used as an energy source by the endosymbionts of the Logatchev hydrothermal vent mussel *B. puteoserpentis*. With 19 mM Logatchev fluids bear the highest endmember amounts of hydrogen ever reported for a hydrothermal system unperturbed by magmatic and eruptive events (Lilley *et al.*, 2003; Schmidt *et al.*, 2007). Two questions were addressed: First, do the symbionts consume hydrogen, and second, does hydrogen consumption result in energy conservation? Furthermore, hydrogen consumption rates of *B. puteoserpentis* symbionts were compared with consumption rates of *B. sp.* symbionts from the basalt-hosted vent fields Comfortless Cove (4°48'S, MAR) and Lilliput (9°33'S, MAR) with hydrogen endmember concentrations ~300 times lower than at Logatchev (Haase *et al.*, 2007a; Haase *et al.*, 2007b). Finally, hydrogen consumption rates were compared to the sulfide consumption rates in these mussels. The importance of hydrogen and sulfide for endosymbionts of bathymodiolin mussels settling in ultramafic- or basalt-hosted vent settings is discussed.

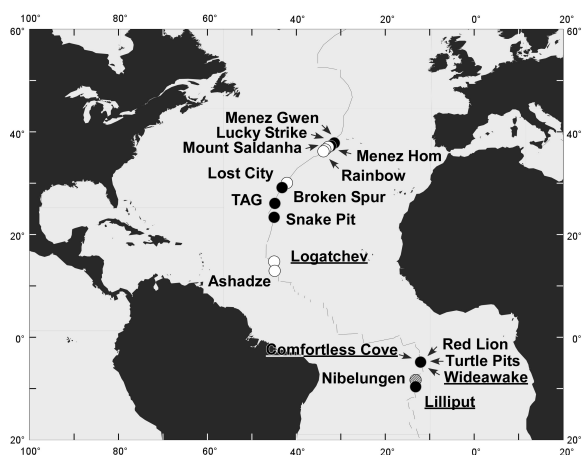


Figure 1. Map showing currently known active hydrothermal vent fields along the Mid-Atlantic Ridge. Fields where hydrogen and /or sulfide consumption experiments were performed are underlined. White and black circles denote ultramafic-hosted and basalt-hosted vent fields, respectively. Fluids of the Nibelungen field support an ultramafic-hosted setting. However, only basaltic were thus far recovered (Koschinsky *et al.*, 2006).

Material and Methods

Sampling sites

Mussels for on board physiological experiments were collected at 4 hydrothermal vent fields on the Mid-Atlantic Ridge (MAR). Specimens of *Bathymodiolus puteoserpentis* were sampled at Logatchev on the northern MAR (14°45'N). Specimens belonging to an undescribed *Bathymodiolus* species (*B. sp.*) were collected at Turtle Pits, Comfortless Cove (4°48'S) and Lilliput (9°33'S) on the southern MAR (Haase *et al.*, 2007a; Haase *et al.*, 2007b) (Figure 1). This species apparently differs from *B. puteoserpentis* (N.N. – personal communication) but has not yet been named. Mussels were sampled using nets (40 cm length, 20 cm diameter opening, mesh size 335 μ m [Hy-

drobios, Kiel, Germany]) handled by the manipulator arm of the ROV Quest (Research Center Ocean Margins, Bremen, Germany) or Jason (Woods Hole Oceanographic Institution, Woods Hole, MA, USA). Tissues from these mussels were also used for molecular purposes. Besides, *B. cf. thermophilus* from a hydrothermal vent field on the Pacific-Antarctic Ridge (PAR), *B. brooksi*, *B. heckerae*, and "*B.*" *childressi* from cold seep sites in the Gulf of Mexico (GoM) as well as *B. cf. boomerang* from a seep at the Gabon-Congo-Angola Continental Margin (GCM) (Olu-Le Roy *et al.*, 2007a; Olu-Le Roy *et al.*, 2007b) were sampled for molecular purposes only and processed as described previously (Duperron *et al.*, 2005; Duperron *et al.*, 2007; Zielinski *et al.*, manuscript II). Sampling sites and coordinates are listed in Table 1.

Mussel dissection

For hydrogen and sulfide consumption experiments and $^{14}\text{CO}_2$ incorporation incubations tissues from 3 and 2 individuals, respectively were used in each experiment. Mussels were opened with a scalpel by cutting through the posterior and anterior adductor muscles. Viability was tested by prodding the food with a dissection needle and only mussels whose foot contracted were used. The foot and both gills were separated from the remaining tissue using dissection scissors. Tissue pieces of 6 mm in diameter were cut out of the gill and the foot tissues using a steel hole puncher. One tissue piece from each individual was frozen in liquid nitrogen for weight determination in the home laboratory. For negative controls, foot tissue that does not contain endosymbiotic bacteria as well as boiled gill tissue was used.

Hydrogen consumption incubations

Experimental setup

For hydrogen partial pressures up to 1000 ppm (in helium) glass serum vials (58°ml) were fully filled with chilled (4°C) sterile-filtered (0.22 µm) bottom seawater retrieved from 3000 m water depth. One piece of gill tissue was placed in the vial, the vial closed with a gas-tight rubber stopper avoiding any inclusion of air bubbles, and crimped with aluminum seals. Control vials contained foot tissue, boiled gill tissue or no tissue at all. 20 ml of hydrogen gas (100 ppm, 250 ppm or 1000 ppm in helium, Linde) were injected through the rubber stopper using a gas-tight syringe with a second syringe allowing pressure compensation through the outflow of seawater. For hydrogen partial pressures above 1000 ppm (in air) glass serum vials were progressed as described above with the exception that the vials were filled with only 38 ml of seawater. Pure hydrogen gas (100%) (Air Liquide) was then injected in the air headspace through the rubber stopper to the desired final concentration (2100 ppm and 3000 ppm) using a gas-tight syringe. All vials were placed upside down to avoid possible gas exchange via the rubber stopper and incubated at 4°C on a slowly rotating table. At given time points a subsample was taken with a gas-tight syringe from the headspace with the pressure decrease compensated through the inflow of chilled sterile-filtered seawater from a second syringe.

Analysis of the headspace hydrogen content

The H₂ concentration in the headspace was determined using a gas chromatograph (Thermo Trace GC ultra) equipped with a packed stainless steel column (Molecular Sieve 5A, carrier gas: He) and a pulse discharge detector (PDD). Recording and calculation of results was performed using a PC operated integration system (Thermo Chrom Card A/D). Analytical procedures were calibrated daily with commercial gas standards (Linde).

Incubation conditions

In incubation vials containing hydrogen up to 1000 ppm in helium as headspace gases the equilibrium between dissolved and headspace gases led to oxygen degassing and hydrogen/helium dissolution. The theoretical concentrations of dissolved hydrogen and oxygen as well as the partial pressure of oxygen in the headspace after establishment of this equilibrium were calculated from (Crozier and Yamamoto, 1974) and (Weiss, 1970) under the assumption of Henry's law i.e. that the concentration of a dissolved gas in a solution is directly proportional to the partial pressure of that gas above the solution. The molar volume of an ideal gas (22.414 l mol⁻¹) was used to convert between the partial pressure of a gas (ppm) and the amount of that gas (moles) in the headspace. Based on these theoretical calculations, oxygen conditions in the incubation vials were sufficient for complete hydrogen oxidation, yet microaerobic. As is typical for mytilid bivalves oxygen consumption rates of Bathymodioline mussels decline with decreasing oxygen concentrations (Kochevar *et al.*, 1992). Therefore, gill oxygen consumption rates are only low under microaerobic conditions (Childress *et al.*, 1986; Kochevar *et al.*, 1992) and do not account for substantial oxygen removal from vials during the time of incubation. Furthermore, the addition of oxygen-saturated seawater for pressure compensation with each subsample taken from the headspace for hydrogen analysis regularly replenished the vials with oxygen. Table 2 lists the calculated dissolved hydrogen and oxygen concentrations under 1 atmosphere of helium or air and different hydrogen partial pressures.

Table 2. Incubation conditions at different H₂ partial pressures in a 58 ml incubation vial filled with 38 ml seawater (4°C, 35 ‰)

H ₂ partial pressure [ppm]	Major headspace gas	O ₂ partial pressure [%]	H ₂ [nmol]	O ₂ [μmol]	O ₂ /H ₂ ratio	Dissolved H ₂ [nM]	Dissolved O ₂ [μM]	O ₂ /H ₂ ratio in solution
100	helium	1*	89	9	101	77	11	143
250	helium	1*	223	9	40	194	11	57
1000	helium	1*	892	9	10	775	11	14
2100	air	21	1874	187	100	1627	324	199
3000	air	21	2677	187	70	2325	324	139

*Although incubation conditions were microaerobic under a helium headspace mitochondrial respiration likely accounted only for low oxygen consumption rates under these conditions (Childress *et al.*, 1986; Kochevar *et al.*, 1992). Furthermore, oxygen was regularly replenished with the addition of oxygen-saturated seawater each time a subsample was taken from the headspace for hydrogen analysis. Thus, oxygen concentrations were sufficient for hydrogen oxidation. Note that for the complete oxidation of hydrogen only half the amount of oxygen is required ($\text{H}_2 + \frac{1}{2} \text{O}_2 \rightarrow \text{H}_2\text{O}$).

Sulfide consumption incubations

For sulfide consumption incubations glass serum vials and tissue pieces were prepared as described for hydrogen consumption incubations with the exception that the seawater to headspace ratio (v/v) was 1/3 and that the headspace always contained air. Control vials contained foot tissue or no tissue at all. A Na₂S stock solution was added to the seawater to a final concentration below 50 μM. The initial dissolved sulfide concentration was determined immediately after sulfide addition as described below and varied between 12 and 41 μM. All vials were incubated at 4°C on a slowly rotating table. Within 3 hours after sulfide addition subsamples were taken and their sulfide content fixed in a zinc acetate solution (2%, w/v). The concentration of the resulting ZnS precipitate was measured spectrophotometrically at 663 nm by means of the methylene blue method according to Pachmayr as described in (Trüper and Schlegel, 1964). The assay volume was adjusted to 10 ml.

Rate calculation

The amount of hydrogen gas in the headspace (in moles) was calculated from the hydrogen concentration (in ppm) using the molar volume of an ideal gas (22.414 l mol⁻¹) for conversion. The rates of hydrogen removal from the headspace and sulfide removal from the seawater (in nmol h⁻¹ (piece tissue)⁻¹) were calculated for the first 1 to 3 hours after addition of the

electron source performing linear regression through the data points obtained during this incubation period and computing the slope. The effect of methodological hydrogen and sulfide removal from the headspace and seawater, respectively through subsampling was considered. The rates at which hydrogen and sulfide vanished from incubation vials containing only seawater but no tissues (chemical oxidation, hydrogen loss by diffusion) were subtracted from the tissue rates. Resulting rates were then normalized to gram wet weight (in nmol h⁻¹ (g wet weight)⁻¹).

¹⁴CO₂ fixation incubations

Incubation conditions

For ¹⁴CO₂ incorporation experiments in the presence of hydrogen or sulfide (H₂S / HS⁻) gill tissue pieces of 6 mm in diameter were prepared as described for hydrogen incubations and incubated for 30, 60, 90, 120, and 180 minutes. Care was taken to use gill tissues from the same individual for all time points and negative controls. Glass serum vials (58 ml) were filled with seawater, one piece of gill tissue, and closed and crimped as described above with the exception that only 10 ml of seawater was added. Vials were supplemented with hydrogen gas or Na₂S to a final concentration of 20 μM while negative controls were left unsupplemented. Pure hydrogen gas (100%) (Air Liq-

uide) was injected to the air headspace through the rubber stopper to a final concentration of 2.6% using a gas-tight syringe thus resulting in a dissolved H_2 concentration of 20 μM (at 4°C, 35 ‰) (Crozier and Yamamoto, 1974). To facilitate the establishment of the equilibrium between hydrogen in the headspace and hydrogen in solution, a stock solution of dissolved hydrogen gas (775 μM , 1 atm H_2 [100%], 4°C, 35 ‰) was injected to the seawater through the rubber stopper to a final concentration of 20 μM using a gas-tight syringe. All vials were supplemented with $^{14}CO_3^{2-}$ to a final activity of 30 kBq/ml (stock solution 37 MBq/ml; Perkin Elmer). Vials were turned upside down and incubated as described above. CO_2 fixation was stopped by adding formaldehyde to a final concentration of 4%.

Measurements of $^{14}CO_2$ incorporation

After formaldehyde treatment the vials were placed upright without shaking to ensure sedimentation of gill tissue. Vials were then opened and a 2 ml seawater subsample was added to a scintillation cocktail (Ultima Gold, Perkin Elmer) to determine the remaining $^{14}CO_3^{2-}$ activity in the medium. To expel the remaining $^{14}CO_3^{2-}$ from the seawater the pH was adjusted to < 2 by adding 1 M HCl. Acidified vials were placed on a shaker under an exhaust hood and shaken for at least 12 h at maximum speed to ensure complete expulsion of CO_2 . To determine the remaining $^{14}CO_2$ activity in the medium after acidification and CO_2 expulsion a seawater subsample was pipetted into a scintillation cocktail. The remaining seawater medium with the gill tissue was poured through a 0.22 μm filter until visually dry. The filter with the gill tissue was covered with a scintillation cocktail and the ^{14}C activity measured with a liquid scintillation counter (Tri-Carb 3100TR, Perkin Elmer).

Amplification of the gene coding for the large subunit (hynL) of a membrane-bound respiratory hydrogen uptake [NiFe]-hydrogenase

DNA extraction, cloning, and sequencing

Total DNA was extracted from gill tissues according to the method described by (Zhou *et al.*, 1996). The previously published primers HUPLX1 and HUPLW2 targeting the highly conserved N- and C-terminal regions of the large subunit of [NiFe] hydrogenases (Csáki *et al.*, 2001) were used to amplify a fragment of approximately 1700 bp length. The reaction mixtures for PCR amplification contained 50 pmol of each primer, 2.5 μmol of each dNTP, 1 \times Eppendorf buffer, 1 U of Eppendorf Taq polymerase, and approximately 200 ng of genomic DNA. The final volume was adjusted to 50 μl with sterile water. The amplification program consisted of an initial denaturation step at 95°C for 5 min, followed by 30 cycles at 95°C for 1 min, 45°C for 1.5 min, and 72°C for 2 min, and a final elongation step at 72°C for 10 min. Due to unspecific amplification, PCR products were separated on a 1% agarose gel. The appropriate band was cut from the gel and purified from gel pieces with the QIAquick PCR purification kit (QIAGEN). Prior to cloning, the PCR product was directly sequenced to confirm specific amplification. Sequences were compared with entries in the public database by using the tBLASTx search algorithm (Altschul *et al.*, 1997). Separated and purified PCR products were ligated at 4°C overnight with the pGEM-T Easy vector (Promega) in the following reaction mixture: 1 \times rapid ligation buffer, 50 ng pGEM-T Easy vector, 3 μl PCR purification product, 3 Weiss units T4 DNA ligase, made up to a final volume of 10 μl with sterile water. The ligation product was used for transformation with the TOPO-TA kit (Invitrogen). Clone libraries of 96 clones were constructed for each individual. The insert size was controlled by PCR screening with vector primers M13F and M13R (Yanisch-Perron *et al.*, 1985). 16 partial sequences were obtained for each individual. Partial sequences were

aligned and compared with BioEdit (Hall, 1999) using the Clustal W implementation (Thompson *et al.*, 1994). An internal primer HUPL540F

(5'-GAAGCAGATTTAATGGCGGTAGC-3') was designed for full sequencing by manual identification of an appropriate site in the alignment. 2 clones from each individual were chosen for full sequencing. Full sequencing was done using plasmid preps (QIAprep Miniprep kit, QIAGEN) and assembled using Sequencher (www.genecodes.com). Sequencing reactions were performed by using ABI BigDye and an ABI PRISM 3100 genetic analyser (Applied Biosystems).

All *hynL* gene sequences obtained from *B. puteoserpentis* (Logatchev – MAR), *B. sp.* (Wideawake – MAR), *B. sp.* (Lilliput – MAR), and *B. cf. thermophilus* (German Flats – PAR) have been deposited at the EMBL database (Kulikova *et al.*, 2007) under accession numbers X00000-X00000, respectively.

Phylogenetic reconstruction

Almost complete *hynL* gene sequences were imported into BioEdit and translated to the corresponding amino acid sequence. Protein sequences used to reconstruct hydrogenase phylogeny in a previous review (Vignais *et al.*, 2001) were imported into BioEdit and aligned with the sequences generated in this study. The alignment generated in BioEdit was imported into ARB (Ludwig *et al.*, 2004), where it was manually corrected. Parsimony and maximum likelihood trees were calculated with the ARB package.

Results

H₂ consumption in *B. puteoserpentis* (Logatchev) and *B. sp.* (Comfortless Cove and Lilliput)

Gill tissues of *B. puteoserpentis* collected from the ultramafic-hosted Logatchev vent field with high in situ hydrogen concentrations consumed hydrogen rapidly from the incubation vials. In contrast, gill tissues collected from the basalt-hosted Comfortless

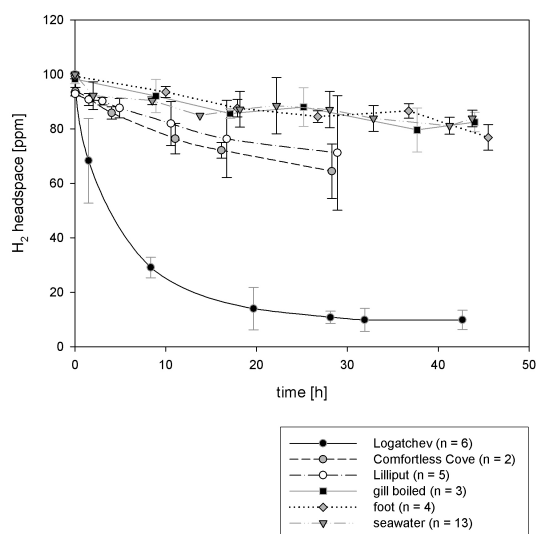


Figure 2. Hydrogen consumption over time in mussel gill tissues. Hydrogen concentrations decreased rapidly in vials with symbiont-containing gill tissues from Logatchev but only moderately in vials with gill tissues from Comfortless Cove and Lilliput. Symbiont-free foot tissue, boiled gill tissue, or seawater barely consumed hydrogen.

Cove and Lilliput vent fields with low in situ hydrogen concentrations consumed hydrogen only moderately. In incubation vials containing the negative controls boiled gill tissue, symbiont-free foot tissue, and 0.22 μm filtered seawater without any tissue hydrogen decreased only marginally (Figure 2). Within nine hours Logatchev gill tissues consumed $\sim 72\%$ of the hydrogen gas whereas Comfortless Cove and Lilliput tissues consumed $\sim 21\%$ and $\sim 16\%$, respectively. The controls accounted for a loss of only $\sim 6\%$. Due to an unfavorable ratio of headspace to seawater volume hydrogen no longer sufficiently dissolved in the seawater after three measurements (20 hours of incubation) and was thus not fully consumed from the headspace. The hydrogen consumption rates were calculated for the first 1-3 hours and were similar for the two Logatchev sampling sites Irina II and Quest. At 100 ppm hydrogen partial pressure Irina II and Quest gill tissues consumed hydrogen at a rate of 478 ± 197 ($n = 3$) and 493 ± 221 ($n = 3$) $\text{nmol h}^{-1} (\text{g wet weight})^{-1}$, respectively. Hydrogen consumption by *B. sp.* gill tissues was 6-fold lower in Comfortless Cove mussels and 13-fold lower in Lilliput mussels.

Hydrogen consumption rates in vials containing boiled gill tissues, foot tissues, and 0.22 μm filtered seawater without any tissue were only low and in the same range with 0.1 ± 0.1 ($n = 3$), 0.2 ± 0.1 ($n = 4$), and 0.2 ± 0.1 nmol h^{-1} ($n = 13$), respectively (Figure 3).

Table 3 Hydrogen consumption rates at different partial pressures in mussels from vent fields with high (Logatchev) and low (Comfortless Cove and Lilliput) hydrogen concentrations

vent field / control	site	tissue	H ₂ headspace [ppm]	Rate (Mean \pm SD) [nmol h ⁻¹ (g wet weight) ⁻¹]	n	H ₂ at site [μM] ^a
Logatchev	Irina II, Quest	gill	100	486 \pm 187	6	4.2-5.9 ^b
	Irina II	gill	100	478 \pm 197	3	5.9 ^b
	Quest	gill	100	493 \pm 221	3	4.2 ^b
Comfortless Cove	Sisters Peak	gill	100	77 \pm 21	2	nd ^c
	Sisters Peak, Golden Valley	gill	1000	446 \pm 223	5	0.1 ^d
Lilliput	Limtoc	gill	100	37 \pm 45	5	0.03 ^e
		gill	250	71 \pm 32	4	
		gill	2100	153 \pm 38	3	
		gill	3000	377 \pm 141	3	
Controls	Irina II	gill boiled	100	0.1 \pm 0.1*	3	5.4 ^b
	Irina II, Sisters Peak, Limtoc	foot	100	0.2 \pm 0.1*	4	-
	-	seawater	100	0.2 \pm 0.1*	13	-

^a as determined by discrete sampling and analysis on board; ^b T. Pape and R. Seifert, personal communication; ^c hydrogen concentrations in Sisters Peaks diffuse fluids were not determined, the endmember concentration at Sisters Peak was 61 μM (Haase *et al.*, 2007b); ^d value refers to the Golden Valley site; ^e values from (Haase *et al.*, 2007a) and A. Koschinsky, personal communication; *rate in nmol h^{-1} , nd – not determined

Effect of H₂ partial pressure on H₂ consumption rate

To investigate the effect of H₂ partial pressure on H₂ consumption rates gill tissues from Comfortless Cove and Lilliput mussels were incubated at partial pressures higher than 100 ppm. At Comfortless Cove a ten-fold increase in partial pressure resulted in a 4-fold increase in H₂ consumption. At Lilliput where only little hydrogen was consumed at 100 ppm an increase in partial pressure to 250 ppm stimulated hydrogen consumption 2-fold (Figure 4). At 2100 ppm and 3000 ppm gill tissues showed 4 and 10-fold higher consumption rates (Figure 5). The values for all consumption rates are listed in Table 3.

Hydrogen vs. sulfide consumption rates

For comparison of hydrogen with sulfide consumption rates gill tissues from the ul-

tramafic-hosted Logatchev field and the basalt-hosted vent fields at 4°48'S were also incubated in the presence of sulfide. Sulfide consumption rates of *B. puteoserpentis* (Logatchev) and *B. sp.* (Wideawake and Lilliput) gill tissues were in the same range. *B. puteoserpentis* and *B. sp.* gill tissues from the Logatchev Quest and Wideawake sites consumed sulfide at a rate of 9.2 ± 3.8 ($n = 3$) and 8.8 ± 1.2 ($n = 4$) $\mu\text{mol h}^{-1}$ (g wet weight)⁻¹, respectively. *B. puteoserpentis* and *B. sp.* gill tissues from the Logatchev Irina II and Lilliput Limtoc sites consumed sulfide at 3 to 4-fold lower rates (Table 4). There was no apparent correlation between the sulfide consumption rates and the total sulfide concentrations at the sampling sites. In general, sulfide consumption rates were higher than hydrogen consumption rates, however, hydrogen con-

sumption experiments were performed at much lower concentrations (0.08-2.3 μM dissolved hydrogen versus 12-41 μM total sulfide). For the Logatchev mussel *B. puteo-serpentis* extrapolation to 5 μM dissolved hydrogen which is consistent with minimum in situ concentrations suggests 3 to 9-fold higher hydrogen than sulfide consumption rates ($31.3 \mu\text{mol h}^{-1} (\text{g wet weight})^{-1}$, Figure 6).

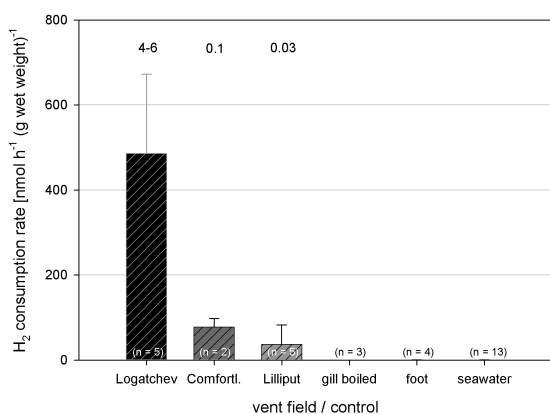


Figure 3. Hydrogen consumption rates in mussels from vent fields with high (Logatchev) and low (Comfortless Cove and Lilliput) hydrogen concentrations. Hydrogen consumption rates were much higher in the gill tissues of mussels from Logatchev than in those from Comfortless Cove and Lilliput. Numbers in the upper part of the graph denote the hydrogen concentrations at the sampling sites. Rates for boiled gill, foot and plain seawater are in nmol h^{-1} .

¹⁴CO₂ Incorporation in the presence of H₂ and H₂S

To investigate if hydrogen consumption is linked to energy conservation and thus CO₂ fixation, gill tissues from Logatchev mussels were incubated with hydrogen in seawater containing ¹⁴CO₃²⁻ (30 kBq ml⁻¹). Control gill tissues were incubated in the presence of sulfide or without an electron source. Under aerobic conditions (1 atm) and in the presence of hydrogen (2.6% H₂ partial pressure, 20 μM dissolved H₂) or sulfide (20 μM) gill tissues clearly incorporated ¹⁴CO₃²⁻. After two hours of incubation ¹⁴C tissue activities were 3.3 (H₂) and 3.9-fold (H₂S) higher than ¹⁴C activities of gill tissues that were incubated without an electron source (Figure 7).

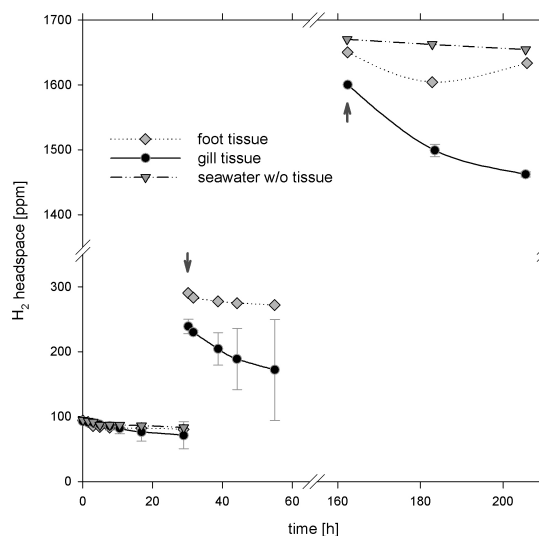


Figure 4. Stimulation of hydrogen consumption in *B. sp.* (Lilliput). At 100 ppm hydrogen was hardly consumed. An increase in partial pressure (arrow) stimulated hydrogen consumption and resulted in an increase in consumption rates. The effect was observed for nearly nine days.

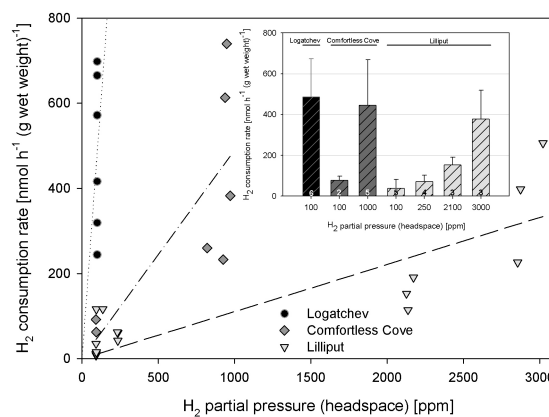


Figure 5. Effect of partial pressure on H₂ consumption rates in *B. sp.* (Comfortless Cove and Lilliput). Consumption rates generally increased with increasing partial pressures. Extrapolation from Logatchev consumption rates at 100 ppm partial pressure (77 nM dissolved H₂) (dotted line) suggests extraordinary high consumption rates at in situ conditions. Inset: Bar chart of the same data with error bars.

Table 4 Sulfide consumption rates in mussels from ultramafic-hosted (Logatchev) and basalt-hosted (Wideawake and Lilliput) hydrothermal vent fields

vent field / control	site	tissue	S ²⁻ _{tot} [μM] ^a	S ²⁻ _{tot} rate (Mean ± SD) [μmol h ⁻¹ (g wet weight) ⁻¹]*	n	S ²⁻ _{tot} at site [μM] ^b
Logatchev	Irina II	gill	12-16	3.3 ± 1.0	10	0.4-6.0 ^c
	Quest	gill	20	9.2 ± 3.8	3	32-70 ^c
Wideawake	-	gill	34-37	8.8 ± 1.2	4	59-115 ^d
Lilliput	Limtoc	gill	18-41	2.2 ± 0.8	6	31-36 ^d
Controls	Irina II, Quest	foot	12-20	-	5	
	Wideawake	foot	34-37	0.1 ± 0.1	2	
	Limtoc	foot	18-41	0.3 ± 0.1	2	

^a sulfide concentrations at which incubations were performed; ^b sulfide concentrations as determined by discrete sampling and analysis on board; ^c values from (Schmidt *et al.*, 2007) and A. Koschinsky, personal communication; ^d A. Koschinsky and H. Strauss, personal communication; * rate of sulfide loss (chemical oxidation) from incubation vials containing only 0.22 μm filtered seawater and no tissue is considered.

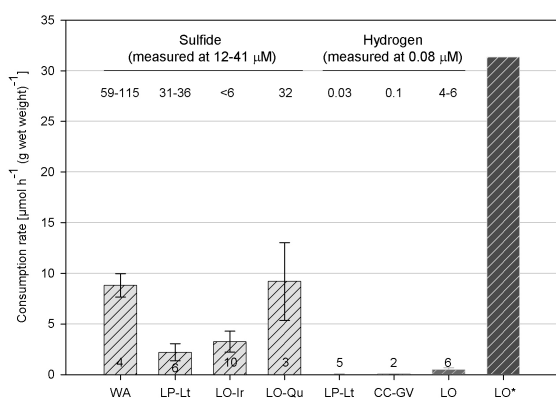


Figure 6. Sulfide and hydrogen consumption rates of *Bathymodiolus* gill tissues from basalt- and ultramafic hosted vent fields. Sulfide consumption rates measured at 12-41 μM (left four bars) were considerably higher than hydrogen consumption rates measured at 0.08 μM (following three bars). However, extrapolation of hydrogen consumption rates of Logatchev mussels to 5 μM, consistent with minimum Logatchev in situ hydrogen concentrations, suggests that hydrogen consumption rates may be 3 to 9-fold higher than sulfide consumption rates at Logatchev (last bar). Numbers in the upper part of the graph denote the sulfide and hydrogen concentrations, respectively at the sampling site as determined by discrete sampling (see Table 3 and Table 4 for references). Numbers at the bottom of the graph denote the number of investigated individuals. Abbreviations: WA – Wideawake; LP-Lt – Lilliput, Limtoc; LO-Ir – Logatchev, Irina II; LO-Qu – Logatchev, Quest; CC-GV – Comfortless Cove, Golden Valley; LO – Logatchev, Irina II and Quest; LO* - Logatchev hydrogen consumption rate extrapolated to 5 μM.

Membrane-bound respiratory hydrogen uptake [NiFe]-hydrogenase

B. puteoserpentis (Logatchev) gill tissues from individuals used for hydrogen consumption experiments were subsequently examined for the presence of bacterial membrane-bound respiratory hydrogen uptake [NiFe]-hydrogenases and the gene coding for the large subunit (*hynL*) of this group of hydrogenases could be amplified. In the light of this result other bathymodiolin mussels both from basalt-hosted vent fields and cold seeps were also investigated for the presence of the *hynL* gene. Whereas the vent mussels *B. sp.* (Lilliput and Wideawake) and *B. cf. thermophilus* (German Flats, PAR) yielded *hynL* amplification products attempts to amplify this gene from the seep mussels *B. brooksi*, *B. heckerae*, and “*B.*” *childressi* from the Gulf of Mexico as well as *B. cf. boomerang* from the Gabon-Congo-Angola Continental Margin have so far been unsuccessful. *B. sp.* (Comfortless Cove) was not included in this study. All *hynL* amplification products comprised 1636 bp translating into 545 amino acids and showed >95% sequence similarity at the amino acid level. Phylogenetic analyses based on the *HynL* amino acid sequence confirmed that *Bathymodiolus* hydrogenases fall within the group of membrane-bound

respiratory hydrogen uptake [NiFe]-hydrogenases (Figure 8). All *Bathymodiolus* hydrogenases form a monophyletic cluster and are most closely related to the hydrogenase from the alphaproteobacterial chemolithoautotroph *Oligotropha carboxidovorans* with a sequence similarity of 78%.

Discussion

Hydrogen is consumed by endosymbionts of bathymodiolin mussels

Bathymodiolin mussels along the Mid-Atlantic Ridge (MAR) live in a dual symbiosis with chemosynthetic bacteria which are housed in gill bacteriocytes (DeChaine and Cavanaugh, 2006; Distel *et al.*, 1995; Duperron *et al.*, 2006). Either one of two energy sources has to date been shown to be utilized by these endosymbionts: reduced sulfur compounds and methane (DeChaine and Cavanaugh, 2006). Here we have shown that gill tissues of MAR bathymodiolin mussels consumed hydrogen. Gill tissues of *B. puteoserpentis* from the ultramafic-hosted Logatchev vent field (14°45'N) with high in situ hydrogen concentrations consumed hydrogen rapidly whereas *B. sp.* gill tissues from the basalt-hosted vent fields Comfortless Cove (4°48'S) and Lilliput (9°33'S) consumed hydrogen only moderately. The fact that symbiont-free foot tissues and boiled gill tissues consumed no hydrogen above the seawater controls indicates that hydrogen consumption is mediated by the chemosynthetic endosymbionts in the gill tissues. Hydrogen consumption by chemosynthetic endosymbionts of hydrothermal vent invertebrates has not been shown previously for any of the deep-sea vent invertebrates.

Hydrogen consumption is coupled to CO₂ incorporation

Candidate hydrogenases for hydrogen consumption

The fact that symbiont-containing gill tissues consumed hydrogen points to the existence of hydrogenases which catalyze the

reversible oxidation of molecular hydrogen. Hydrogenases comprise three phylogenetically distinct classes, [NiFe]-hydrogenases, [FeFe]-hydrogenases, and iron-sulfur cluster-free [Fe]-hydrogenases (Schwartz and Friedrich, 2006; Vignais *et al.*, 2001; Vignais and Colbeau, 2004; Vignais *et al.*, 2004). The latter class has thus far only been detected in methanogenic archaea (Vignais and Colbeau, 2004). [FeFe]-hydrogenases occur mainly in bacteria but are rather involved in hydrogen production (Vignais *et al.*, 2004). Thus, these two classes of hydrogenases are unlikely candidates for hydrogen consumption by bathymodiolin gill tissues. [FeFe]-hydrogenases have also been found in eukaryotes but appear to be restricted to anaerobic hydrogenosome-possessing protists and chloroplasts of green algae (Vignais *et al.*, 2001; Vignais *et al.*, 2004). Therefore it is highly unlikely that bathymodiolin hydrogen consumption is of eukaryotic origin. The most likely candidate for hydrogen consumption by bathymodiolin gill tissues are [NiFe]-hydrogenases of endosymbiotic origin. First, [NiFe]-hydrogenases tend to be involved in hydrogen consumption, second, they appear to be present only in bacteria and archaea and third, to date they have remained undetected in eukaryotes (Vignais *et al.*, 2001; Vignais *et al.*, 2004).

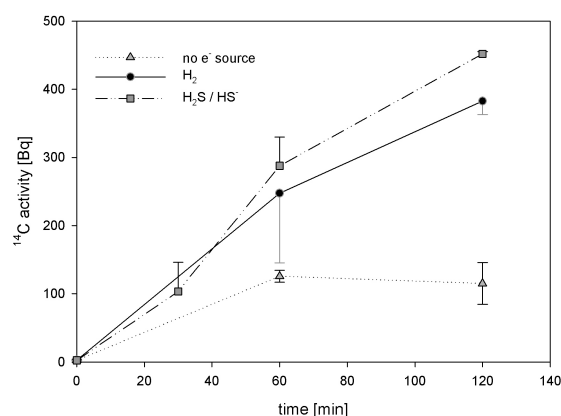


Figure 7. ¹⁴C activity in Logatchev gill tissues after incubation with ¹⁴CO₃²⁻ in the presence of hydrogen or sulfide and without an electron source. CO₂ fixation is clearly stimulated in the presence of hydrogen and sulfide. CO₂ incorporation rates are comparable for both electron sources. Data are from mussels collected from the Quest site. Gill tissues of two individuals each were used in the incubations. Error bars for H₂ and H₂S plots are given in only one direction.

Candidate [NiFe]-hydrogenases for hydrogen consumption

Two phylogenetically distinct groups of [NiFe]-hydrogenases could in theory account for endosymbiotic hydrogen consumption, a membrane-associated respiratory hydrogen uptake [NiFe]-hydrogenase (Group 1) of the membrane-bound and periplasmically oriented type or a cytoplasmic heteromultimeric reversible [NiFe]-hydrogenase (Group 3) of the bidirectional NAD-linked type (Group 3d) (Vignais *et al.*, 2001). Group 1 [NiFe]-hydrogenases are directly involved in energy conservation along the respiratory chain. They split hydrogen on the periplasmic site of the cell membrane and feed the electrons into the respiratory chain. Thus they contribute to a proton motive force and subsequent ATP production (Vignais *et al.*, 2001; Vignais and Colbeau, 2004; Vignais *et al.*, 2004). Group 3d [NiFe]-hydrogenases couple the oxidation of hydrogen to the reduction of NAD(P)⁺ or vice versa. Thus they may generate NAD(P)H needed for CO₂ fixation via the Calvin cycle and biosynthetic pathways. However, they are not directly involved in energy conservation. Yet, they may indirectly contribute to a proton motive force if the generated NADH is reoxidized by a respiratory NADH dehydrogenase. Direct coupling of a NAD(P)-dependent bidirectional [NiFe]-hydrogenase with a respiratory NADH dehydrogenase and thus energy conservation has for example been suggested for the cyanobacterium *Synechocystis* to complement the missing NADH binding subunit of its NADH dehydrogenase but has not yet been proven (Vignais *et al.*, 2004).

Hydrogen consumption and energy conservation

Incorporation of ¹⁴CO₂ by gill tissues of *B. puteoserpentis* (Logatchev) in the presence of hydrogen shows that hydrogen stimulates carbon fixation and indicates that hydrogen consumption is linked to energy conservation. Evidence for the latter is supported by the existence of the gene coding for the large subunit of a membrane-bound respiratory hydrogen uptake (Group 1)

[NiFe]-hydrogenase. This indicates that an energy-transducing [NiFe]-hydrogenase is present. The occurrence of the *hynL* gene in *B. sp.* (Wideawake and Lilliput - MAR), and *B. cf. thermophilus* (German Flats – Pacific Antarctic Ridge) from basalt-hosted vent fields implies that these mussels, too may derive energy from hydrogen consumption.

Which symbiont consumes hydrogen

Theoretical considerations

Since MAR bathymodiolin mussels live in dual symbiosis with both a chemoautotroph and a methanotroph (Duperron *et al.*, 2006) the question arises which of the two endosymbionts accounts for hydrogen consumption. Among free-living bacteria both sulfur-oxidizing chemoautotrophs and methanotrophs have been shown to use hydrogen as an energy source. Growth on hydrogen has for example been shown for the free-living sulfur-oxidizing chemoautotroph *Acidithiobacillus ferrooxidans* (Drobner *et al.*, 1990; Ohmura *et al.*, 2002). Besides, the potential to grow on hydrogen has been inferred from the complete genomes of the sulfur-oxidizing chemolithoautotrophs *Thiobacillus denitrificans* and *Thiomicrospira crunogena* (Beller *et al.*, 2006; Scott *et al.*, 2006). Methanotrophs have long been known to oxidize hydrogen in addition to methane since the enzyme methane monooxygenase which catalyzes the first step in methane oxidation co-oxidizes a variety of other substrates including hydrogen. However, no energy is yielded from this process (DiSpirito *et al.*, 2004). On the other hand, a gene cluster coding for a membrane-bound respiratory uptake [NiFe] hydrogenase has been found in the type X methanotroph *Methylococcus capsulatus* (Bath) suggesting hydrogen-dependent energy conservation in this strain (Csáki *et al.*, 2001; Ward *et al.*, 2004). The respective enzyme has biochemically been characterized revealing a high affinity for hydrogen (Hanczár *et al.*, 2002). Furthermore, a soluble cytoplasmic NAD reducing hydrogenase has also been found in this strain (Hanczár *et al.*, 2002; Ward *et al.*, 2004) which has been shown to provide

NADH needed for the oxidation of methane to methanol by methane monooxygenase (Hanczár *et al.*, 2002). Thus, both the sulfur- and the methane-oxidizing endosymbiont of MAR bathymodiolin mussels could in theory account for hydrogen consumption and exploit hydrogen as an energy source.

Experimental facts

Incorporation of $^{14}\text{CO}_2$ by gill tissues of *B. puteoserpentis* (Logatchev) in the presence of hydrogen indicates that the chemoautotrophic symbiont is a likely candidate for using hydrogen as an energy source. In all methanotrophs investigated so far CO_2 fixation via the Calvin cycle has only been found in type X methanotrophs (Bowman, 2006). However, the methane-oxidizing symbiont of bathymodiolin mussels is most closely related to type I methanotrophs (Cavanaugh *et al.*, 2006). Nevertheless, we can currently not exclude that the methanotrophic endosymbiont contributes to hydrogen consumption with or without conserving energy from this process.

The assumption that the chemoautotroph uses hydrogen as an energy source is supported by the fact that the *hynL* gene was also found in the vent mussel *B. cf. thermophilus* (German Flats – Pacific Antarctic Ridge), a mussel that solely hosts sulfur-oxidizing chemoautotrophic endosymbionts whereas methanotrophs are absent (J. M. Struck and N. Dubilier, unpublished data). This indicates that hydrogen-dependent energy conservation can be attributed to the physiological capabilities of the chemoautotrophic endosymbiont rather than to the methanotrophic symbiont. Thus, our data strongly imply that the sulfur-oxidizing chemoautotrophic endosymbiont of *B. puteoserpentis* uses hydrogen as an energy source.

Hydrogen consumption rates

Hydrogen consumption rates of MAR bathymodiolin gill tissues were considerably higher in *B. puteoserpentis* from the ultramafic-hosted Logatchev vent field than in *B. sp.* from the basalt-hosted Comfortless Cove and Lilliput fields. This is consistent with the

high and low hydrogen concentrations at these vent fields (Table 3). At Logatchev where hydrogen consumption experiments were performed with mussels from two distinct sites (Irina II and Quest) consumption rates were in the same range consistent with hydrogen concentrations at the sampling sites which did not vary greatly either (Irina II 5.9 μM , Quest 4.2 μM). The low hydrogen consumption rates of *B. sp.* gill tissues from basalt-hosted vent fields may be explained by transcriptional regulation of the genes coding for the uptake [NiFe]-hydrogenase. In the free living aerobic hydrogen-oxidizing bacteria *Ralstonia eutotropha* and *Rhodobacter capsulatus* which have extensively been investigated for the regulation of the operons coding for respiratory uptake [NiFe]-hydrogenases, expression of the respective genes is inhibited in the absence of hydrogen (Schwartz and Friedrich, 2006). Thus, the lack of hydrogen at basalt-hosted vent fields may inhibit the expression of genes involved in symbiotic hydrogen uptake. Therefore, under experimental conditions the expression of respective genes must first be induced and the [NiFe]-hydrogenase as well as the enzymes involved in electron transport along the respiratory chain be synthesized before hydrogen uptake can even start. It appears reasonable to assume that the experimental conditions (Table 2) may not have favored sufficient expression of hydrogen uptake genes in mussels from low hydrogen basalt-hosted vent fields to fully exploit the hydrogen uptake machinery. Nevertheless, the fact that hydrogen consumption could be stimulated with increasing hydrogen partial pressures in Comfortless Cove and Lilliput mussels indicates that the symbionts may have responded to the increase in hydrogen by switching from sulfur and methane oxidation to hydrogen oxidation. An alternative explanation for the low hydrogen consumption rates of *B. sp.* gill tissues from basalt-hosted vent fields may be the activity of a constitutively expressed cytoplasmic NAD-linked [NiFe]-hydrogenase (Group 3d) as is apparently the case in the type X methanotroph *Methylococcus capsulatus* (Bath) (Hanczár *et al.*, 2002).

Importance of hydrogen over sulfide

Hydrogen versus sulfide consumption rates

Experimental hydrogen consumption rates were lower than sulfide consumption rates, however, hydrogen consumption experiments were performed at much lower concentrations (0.08–2.3 μM dissolved hydrogen versus 12–41 μM total sulfide). The fact that hydrogen consumption rates increased with increasing dissolved hydrogen concentrations suggests considerably higher consumption rates at higher dissolved hydrogen concentrations. Furthermore, a considerable drawback of sulfide consumption experiments using mussel tissues is the problem that endosymbiotic sulfide consumption can not reliably be distinguished from host mitochondrial sulfide consumption. Mitochondrial sulfide oxidation has first been shown for the coastal clam *Solemya reidi* (Powell and Somero, 1986a) which like bathymodiolin mussels hosts chemoautotrophic endosymbionts. Subsequently, this phenomenon has been demonstrated across a wide range of organisms including polychaete worms, clams, fishes and chickens (Grieshaber and Volkel, 1998; Yong and Searcy, 2001). Obviously, mitochondrial sulfide oxidation is a means of sulfide detoxification, however, appears also to be a means of energy conservation (Powell and Somero, 1986b; Yong and Searcy, 2001). Therefore, sulfide consumption of *Bathymodiolus* gill tissues is certainly the sum of endosymbiotic and mitochondrial sulfide oxidation. Even if the sulfide oxidation rate of foot tissue is subtracted from the gill tissue rate the resulting rate may not reliably be attributed to the chemoautotrophic endosymbionts. This is mainly because gill tissue which primarily serves as an oxygen uptake organ (from an evolutionarily point of view) is undeniably more efficient in gas and solute uptake than the structurally, morphologically, and physiologically differing foot tissue. These considerations indicate that hydrogen and sulfide consumption rates may not directly be comparable.

For *B. sp.* mussels from the basalt-hosted Comfortless Cove and Lilliput vent

fields comparison of hydrogen and sulfide consumption rates at similar experimental concentrations does not make much sense anyway since hydrogen concentrations at the sampling sites are also only in the nanomolar range, much lower than sulfide concentrations which are in the micromolar range (A. Koschinsky and R. Seifert, personal communication). However, for *B. puteoserpentis* from the ultramafic-hosted Logatchev field direct comparison of hydrogen and sulfide consumption rates is useful since hydrogen and sulfide concentrations at the sampling site are at least in the micromolar range (A. Koschinsky and R. Seifert, personal communication). Extrapolation to 5 μM dissolved hydrogen which is consistent with lower range in situ concentrations at the sampling site suggests higher hydrogen than sulfide consumption rates for *B. puteoserpentis* gill tissues (31 versus 3–9 $\mu\text{mol h}^{-1}$ (g wet weight)⁻¹).

Hydrogen and sulfide concentrations in different vent settings

A way to estimate the importance of hydrogen and sulfide at basalt- and ultramafic-hosted vent fields is to compare the ratio between dissolved hydrogen and total dissolved sulfide ($\text{H}_2/[\text{S}^{2-}_{\text{tot}}]$) at the sampling sites. The respective concentrations are usually obtained by discrete sampling followed by analysis on board. However, it should be noted that this approach may result in erroneously low sulfide concentrations due to redox processes during fluid transport or possible sulfide loss during recovery (Schmidt *et al.*, 2007). In situ measurements of hydrogen sulfide in diffuse hydrothermal fluids reveal generally higher sulfide concentrations than is suggested by discrete sampling (Zielinski *et al.*, manuscript I). According to discrete sampling the $\text{H}_2/[\text{S}^{2-}_{\text{tot}}]$ ratio at the Comfortless Cove sampling site (Golden valley) was between 0.1 and 0.01 (A. Koschinsky and R. Seifert, personal communication). At the Lilliput sampling site (Limtoc) this ratio was ~ 0.0001 (Haase *et al.*, 2007a). Thus, hydrogen concentrations at these basalt-hosted vent fields are only low compared to sulfide concentrations even

if the sulfide bias due to discrete sampling is ignored. The $H_2/[S^{2-}_{tot}]$ ratio at the Logatchev Irina II and Quest sampling sites were 10 to 1 and ~ 0.1 , respectively. Recent measurements suggest a ratio of ~ 30 with hydrogen concentrations exceeding 1 mM (A. Koschinsky and R. Seifert, personal communication). Logatchev endmember concentrations suggest a ratio of 7.6 (Schmidt *et al.*, 2007). Thus, an excess of hydrogen over sulfide is generally apparent in Logatchev diffuse hydrothermal fluids.

Considering experimental data and fluid chemistry indicates that energy conservation by chemoautotrophic endosymbionts of MAR bathymodiolin mussels may be sulfur-based at the basalt-hosted Comfortless Cove and Lilliput vent fields but hydrogen-based at the ultramafic-hosted Logatchev vent field.

General importance of hydrogen as an energy source

Implications for B. azoricus at Rainbow and Lost City

The above outlined hypothesis may apply to basalt- and ultramafic-hosted vent fields in general. Thus, hydrogen-based energy conservation by chemoautotrophic endosymbionts of bathymodiolin mussels may also be considered for the ultramafic-hosted Rainbow and Lost City vent fields with H_2/H_2S endmember ratios of 13 and 4 to 7, respectively (Charlou *et al.*, 2002; Kelley *et al.*, 2001). However, whereas *Bathymodiolus azoricus* is abundant at Rainbow (Desbruyères *et al.*, 2001) only two live specimens have to date been found at Lost City (DeChaine *et al.*, 2006). It has been suggested that the generally low biomass at Lost City is the result of hydrogen-rich fluids poor in the sulfide species that are typically relied on by vent faunal assemblages (Kelley *et al.*, 2005). However, the discovery of a dense aggregation of fragmentary valves belonging *B. azoricus* in the Lost City area (Lost Village) indicates that large populations have existed at Lost City in recent times (Galkin, 2006) and points to the potential of Lost City fluids to support chemo-

synthesis-based symbioses. Since hydrothermal activity at Lost City has been ongoing for at least 30,000 years (Früh-Green *et al.*, 2003) sulfide concentrations have likely also been low at the time when Lost Village mussels flourished, i.e. decades ago (Galkin, 2006). Thus, the chemoautotrophic symbiont of Lost Village mussels may rather have relied on hydrogen rather than on sulfide until a shutdown of hydrothermal activity may have caused the extinction of this mussel population.

In situ measurements of H_2S concentrations in hydrothermal diffuse fluids at the ultramafic-hosted Logatchev field revealed sufficient sulfide concentrations ($\sim 30 \mu M$) to support the chemoautotrophic endosymbiont of *B. puteoserpentis* (Zielinski *et al.*, manuscript I). Unfortunately, no in situ sulfide data are available for Rainbow and Lost City. The endmember H_2S concentration at Rainbow is 1.2 mM (Charlou *et al.*, 2002). In contrast, the Lost City sulfide endmember is only 0.064 mM. (Kelley *et al.*, 2001). Either way, since sulfide does not mix conservatively with seawater due to precipitation with metal ions and biological consumption (Johnson *et al.*, 1988) sulfide abundance in the endmember fluid does not necessarily reflect sulfide availability in diffuse fluids. Especially at Rainbow where ferrous iron exceeds H_2S by a factor of 24 (Douville *et al.*, 2002) sulfide may be completely precipitated and not be present as bioavailable H_2S/HS^- in diffuse fluids. Therefore it remains unclear if the Rainbow and Lost City chemoautotrophic endosymbionts could in theory rely on sulfide. The Rainbow and Lost City fluid compositions indicate that endosymbiotic chemoautotrophy may rather be based on hydrogen.

Implications for B. puteoserpentis at Logatchev

At Logatchev where both hydrogen and H_2S concentrations in diffuse fluids are sufficient to support hydrogen and sulfur-based chemoautotrophy, the chemoautotrophic endosymbiont of *B. puteoserpentis* may switch between hydrogen and sulfide depending on the availability of these electron donors or

use both simultaneously. Interestingly, hydrogen oxidation in the free-living sulfur- and ferrous iron oxidizing chemoautotroph *Acidithiobacillus ferrooxidans* appears to be repressed in the presence of sulfur and ferrous iron suggesting preferential growth on these substrates (Drobner *et al.*, 1990). This is surprising given the fact that the energy yield from aerobic hydrogen oxidation is higher than from aerobic sulfide or Fe²⁺ oxidation and that aerobic hydrogen oxidation does not require reverse electron transport in order to generate reducing equivalents. Further work is needed to shed light on this issue.

Attempts to correlate in situ sulfide and methane concentrations with symbiont abundance and activity at ultramafic vent settings must take in situ hydrogen concentrations into consideration as in situ sulfide concentrations may be low (Rainbow, Lost City) but the sulfur-oxidizing chemoautotrophic symbiont nonetheless abundant (DeChaine *et al.*, 2006).

Implications for cold seep bathymodiolin mussels

Hydrogen does apparently not occur in relevant concentrations in cold seep fluids (Jørgensen and Boetius, 2007; Sibuet and Olu-Le Roy, 2002; Sibuet and Olu, 1998). Therefore, cold-seep bathymodiolin mussels may exclusively rely on methane and/or sulfide provided with cold-seep fluids. The fact that the *hynL* gene could not be amplified from any of the investigated seep mussels indicates that the chemoautotrophic strains of seep bathymodiolin mussels may not be equipped with a membrane-bound respiratory hydrogen uptake [NiFe]-hydrogenase.

Implications of the presence / absence of an uptake [NiFe]-hydrogenase in vent and seep mussels, respectively

(Jones and Vrijenhoek, 2006; Jones *et al.*, 2006) have recently resolved the phylogenetic relationship within bathymodiolin mussels. Accordingly, bathymodiolin mussels fall within two clades the “childressi” clade comprising mainly seep mussels (in-

cluding “*B.*” *childressi*) and the “thermophilus” clade comprising both seep mussels (*B. brooksi* and *B. heckerae*) and vent mussels (including among others *B. cf. thermophilus* and *B. puteoserpentis*). One conclusion drawn from the phylogenetic relationship was that *B. brooksi* and *B. heckerae* have independently invaded deep-sea cold seeps. Within the “thermophilus” clade *B. brooksi* constitutes the most basal lineage whereas *B. heckerae* branched off last from its common ancestor with the *B. puteoserpentis* / *B. azoricus* lineage. Regarding the presence or absence of an uptake [NiFe]-hydrogenase in members of the “thermophilus” clade the phylogenetic pattern suggests two scenarios: First, the chemoautotrophic symbiont of the common ancestor of the “thermophilus” clade acquired an uptake [NiFe]-hydrogenase by horizontal gene transfer which was then secondarily lost in *B. brooksi*, and *B. heckerae* as an adaptation to the hydrogen deficient seep environment where an energy transducing hydrogenase is dispensable. Second, the uptake [NiFe]-hydrogenase was acquired by the common ancestor of all other mussels in the “thermophilus” clade including *B. cf. thermophilus* and *B. puteoserpentis* and was then secondarily lost only in *B. heckerae*. Either way secondarily loss of the [NiFe]-hydrogenase is a more parsimonious explanation than multiple or independent acquisition of closely related [NiFe]-hydrogenases in “thermophilus” clade vent mussels.

Due to the existence of uptake [NiFe]-hydrogenases in all vent mussels investigated so far and belonging to the “thermophilus” clade we hypothesize that all vent members of the “thermophilus” clade are equipped with uptake [NiFe]-hydrogenases given the fact that hydrogen is generally present in vent diffuse fluids even though concentrations are only low at basalt-hosted vent systems.

Estimation of total hydrogen consumption mediated by *B. puteoserpentis* endosymbionts

Hydrogen consumption experiments were performed under normal pressure and

at low dissolved hydrogen concentrations for Logatchev mussels (~ 77 nM). Therefore, hydrogen consumption rates of *B. puteoserpentis* endosymbionts may be far from the rates at which hydrogen is oxidized at Logatchev in situ where dissolved hydrogen concentrations of $6 \mu\text{M}$ may be the minimum in diffuse fluids (T. Pape and R. Seifert, personal communication). This assumption is supported by the fact that an increase in hydrogen partial pressure in experiments with Comfortless Cove and Lilliput mussels resulted in an increase in hydrogen consumption rates. Using data from Comfortless Cove, extrapolation to $5 \mu\text{M}$ dissolved hydrogen suggests a hydrogen consumption rate of $\sim 3.2 \mu\text{mol h}^{-1} (\text{g wet weight})^{-1}$ for Logatchev mussel symbionts. Higher consumption rates of around $31 \mu\text{mol h}^{-1} (\text{g wet weight})^{-1}$ are in theory possible when extrapolating from zero through Logatchev rates at 100 ppm (Figure 5, dotted line). Even higher hydrogen consumption rates of $\sim 47 \mu\text{mol h}^{-1} (\text{g wet weight})^{-1}$ were measured in incubation experiments with Logatchev gill tissues in hydrogen-saturated seawater ($775 \mu\text{M}$ at 4°C , 35‰) using Clark-type H_2 sensors (Frank Wenzhöfer, unpublished data). Either way, neglecting the effect of hydrostatic pressure on hydrogen consumption rates our data allow at first approximation an estimation of hydrogen oxidation mediated by *B. puteoserpentis* endosymbionts under in situ conditions. Neglecting the influence of pressure may be justified since (Belkin *et al.*, 1986) have shown that CO_2 incorporation rates for the sulfide-oxidizing endosymbiont of *B. thermophilus* were not significantly different at 1 atm and under in situ pressure (250 atm). Therefore, assuming a gill weight of around 1 g one single *B. puteoserpentis* specimen may account for the oxidation of $60 \mu\text{mol}$ hydrogen h^{-1} . At Logatchev, *B. puteoserpentis* accounts for most of the invertebrate biomass and exceeds 70 kg m^{-2} (wet weight with shells) in Irina II mussel beds (Gebruk *et al.*, 2000). Mussel aggregations at Logatchev range from small patches 20-30 cm in diameter to larger aggregations and mus-

sel beds covering an area of 3 m^2 (for example at Quest) and 12 m^2 (for example at Irina II), respectively (Jens Stecher, personal communication). (Gebruk *et al.*, 2000) described the extended mussel beds at Irina II as 20 m in diameter. Based on these data and personal observations we estimate the mussel population at Logatchev to range between 200,000 and half a million individuals. This population may thus remove 12-30 mol hydrogen h^{-1} corresponding to 270-670 liters of pure hydrogen. Mussel patches, aggregations, and beds of *B. puteoserpentis* may therefore play an appreciable role in hydrogen removal from diffuse fluids before hydrogen is issued into the open ocean.

Acknowledgements

This work would not have been possible without the skill and cooperation of the chief scientists, the shipboard scientific parties, the captains and crews of the R/Vs and the engineers and pilots of the ROVs. We especially thank the chief scientists Klas Lackschewitz (M64/2), Andrea Koschinsky (M68/1), and Christian Borowski (MSM04/3), captain Martin Kull and the crew of the R/V Meteor, captain Friedhelm von Staa and the crew of the R/V Maria S. Merian as well as Volker Rathmeyer, Götz Ruhland, Christian Seiter and crew of the ROV Quest and N.N. and crew of the ROV Jason for their best support to collect mussels and perform experiments on board. Sébastien Duperron is acknowledged for providing gill tissues from cold seep bathymodiolin mussels. This work was supported by grants from the priority program 1144 of the German Science Foundation (DFG). This is publication number XY of the priority program 1144 "From Mantle to Ocean: Energy-, Material- and Life cycles a Spreading Axes" of DFG.

References

- Allen, D.E., Seyfried, W.E., 2003. Compositional controls on vent fluids from ultramafic-hosted hydrothermal systems at mid-ocean ridges: An experimental study at 400°C , 500 bars. *Geochim. Cosmochim. Acta* 67 (8), 1531-1542.
- Allen, D.E., Seyfried, W.E., 2004. Serpentinization and heat generation: Constraints from Lost City and

- Rainbow hydrothermal systems. *Geochim. Cosmochim. Acta* 68 (6), 1347-1354.
- Altschul, S.F., Madden, T.L., Schaffer, A.A., Zhang, J.H., Zhang, Z., Miller, W., Lipman, D.J., 1997. Gapped BLAST and PSI-BLAST: a new generation of protein database search programs. *Nucleic Acids Res.* 25 (17), 3389-3402.
- Amend, J.P., Shock, E.L., 2001. Energetics of overall metabolic reactions of thermophilic and hyperthermophilic Archaea and Bacteria. *FEMS Microbiol. Rev.* 25 (2), 175-243.
- Bach, W., Garrido, C.J., Paulick, H., Harvey, J., Rosner, M., 2004. Seawater-peridotite interactions: First insights from ODP Leg 209, MAR 15°N. *Geochim. Geophys. Geosyst.* 5, doi: 10.1029 / 2004GC000744.
- Bach, W., Paulick, H., Garrido, C.J., Ildefonse, B., Meurer, W.P., Humphris, S.E., 2006. Unraveling the sequence of serpentinization reactions: petrography, mineral chemistry, and petrophysics of serpentinites from MAR 15°N (ODP Leg 209, Site 1274). *Geophys. Res. Lett.* 33 (13).
- Belkin, S., Nelson, D.C., Jannasch, H.W., 1986. Symbiotic assimilation of CO₂ in two hydrothermal vent animals, the mussel *Bathymodiolus thermophilus* and the tube worm *Riftia pachyptila*. *Biol. Bull.* 170 (1), 110-121.
- Beller, H.R., Chain, P.S.G., Letain, T.E., Chakicherla, A., Larimer, F.W., Richardson, P.M., Coleman, M.A., Wood, A.P., Kelly, D.P., 2006. The genome sequence of the obligately chemolithoautotrophic, facultatively anaerobic bacterium *Thiobacillus denitificans*. *J. Bacteriol.* 188 (4), 1473-1488.
- Berndt, M.E., Allen, D.E., Seyfried, W.E., 1996. Reduction of CO₂ during serpentinization of olivine at 300°C and 500 bar. *Geology* 24 (4), 351-354.
- Borowski, C., Asendorf, V., Bürk, D., Jr., A.C., Elder, R., Fabian, M., Forte, P., Fuhrmann, R., Hansen, S., Jost, C.L., Keir, R., Kevis-Stirling, J., Kevis-Stirling, N., Perner, M., Petersen, J.M., Røy, H., Schauer, R., Schmale, O., Schmidt, K., Scott, D., Waters, R., Wefers, P., Wetzell, S., 2007. New coordinates for the hydrothermal structures in the Logatchev vent field at 14°45'N on the Mid-Atlantic Ridge. *InterRidge News* 16, 13-14.
- Bowman, J., 2006. The methanotrophs - the families Methylococcaceae and Methylocystaceae. In: Dworkin, M., Falkow, S., Rosenberg, E., Schleifer, K.H., Stackebrandt, E. (Eds.), *The Prokaryotes*. Springer-Verlag, Berlin, Heidelberg, pp. 266-289.
- Cavanaugh, C.M., McKiness, Z.P., Newton, I.L.G., Stewart, F.J., 2006. Marine chemosynthetic symbioses. In: Dworkin, M., Falkow, S., Rosenberg, E., Schleifer, K.H., Stackebrandt, E. (Eds.), *The Prokaryotes*. Springer-Verlag, Berlin, Heidelberg, pp. 473-507.
- Charlou, J.L., Donval, J.P., Fouquet, Y., Jean-Baptiste, P., Holm, N., 2002. Geochemistry of high H₂ and CH₄ vent fluids issuing from ultramafic rocks at the Rainbow hydrothermal field (36°14'N, MAR). *Chem. Geol.* 191 (4), 345-359.
- Charlou, J.L., Donval, J.P., Jean-Baptiste, P., Dapigny, A., 1996. Gases and helium isotopes in high temperature solutions sampled before and after ODP Leg 158 drilling at TAG hydrothermal field (26°N, MAR). *Geophys. Res. Lett.* 23 (23), 3491-3494.
- Childress, J.J., Fisher, C.R., Brooks, J.M., Kennicutt, M.C., Bidigare, R., Anderson, A.E., 1986. A methanotrophic marine molluscan (Bivalvia, Mytilidae) symbiosis: mussels fueled by gas. *Science* 233 (4770), 1306-1308.
- Crozier, T.E., Yamamoto, S., 1974. Solubility of hydrogen in water, seawater, and NaCl solutions. *J. Chem. Eng. Data* 19 (3), 242-244.
- Csáki, R., Hanczár, T., Bodrossy, L., Murrell, J.C., Kovács, K.L., 2001. Molecular characterization of structural genes coding for a membrane bound hydrogenase in *Methylococcus capsulatus* (Bath). *FEMS Microbiol. Lett.* 205 (2), 203-207.
- DeChaine, E.G., Bates, A.E., Shank, T.M., Cavanaugh, C.M., 2006. Off-axis symbiosis found: characterization and biogeography of bacterial symbionts of *Bathymodiolus* mussels from Lost City hydrothermal vents. *Environ. Microbiol.* 8 (11), 1902-1912.
- DeChaine, E.G., Cavanaugh, C.M., 2006. Symbioses of methanotrophs and deep-sea mussels (Mytilidae: Bathymodiolinae). In: Overmann, J. (Ed.), *Molecular Basis of Symbiosis*. Springer-Verlag, Berlin, Heidelberg, pp. 227-249.
- Desbruyères, D., Biscoito, M., Caprais, J.-C., Colaço, A., Comtet, T., Crassous, P., Fouquet, Y., Khipounoff, A., Le Bris, N., Olu, K., Riso, R., Sarradin, P.M., Segonzac, M., Vangriesheim, A., 2001. Variations in deep-sea hydrothermal vent communities on the Mid-Atlantic Ridge near the Azores plateau. *Deep-Sea Res. I* 48 (5), 1325-1346.
- DiSpirito, A.A., Kunz, R.C., Choi, D.-W., Zahn, J.A., 2004. Respiration in methanotrophs. In: Zannoni, D. (Ed.), *Respiration in archaea and bacteria*. Vol 2: Diversity of prokaryotic respiratory systems. Springer, Dordrecht, The Netherlands, pp. 149-168.
- Distel, D.L., Lee, H.K.W., Cavanaugh, C.M., 1995. Intracellular coexistence of methanotrophic and thioautotrophic bacteria in a hydrothermal vent mussel. *Proc. Natl. Acad. Sci. USA* 92 (21), 9598-9602.
- Douville, E., Charlou, J.L., Oelkers, E.H., Biennu, P., Colon, C.F.J., Donval, J.P., Fouquet, Y., Prieur, D., Appriou, P., 2002. The rainbow vent fluids (36°14'N, MAR): the influence of ultramafic rocks

- and phase separation on trace metal content in Mid-Atlantic Ridge hydrothermal fluids. *Chem. Geol.* 184 (1-2), 37-48.
- Drobner, E., Huber, H., Stetter, K.O., 1990. *Thiobacillus ferrooxidans*, a facultative hydrogen oxidizer. *Appl. Environ. Microbiol.* 56 (9), 2922-2923.
- Duperron, S., Bergin, C., Zielinski, F., Blazejak, A., Pernthaler, A., McKiness, Z.P., DeChaine, E., Cavanaugh, C.M., Dubilier, N., 2006. A dual symbiosis shared by two mussel species, *Bathymodiolus azoricus* and *Bathymodiolus puteoserpentis* (Bivalvia: Mytilidae), from hydrothermal vents along the northern Mid-Atlantic Ridge. *Environ. Microbiol.* 8 (8), 1441-1447.
- Duperron, S., Nadalig, T., Caprais, J.C., Sibuet, M., Fiala-Medioni, A., Amann, R., Dubilier, N., 2005. Dual symbiosis in a *Bathymodiolus* sp. mussel from a methane seep on the Gabon continental margin (southeast Atlantic): 16S rRNA phylogeny and distribution of the symbionts in gills. *Appl. Environ. Microbiol.* 71 (4), 1694-1700.
- Duperron, S., Sibuet, M., MacGregor, B.J., Kuypers, M.M.M., Fisher, C.R., Dubilier, N., 2007. Diversity, relative abundance and metabolic potential of bacterial endosymbionts in three *Bathymodiolus* mussel species from cold seeps in the Gulf of Mexico. *Environ. Microbiol.* 9 (6), 1423-1438.
- Fisher, C.R., Takai, K., Le Bris, N., 2007. Hydrothermal vent ecosystems. *Oceanography* 20 (1), 14-23.
- Früh-Green, G.L., Kelley, D.S., Bernasconi, S.M., Karson, J.A., Ludwig, K.A., Butterfield, D.A., Boschi, C., Proskurowski, G., 2003. 30,000 years of hydrothermal activity at the Lost City vent field. *Science* 301 (5632), 495-498.
- Galkin, S.V., 2006. Lost Village - a "faubourg" of Lost City: benthic studies using Mir submersibles at North Atlantic hydrothermal sites in 2005. *InterRidge News* 15, 18-24.
- Gebrek, A.V., Chevaldonné, P., Shank, T., Lutz, R.A., Vrijenhoek, R.C., 2000. Deep-sea hydrothermal vent communities of the Logatchev area (14°45'N, Mid-Atlantic Ridge): diverse biotopes and high biomass. *J. Mar. Biol. Assoc. U.K.* 80 (3), 383-393.
- Grieshaber, M.K., Volkel, S., 1998. Animal adaptations for tolerance and exploitation of poisonous sulfide. *Annu. Rev. Physiol.* 60, 33-53.
- Haase, K.M., Koschinsky, A., Devey, C.W., Fretzdorff, S., German, C., Lackschewitz, K.S., Melchert, B., Petersen, S., Seifert, R., Stecher, J., Giere, O., Paulick, H., Yoerger, D., M64/1, M68/1, 2007a. Diking, young volcanism and diffuse hydrothermal activity on the southern Mid-Atlantic Ridge. *Marine Geology*, submitted.
- Haase, K.M., Petersen, S., Koschinsky, A., Seifert, R., Devey, C.W., Keir, R., Lackschewitz, K.S., Melchert, B., Perner, M., Schmale, O., Süling, J., Dubilier, N., Zielinski, F., Fretzdorff, S., Garbe-Schönberg, D., Westernströer, U., German, C.R., Shank, T.M., Yoerger, D., Giere, O., Kuever, J., Marbler, H., Mawick, J., Mertens, C., Stöber, U., Ostertag-Henning, C., Paulick, H., Peters, M., Strauss, H., Sander, S., Stecher, J., Warmuth, M., Weber, S., 2007b. Young volcanism and related hydrothermal activity at 5°S on the slow-spreading southern Mid-Atlantic Ridge. *Geochem. Geophys. Geosyst.* 8 (11), Q11002, doi: 11010.11029 / 12006GC001509.
- Hall, T.A., 1999. BioEdit: a user-friendly biological sequence alignment editor and analysis program for Windows 95/98/NT. *Nucleic Acids Symp Ser* 41 (95-98).
- Hanczár, T., Csáki, R., Bodrossy, L., Murrell, J.C., Kovács, K.L., 2002. Detection and localization of two hydrogenases in *Methylococcus capsulatus* (Bath) and their potential role in methane metabolism. *Arch. Microbiol.* 177 (2), 167-172.
- Hipp, W.M., Pott, A.S., ThumSchmitz, N., Faath, I., Dahl, C., Truper, H.G., 1997. Towards the phylogeny of APS reductases and sirohaem sulfite reductases in sulfate-reducing and sulfur-oxidizing prokaryotes. *Microbiology* 143, 2891-2902.
- Jannasch, H.W., Mottl, M.J., 1985. Geomicrobiology of deep-sea hydrothermal vents. *Science* 229 (4715), 717-725.
- Johnson, K.S., Childress, J.J., Hessler, R.R., Sakamoto-Arnold, C.M., Beehler, C.L., 1988. Chemical and biological interactions in the Rose Garden hydrothermal vent field, Galapagos spreading center. *Deep-Sea Res. A* 35 (10-11), 1723-1744.
- Jones, W.J., Vrijenhoek, R.C., 2006. Evolutionary relationships within the "*Bathymodiolus*" *childressi* group. *Cah. Biol. Mar.* 47 (4), 403-407.
- Jones, W.J., Won, Y.J., Maas, P.A.Y., Smith, P.J., Lutz, R.A., Vrijenhoek, R.C., 2006. Evolution of habitat use by deep-sea mussels. *Mar. Biol.* 148 (4), 841-851.
- Jørgensen, B.B., Boetius, A., 2007. Feast and famine - microbial life in the deep-sea bed. *Nat. Rev. Microbiol.* 5 (10), 770-781.
- Kelley, D.S., Karson, J.A., Blackman, D.K., Früh-Green, G.L., Butterfield, D.A., Lilley, M.D., Olson, E.J., Schrenk, M.O., Roe, K.K., Lebon, G.T., Rivizzigno, P., 2001. An off-axis hydrothermal vent field near the Mid-Atlantic Ridge at 30°N. *Nature* 412 (6843), 145-149.
- Kelley, D.S., Karson, J.A., Früh-Green, G.L., Yoerger, D.R., Shank, T.M., Butterfield, D.A., Hayes, J.M., Schrenk, M.O., Olson, E.J., Proskurowski, G., Jakuba, M., Bradley, A., Larson, B., Ludwig, K., Glickson, D., Buckman, K., Bradley, A.S., Brazelton,

- W.J., Roe, K., Elend, M.J., Delacour, A., Bernasconi, S.M., Lilley, M.D., Baross, J.A., Summons, R.T., Sylva, S.P., 2005. A serpentinite-hosted ecosystem: The Lost City hydrothermal field. *Science* 307 (5714), 1428-1434.
- Kochevar, R.E., Childress, J.J., Fisher, C.R., Minnich, E., 1992. The methane mussel: roles of symbiont and host in the metabolic utilization of methane. *Mar. Biol.* 112 (3), 389-401.
- Koschinsky, A., Billings, A., Devey, C.W., Dubilier, N., Duester, A., Edge, D., Garbe-Schönberg, D., German, C.R., Giere, O., Keir, R., Lackschewitz, K.S., Mai, H.A., Marbler, H., Mawick, J., Melchert, B., Mertens, C., Peters, M., Sandler, S., Schmale, O., Schmidt, W., Seifert, R., Seiter, C., Stöber, U., Suck, I., Walter, M., Weber, S., Yoerger, D., Zarrouk, M., Zielinski, F., 2006. Discovery of new hydrothermal vent fields on the Southern Mid-Atlantic Ridge (4°S - 10°S) during Cruise M68/1. *InterRidge News* 15, 9-15.
- Kulikova, T., Akhtar, R., Aldebert, P., Althorpe, N., Andersson, M., Baldwin, A., Bates, K., Bhattacharyya, S., Bower, L., Browne, P., Castro, M., Cochrane, G., Duggan, K., Eberhardt, R., Faruque, N., Hoad, G., Kanz, C., Lee, C., Leinonen, R., Lin, Q., Lombard, V., Lopez, R., Lorenc, D., McWilliam, H., Mukherjee, G., Nardone, F., Pastor, M.P.G., Plaister, S., Sobhany, S., Stoehr, P., Vaughan, R., Wu, D., Zhu, W., Apweiler, R., 2007. EMBL Nucleotide Sequence Database in 2006. *Nucl. Acids Res.* 35 (suppl_1), D16-D20.
- Lilley, M.D., Butterfield, D.A., Lupton, J.E., Olson, E.J., 2003. Magmatic events can produce rapid changes in hydrothermal vent chemistry. *Nature* 422 (6934), 878-881.
- Ludwig, W., Strunk, O., Westram, R., Richter, L., Meier, H., Yadukumar, Buchner, A., Lai, T., Steppi, S., Jobb, G., Forster, W., Brettske, I., Gerber, S., Ginhart, A.W., Gross, O., Grumann, S., Hermann, S., Jost, R., König, A., Liss, T., Lussmann, R., May, M., Nonhoff, B., Reichel, B., Strehlow, R., Stamatakis, A., Stuckmann, N., Vilbig, A., Lenke, M., Ludwig, T., Bode, A., Schleifer, K.H., 2004. ARB: a software environment for sequence data. *Nucleic Acids Res.* 32 (4), 1363-1371.
- Nelson, D.C., Hagen, K.D., Edwards, D.B., 1995. The gill symbiont of the hydrothermal vent mussel *Bathymodiolus thermophilus* is a psychrophilic, chemoautotrophic, sulfur bacterium. *Mar. Biol.* 121 (3), 487-495.
- Ohmura, N., Sasaki, K., Matsumoto, N., Saiki, H., 2002. Anaerobic respiration using Fe³⁺, S⁰, and H₂ in the chemolithoautotrophic bacterium *Acidithiobacillus ferrooxidans*. *J. Bacteriol.* 184 (8), 2081-2087.
- Olu-Le Roy, K., Caprais, J.C., Fifi, A., Fabri, M.C., Galéron, J., Budzinsky, H., Le Ménach, K., Khripounoff, A., Ondreas, H., Sibuet, M., 2007a. Cold-seep assemblages on a giant pockmark off West Africa: spatial patterns and environmental control. *Mar. Ecol.* 28 (1), 115-130.
- Olu-Le Roy, K., von Cosel, R., Hourdez, S., Carney, S.L., Jollivet, D., 2007b. Amphi-Atlantic cold-seep *Bathymodiolus* species complexes across the equatorial belt. *Deep-Sea Res.* 54 (11), 1890-1911.
- Paulick, H., Bach, W., Godard, M., De Hoog, J.C.M., Suhr, G., Harvey, J., 2006. Geochemistry of abyssal peridotites (Mid-Atlantic Ridge, 15°20'N, ODP Leg 209): Implications for fluid/rock interaction in slow spreading environments. *Chem. Geol.* 234 (3-4), 179-210.
- Pernthaler, A., Ward, J.E., Zielinski, F., Borowski, C., Dubilier, N., in prep. Expression patterns of *pmoA* and *aprA* in symbionts of the hydrothermal vent mussel *Bathymodiolus puteoserpentis*.
- Pimenov, N.V., Kalyuzhnaya, M.G., Khmelenina, V.N., Mityushina, L.L., Trotsenko, Y.A., 2002. Utilization of methane and carbon dioxide by symbiotrophic bacteria in gills of Mytilidae (*Bathymodiolus*) from the Rainbow and Logachev hydrothermal fields on the Mid-Atlantic Ridge. *Microbiology* 71 (5), 587-594.
- Powell, M.A., Somero, G.N., 1986a. Adaptations to sulfide by hydrothermal vent animals: sites and mechanisms of detoxification and metabolism. *Biol. Bull.* 171 (1), 274-290.
- Powell, M.A., Somero, G.N., 1986b. Hydrogen sulfide oxidation is coupled to oxidative phosphorylation in mitochondria of *Solemya reidi*. *Science* 233 (4763), 563-566.
- Robinson, J.J., Polz, M.F., Fiala-Medioni, A., Cavanaugh, C.M., 1998. Physiological and immunological evidence for two distinct C₁-utilizing pathways in *Bathymodiolus puteoserpentis* (Bivalvia: Mytilidae), a dual endosymbiotic mussel from the Mid-Atlantic Ridge. *Mar. Biol.* 132 (4), 625-633.
- Sánchez, O., Ferrera, I., Dahl, C., Mas, J., 2001. In vivo role of adenosine-5'-phosphosulfate reductase in the purple sulfur bacterium *Allochrochromatium vinosum*. *Arch. Microbiol.* 176 (4), 301-305.
- Schmidt, K., Koschinsky, A., Garbe-Schönberg, D., de Carvalho, L.M., Seifert, R., 2007. Geochemistry of hydrothermal fluids from the ultramafic-hosted Logatchev hydrothermal field, 15°N on the Mid-Atlantic Ridge: Temporal and spatial investigation. *Chem. Geol.* 242 (1-2), 1-21.
- Schwartz, E., Friedrich, B., 2006. The H₂-metabolizing prokaryotes. In: Dworkin, M., Falkow, S., Rosenberg, E., Schleifer, K.H., Stackebrandt, E. (Eds.), *The Prokaryotes*. Springer-Verlag, Berlin, Heidelberg, pp. 496-563.
- Scott, K.M., Sievert, S.M., Abril, F.N., Ball, L.A., Barrett, C.J., Blake, R.A., Boller, A.J., Chain, P.S.G.,

- Clark, J.A., Davis, C.R., Detter, C., Do, K.F., Dobrinski, K.P., Faza, B.I., Fitzpatrick, K.A., Freyermuth, S.K., Harmer, T.L., Hauser, L.J., Hügler, M., Kerfeld, C.A., Klotz, M.G., Kong, W.W., Land, M., Lapidus, A., Larimer, F.W., Longo, D.L., Lucas, S., Malfatti, S.A., Massey, S.E., Martin, D.D., McCuddin, Z., Meyer, F., Moore, J.L., Ocampo, L.H., Paul, J.H., Paulsen, I.T., Reep, D.K., Ren, Q.H., Ross, R.L., Sato, P.Y., Thomas, P., Tinkham, L.E., Zeruth, G.T., 2006. The genome of deep-sea vent chemolithoautotroph *Thiomicrospira crunogena* XCL-2. *PLoS Biol.* 4 (12), 2196-2212.
- Sibuet, M., Olu-Le Roy, K., 2002. Cold seep communities on continental margins: Structure and quantitative distribution relative to geological and fluid venting patterns. In: Wefer, G., Billett, D., Hebbeln, D., Jørgensen, B.B., Schlüter, M., Van Weering, T. (Eds.), *Ocean Margin Systems*. Springer-Verlag, Berlin, Heidelberg, pp. 235-251.
- Sibuet, M., Olu, K., 1998. Biogeography, biodiversity and fluid dependence of deep-sea cold-seep communities at active and passive margins. *Deep-Sea Res. II* 45 (1-3), 517-567.
- Sleep, N.H., Meibom, A., Fridriksson, T., Coleman, R.G., Bird, D.K., 2004. H₂-rich fluids from serpentinization: geochemical and biotic implications. *Proc. Natl. Acad. Sci. USA* 101 (35), 12818-12823.
- Stewart, F.J., Newton, I.L.G., Cavanaugh, C.M., 2005. Chemosynthetic endosymbioses: adaptations to oxic-anoxic interfaces. *Trends Microbiol.* 13 (9), 439-448.
- Suen, G., Goldman, B.S., Welch, R.D., 2007. Predicting prokaryotic ecological niches using genome sequence analysis. *PLoS ONE* 2 (8), e743.
- Thompson, J.D., Higgins, D.G., Gibson, T.J., 1994. Clustal W: improving the sensitivity of progressive multiple sequence alignment through sequence weighting, position-specific gap penalties and weight matrix choice. *Nucleic Acids Res.* 22 (22), 4673-4680.
- Trüper, H.G., Schlegel, H.G., 1964. Sulphur metabolism in Thiorhodaceae I. Quantitative measurements on growing cells of *Chromatium okenii*. *Antonie Van Leeuwenhoek* 30 (3), 225-238.
- Vignais, P.M., Billoud, B., Meyer, J., 2001. Classification and phylogeny of hydrogenases. *FEMS Microbiol. Rev.* 25 (4), 455-501.
- Vignais, P.M., Colbeau, A., 2004. Molecular biology of microbial hydrogenases. *Curr. Issues Mol. Biol.* 6, 159-188.
- Vignais, P.M., Willison, J.C., Colbeau, A., 2004. Hydrogen Respiration. In: Zannoni, D. (Ed.), *Respiration in Archaea and Bacteria. Vol 2: Diversity of Prokaryotic Respiratory Systems*. Springer, Dordrecht, The Netherlands, pp. 233-260.
- Ward, N., Larsen, O., Sakwa, J., Bruseth, L., Khouri, H., Durkin, A.S., Dimitrov, G., Jiang, L.X., Scanlan, D., Kang, K.H., Lewis, M., Nelson, K.E., Methé, B., Wu, M., Heidelberg, J.F., Paulsen, I.T., Fouts, D., Ravel, J., Tettelin, H., Ren, Q.H., Read, T., DeBoy, R.T., Seshadri, R., Salzberg, S.L., Jensen, H.B., Birkeland, N.K., Nelson, W.C., Dodson, R.J., Grindhaug, S.H., Holt, I., Eidhammer, I., Jonassen, I., Vanaken, S., Utterback, T., Feldblyum, T.V., Fraser, C.M., Lillehaug, J.R., Eisen, J.A., 2004. Genomic insights into methanotrophy: the complete genome sequence of *Methylococcus capsulatus* (Bath). *PLoS Biol.* 2 (10), 1616-1628.
- Weiss, R.F., 1970. Solubility of Nitrogen, Oxygen and Argon in Water and Seawater. *Deep-Sea Res. Oceanogr. Abstr.* 17 (4), 721-735.
- Wetzel, L.R., Shock, E.L., 2000. Distinguishing ultramafic- from basalt-hosted submarine hydrothermal systems by comparing calculated vent fluid compositions. *J. Geophys. Res.* 105 (B4), 8319-8340.
- Yanisch-Perron, C., Vieira, J., Messing, J., 1985. Improved M13 phage cloning vectors and host strains: nucleotide sequences of the M13mp18 and pUC19 vectors. *Gene* 33 (1), 103-119.
- Yong, R., Searcy, D.G., 2001. Sulfide oxidation coupled to ATP synthesis in chicken liver mitochondria. *Comp. Biochem. Physiol. B Biochem. Mol. Biol.* 129 (1), 129-137.
- Zhou, J.Z., Bruns, M.A., Tiedje, J.M., 1996. DNA recovery from soils of diverse composition. *Appl. Environ. Microbiol.* 62 (2), 316-322.
- Zielinski, F.U., Borowski, C., Gennerich, H.H., Dubilier, N., Wenzhöfer, F., manuscript I. *In situ* measurements of hydrogen sulfide, oxygen, and temperature in diffuse fluids of the ultramafic-hosted Logatchev hydrothermal vent field (Mid-Atlantic Ridge): implications for symbiont-containing *Bathymodiolus* mussels. Intended as article in *Deep-Sea Research I*.
- Zielinski, F.U., Pernthaler, A., Duperron, S., Raggi, L., Giere, O., Borowski, C., Dubilier, N., manuscript II. Widespread occurrence of an intranuclear bacterial parasite in vent and seep mussels. submitted to *PLoS Biology*.

Curriculum Vitae

Personal Information

Name: **Frank Zielinski
Biologist (Dipl.)**

Date of Birth: February 27, 1974

Children: Béla A. Zielinski (3)

Address: Möckernsche Str. 30
04155 Leipzig

Phone (Office): 0341-235-1373

Email: frank.zielinski@ufz.de
fzielins@mpi-bremen.de

Web: http://marmic.mpg.de/marmic_cms/participating.php?section=students&profile=fzielins



Education

- since Jun 2007 **Helmholtz Centre for Environmental Research**
Department of Environmental Microbiology
- since Nov 2003 **PhD student in the field of Molecular Ecology**
- Intern. Max-Planck Research School of Marine Microbiology (MarMic)
Max Planck Institute for Marine Microbiology, Bremen, Germany
Department of Molecular Ecology / Marine Symbioses
 - California Institute of Technology, Pasadena, USA
Department of Geological and Planetary Sciences / Geobiology
Thesis subject: Geobiological coupling of hydrothermal vent fluids with endosymbiotic primary producers of deep-sea mussels inhabiting hydrothermal vents on the Mid-Atlantic Ridge
Paternity leave from Aug-Oct 2005
- 2003 **Diploma in Biology**
- Thesis subject: MalR – the negative regulator of the gene cluster for starch metabolism from the grampositive bacterium *Alicyclobacillus acidocaldarius*. Purification and *in vitro* DNA-binding assays.
- Department of Bacterial Physiology
under the supervision of Prof. Dr. Erwin Schneider
- 1995-2003 **Studies in Biology**
- Major: **Microbiology**
Minors: **Biochemistry, Zoology**
- Humboldt University, Berlin
 - Bates College, Lewiston Maine, USA
- 1994 **Studies in Conservation and Preservation of Historic buildings and Monuments**
Fachhochschule Potsdam
- 1992 **Studies in Classical Philology and Archaeology**
Humboldt University, Berlin
- 1992 **Abitur**
3rd Gymnasium Mitte, Berlin

Erklärung

Gemäß § 6 (5) Promotionsordnung erkläre ich hiermit, dass ich die Arbeit mit dem Titel:

Geobiological coupling of hydrothermal vent fluids with endosymbiotic primary producers of *Bathymodiolus* mussels from hydrothermal vents on the Mid-Atlantic Ridge

selbständig verfasst und geschrieben, außer den angegebenen Quellen keine weiteren Hilfsmittel verwendet und die den benutzten Werken wörtlich oder inhaltlich entnommenen Stellen als solche kenntlich gemacht habe.

Ebenfalls erkläre ich hiermit, dass es sich bei den von mir abgegebenen Arbeiten um drei identische Exemplare handelt.

Frank Zielinski

Ort, Datum